VOLUME 86 NO. WW1
MARCH 1960
PART 1

JOURNAL of the

Waterways and Harbors Division

PROCEEDINGS OF THE
AMERICAN SOCIETY
OF CIVIL ENGINEERS

BASIC REQUIREMENTS FOR MANUSCRIPTS

Original papers and discussions of current papers should be submitted to the Manager of Technical Publications, ASCE. Authors should indicate the technical division to which the paper should be referred. The final date on which a discussion should reach the Society is given as a footnote with each paper. Those who are planning to submit material will expedite the review and publication procedures by complying with the following basic requirements:

1. Titles must have a length not exceeding 50 characters and spaces.

2. A 50-word summary must accompany the paper.

3. The manuscript (a ribbon copy and two copies) should be double-spaced on one side of 8½-in. by 11-in. paper. Papers that were originally prepared for oral presentation must be rewritten into the third person before being submitted.

4. The author's full name, Society membership grade, and footnote reference stating present employment must appear on the first page of the paper.

5. Mathematics are recomposed from the copy that is submitted. Because of this, it is necessary that letters be drawn carefully, and that special symbols be properly identified.

6. Tables should be typed (ribbon copies) on one side of 8½-in. by 11-in. paper. Specific reference and explanation must be made in the text for each table.

7. Illustrations must be drawn in black ink on one side of 8½-in. by 11-in. paper. Because illustrations will be reproduced with a width of between 3-in. and 4½-in., the lettering must be large enough to be legible at this width. Photographs should be submitted as glossy prints. Explanations and descriptions must be made within the text for each illustration.

8. Papers should average about 12,000 words in length and must be no longer than 18,000 words. As an approximation, each full page of typed text, table, or illustration is the equivalent of 300 words.

Further information concerning the preparation of technical papers is contained in the "Technical Publications Handbook" which can be obtained from the Society.

Reprints from this Journal may be made on condition that the full title of the paper, name of author, page reference, and date of publication by the Society are given. The Society is not responsible for any statement made or opinion expressed in its publications.

This Journal is published quarterly by the American Society of Civil Engineers. Publication office is at 2500 South State Street, Ann Arbor, Michigan. Editorial and General Offices are at 33 West 39 Street, New York 18, New York. $4.00 of a member's dues are applied as a subscription to this Journal. Second-class postage paid at Ann Arbor, Michigan.

Subject and author indexes, with abstracts, are published at the end of each year for the Proceedings of ASCE. The index for 1958 was published as Proc. Paper 1891; indexes for previous years are also available.

EM.HW.R.WW

Journal of the

WATERWAYS AND HARBORS DIVISION

Proceedings of the American Society of Civil Engineers

WATERWAYS AND HARBORS DIVISION
EXECUTIVE COMMITTEE
Joe W. Johnson, Chairman; Richard O. Eaton, Vice-Chairman;
Lawrence B. Feagin; Evan W. Vaughan; Robert J. Winters, Secretary

COMMITTEE ON PUBLICATIONS
Jay V. Hall, Jr., Chairman; W. Mack Angas; Joseph M. Caldwell;
Ellsworth I. Davis; James W. Dunham

CONTENTS

March, 1960

Papers

	Page
Transmission of Waves Past a Rigid Vertical Thin Barrier by Robert L. Wiegel	1
Hydrodynamic Wave Pressure on Breakwaters by M. A. Gouda	13
Discussion	27
Canadian Section of the St. Lawrence Seaway by Lawrence H. Burpee	53
Design and Construction of Navy's Largest Drydock by S. P. Zola and P. M. Boothe	85
Waves in Navigation Canals due to Lock Filling by Hans-Werner Partenscky	123
Mean Direction of Waves and Wave Energy by Omar J. Lillevang	145

Copyright 1960 by the American Society of Civil Engineers.

Journal of the
WATERWAYS AND HARBORS DIVISION
Proceedings of the American Society of Civil Engineers

TRANSMISSION OF WAVES PAST A RIGID VERTICAL THIN BARRIER

By Robert L. Wiegel[1]

SYNOPSIS

A theory is presented for the transmission of waves past a rigid vertical thin barrier extending from above the water surface to some distance below the surface. This theory is based on consideration of wave-power transmission. Laboratory data are presented to show that this theory is useful from the engineering design standpoint, but that improvements are desirable.

INTRODUCTION

One possible type of breakwater consists of a thin rigid barrier extending from above the water surface to some distance below the water surface. This barrier may be siding mounted on a pile structure, for example. One of the problems in the design of such a structure is to determine the distance below the free surface to which such a barrier must extend in order to function effectively. The theory of such a structure is developed here together with the results of laboratory tests on a model structure under a variety of wave conditions.

Note.—Discussion open until August 1, 1960. To extend the closing date one month, a written request must be filed with the Executive Secretary, ASCE. This paper is part of the copyrighted Journal of the Waterways and Harbors Division, Proceedings of the American Society of Civil Engineers, Vol. 86, No. WW 1, March, 1960.

[1] Assoc. Research Engr., Univ. of Calif., Dept. of Engrg., Inst. of Engrg. Research, Berkeley, Calif.

THEORY

Two theories are given, one developed herein and one due to F. Ursell.[2]

Deep Water—Ursell's Theory.—In 1947 Ursell developed a theory for the partial transmission and partial reflection of water gravity waves in deep water for a fixed vertical infinitely thin barrier extending from the water surface to some depth below this surface. He found that:

$$\frac{H_T}{H_I} = \frac{K_1 (2\pi l/L)}{\sqrt{\pi^2 I_1^2 (2\pi l/L) + K_1^2 (2\pi l/L)}} \quad \ldots\ldots\ldots \quad (1)$$

where H_T is the transmitted wave height, H_I denotes the incident wave height, $I_1 (2\pi l/L)$ and $K_1 (2\pi l/L)$ are modified Bessel functions, and L is the wave length. The ratio H_T/H_I is plotted in Fig. 1 together with the experimental data.

Power Transmission Theory.—Consider an infinite series of uniform long-crested periodic waves. The average power (averaged over one wave period) that is transmitted past a vertical plane is

$$P_{y_s-y} = \frac{1}{T} \int_0^T \int_y^{y_s} p\, u\, dt\, dy \quad \ldots\ldots\ldots\ldots\ldots \quad (2)$$

where P_{y_s-y} is the power per foot of wave crest for the section of the vertical plane between y and the surface y_s, T denotes the wave period, p is the pressure in the fluid, u represents the horizontal component of water particle velocity, y is the vertical coordinate measured negative downward from the still water level, and y_s denotes the free surface ordinate.

Now

$$p = \rho g y + \rho g a \frac{\cosh k (y+d)}{\cosh k d} \cos (k x - \sigma t) \ldots\ldots\ldots \quad (3a)$$

and

$$u = \frac{g a k}{\sigma} \frac{\cosh k (y+d)}{\cosh k d} \cos (k x - \sigma t) \quad \ldots\ldots\ldots\ldots \quad (3b)$$

where ρ is the fluid mass density, g denotes the acceleration of gravity, a is one-half the wave height H, $k = 2\pi/L$, L is the wave length, d represents the still water depth, $\sigma = 2\pi/T$, x is the horizontal coordinate measured positive in the direction of wave advance from the wave crest, and t denotes time. It follows then that

$$P_{y_s-y} = \frac{\rho g^2 a^2 k}{T\sigma \cosh^2 k d} \left[\int_0^T \int_y^{y_s} \cosh^2 \Big(k (y+d)\Big) \cos^2 (k x - \sigma t)\, dt\, dy \right.$$

$$\left. - \frac{\cosh k d}{a} \int_0^T \int_y^{y_s} y \cosh \Big(k (y+d)\Big) \cos (k x - \sigma t)\, dt\, dy \right] \ldots\ldots \quad (4)$$

---

[2] "The Effect of a Fixed Vertical Barrier on Surface Waves in Deep Water," by F. Ursell, Proc. Cambridge Phil. Soc., Vol. 43, Part 3, pp 374-382, July 1947.

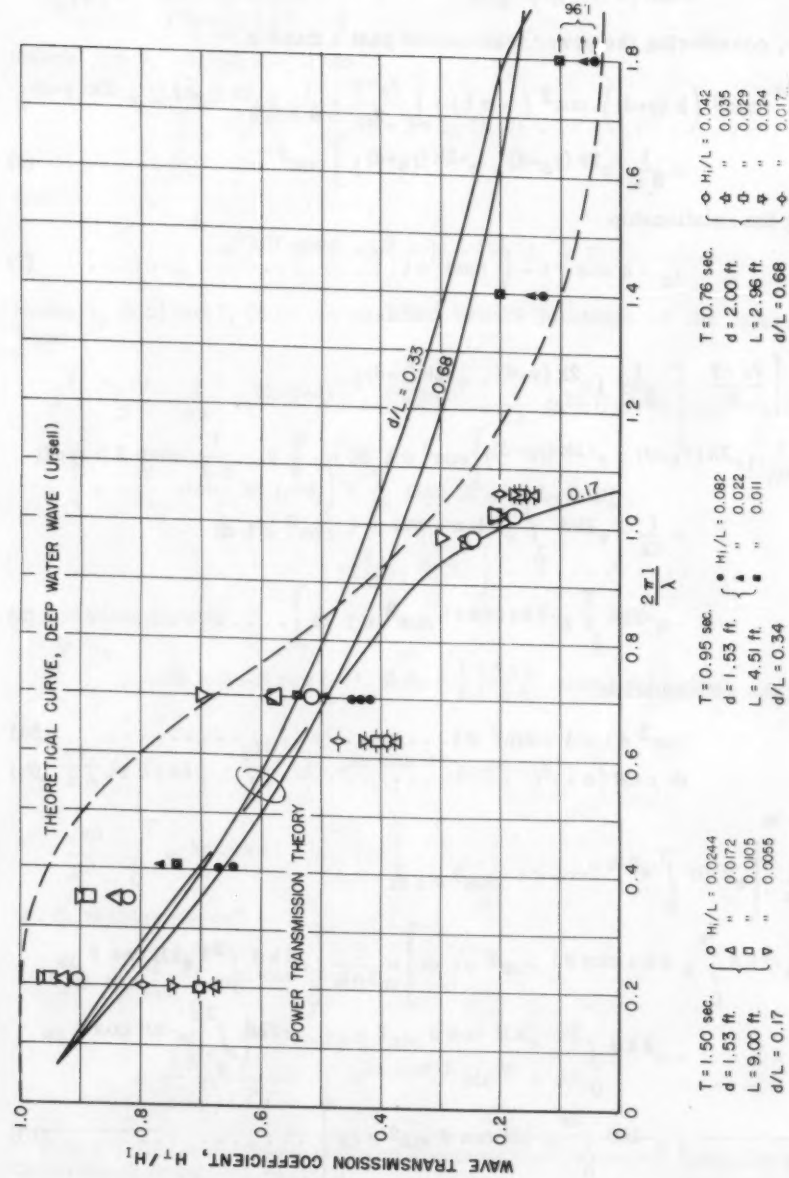

FIG. 1.—TRANSMISSION COEFFICIENT FOR BARRIER IMMERSED TO VARIOUS DEPTHS

with the resulting equation applying only when y is below the wave trough. Now

$$\cosh\Big(k\,(y+d)\Big) = \frac{1}{2}\,(e^{k(y+d)} + e^{-k(y+d)}); \quad \ldots\ldots\ldots \quad (5)$$

hence, considering the power transmitted past a fixed x

$$\int_{y}^{y_s} \cosh^2\Big(k\,(y+d)\Big)\,\cos^2(-\sigma t) = \Big[\frac{y_s - y}{2} - \frac{1}{8k}\,(e^{2k(y+d)} - e^{-2k(y+d)}) + \frac{1}{8k}\,(e^{2k(y_s+d)} - e^{-2k(y_s+d)})\Big]\cos^2\sigma t \quad \ldots\ldots\ldots \quad (6)$$

Using the relationship

$$y_s = a\cos\sigma t + \frac{H}{2}\cos\sigma t \quad \ldots\ldots\ldots\ldots\ldots\ldots \quad (7)$$

leads to

$$\int_0^T \Big[\frac{y_s - y}{2} - \frac{1}{8k}\,(e^{2k(y+d)} - e^{-2k(y+d)}) + \frac{1}{8k}\,(e^{2k(y_s+d)} - e^{-2k(y_s+d)})\Big]\cos^2\sigma t\ dt = -\frac{T}{4}\,y - \frac{T}{8k}\sinh 2k\,(y+d) + \frac{1}{8k}\Big[e^{2kd}\int_0^T e^{2ka\cos\sigma t}\cos^2\sigma t\ dt - e^{-2kd}\int_0^T e^{-2ka\cos\sigma t}\cos^2\sigma t\ dt\Big] \quad \ldots\ldots\ldots\ldots \quad (8)$$

Using the relationships

$$\cos^2\sigma t = 1 - \sin^2\sigma t \quad \ldots\ldots\ldots\ldots\ldots\ldots\ldots\ldots \quad (9a)$$

$$dt = d\theta/\sigma \quad \ldots\ldots\ldots\ldots\ldots\ldots\ldots\ldots\ldots\ldots\ldots \quad (9b)$$

leads to

$$\frac{1}{8k}\Big[e^{2kd}\int_0^T e^{2ka\cos\sigma t}\cos^2\sigma t\ dt - e^{-2kd}\int_0^T e^{-2ka\cos\sigma t}\cos^2\sigma t\ dt\Big] = \frac{1}{8\sigma k}\Big[e^{2kd}\int_0^{2\pi} e^{kH\cos\theta}\,d\theta - e^{2kd}\int_0^{2\pi} e^{kH\cos\theta}\sin^2\theta\,d\theta - e^{-2kd}\int_0^{2\pi} e^{-kH\cos\theta}\,d\theta + e^{-2kd}\int_0^{2\pi} e^{-kH\cos\theta}\sin^2\theta\,d\theta\Big] \quad \ldots\ldots\ldots\ldots \quad (10)$$

G. N. Watson gives[3] the following functions:

$$I_\nu(z) = \frac{\left(\frac{1}{2}z\right)^\nu}{\Gamma\left(\nu+\frac{1}{2}\right)\Gamma\left(\frac{1}{2}\right)} \int_0^\pi e^{+z\cos\theta} \sin^{2\nu}\theta \, d\theta$$

where $\nu = 0, \pm1, \pm2, \ldots$; so

$$\int_0^{2\pi} e^{+kH\cos\theta} \, d\theta = 2\pi I_0(kH) \quad \ldots\ldots\ldots\ldots \quad (11a)$$

and

$$\int_0^{2\pi} e^{+kH\cos\theta} \sin^2\theta \, d\theta = \frac{2\pi}{kH} I_1(kH) \quad \ldots\ldots\ldots \quad (11b)$$

where $I_0(kh)$ and $I_1(kH)$ are modified Bessel functions of the first kind. Thus

$$\int_0^T \left[\frac{y_s - y}{2} - \frac{1}{8k}\left(e^{2k(y+d)} - e^{-2k(y+d)}\right) + \frac{1}{8k}\left(e^{2k(y_s+d)}\right)\right]\cos^2\sigma t \, dt$$

$$= -\frac{T}{4}y - \frac{T}{8k}\sinh\left(2k(y+d)\right) + \frac{T}{4k}\sinh(2kd)\left[I_0(kH) - \frac{1}{kH}I_1(kH)\right] \quad \ldots\ldots\ldots\ldots\ldots \quad (12)$$

In a similar manner

$$\int_0^T \int_y^{y_s} y\cosh k(y+d)\cos(-\sigma t)\, dt\, dy = \frac{1}{2}\left\{\frac{4\pi a}{\sigma k}\sinh kd\left[I_0(ka) - \frac{1}{ka}I_1(ka)\right] - \frac{e^{kd}}{k^2}\int_0^T e^{ka\cos\sigma t}\cos\sigma t\, dt - \frac{e^{kd}}{k^2}\int_0^T e^{-ka\cos\sigma t}\cos\sigma t\, dt\right\} \quad \ldots\ldots\ldots\ldots\ldots\ldots \quad (13)$$

W. G. Bickley shows[4]

$$I_n(ka) = \frac{1}{\pi}\int_0^\pi e^{ka\cos\theta}\cos n\theta \, d\theta$$

$$= \frac{\left(\frac{1}{2}ka\right)^n}{\left(n-\frac{1}{2}\right)!\sqrt{\pi}} \int_0^\pi e^{ka\cos\theta}\sin^{2n}\theta \, d\theta, \quad \ldots\ldots\ldots \quad (14)$$

---

3 "A Treatise on the Theory of Bessel Functions," by G. N. Watson, University Press, Cambridge, England, 804, pp. 1944.

4 "Bessel Functions and Formulae," by W. G. Bickley, Royal Society (London), University Press, Cambridge, England, 40 pp, 1953.

and as

$$I_1(-k\,a) = I_1(k\,a), \quad \ldots\ldots\ldots\ldots\ldots\ldots \quad (15)$$

we find

$$\int_0^T \int_y^{y_s} y \cosh k(y+d) \cos(-\sigma t)\, dt\, dy$$

$$= \frac{1}{2}\left\{\frac{4\pi a}{\sigma k} \sinh k\,d \left[I_0(k\,a) - \frac{2}{k\,a} I_1(k\,a)\right]\right\}; \quad \ldots\ldots\ldots\ldots\ldots\ldots \quad (16)$$

using the relationship

$$C = \frac{g}{\sigma} \tanh(k\,d). \quad \ldots\ldots\ldots\ldots\ldots\ldots \quad (17)$$

we find finally

$$P_{y_s - y} = \frac{1}{2}\rho g a^2 C \frac{1}{2}\left\{ - \frac{2\,k\,y}{\sinh 2\,k\,d} - \frac{\sinh 2k(y+d)}{\sinh 2\,k\,d} + 2\left[I_0(2\,k\,a) - \frac{1}{2\,k\,a} I_1(2\,k\,a)\right] + 4\left[-I_0(k\,a) + \frac{2}{k\,a} I_1(k\,a)\right]\right\} \quad \ldots\ldots\ldots\ldots \quad (18)$$

The power from the ocean bottom, y = -d, to the surface is given by

$$P_{y_s - d} = \frac{1}{2}\rho g a^2 C \frac{1}{2}\left\{ \frac{2\,k\,d}{\sinh 2\,k\,d} + 2\left[I_0(2ka) - \frac{1}{2\,k\,a} I_1(2\,k\,a)\right] + 4\left[-I_0(k\,a) + \frac{2}{k\,a} I_1(k\,a)\right]\right\} \quad \ldots\ldots\ldots\ldots \quad (19)$$

The power transmitted between the bottom and some level y located below the wave trough is given by

$$P_{y-d} = \frac{1}{2}\rho g a^2 C \frac{1}{2}\left\{ \frac{2k(y+d)}{\sinh 2kd} + \frac{\sinh 2k(y+d)}{\sinh 2\,k\,d}\right\} \quad \ldots\ldots\ldots\ldots \quad (20)$$

If the rigid vertical barrier extends to a distance y below the still water surface, the wave height (H = 2 a) in the lee of the curtain can be obtained by assuming that the only power transmitted is that from - d to y; that is, the power between y and y_s is reflected.

Now for waves of small amplitude, and using the approximate series for I_0 and I_1, Bickley[4] shows:

$$I_0(k\,a) = 1 + \left(\frac{k\,a}{2}\right)^2 + \ldots \quad \ldots\ldots\ldots\ldots\ldots\ldots \quad (21)$$

$$I_n(k\,a) = \frac{\left(\frac{1}{2}k\,a\right)^n}{n!}\left(1 + \frac{\left(\frac{1}{2}k\,a\right)^2}{1\,(n+1)} + \ldots\right) \quad \ldots\ldots\ldots\ldots\ldots\ldots \quad (22)$$

So: $I_0 (k a) \sim 1$, $I_0 (2 k a) \sim 1$, $I_1 (k a) \sim -k a$ and $I_1 (2 k a) \sim k a$; and

$$P_{y_s - d} = \frac{1}{2} \rho g a^2 \frac{1}{2} \left(1 + \frac{2 k d}{\sinh 2 k d} \right), \quad \ldots\ldots\ldots\ldots\ldots \quad (23)$$

which is the generally accepted expression for small amplitude waves.

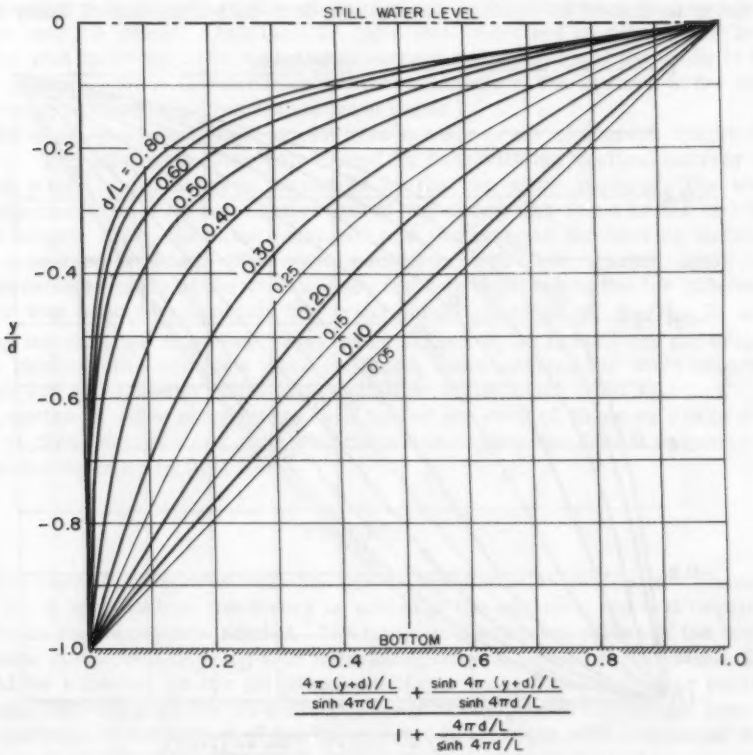

FIG. 2.—FIRST APPROXIMATION OF WAVE POWER TRANSMITTED BETWEEN BOTTOM AND DEPTH y/d

The portion of wave power transmitted between the bottom and the depth y/d below the still water level for waves of small amplitude is:

$$\frac{P_T}{P_I} = \frac{\frac{4\pi (y+d)/L}{\sinh 4\pi d/L} + \frac{\sinh 4\pi (y+d)/L}{\sinh 4\pi d/L}}{1 + \frac{4\pi d/L}{\sinh 4\pi d/L}} \quad \ldots\ldots\ldots\ldots\ldots \quad (24)$$

This function is shown in Fig. 2. For the case of deep water it reduces to

$$\frac{P_T}{P_I} \sim e^{4\pi y/L} \quad \ldots\ldots\ldots\ldots\ldots \quad (25)$$

where y is measured as negative downward.

The portion of the wave height transmitted between the bottom and the depth y/d below the still water level for waves of small amplitude is:

$$\frac{H_T}{H_I} = \sqrt{\frac{P_t}{P_I}} \quad \ldots\ldots\ldots\ldots\ldots\ldots\ldots\ldots \quad (26)$$

This function is shown in Fig. 3. It is this fact that the ratio of the transmitted to incident wave height is proportional to the square root of the ratio of the transmitted to incident wave power that makes the use of many forms

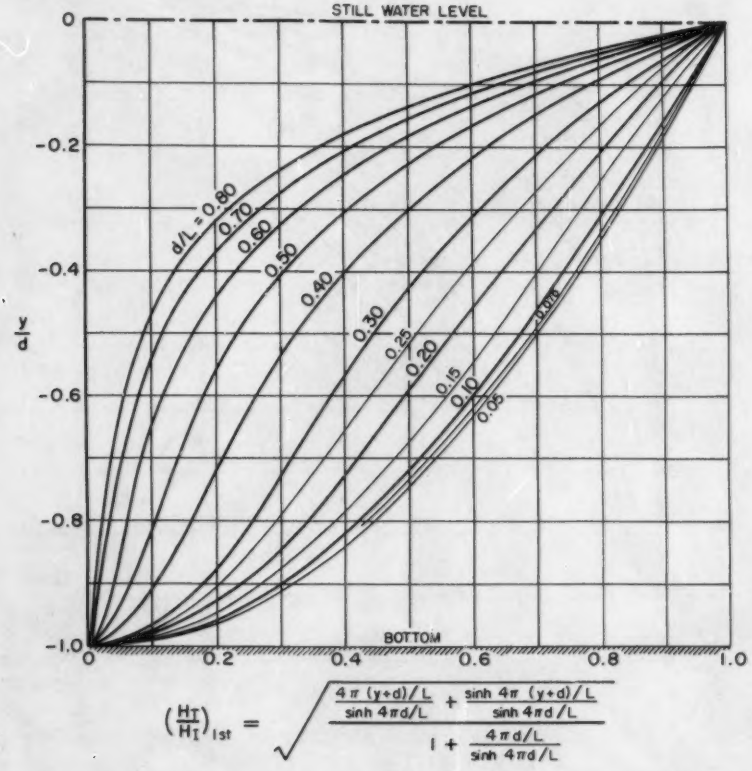

FIG. 3.—FIRST APPROXIMATION OF RATIO OF TRANSMITTED TO INCIDENT WAVE HEIGHT AS A FUNCTION OF BARRIER DEPTH

of partial breakwaters relatively ineffective. For example, if only 4% of the power is transmitted, 20% of the wave height is transmitted.

The effect of the terms I_0 and I_1 can be neglected for the most practical purposes. For example, if the wave steepness H/L were 0.1, k a = π H/L = 0.314 and 2 k a = 2 π H/L = 0.628, I_0 (k a) = 1.025, I_1 (k a) = 0.158, I_0 (2 k a) = 1.101, I_1 (2 k a) = 0.330, and the term

$$\left\{ 2 \left[I_0 (2\,k\,a) - \frac{1}{2\,k\,a} I_1 (2\,k\,a) \right] + 4 \left[- I_0 (k\,a) + \frac{2}{k\,a} I_1 (k\,a) \right] \right\} = 1.076 ,$$

which is only about 7% to 8% greater than unity; the values of I_0 and I_1 have been tabulated by Andrew Gray, G. B. Mathews, and T. M. MacRobert.[5]

EXPERIMENTAL EQUIPMENT AND PROCEDURES

The experiments were performed in the 1 ft wide by 3 ft deep by 106 ft long wave channel at the University of California at Berkeley.[6] The rigid vertical thin barrier was fitted into that channel about halfway between the wave generator and the beach. Considerable care was exercised in placing the barrier so that there would be no leakage between the barrier and the walls of the wave channel. Wave measurements were made about 6 ft in front of the barrier using parallel wire resistance wave gages.[7]

The wave generator was set to give a wave train of a given height and period. The wave generator was turned on first with the vertical barrier out of the water and the waves measured by the two wave meters. The wave heights measured with the barrier out of the water was taken as the incident wave height. Then the wave generator was stopped and the barrier installed in the desired position. The wave generator was then started again and measurements made of the waves. Only the data obtained on the lee side wave meter was used in computing the transmission coefficient, H_T/H_I. In analyzing the data the first few waves were passed by as these were not of constant period. The next few were analyzed, these passing the wave recorder before any wave energy could be reflected from the beach (Fig. 4).

A series of wave steepnesses was tested for each of three values of d/L. Two of these series were done with the water depth being 1.53 ft and one with the water depth being 2.01 ft.

RESULTS

The results, compared with the power transmission theory are shown in Fig. 5. It appears that the theory is useful to the engineer, but that improvements in the theory are needed. The trend of decreasing values of the transmission coefficient (H_T/H_I) with increasing wave stepness is consistent. This would be expected as for all other conditions being equal the water particle velocity increases as the wave steepness increases, hence the energy loss due to separation at the bottom of the barrier would increase with increasing wave steepness resulting in a decrease in the transmission coefficient.

The same data are plotted in Fig. 1. The power-transmission theory predicts the transmission coefficient more closely for the deep water wave (d/L = 0.68) than does the deep-water theory for the smaller values of barrier im-

---

[5] "A Treatise on Bessel Functions and Their Applications to Physics," by Andrew Gray, G. B. Mathews, and T. M. MacRobert, MacMillan and Co., Ltd., London, 327 pp, 1931.

[6] "Laboratory Facilities for Studying Water Gravity Wave Phenomena," by C. M. Snyder, R. L. Wiegel, and Karl J. Bermel, Proc. of the Sixth Conf. on Coastal Engineering, Council on Wave Research, The Engineering Foundation, Berkeley, Calif., pp 231-251, 1958.

[7] "Parallel Wire Resistance Wave Meter," by R. L. Wiegel, Proc. First Conf. on Coastal Engineering Instruments, Council on Wave Research, The Engineering Foundation, Berkeley, Calif., pp 39-43, 1956.

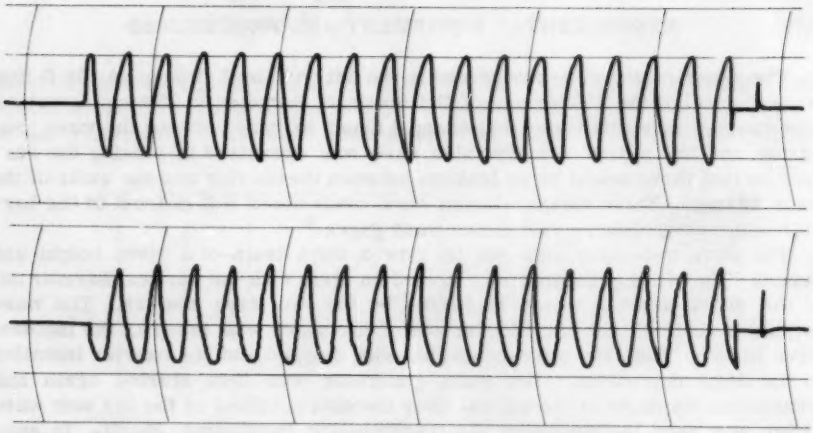

a. Barrier out of water - T = 1.5 sec., d = 1.53 ft., H_I = 0.22 ft.

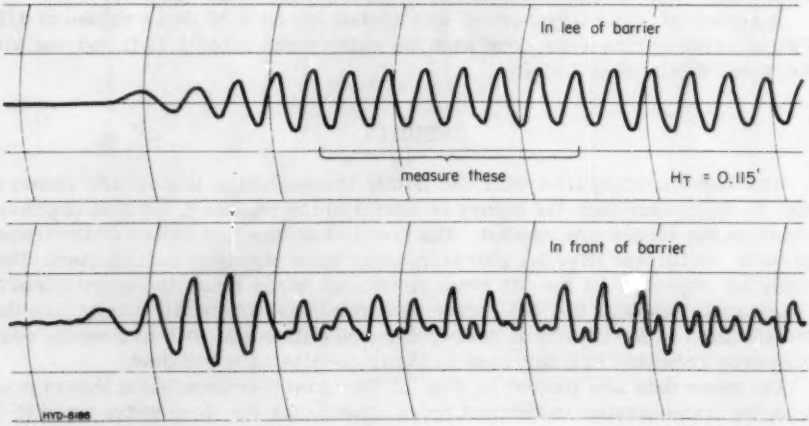

b. Barrier in the water - T = 1.5 sec., d = 1.53 ft., H_T = 0.115 ft.

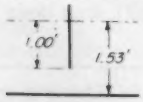

FIG. 4.—SAMPLE WAVE RECORD

mersion while the deep-water theory predicts the transmission coefficient more closely for the larger values of barrier immersion.

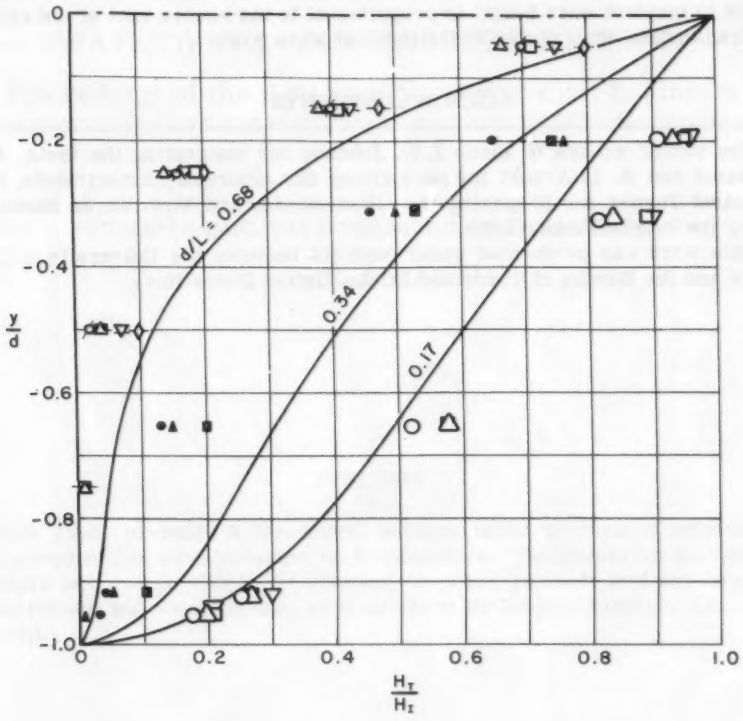

T = 1.50 sec.
d = 1.53 ft.
L = 9.00 ft.
d/L = 0.17

○ H_i/L = 0.0244
△ " 0.0172
□ " 0.0105
▽ " 0.0055

T = 0.95 sec.
d = 1.53 ft.
L = 4.51 ft.
d/L = 0.34

● H_i/L = 0.082
▲ " 0.022
■ " 0.011

T = 0.76 sec.
d = 2.00 ft.
L = 2.96 ft.
d/L = 0.68

ø H_i/L = 0.042
⛢ " 0.035
⛋ " 0.029
⛛ " 0.024
⛊ " 0.017

FIG. 5.—COMPARISON OF MEASURED TRANSMITTED WAVE HEIGHT AND THE FIRST-ORDER POWER-TRANSMISSION THEORY

CONCLUSIONS

The power-transmission theory predicts the transmission coefficient adequately for some engineering purposes.

A consistent trend of decreasing transmission coefficient with increasing wave steepness is evident in the laboratory measurements, all other conditions being equal.

Except under certain special circumstances the use of a rigid barrier extending only a short distance below the surface does not appear to be useful. The main reason for this is the fact that the ratio of the transmitted wave height to incident wave height is proportional to the square root of the ratio of the transmitted wave power to the incident wave power.

ACKNOWLEDGMENTS

The writer wishes to thank J. W. Johnson for suggesting the tests, J. A. Williams and A. L. Arnold for performing the laboratory experiments, Mrs. Margaret Turner for preparing the illustrations, and Mrs. Verda Bauer for typing the original manuscript.

This work was performed under contract between the University of California and the Bureau of Yards and Docks, United States Navy.

Journal of the
WATERWAYS AND HARBORS DIVISION
Proceedings of the American Society of Civil Engineers

HYDRODYNAMIC WAVE PRESSURE ON BREAKWATERS

By M. A. Gouda[1]

SYNOPSIS

This paper presents a theoretical solution to the problem of determining the hydrodynamic wave pressure on breakwaters. The pressures derived are in close agreement with those obtained by other methods that are based on observations and experiments, such as those by Luiggi, Sainflou, Cagli, and Benedit.

INTRODUCTION

The problem of wave pressure on breakwaters is of much importance to port and harbor engineers.

Previous investigators discussing this problem based their work mostly on observations and experiments. Results are given in the form of diagrams and empirical formulae such as that given by Luiggi, Sainflou, Cagli, Benedit, and others.

An attempt is made herein to obtain a solution for this problem based totally on the theory of hydrodynamics. This theoretical investigation is of great practical value as engineers in increasing numbers are drawing extensively

Note.--Discussion open until August 1, 1960. To extend the closing date one month, a written request must be filed with the Executive Secretary, ASCE. This paper is part of the copyrighted Journal of the Waterways and Harbors Division, Proceedings of the American Society of Civil Engineers, Vol. 86, No. WW 1, March, 1960.

[1] Ass't. Prof., Civ. Engrg. Dept., Alexandria Univ., Chatby, Alexandria, Egypt.

on the results of mathematical analysis as an aid in their design work. Moreover, results obtained for a specific wave problem by applying the mentioned diagrams and equations are of such different values that a theoretical investigation is needed.

SURFACE AND STANDING WAVES

Consider the oscillation of a horizontal sheet of water where the depth is very great. The motion, being such as could be produced from rest by natural forces, is irrotational and the velocity potential ϕ has to satisfy the differential equation[2]

$$\frac{\partial^2 \phi}{\partial y^2} + \frac{\partial^2 \phi}{\partial z^2} = 0 \quad \ldots\ldots\ldots\ldots\ldots\ldots \quad (1)$$

with the condition $\partial \phi / \partial n = 0$ at a fixed barrier in the z-x plane, where $\frac{\partial}{\partial n}$ denotes differentiation with respect to definite distance from the barrier.

The pressure at any point (x, y, z) at time t is given by:

$$\frac{p}{\rho} = -g z - \frac{1}{2} q^2 + \dot{\phi} + f(t) \ldots\ldots\ldots\ldots\ldots\ldots \quad (2)$$

where p is pressure, ρ denotes density of liquid, q is velocity, and f(t) represents an arbitrary function of the time which may be supposed merged in $\dot{\phi}$.

Thus the pressure will be

$$\frac{p}{\rho} = -g z - \frac{1}{2} q^2 + \dot{\phi} \quad \ldots\ldots\ldots\ldots\ldots\ldots \quad (3)$$

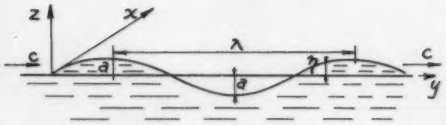

FIG. 1.—ELEMENTS OF A STANDING WAVE

Referring to Fig. 1 for a standing wave of amplitude a, wavelength λ, and velocity of propagation c, it is known that $c^2 = g/K$ where $K = 2\pi/\lambda$ and in deep water, the elevation of the free surface[3]

$$\eta = 2a \cos(K y) \cos(K c t) \quad \ldots\ldots\ldots\ldots\ldots\ldots \quad (4)$$

To arrive at a practical solution for the problem, the following assumptions have to be considered:

1. The barrier is assumed very long and thus the solution is independent of x.
2. The solution is periodic in the time t and the period being $\frac{\lambda}{c} = \frac{2\pi}{K c}$ also it is periodic in y, its period being $\lambda = 2\pi/K$.
3. At the barrier where $y = 0$ the horizontal velocity $v = \partial \phi / \partial y = 0$ also at the bottom of the sea where $z = -\infty$, the vertical velocity $w = -\frac{\partial \phi}{\partial z} = 0$.

---

2 "A Treatise on Hydro-Mechanics," Part II, "Hydrodynamics," by Arthur S. Ramsey, pp. 267.

3 "Theoretical Hydrodynamics," by L. M. Milin - Thomson, pp. 354.

4. At the free surface where $z = \eta$, the pressure $p = 0$. Hence by substituting in Eq. 3, $\phi - \frac{1}{2} q^2 = g z$.

5. The surface of waves is expected to be of the form

$$\eta = 2 a \cos (K y) \cos (K c t) + \eta' \quad \ldots\ldots\ldots\ldots \quad (5)$$

where η' is a function of y and t and $K = g/c^2$

SOLUTION OF THE PRESSURE DIFFERENTIAL EQUATION

The semi-inverse method is used to obtain the potential ϕ satisfying Eq. 3. The velocity v could be written in the form

$$v = V \sin (K y) \sin (K c t) = \frac{\partial \phi}{\partial y} \quad \ldots\ldots\ldots\ldots \quad (6)$$

and since

$$\frac{\partial^2 v}{\partial y^2} + \frac{\partial^2 v}{\partial z^2} = O \quad \ldots\ldots\ldots\ldots\ldots\ldots \quad (7)$$

therefore

$$- K^2 V \sin (K y) \sin (K c t) + \frac{d^2 V}{dz^2} \sin (K y) \sin (Kct) = O \ldots\ldots \quad (8)$$

or

$$\frac{d^2 V}{dz^2} - K^2 V = O \ldots\ldots\ldots\ldots\ldots\ldots\ldots \quad (9)$$

thus

$$V = A_1 e^{K z} + A_2 e^{-K z} \quad \ldots\ldots\ldots\ldots\ldots \quad (10)$$

Substituting from Eq. 10 into Eq. 6 yields

$$v = (A_1 e^{Kz} + A_2 e^{-Kz}) \sin (K y) \sin (K c t) \ldots\ldots\ldots\ldots \quad (11)$$

but since

$$\frac{\partial w}{\partial y} = - \frac{\partial^2 \phi}{\partial y \partial z} = - \frac{\partial}{\partial z} \frac{\partial}{\partial y} = \frac{\partial v}{\partial z}$$

$$= K (A_1 e^{K z} - A_2 e^{-K z}) \sin (K y) \sin (K c t) \ldots\ldots\ldots\ldots \quad (12)$$

and

$$\frac{\partial w}{\partial z} = - \frac{\partial^2 \phi}{\partial z^e} = \frac{\partial^2 \phi}{\partial y^2} = - \frac{\partial v}{\partial y}$$

$$= -K (A_1 e^{K z} + A_2 e^{-K z}) \cos (K y) \sin (K c t) \ldots\ldots\ldots\ldots \quad (13)$$

Thus from Eqs. 12 and 13 the vertical velocity w will be

$$w = - (A_1 e^{K z} - A_2 e^{-K z}) \cos (K y) \sin (K c t) \quad \ldots\ldots\ldots\ldots (14)$$

and since, from assumption 3, $w = O$ when $z = - \infty$, therefore $A_2 = O$. Hence the horizontal and vertical velocities v and w will be

$$v = A_1 e^{Kz} \sin (K y) \sin (K c t) \quad \ldots\ldots\ldots\ldots\ldots\ldots\ldots (15a)$$

and

$$w = - A_1 e^{Kz} \cos (K y) \sin (K c t) \quad \ldots\ldots\ldots\ldots\ldots\ldots\ldots (15b)$$

From previous expressions of the velocities and since $v = - \partial \phi / \partial y$ and $w = - \partial \phi / \partial z$ then

$$\phi = \frac{A_1}{K} e^{Kz} \cos (K y) \sin (K c t) + f(t) \quad \ldots\ldots\ldots\ldots\ldots\ldots (16)$$

or

$$\phi = A e^{K z} \cos (K y) \sin (K c t) + f(t) \quad \ldots\ldots\ldots\ldots\ldots\ldots (17)$$

where $A = A_1/K$, but since $q^2 = v^2 + w^2$, and by expressing values of v and w from Eq. 15, thus

$$q^2 = A^2 K^2 e^{2 K z} \sin^2 (K c t) \quad \ldots\ldots\ldots\ldots\ldots\ldots\ldots\ldots (18)$$

From expression of ϕ in Eq. 17,

$$\phi = \frac{\partial \phi}{\partial t} = A K c e^{K z} \cos (K y) \cos (K c t) + f'(t) \quad \ldots\ldots\ldots (19)$$

Substituting from Eqs. 18 and 19 into Eq. 3,

$$\frac{p}{\rho} = - g z - \frac{1}{2} A^2 K^2 e^{2 K z} \sin^2 (K c t)$$

$$+ A K c e^{Kz} \cos (K y) \cos (K c t) + f'(t) \quad \ldots\ldots\ldots\ldots\ldots\ldots (20)$$

At the free surface where z equals η and by expanding terms $e^{2 K z}$ and $e^{K z}$ in power series and neglecting high orders in Eqs. 18 and 19 thus

$$\phi = A K c (1 + K \eta) \cos (K y) \cos (K c t) + f'(t) \quad \ldots\ldots\ldots\ldots (21)$$

and

$$q^2 = A^2 K^2 \sin^2 (K c t) \quad \ldots\ldots\ldots\ldots\ldots\ldots\ldots\ldots\ldots (22)$$

and by substituting previous expressions in Eq. 3 for the free surface where $p = O$ and $z = \eta$, therefore

$$O = - \eta - \frac{1}{2} \frac{A^2 K^2}{g} \sin^2 (K c t)$$

$$+ \frac{A K c}{g} (1 + K \eta) \cos (K y) \cos (K c t) + \frac{1}{g} f'(t) \quad \ldots\ldots\ldots\ldots\ldots (23)$$

so that the equation of the free wave surface will be

$$\eta = \frac{A K c}{g} \cos(K y) \cos(K c t)$$

$$+\frac{A K^2 c}{g} \cos(K y) \cos(K c t) - \frac{1}{2} \frac{A^2 K^2}{g} \sin^2(K c t) + \frac{1}{g} f'(t) \ldots . \quad (24)$$

Putting $2 a = A K c/g = A/c$ (since $K = g/c^2$), therefore

$$\eta = 2 a \cos(K y) \cos(K c t) + 2 a K \cos(K y) \cos(K c t)$$

$$- 2 a^2 \frac{g}{c^2} \sin^2(K c t) + \frac{1}{g} f'(t) \ldots \quad (25)$$

In the last expression by equating the elevation of the wave's free surface η to the first term only as a first approximation,

$$\eta = 2a \cos(K y) \cos(K c t) \ldots \quad (26)$$

By substituting from Eq. 26 into Eq. 25, to get a better second approximation,

$$\eta = 2 a \cos(K y) \cos(K c t) + 4 a^2 K \cos(K y) \cos(K c t) \cos(K y) \cos(K c t)$$

$$- 2 a^2 \frac{g}{c^2} \sin^2(K c t) + \frac{1}{g} f'(t) = 2 a \cos(K y) \cos(K c t) + \frac{a^2 g}{c^2} \left[\cos(2 K y)\right.$$

$$\left. + 2 \cos(2 K c t) + \cos(2 K y) \cos(2 K c t)\right] + \frac{1}{g} f'(t) = 2 a \cos(K y) \cos(K c t)$$

$$+ \frac{a^2 g}{c^2} \left[\cos(2 K y) + \cos(2 K y) \cos(2 K c t)\right] \ldots \quad (27)$$

where

$$\frac{a^2 g}{c^2} 2 \cos(2 K c t) + \frac{1}{g} f'(t) = 0 \ldots \quad (28)$$

that is,

$$\frac{1}{g} f'(t) = -2 a^2 K \cos(2 K c t) \ldots \quad (29)$$

THE PRESSURE AND FREE SURFACE EQUATIONS

By substituting Eq. 29 into Eq. 20, the pressure at any point (z, y) at or away from the breakwater and at any instant t is:

$$\frac{p}{\rho g} = -z - 2 a^2 K e^{2 K z} \sin^2(K c t) + 2 a e^{K z} \cos(K y) \cos(K c t)$$

$$- 2 a^2 K \cos(2 K c t)$$

Putting $P = \frac{p}{\rho g}$ leads to

$$P = -z + 2a\,[e^{Kz}\cos(Ky)\cos(Kct) - aKe^{2Kz}\sin^2(Kct) - aK\cos(2Kct)] \quad \ldots\ldots (30)$$

From Eq. 27 the free surface

$$\eta = 2a\cos(Ky)\cos(Kct) + 2a^2K\cos(2Ky)\cos^2(Kct)$$
$$= 2a\,[\cos(Ky)\cos(Kct) + aK\cos(2Ky)\cos^2(Kct)] \quad \ldots\ldots (31)$$

From previous approximations until derivation of the final pressure and surface Eqs. 30 and 31, terms whose amplitude is of order (aK) were retained and higher powers were neglected.

This approximation is then satisfactory if these terms can be neglected numerically.

If $a^2K^2 \leq 0.09$ therefore $aK \leq 0.3$ and since $K = 2\pi/\lambda$ therefore $\frac{2a\pi}{\lambda} \leq 0.3$ or $\frac{2a}{\lambda} \leq 0.3/\pi$ and hence $\frac{\lambda}{2a} \geq \frac{\pi}{0.3} = 10.46$

This means that Eqs. 30 and 31 are applicable for all wave cases where

$$\frac{\text{length of wave}}{\text{height of wave}} = \frac{\lambda}{2a} \geq 10$$

Such limitation is within all practical values.

PRESSURE DISTRIBUTION ON BREAKWATERS (VERTICAL WALL)

The pressure on the breakwater can be obtained by substituting $y = O$ in Eq. 30 for any time t.

$$P = -z + 2a\,[e^{Kz}\cos(Kct) - aKe^{2Kz}\sin^2(Kct) - aK\cos(2Kct)] \quad \ldots\ldots (32)$$

The first term in Eq. 32 represents the hydrostatic pressure, while the second terms represent the hydrodynamic pressure. Thus, hydrodynamic-pressure equations will be:

$$P = 2a\,[e^{Kz}\cos(Kct) - aKe^{2Kz}\sin^2(Kct) - aK\cos(2Kct)] \quad \ldots\ldots (33)$$

where $-\infty < z \leq O$ and

$$P = -z + 2a\,[e^{Kz}\cos(Kct) - aKe^{2Kz}\sin^2(Kct) - aK\cos(aKct)] \quad \ldots\ldots (34)$$

where $O \leq 2 \leq \eta$ and

$$\eta = 2a\cos(Kct) + aK\cos Kct \quad \ldots\ldots (35)$$

It should be noticed that the pressure distribution obtained by Eq. 33 is of great value when $t = O$. This may be examined easily from the value of

cos (K c t) which varies between a minimum of zero for $t = \frac{\pi}{2 K c}$ and a maximum of unity for t = O. Thus, at the breakwater for t = O, the hydrodynamic pressure:

$$P = 2 a (e^{Kz} - a K) \quad \ldots\ldots\ldots\ldots\ldots\ldots \quad (36)$$

where $-\infty < z \leq O$, and

$$P = -z + 2 a (e^{Kz} - a K) \quad \ldots\ldots\ldots\ldots\ldots\ldots \quad (37)$$

where $O \leq z \leq \eta$ and the free surface for t = O

$$\eta = 2 a (1 + a K) \quad \ldots\ldots\ldots\ldots\ldots\ldots \quad (38)$$

In Fig. 2, the distribution of hydrodynamic wave pressure on a breakwater wall is given for a wave 5.0 m high and 75.0 m long at different times t.

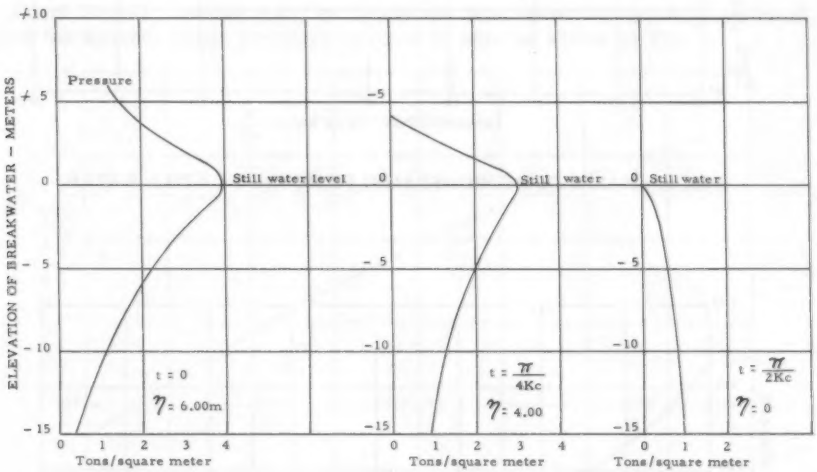

FIG. 2.—HYDRODYNAMIC PRESSURE ON BREAKWATER WALL (FOR A WAVE 5.00 m HIGH AND 75.00 m LONG AT DIFFERENT TIMES t)

PRACTICAL CURVES

Eqs. 36 and 37 give a picture of the distribution of the hydrodynamic pressure at the breakwater when the height of the free surface is limited by Eq. 38.

It may be seen from Eqs. 36 and 37 that the maximum pressure occurs at the mean sea water level, that is, at z = O, and hence:

$$P_{max} = 2 a (1 - a K)$$

and since $K = 2\pi / \lambda$

$$P_{max} = 2 a \left(1 - \frac{2 a \pi}{\lambda}\right) \quad \ldots\ldots\ldots\ldots\ldots\ldots \quad (39)$$

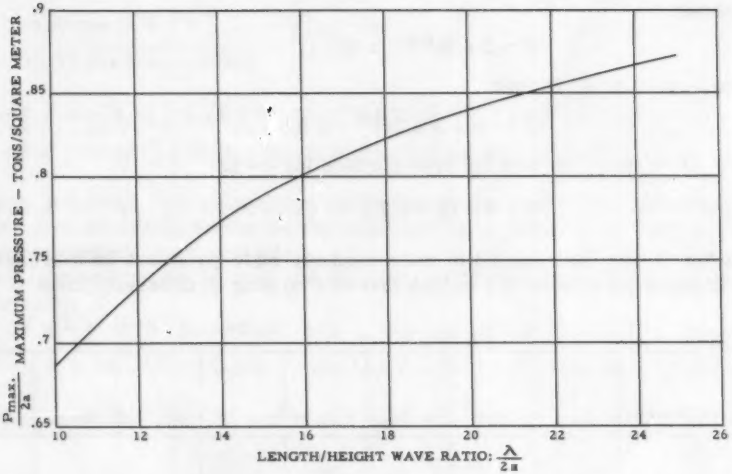

FIG. 3.—MAXIMUM HYDRODYNAMIC PRESSURE AT STILL WATER

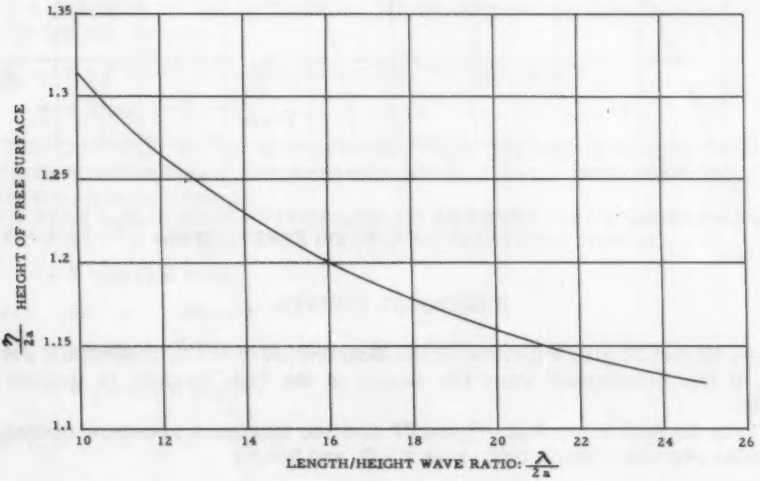

FIG. 4.—HEIGHT OF FREE SURFACE AT BREAKWATER

and

$$\eta = 2a\left(1 + \frac{2a\pi}{\lambda}\right) \quad \ldots\ldots\ldots\ldots\ldots\ldots\ldots\ldots \quad (40)$$

From Eq. 39 and 40, curves may be drawn relating the length/height wave ratio ($\lambda/2a$) to the maximum hydrodynamic pressure at the mean sea water level or to the maximum height of the free surface of the wave at the breakwater as shown in Figs. 3 and 4.

It may be noticed from Eqs. 36 and 37 that the hydrodynamic pressure P will be equal to zero when

$$e^{Kz} = aK$$

or

$$z = \frac{1}{K}\log(aK) = \frac{\lambda}{2\pi}\log\frac{2a\pi}{\lambda} \quad \ldots\ldots\ldots\ldots\ldots \quad (41)$$

From Eq. 41, curves may be drawn to determine the depth of water at which the hydrodynamic pressure is equal to zero as shown in Fig. 5.

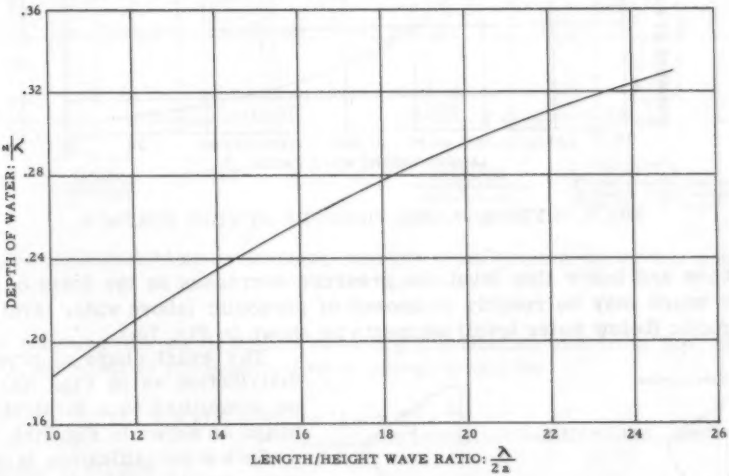

FIG. 5.—DEPTH OF WATER AT ZERO HYDRODYNAMIC WAVE PRESSURE

By substituting the height of the wave at the free surface from Eq. 40 into Eqs. 36 and 37, the value of the pressure will be

$$P_\eta = 2a\left[-\beta + \left(e^{4\pi a\beta/\lambda} - \frac{2a\pi}{\lambda}\right)\right] \quad \ldots\ldots\ldots\ldots \quad (42)$$

where $\beta = \left(1 + \frac{2a\pi}{\lambda}\right)$.

Eq. 42 may be used to plot curves relating the length/height wave ratio to the pressure at the free surface as shown in Fig. 6.

SIMPLE AND PRACTICAL WAVE PRESSURE DISTRIBUTION

The pressure distribution at the breakwater obtained by Eqs. 36 and 37 shows that the maximum pressure of the wave occurs at the mean sea water level in agreement with the results of Luiggi or Cagli.

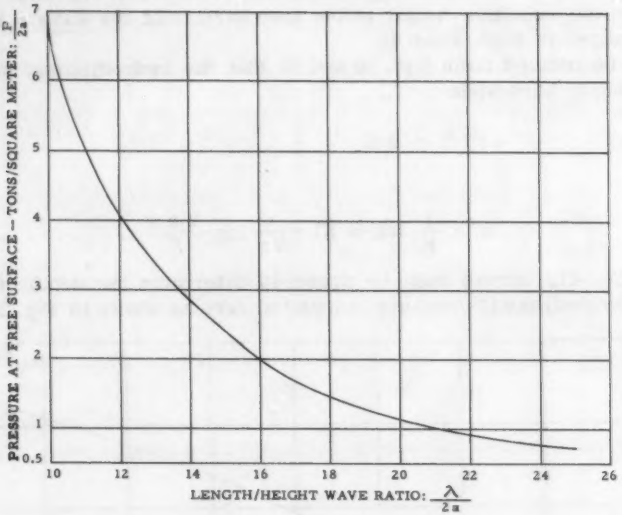

FIG. 6.—HYDRODYNAMIC PRESSURE AT FREE SURFACE

Above and below this level the pressure decreases in the form of some curve which may be roughly composed of parabolic (above water level) and hyperbolic (below water level) segments as shown in Fig. 7(a).

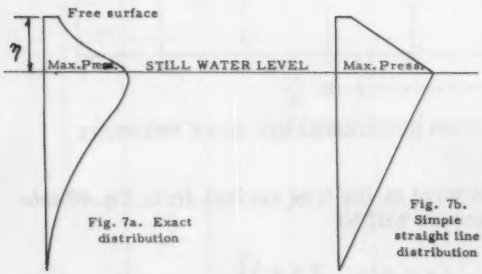

FIG. 7.—DISTRIBUTION OF WAVE PRESSURE AGAINST BREAKWATER

The exact shape of pressure distribution as in Fig. 7(a) may be simplified to a straight line shape as shown in Fig. 7(b).

Such a simplification is much more on the safe side and will give a simple and practical pressure distribution.

By the help of curves on Figs. 3, 4, 5, and 6, the straight-line diagram of pressure distribution may be determined at once for any wave. Considering the case of a wave 5 m high and 110 m long, the pressure distribution according to Luiggi, Cagli, and the writer's exact and simple straight line distributions are shown on Fig. 8.

DETERMINATION OF THE RESULTANT OF WAVE PRESSURE

In the design of breakwaters, it is very important to determine the amount and position of the resultant of wave pressure. Thus, by integrating in Eqs. 36 and 37 with respect to z from $z = -D$ to $z = \eta$ (where D = depth of breakwater), the value of the resultant wave pressure may be evaluated.

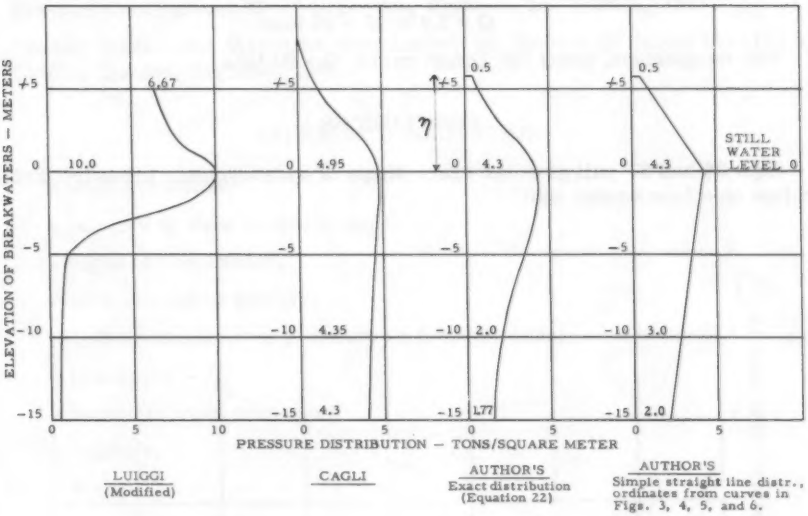

FIG. 8.—HYDRODYNAMIC PRESSURE DISTRIBUTION (FOR A WAVE 5.0 m HIGH AND 110 m LONG)

By adopting the straight-line pressure distribution and from Eqs. 39, 40, and 41, the value of the resultant wave pressure will be

$$Q = 2a(1 - aK)\left[a(1 + aK) + \frac{D}{2}\right] \quad \ldots\ldots\ldots\ldots\ldots\ldots (43)$$

and since $K = 2a\pi/\lambda$

$$Q = 2a\left(1 - \frac{2a\pi}{\lambda}\right)\left[a\left(1 + \frac{2a\pi}{\lambda}\right) + \frac{D}{2}\right] \quad \ldots\ldots\ldots\ldots\ldots\ldots (44)$$

where $D >$ twice wave height.

In case of a deep breakwater where all wave pressure may be assumed acting

$$Q = 2a\left(1 - \frac{2a\pi}{\lambda}\right)\left[a\left(1 + \frac{2a\pi}{\lambda}\right) + \frac{\lambda}{2\pi}\log\frac{2a\pi}{\lambda}\right] \quad \ldots\ldots\ldots\ldots (45)$$

From Eq. 45, a curve may be drawn relating the value of the resultant wave pressure to the length/height wave ratio, as shown in Fig. 9.

Using the example of a wave 5.0 m in height and 110.0 m in length,

$$\frac{\lambda}{2\,a} = \frac{110}{5} = 22$$

From the curve (Fig. 9),

$$\frac{Q}{(2\,a)^2} = 3.4$$

and

$$Q = 3.4 \times 25 = 85 \text{ tons}$$

For comparison, using the Luiggi curve, Q = 90 tons.

CONCLUSIONS

Eqs. 36 and 37 will give the exact shape of hydrodynamic pressure distribution on a breakwater wall.

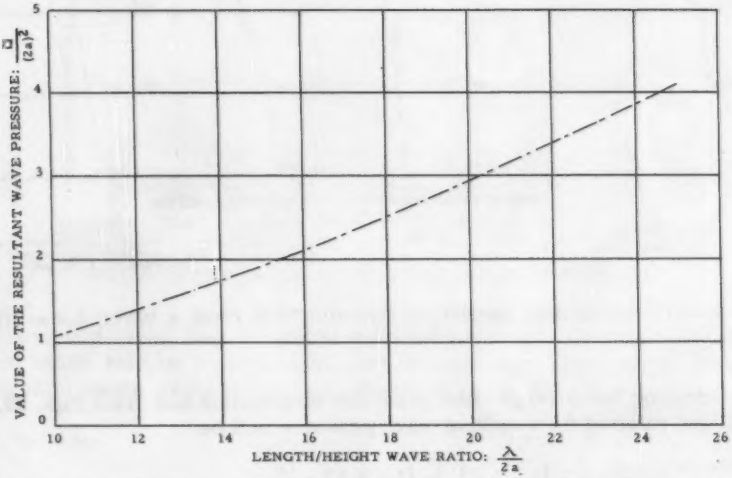

FIG. 9.—VALUE OF THE RESULTANT WAVE PRESSURE

The maximum intensity of pressure is at the still water level. (Values obtained by previous investigators Cagli, Sainflou, and Minikin do not differ much from those given by Eqs. 36 and 37.)

Above and below sea-water level, the intensity of pressure decreases in the form of a curve. (Values given by previous investigators below still water level are greater than those given by Eqs. 36 and 37.)

The maximum pressure distribution on a breakwater will be for time t = 0 (for the period = $2\,\pi / K\,C$).

The pressure distribution depends on the height and length of the wave.

Simple and practical pressure distribution may be obtained by following straight-line pressure diagrams using Figs. 3, 4, 5, and 6.

APPENDIX I.—ADDITIONAL REFERENCES

1. "Hydrodynamics" by Horace Lamb, Cambridge Univ. Press, 6th Edition, 1932.

2. "The Interruption of Surface Waves" by H. Y. Hammad.

3. "A Treatise on the Principles and Practice of Harbour Engineering" by Brysson Cunningham, Griffin, London, England, 3rd Edition, 1928.

4. "Winds Waves and Maritime Structures" by Robert C. Royal Minikin, Griffin, London, England, 1950.

APPENDIX II.—NOTATION

a = wave amplitude;

c = velocity of wave propagation;

D = depth of breakwater;

g = acceleration of gravity;

P = hydrodynamic wave pressure on a breakwater;

p = pressure;

Q = resultant wave pressure;

q = velocity;

t = time;

v = horizontal velocity;

w = vertical velocity;

$\beta = \left(1 + \frac{2\,a\,\pi}{\lambda}\right)$;

η = elevation of free water surface;

λ = wave length;

ρ = density of liquid; and

ϕ = velocity potential:

Journal of the
WATERWAYS AND HARBORS DIVISION
Proceedings of the American Society of Civil Engineers

CANADIAN SECTION OF THE ST. LAWRENCE SEAWAY

By Lawrence H. Burpee,[1] M. ASCE

SYNOPSIS

This paper describes the St. Lawrence Seaway project and summarizes many of the facts relating to the navigation features of the Canadian share of the work. Preliminary facts relating to operation are given.

INTRODUCTION

The Canadian share of the St. Lawrence Seaway project comprises all of the navigation work in the Canadian section of the St. Lawrence River which extends for a distance of 77 miles from Mile 0 at the entrance from the harbor of Montreal to the head of Lake St. Francis, together with several features of the project in the 113-mile International Section of the River upstream from Lake St. Francis to Lake Ontario.

During the past five years (1955-1960), the combined power and navigation development of the River has been completed. Power in the International Section has been developed by The Power Authority of the State of New York and by The Hydro-Electric Power Commission of Ontario, and power in the Canadian section has been developed by the Quebec Hydro-Electric Commission. Navigation works have been constructed by the Corps of Engineers for The Saint Lawrence Seaway Development Corporation (United States), and by The St. Lawrence Seaway Authority (Canada). The comprehensive development of the

Note.—Discussion open until August 1, 1960. To extend the closing date one month, a written request must be filed with the Executive Secretary, ASCE. This paper is part of the copyrighted Journal of the Waterways and Harbors Division, Proceedings of the American Society of Civil Engineers, Vol. 86, No. WW 1, March 1960.

[1] Deputy Chf. Engr., The St. Lawrence Seaway Authority, Montreal, Quebec, Canada.

St. Lawrence River has been a great international project, in which five constructing entities have taken part. The cooperation has been excellent.

Regarding the construction of the navigation works, it was agreed between the United States and Canada in August 1954 that the entire Seaway would be completed and ready for operation by the opening of the 1959 season. Decisions were also made in August 1954 which set the standards to which all of the navigation works would be built.

This paper deals with the parts of the Seaway constructed by Canada.

Fig. 1 shows the St. Lawrence and the Great Lakes Region. Fig. 2 shows the river from Montreal Harbor to Lake Ontario, and on it are shown the areas covered by the work. Fig. 3 is an enlargement of the 48-mile reach of river from Montreal Harbor up to the foot of Lake St. Francis, in which there is a rise of 133 ft, made up of 50 ft in the Lachine Rapids and 83 ft in the Soulanges Rapids. Four of the five Canadian locks are in this reach. The mileages shown on Fig. 3 will serve to locate the various locks and other structures.

The work constructed in the Canadian section of the River includes an 18 $\frac{1}{2}$-mile side canal and two locks to bypass the Lachine Rapids, modifications to the 15-mile Beauharnois Power Canal (Quebec Hydro) and two locks to bypass the Soulanges Rapids, dredging, modifications to or construction of eleven bridges, construction of a four-lane highway tunnel under Lower Beauharnois Lock, and miscellaneous railway, highway, power and municipal relocations.

The work constructed by Canada in the International Section of the River includes the short canal and the lock to bypass the Iroquois Control Dam, part of the dredging, some channel improvements, and a share in the Cornwall-Massena International Bridge.

The cost of the Canadian section of the navigation works, split up into the several areas, is presented in Table 1.

Water Levels.—The water level at the Seaway entrance in Montreal Harbor has varied during the open-water season from an extreme low of 15 ft above mean sea level to a flood stage of 33 ft. The range of water levels on Lake St. Louis (Mile 19-31) has been from 65 ft to 75 ft above mean sea level, with a normal elevation of around 69 ft. The water levels at Montreal and on Lake St. Louis are influenced to a large extent by the wide range of flow of the Ottawa River.

Lake St. Francis (Mile 47-77) has a natural range of level between 149 ft and 154 ft. In 1935, the series of control dams across the four channels at the outlet of Lake St. Francis were completed as features of the Beauharnois Power Development, and the water level of the Lake has, for many years, been generally controlled at a minimum elevation of 152 ft.

The new Lake St. Lawrence, (Mile 87-112) created by the St. Lawrence Power Project, will have a water elevation ranging from 238 ft to 242 ft. The slope in the upstream end of Lake St. Lawrence up to the Control Dam at Iroquois, and from the dam to Lake Ontario, will vary according to the plan for regulation of Lake Ontario levels and outflows established by International Agreements. Lake Ontario will have a controlled range of water level generally between 244 ft and 248 ft.

Channels.—All channels have a minimum depth of 27 ft. The channel below the St. Lambert lock (Mile 3) to Montreal Harbor has a bottom width of 225 ft, which was considered to be the minimum for good operation where ships first enter the Seaway. The bottom width of the channel above St. Lambert Lock and around Laprairie Basin to Côte Ste-Catherine Lock (Mile 12) was adopted at

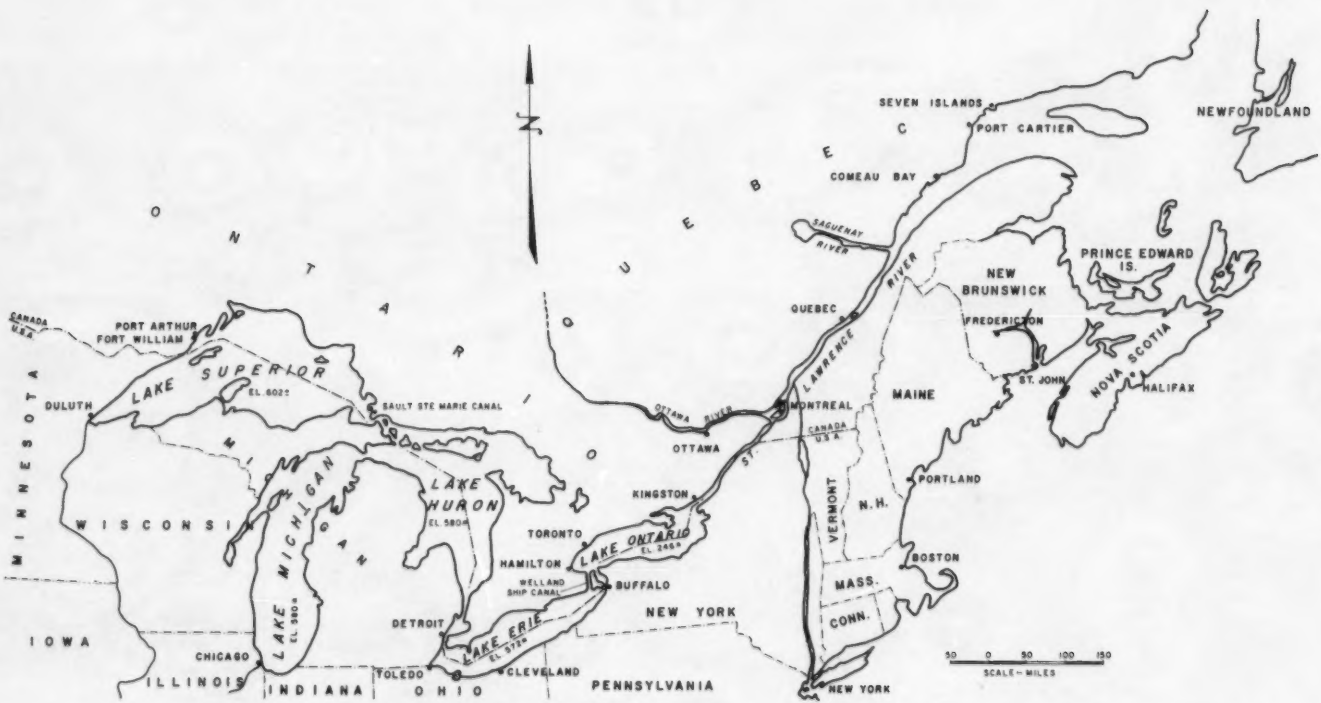

FIG. 1.—ST. LAWRENCE AND GREAT LAKES REGION

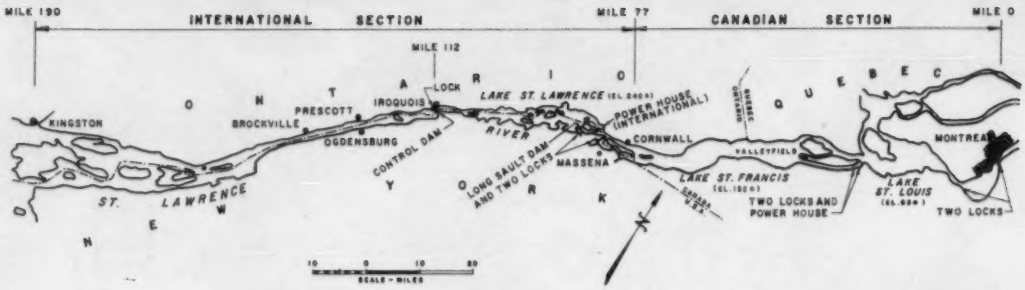

FIG. 2.—MONTREAL TO LAKE ONTARIO

FIG. 3.—MONTREAL TO LAKE ST. FRANCIS

300 ft, which provides an extra width of channel around the long curve. The decision as to the width of this part of the channel was also influenced by the necessity to have adequate materials of suitable types for dike construction. From Côte Ste-Catherine Lock to the canal entrance (Mile 19) at Lake St. Louis the bottom width is 250 ft.

Dredged channels in the 12-mile Lake St. Louis are generally 600-ft wide.

In the Soulanges Section (Mile 31-47) there already existed a 15-mile power canal 3,000-ft wide. In the approval of plans for this power-development work in 1929, the Government of Canada required that it be constructed to standards which would make it available as a part of the future St. Lawrence Seaway. Thus, a 600-ft wide portion of the power canal has been excavated by the Quebec Hydro-Electric Commission which provides the navigation channel.

Dredged channels in the 30-mile Lake St. Francis are generally 450-ft wide.

The navigation channel in the river on the south side of Cornwall Island (Mile 77-81) has been constructed jointly by the United States and by Canada.

TABLE 1.—COST OF CANADIAN NAVIGATION WORK

Item	Cost
Lachine (with two locks)	$145,000,000
Soilanges (with two locks)	55,000,000
Iroquois (with one lock)	20,000,000
Dredging (all areas)	55,000,000
Miscellaneous	25,000,000[a]
Total (not including interest during construction)	$300,000,000[b]

[a] Includes contribution to "Power" of $9,000,000, Head Office building in Cornwall, Cornwall Bridge work, and various other items. [b] This does not include work done on deepening the Welland Canal.

The River has been straightened by excavation of points of land along each shore, and has been deepened by dredging to provide channel depth and to reduce the river velocity from about 8 ft per sec to around 4 ft per sec.

Channels made available for navigation by reason of the International Power Development are in all cases not less than 600 ft.

The short channels below and above Iroquois Lock (Mile 112) are not less than 600-ft wide at the junctions with the channel improvements made by the two power entities.

The Thousand Islands Section extends from Mile 124 to Mile 190 and contained many dangerous shoals. Canadian channel widths have been in general dredged to not less than 580 ft, with about 3 miles at 450 ft. The dredging has been done by United States or Canada depending on which side of the International Boundary the channel lies. The greater part of this dredging was in United States.

Locks.—The locks built by Canada and those built by the United States are of similar basic dimensions, that is to say, 80 ft wide by 765 ft usable length from fender to breast wall, and 30-ft depth of water on the sills at low water level. These are also the dimensions of the eight locks on the Welland Canal.

Table 2 shows the mileages, and summarizes the water level ranges and lifts at the five Canadian locks.

Lock Entrance Walls.—Entrance walls to guide the ships into the locks have been layed out to suit the local site conditions, and have been designed to provide tie-up space for ships waiting to enter the locks. The objective has been to design all entrance walls to get all types of ships into the respective locks with a minimum of lost time.

Fig. 4 is a plan showing the five Canadian locks with the arrangements and dimensions of the entrance walls at each.

GENERAL LAYOUT AND CONSTRUCTION FEATURES

Lachine Section.—Over 50% of the Canadian construction work and dredging was in the immediate area of Montreal. This section has been constructed as a Seaway Project only, but with all structures located to avoid interference

TABLE 2

Lock	Miles from Montreal	Water Level Range, Above Mean Sea Level		Approximate normal lift, in feet	Possible Limit of Lift, in Feet	
		Below lock	Above lock		Minimum	Maximum
Iroquois	112	237.5 to 244	238 to 246	$\frac{1}{2}$ to 2	$\frac{1}{4}$	18[a] 6[b]
Upper Beauharnois	32.5	108 to 112	149 to 154	41	39	44
Lower Beauharnois	31.5	68 to 75	108 to 112	41	35	45
Cote Ste-Catherine	12	35 to 38	65 to 75	35	30	40
St. Lambert	3	15 to 33	35 to 38	15 to 20	2	23

[a] During construction only, and only for 14-ft draft vessels. [b] A possible extreme condition with high level on Lake Ontario, low controlled outflow from Lake Ontario, and a low controlled operating level at the power house forelay.

with a future development of the power from the 50 ft of head in this reach. The principal features of this part of the work are shown in Fig. 3. The 18.5 miles of canal from Montreal Harbor to Lake St. Louis required the excavation in the dry of 19,000,000 cu yd of common material and over 20,000,000 cu yd of rock. The two locks required a total of 870,000 cu yd of concrete. The connecting dikes required 9,000,000 cu yd of fill. In addition, a total of over 7,000,000 cu yd have been excavated by dredging at Montreal Harbor and in Lake St. Louis. The canal and its two locks were constructed by ten main contracts, two of which covered the St. Lambert and Côte Ste-Catherine Locks with adjacent parts of the channel and dike. The other eight contracts made up the remaining 15 $\frac{1}{2}$ miles of channels and dikes.

Early plans for the work in this section dating from 1920 up to nearly 1950 were all based on a side canal located on the north side of the river. The continued expansion in recent years of Greater Montreal with its harbor and railway developments made it necessary to construct the Seaway on the South Shore.

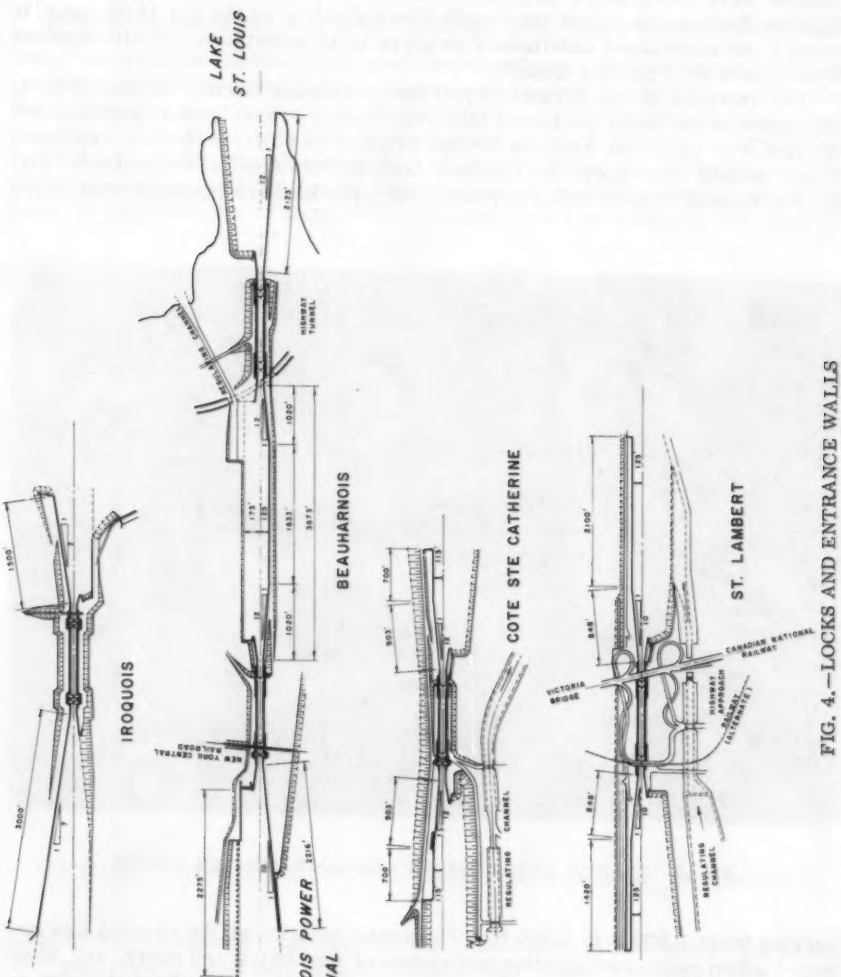

FIG. 4.—LOCKS AND ENTRANCE WALLS

The length of the canal became 18 $\frac{1}{2}$ miles, instead of 12 miles for the north-side site, but the problems of construction and coordination with existing facilities were much more practical and less costly. The new works in the Lachine Section are called the "South Shore Canal", as the old 14-ft canal is going to be maintained indefinitely to serve local industries. It will continue to be called the "Lachine Canal".

The entrance to the Seaway is just below Jacques Cartier Bridge (Fig. 5) and opposite the upper portion of Montreal Harbor. Three miles upstream are St. Lambert Lock and Victoria Bridge (Figs. 6 and 7). An 8-mile regulated reach extends from above St. Lambert Lock to Côte Ste-Catherine Lock (Fig. 8). The Seaway channel follows around Laprairie Basin at distances from shore

FIG. 5.—SEAWAY ENTRANCE AND JACQUES CARTIER BRIDGE

varying from 1,000 ft to 2,500 ft. The actual location of the channel was selected after many comparative estimates of quantities and costs, and after many studies of suitable navigation alignment. From Côte Ste-Catherine to Caughnawaga the canal had to be located inshore, thus providing sufficient space between the Seaway and the river shore for a future enlargement of the river cross section by Quebec Hydro for the Lachine power development. Four miles above Côte Ste-Catherine Lock are the Honore Mercier and Canadian Pacific Railway bridges (Fig. 9). Two and a half more miles of canal lead to deep water in Lake St. Louis. From just west of the Canadian Pacific Railway and around Caughnawaga village, (an Indian Reserve), the channel has again been located in the river. The cost would have been prohibitive and the number of persons displaced would have been too great to have constructed the channel overland

through the town. It was important to keep the restriction of the river to a minimum, to avoid affecting the water level of Lake St. Louis, and the channel therefore follows close to the shoreline.

Thirteen miles of the 18 $\frac{1}{2}$-mile canal has been constructed in the former bed of the river and the construction of the cofferdams was a major construction problem and a large item of cost. Of the ten contracts for this canal, only the three extending for 4 miles from above Côte Ste-Catherine lock to a little beyond the C.P.R. embankment were constructed on land. The six contracts below Côte Ste-Catherine were entirely constructed in the bed of the river. The cofferdams throughout this part of the work were made of materials obtained from the excavations. The contract covering over 2 miles along the river at

FIG. 6.—ST. LAMBERT LOCK AND VICTORIA BRIDGE DURING CONSTRUCTION

Caughnawaga required large cofferdams constructed in fast water, for which the major part consisted of rockfilled timber cribs with steel sheet pile sheathing.

The topography of the Lachine Section required two locks to provide the lift from Montreal Harbor to Lake St. Louis with the lower lock near the City of St. Lambert, opposite Montreal, and the upper lock near the foot of the Lachine Rapids. It was impractical to split the lift into equal parts and make the two locks similar. The selected location of St. Lambert Lock immediately upstream from Victoria Bridge made possible an arrangement for uninterrupted highway and railway traffic by the use of duplicate bridges. Côte Ste-Catherine Lock was located for the most economical layout of channels and dikes.

St. Lambert and Côte Ste-Catherine Locks are both located in an area where the foundations are shale. These two locks have therefore been constructed with complete concrete floors and with the side walls designed as full gravity structures. The floor slab is nominally 3 ft thick, but is generally more due to the shale breaking along its bedding plains. Rock anchors have been used to overcome the full uplift under the slab. Fig. 10 shows the plan and cross section of the Côte Ste-Catherine Lock. St. Lambert Lock is generally similar except for the height of lift. At each of these two locks, the north wall has been designed as a gravity dam with full water level in the lock and excavated on the

FIG. 7.—ST. LAMBERT LOCK AND VICTORIA BRIDGE

outside, a condition which would occur during the period of the future twinning of the locks.

The St. Lambert and Côte Ste-Catherine locks are located in a continuous confined channel with limited space available. Consequently, the entrance walls have been constructed with the mooring portion of the wall built parallel to the canal. St. Lambert Lock has a much longer downstream wall to accommodate incoming ships.

Construction of St. Lambert Lock.—The St. Lambert Lock is located just upstream of Victoria Bridge and in the former bed of the river. The first step was the construction of a large cofferdam to unwater an area of about 150 acres.

This cofferdam had a length of approximately 1 mile parallel to the river with connections to the shore at each end. The part parallel to the river was constructed to the full section and quality required for the permanent dike of which it later became a part, which was necessary to meet winter ice conditions. The upstream shore connection was of similar construction. The downstream shore connection was of a somewhat lighter construction as no ice shoves were possible. As the schedule of lock construction required uninterrupted work throughout two winters, it was necessary to construct the cofferdam to an elevation which would make it safe against overtopping by floods caused by ice jams.

FIG. 8.—COTE STE-CATHERINE LOCK (LOOKING DOWNSTREAM)

This cofferdam was therefore constructed to El. 49, to take a 20-ft rise of water level above summer stages.

The whole cofferdam in the St. Lambert Lock area was constructed during the fall of 1955 in advance of the awarding of the general lock contract, and was turned over to the lock contractor in an unwatered condition, ready for the start of excavation. The total construction time available to the general lock contractor was 32 months (January 1956 to August 1958).

All blasting had to be conducted under very strict regulations, particularly as the excavation approached close to and under Victoria Bridge. Highway traffic on this bridge, (up to 2,000 cars per hr), had to be interrupted for every blast.

The contractor was allowed 8 months in which to advance the excavation and to start on concrete. Good production performance was made by the contractor and concrete was completed during 1957, reaching a peak rate of over 70,000 cu yd per month. St. Lambert Lock and entrance walls has a total concrete quantity of 490,000 cu yd.

The construction procedure for the strengthening and enlarging of the south abutment and the adjacent pier of Victoria Bridge was one of the most critical problems of the job. The piers of this bridge are stone masonry and were constructed over 90 yr ago, and are founded on shale, therefore it was necessary to take extreme precautions to avoid any damage. The excavation for the lock required going about 40 ft below the elevation of the river bottom shale on

FIG. 9.—THE HONORE MERCIER AND CANADIAN PACIFIC RAILWAY BRIDGES (MILE 16)

which the piers were founded. The first operation was the excavation of a 100-ft wide cut to grade for a distance of over 200 ft along the centerline of the lock under the bridge. The next step was the excavation of a lateral trench in shale to grade through to the abutment on the one side of the lock and to the pier on the other side of the lock. A 12-ft section of the lock structure was then constructed as a buttress against the rock underlying the pier and the south abutment. In a series of seven steps the shale was excavated up to the backline of the concrete in 12-ft trenches, and was followed after each excavation step by the construction of another 12-ft block of concrete. The whole operation of constructing the portion of the lock about 100 ft along the bridge pier and along the south abutment required a total time of almost 1 year. It was not until this

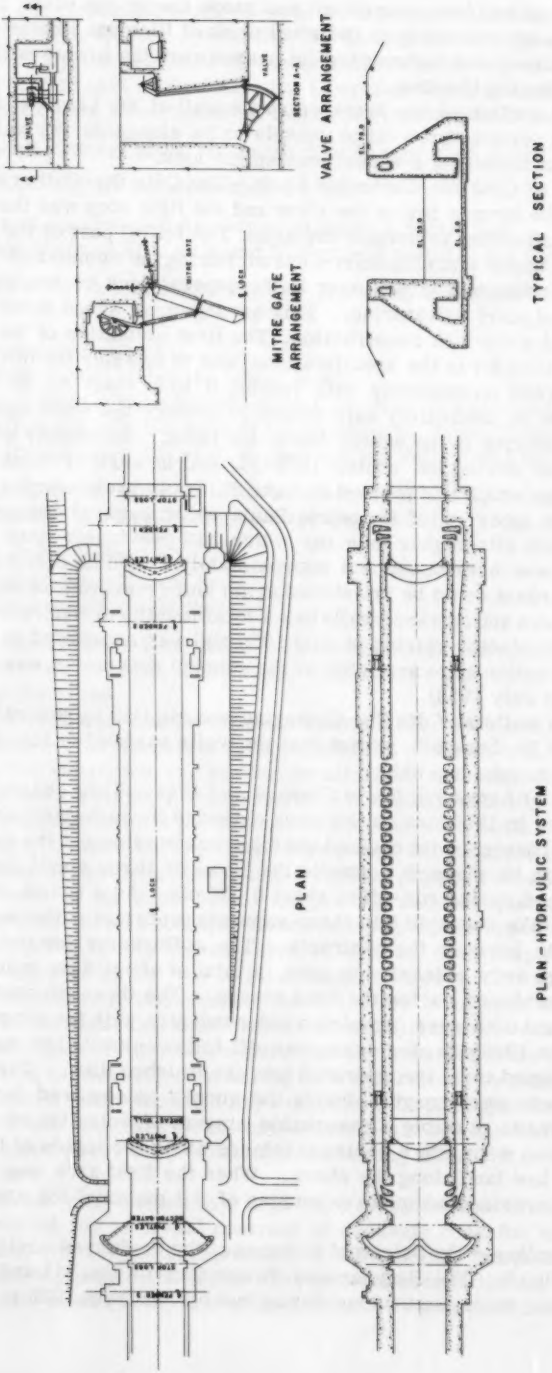

FIG. 10.—COTE STE-CATHERINE LOCK

portion of the lock had been completed and made the bridge piers completely safe that any change was made in the steel work of Victoria Bridge. All during this time, railway and highway traffic passed over the bridge without interruption, except during blasting.

The mooring portion of the lower entrance wall at St. Lambert is 2,100 ft long, which will permit three large vessels to lie alongside the wall awaiting entrance, without hindering a vessel leaving the lock.

Construction of Côte Ste-Catherine Lock.—The Côte Ste-Catherine Lock is also located in the former bed of the river and the first step was the construction of a large cofferdam to unwater the area. The initial part of the cofferdam was constructed under a preliminary contract during the summer of 1955. This initial low cofferdam was turned over to the general lock contractor ready to set up pumps and start unwatering. This arrangement saved about 4 months in overall time for the lock construction. The first obligation of the lock contractor, as provided for in the specifications, was to unwater the initial cofferdam and to proceed immediately with raising it to at least El. 50 which was considered to be an adequately safe height to protect the work against high-water-level conditions in the winter due to ice jams. Extremely severe conditions did occur during the winter 1955-56, and in early February a large amount of the ice which had formed in Lake St. Louis broke away and formed an ice jam at the upper end of Laprairie Basin, which created water-level conditions at the lock site higher than any which had previously been recorded. The cofferdam was overtopped and approximately 2 months of time was lost before the cofferdam could be unwatered again and excavation resumed. Côte Ste-Catherine Lock and entrance walls has a total quantity of concrete of 380,000 cu yd. Concrete placing started in July 1956 and was completed in July 1958. The total construction time available to the general contractor was 34 months (October 1955 to July 1958).

The entrance walls at Côte Ste-Catherine are similar in general arrangement to those at St. Lambert, except that the walls parallel to the channel are only 700 ft long to take one ship.

Construction of Laprairie Basin Channel and Dike.—This channel and dike work was started in 1955, and as the work extended through parts of four seasons, the general design of the channel and dike construction and the contractor's operations had to be planned to handle the flows of three small local rivers having a combined spring run-off of about 6,000 cfs. As a result, this part of the channel and dike was split into three separate contracts with specified gaps left at two points between the contracts. The cofferdams for the Laprairie Basin work were very extensive in area, a total of about 4 sq miles of river bottom being unwatered during the final stages. The three separate sections of the channel and dike were completed independently, with the closures at the two gaps made in 1958 after the spring run-off had occurred. The main cofferdams were designed to be incorporated into the finished dike. The quantities of excavation here were roughly double the quantities required for dike construction, and made possible a reasonable amount of selection of materials. Excess excavation went into a series of islands along the inside of the channel and to reclaim low land along the shore. When the first area was unwatered during 1955, it provided adequate quantities of fill material for extending the cofferdams.

Soulanges Section.—The principal features of the Soulanges part of the work are shown on Fig. 3. The Beauharnois Power Canal (Fig. 11) and the initial power installation were constructed during the period from 1929 to 1932. The

project was developed and financed by private power interests, but was subsequently acquired by Quebec Hydro Electric Commission. Approval of the work was dependent on the provision of many features which would make the canal suitable for use as part of the future St. Lawrence Seaway. Among the requirements set out by the Government at that time were the following:

1. A 600-ft channel along the north dike having 27-ft depth;
2. A mean velocity not exceeding $2\frac{1}{4}$ fps;
3. Space to be provided for future navigation locks; and
4. Bridge piers at St. Louis and Valleyfield suitable for future lift spans.

The work done in this section by the Authority to complete the Seaway included:

a. Construction of locks;
b. Highway tunnel under the lower lock;
c. Swing bridge across the upper lock for New York Central Railroad;
d. Construction of a lift span in the existing St. Louis Bridge; and
e. Construction of a lift span in the existing Valleyfield Bridge.

Consideration was given to three alternates for the 82-ft (normal) lift from Lake St. Louis to the Beauharnois Power Canal:

(1) Twin flight locks;
(2) A single high lift lock; and
(3) Two separated single locks.

The third alternative with two locks was adopted as the most desirable from the points of view of costs, reliability, uniformity of all locks and equipment, and construction time.

The lower lock was located to obtain minimum overall costs considering the variable factors of cofferdams, rock excavation, and concrete. After a series of comparative estimates, and setting the minimum desirable distance between the locks at around 3,600 ft, the position of the lower lock was fixed.

A main highway follows the south shore of Lake St. Louis, which required maintenance of traffic during construction and uninterrupted flow of traffic after the Seaway had been completed. The old highway crossed the work at about the center of the lower lock. To provide uninterrupted traffic, a four-lane twin-tube tunnel was constructed under the upstream approach to the lower lock. By completing this highway diversion as the first step in construction, traffic was kept out of the way of all subsequent work. The tunnel itself has no unusual features. It was constructed in the dry in an open cut. The stratified nature of the sandstone rock created some difficulties in sealing the tunnel.

The greater part of the lower approach excavation was made inside a cofferdam, the extent of the cofferdam having been determined by the estimated comparative costs of cofferdams and dry excavation of rock against costs of dredging rock. It was decided that the cofferdam would be constructed out into the lake to the point where rock excavation exceeding about 7 ft in depth would be done in the dry.

This lock was constructed in a total time of 32 months, of which the first 4 months provided for an initial contract to excavate rock for the highway diversion tunnel and for the construction of the Lake St. Louis cofferdam using rock from the highway excavation. The general contractor for the lock excavated 1,200,000 cu yd of rock and placed 390,000 cu yd of concrete in 28 months.

To provide the entrance to Lower Beauharnois from Lake St. Louis, it was desirable to have as broad an opening as possible for ships to enter the protected approach area. Consequently, the wall for this entrance extends in a straight line for a little over 2,100 ft on a flare of 1:12. At the outer end of the entrance wall, the water in Lake St. Louis is over 50 ft in depth. This part of the wall consists of twelve reinforced concrete cribs, each 115 ft long, founded on a prepared base of heavy rockfill. The tops of the cribs were designed to be just above normal water level, which provided for an 8-ft cast-in-place concrete coping on top of the cribs.

The pool between the two Beauharnois locks has a continuous wall along the south side.

The New York Central Railroad crosses the Beauharnois Power Canal on a 3,000-ft long bridge. It was desirable to locate the upper lock either just above

FIG. 11.—BEAUHARNOIS POWER CANAL QUEBEC HYDRO POWER DEVELOPMENT (2,2000,000 HP) AND THE TWO BEAUHARNOIS LOCKS

or just below the existing New York Central Railroad crossing, in order to use a movable railroad span with an 80-ft gap, as compared to a much longer span if the bridge were separated from the lock. It was decided to locate the lock below the bridge for the following reasons:

(a) A longer entrance channel from the power canal, and therefore a greater distance in which ships can reduce speed;

(b) Reduced effect of any interference between trains and ships. Ships will always be able to pass between the upper and lower locks; and

(c) Lower cost.

One of the site problems was the maintenance of railway traffic during the construction of the lock and bridge. A work program using two stages of diversion was adopted. The first diversion permitted the construction of a short

length of lock walls at the location of the existing railway. The second diversion crossed the completed lock walls section, just clear of the future swing bridge. This permitted the remainder of the lock excavation and concrete to proceed with no further hindrance from the railroad.

This lock was constructed in a total time of 29 months. The major quantities included 1,000,000 cu yd of common excavation, 1,400,000 cu yd of rock excavation and 330,000 cu yd of concrete.

The entrance to Upper Beauharnois Lock from the power canal required that no serious obstruction be imposed on the flow to the existing power house. The south wall for this entrance extends for a little over 2,200 ft in a straight line on a flare of 1:10. Because of the current in the power canal, and the long distance from a good anchorage, a 2,200-ft snubbing wharf has been constructed along the north side of the entrance to the lock. This is long enough to accommodate two large vessels awaiting entrance to the lock.

A major problem of construction for the two Beauharnois locks related to the large amount of work going on at one time by The Seaway Authority and by Quebec Hydro. A total of over 4,000,000 cu yd of hard sandstone rock was excavated by four contractors (three for the Authority and one for Quebec-Hydro) in the one congested area. The problem was made more difficult by the many existing high tension transmission lines which had to be protected and relocated.

Canal and Lock at Iroquois (Fig. 12).—This lock by-passes the Control Dam constructed by the New York State Power Authority. One of the many features of cooperation between power and navigation was the necessity to complete the Iroquois Lock in early 1958 to permit the abandonment of parts of the existing 14-ft canal in order to permit the flooding of the new power pool.

A 3,000-ft entrance wall has been constructed above the lock in order to provide a safe mooring place for at least three large downbound vessels. A 1,500-ft wall has been constructed for the downstream entrance.

There were no particular construction problems at Iroquois other than the excavation of 4,500,000 cu yd of dense glacial till and the placing of 320,000 cu yd of concrete.

Hydraulic Design of Locks.—Iroquois Lock is filled and emptied by the operation of the main lock gates (sector type).

The four downstream Canadian locks have all been constructed with side culverts and lateral ports, with the flow for filling and emptying controlled by sector-type valves at the upstream and downstream ends of the culverts. The valves (12 ft by 14 ft) are identical for all locks, and the culverts and ports have essentially similar cross-sectional areas. The actual culvert shapes and the size and number of lateral ports have been varied to suit the structural shape of the different lock walls. The hydraulic details were developed by use of a 1/30 scale model.

At St. Lambert and Côte Ste-Catherine, the lock walls are complete gravity structures built on excavated shale foundations. The culverts are 16 ft 6 in. wide at the base by 20 ft. 0 in. high. The culvert is shaped as shown on Fig. 10. There are twenty lateral ports in each wall located in the middle 400-ft length of the lock. The ports are all 2 ft 7 in. wide by 3 ft 7 in. high.

At the two Beauharnois locks, the walls have been constructed in sound durable sandstone and the wall thickness has been governed mainly by the space requirements for the culverts. To maintain essentially similar hydraulic characteristics as for Côte Ste-Catherine and St. Lambert, the culverts at Beauharnois have been made narrower and higher. The concrete wall separating the culvert from the lock chamber has also been made narrower here.

The culverts are 13 ft 6 in. wide at the base by 25 ft 0 in. high. There are forty lateral ports in each wall located in the middle 400-ft length of the lock. The ports are 1 ft 3 $\frac{1}{2}$ in. wide by 3 ft 6 in. high.

Table 3 shows some of the dimensional characteristics of the lock hydraulic systems. All figures relate to one wall. The other wall is similar.

Under the maximum head and discharge valves full open conditions at Beauharnois, the flow in each culvert will be around 6,000 cfs.

FIG. 12.—IROQUOIS LOCK AND IROQUOIS CONTROL DAM

The calculated operating times for the Beauharnois locks, based on the hydraulic model tests were:

Fill	6.5 min
Empty	7.3 min

Actual operating results have shown that for a 41-ft lift, and with a valve movement time of 2 min (fill) and of 1 min (empty) the possible times are approximately:

Fill	6.5 min
Empty	6 min

The operating times for the other locks are less, and are roughly proportional to the head.

Up to the present time (1960), for precautionary reasons, the locks have been operated to fill and empty in times varying from 6 min to 12 min while operators are becoming familiar with the hydraulic characteristics.

LOCK EQUIPMENT

Canadian policy for the Seaway construction has been to provide all equipment under "supply and erect" contracts, separated from the general construction contracts. Equipment contracts providing uniform equipment for the locks have included: miter gates, sector gates, gate operating machinery (similar for miter and sector gates), valves, valve machinery, fenders, stoplogs, stiffleg derricks for stoplogs, de-watering pumps, line haulers, and diesel generator units.

Electrical equipment has been generally standardized throughout all locks. The motors for all of the gates and for all of the valves and the fenders are of the same size and characteristics. All of these motors were purchased under one contract.

TABLE 3.—AREAS, IN SQUARE FEET, OF LOCK HYDRAULIC SYSTEMS

Item	St. Lambert and Cote Ste-Catherine	Lower and Upper Beauharnois
Inlet area	504	504
Area at valve	168	168
Culvert	300	305
Lateral ports (each)	9.25	4.5
Total port area	185	180
Discharge area	427	435

Miter Gates.—A miter gate consists of two horizontally framed leaves which, when closed, form a three-hinged arch against the hydrostatic load. All miter-gate leaves are approximately 5 ft thick and 46 ft wide. The gate leaf in the closed position is at an angle of 1 in 3 to the face of the lock.

The horizontal girders in a leaf terminate at each of the vertical leaf edges in the quoin and miter posts. The quoin post forms the edge next to the lock wall. The miter post forms the edge next to the lock center line when the leaf is in a closed position. The bottom hinges on which the gate leaves turn, are pintles, identical in every case, of 21-in. diameter. The upper hinges are of a simple pin type and are also identical in every case. Each leaf has a skin plate on the upstream side only, the other side being left open for economy and ease of maintenance, but has adjustable diagonal members. The adjustable diagonal members when prestressed give the gate leaf its required additional stiffness for operation. All lock gates are poly-vinyl coated for protection against corrosion.

The pintle assembly consists of a heel casting, which is attached by means of tuned bolts to the bottom of a gate leaf at the quoin end, a phosphor bronze bushing inserted in the heel casting, a nickel steel hemispherical pintle on

which the bronze bushing bears and a base casting embedded in concrete which supports the pintle and gate leaf.

The miter gates have been designed to withstand the hydrostatic loads and to be operated against a differential head of 0.50 ft. The dead-load forces are those which result from the weights of the gates.

The gates are operated by a horizontal sector gear with a strut attached near the top of the gate. The machine is designed to exert a thrust of 1,480 ft-kips through a spring-loaded strut. The gate machine arrangement is shown in Fig. 10. The motors are wound-rotor type of 20 hp.

Gate machines are identical for all gates (miter and sector). Thirty-four gate machines were supplied under one contract.

The gates are of welded construction, in vertical sections from 12 ft to 14 ft. The field connections are bolted with high tensile bolts.

The normal time for opening or closing a miter gate is approximately 2 min. Miter gates installed at the downstream end of a lock may be subjected, at times, to a severe back surge either from dumping the lock, or from ship propellers if the gates are being closed immediately after a downbound vessel leaves the lock. Provision has been made to release such a gate from the operating machine if the force due to the back surge exceeds a strut load of 140,000 lb plus or minus 10%, when the gate is near the mitering position. Release is accomplished by the shearing of pins in the gate machinery.

Table 4 shows the miter gate installation at each of the locks.

TABLE 4

Lock	Upper End	Lower End
St. Lambert	1 pair 1 pair (space non-operating)	2 pairs
Cote Ste-Catherine	1 pair	1 pair 1 pair (spares non-operating)
Lower Beauharnois	2 pairs	2 pairs
Upper Beauharnois	1 pair	1 pair
Iroquois	none	none

The weights of the individual gate leaves are:

All upper gates	- 132 tons
St. Lambert Lower Gates	- 175 tons
Côte Ste-Catherine Lower Gates	- 238 tons
Beauharnois Lower Gates	- 258 tons

A floating gate lifter having a lift capacity of 300 tons is being designed. If a gate should be damaged before the delivery of the lifter, and this is a calculated risk, temporary rigging will be required.

Sector Gates.—Each sector gate consists of two vertical sectorial prisms. The radius of each sector is 48.7 ft, with a 43° angle included between its radial members and having a height of about 43 ft. The sector framing consists of

seven horizontal structural steel sector frames. The skin plate on the outer faces of the curved steel girders forms the curved vertical face of the prism. The outer faces of the radial horizontal frames form the two vertical faces of the prism. The two outer vertical edges of the curved face extend approximately 8 ft beyond each radial vertical face. The two radial faces of each sector are of open framing with vertical and horizontal members, except for the ice guard gratings, the diagonal braces and the plate girders at the bottom of these faces. A vertical girder of V-section extends the full height of gate from heel casting to top anchorage. This girder transfers all the water load to pintle and top bearing. The heel casting is fitted with a bronze bushing which turns on a nickel steel 30-in. diameter pintle. The pintle is set in a base casting which in turn is connected to an anchorage which extends back into the concrete monolith.

The weight of each sector is supported at three main points—on a pintle beneath the junction of the two radial faces and on the two roller trucks which are beneath the outer ends of the radial faces. The rollers travel on a curved steel track and are close to the skin plate. In addition to the three main points of support there is a hinge at the top of each sector, directly above the pintle. The top hinge and the pintle have embedded anchorages which are designed to withstand the entire horizontal loads.

The sector gates are operated by operating machines identical with those provided for the miter gates. The weight of each sector is 246 tons.

Iroquois Lock has four pairs of sector gates, two pairs at each end, Upper Beauharnois has one pair, and Côte Ste-Catherine has one pair. At Iroquois the four pairs of gates are completely equipped with operating machinery so that, in case of one gate being damaged, the adjacent pair can be immediately brought into use. They serve as lock-operating gates and also as the means of filling and emptying the lock. For a three-month period during construction of the power project, it was necessary to operate these Iroquois sector gates under a head of 18 ft. The operation under those head conditions was smooth and uneventful with a filling flow of around 3,000 cfs. Permanent operating conditions will be under a head range of from $\frac{1}{2}$ ft to 2 ft and occasionally a head of up to 6 ft.

The sector gates at Upper Beauharnois and Côte Ste-Catherine have been provided as emergency gates, which can be closed against a flow of water in case of any accident to the downstream miter gates. All sector gates have been designed for a hydrostatic head of 40 ft, which can occur at Upper Beauharnois or at Côte Ste-Catherine with the upper miter gates open and the lock at its low water level. The regulations established for operating procedure require that the operator starts closing the sector gates promptly after the stern of a downbound ship passes these gates. If a ship should crash through the fender and knock out the downstream gate, the damage would be limited to the gate, the fender, and the vessel. The water suddenly released would be little more than the volume contained in the lock, as the sector gate would quickly close off the flow at the upper end of the lock.

Lock Valves.—The sixteen filling and emptying valves for the four locks (excluding Iroquois) are identical and interchangeable except for the operating strut arms. All valves were supplied and erected under one contract. The weight of one valve is 25 tons. The valves are 12 ft wide by 14 ft high and can be opened or closed in 1 min. The bottom seal is steel on babbit. The side and lintel seals are rubber. Each valve is set in a well extending down from the

coping, large enough so that a complete valve can be removed and replaced in case of a breakdown. Two spare valves are on hand.

Fig. 10 shows the general arrangement of a valve and its operating machine. The strut arm has a spring mounting having a total compression of 8 in. The strut arm and machine can exert a pull of 166,000 lb. The motors are 20 hp.

Wire Rope Fenders.—Wire rope fenders are installed on each side of the lower lock gates for the purpose of protection against ships which have travelled beyond the prescribed limit. Fenders are also installed upstream from the upper gates at all locks, and downstream from the upper gates at St. Lambert and Iroquois. At the other three locks, the breastwall protects the downstream side of the upper gates. If a ship hits the fender its bow will come in contact with a three-part double system of $1\frac{3}{4}$-in. diameter wire ropes stretched across the lock. These ropes are reeved through sheaves anchored to bollards encased in the lock wall. As the ship continues to advance the ropes unwind from two drums against four friction brakes gear-connected to the drums, thus maintaining a steady rope pull. The kinetic energy from the moving ship is dissipated through the ropes sliding across and along the bow, over a friction bollard just ahead of the drum, and through the drum brakes. The fenders have been designed to absorb the energy of a ship weighing 40,000 tons moving at a speed of 3 mph through a distance of 68 ft.

Two types of machine elements comprise the complete fender machinery. The exposed machine elements, the sheaves, the boom, the bascule, the boom latch, the bascule frame with driving screws, the bollards, and that portion of the rope which stretches across the lock, are outside on top of the lock walls. The housed machinery elements, the rope drums with brakes, the rewinding and brake scouring machine and the bascule drive unit are inside in a machine room within the lock wall.

Stoplogs.—Any of the five Canadian locks can be completely unwatered in case of emergency or for maintenance by placing the stoplogs which are provided at each end of all locks. There are two types of steel stoplogs (80-ft clear span) standard for all locks, and a third type required for the lower end of St. Lambert only. They are all of approximately the same weight, a little over 30 tons, but vary in height and strength to suit the range of head conditions. All stoplogs have two rollers at each end to permit placing in flowing water. The stoplog gains are located at the ends of the lock to permit unwatering of the entire lock area in which all of the operating equipment is located. The stoplogs are not heated and require a portable steam generator for winter handling.

Permanently installed stiff-leg derricks at each end of all locks place and remove the logs. The derricks are rated at 55 tons at 55-ft radius and have 75-hp motors.

The heights, weights and distribution of the three types of logs are shown in Table 5.

Unwatering Pumps.—Each lock can be dewatered within an interval of from 15 hr to 18 hr by means of the permanent pumping installations. St. Lambert, Cote Ste-Catherine, Lower Beauharnois and Iroquois Locks are each equipped with two vertical 24-in. propeller type pumps capable of discharging an average total of around 40,000 gpm. Upper Beauharnois Lock has no dewatering pumps, but can be drained by gravity through the lower lock. All eight pumps are similar except for the length of the riser and shaft, and they were purchased and erected under one contract. They are driven by 250-hp motors.

Line Haulers.—The four locks (excluding Iroquois) have line haulers spaced along the side of the lock wall on which the ship is moored. These line haulers are provided to facilitate the handling of wire ropes from the ship up to the coping and are particularly important for upbound ships where the height from the deck of the ship up to the coping is of the order of 40 ft.

Power Supply.—The main power supply at all locks is furnished by the public utility in the area. At. St. Lambert, Côte Ste-Catherine and Iroquois locks, and at all of the lift bridges, there are individual diesel electric units for use in cases of emergency. The size of the diesel electric units at the locks is 300 kva.

TABLE 5.—STOPLOGS

(a) Types

Type	Height of log	Design head, in feet	Remarks
A	3 ft 8-7/8 in.	43	Bottom group, all except lower end of St. Lambert
B	4 ft 10-1/4 in.	24	Top group, all locks
C	3 ft 8-7/8 in.	59	For lower end of St. Lambert only, using high-tensile steel

(b) Distribution

Lock	Type A	Type B	Type C
Iroquois	10	10	. . .
Upper Beauharnois	10	9	. . .
Lower Beauharnois	10	10	. . .
Cote Ste-Catherine	10	9	. . .
St. Lambert	5	7	12
Total	45	45	12

BRIDGES

Brief notes relative to the modification of existing bridges or construction of new bridges follow.

Jacques Cartier Bridge (existing, Mile 1).—This is the most important highway bridge (five traffic lanes) from Montreal to the South Shore. It was built in the 1920's, and has a high-level crossing over the north channel. The high clearance permitted access to the upper part of Montreal Harbor and also to the proposed entrance to the Seaway which at that time was planned to be located along the north shore. The part of the bridge south of St. Helen's Island sloped at an easy grade down to the south shore. At the Seaway channel location the bottom of the steelwork of the bridge was only 40 ft clear of the high-water level in the river. In order to avoid a lift span, 120 ft clearance has been obtained by jacking up the bridge by 50 ft, and by replacing one deck span by a new through truss to gain an additional 33 ft. The new truss was erected on falsework on the upstream side of the bridge, and other falsework was constructed on the opposite side for dismantling the old truss. The only complete

traffic interruption was one of about 6 hr in October 1957 when the old span was shifted out and the new one moved in.

Victoria Bridge (existing, Mile 3).—This bridge carries the double track main line of the Canadian National Railways and is an important highway crossing. As it was impractical and would have been of very great cost to carry the railway over the Seaway at a high level, and a tunnel would have been of even greater cost, a lift span had to be provided. There were strong objections from the public about the highway-traffic interruptions which would occur, and the Canadian Government concluded that arrangements must be made for uninterrupted highway traffic over this bridge. This decision was a major factor which influenced the precise location of St. Lambert Lock. By locating the lock immediately upstream from the bridge, it was possible to provide for uninterrupted highway traffic by having duplicate bridges, one at each end of the lock. Normally, all traffic uses the downstream lift span (which is the south span of Victoria Bridge). When this span is raised for an upbound ship entering the lock or a downbound ship leaving it, all vehicular traffic will be diverted to the other bridge. After this plan had been adopted for the highway traffic, the Canadian National Railway decided that a similar arrangement of alternate routes should be provided to permit uninterrupted railway traffic. This railway diversion bridge will be completed in 1961.

Victoria Bridge - Alternate (new, Mile 3.2).—A vertical-lift span has been constructed across the upper end of St. Lambert Lock to provide the alternate route during periods when Victoria Bridge is raised.

Côte Ste-Catherine (new, Mile 12).—A rolling lift bridge has been constructed across the upper end of Côte Ste-Catherine Lock for access to the dike. It has cast steel segmental and track girders. It is a service bridge only.

Honoré Mercier (new approaches to existing bridge, Mile 16.4).—This is an important highway crossing. The old approach ramp has been demolished, and an entirely new high level approach structure has been built.

Canadian Pacific Railway Bridge (new, Mile 16.6).—This bridge carries the double-track main line of the Canadian Pacific Railway. Two single-track vertical-lift bridges have been constructed close to the former embankment. The bridges were constructed complete on a new alinement about 100 ft east of the existing embankment, and after diversion of the railway onto the bridges, the old embankment was excavated. The use of two single-track bridges will permit mechanical maintenance on one bridge in the raised position, with negligible interference to railway or Seaway traffic.

New York Central Railroad (new, Mile 33).—A bob-tail swing span has been constructed across the upper end of the Upper Beauharnois Lock. It is also used as a service bridge.

St. Louis Bridge (existing, Mile 39).—This is a combined railway (Canadian National) and highway structure across the Beauharnois Power Canal. Two old 100-ft fixed-girder spans have been replaced by a new 200-ft vertical-lift span weighing 1300 tons. One old pier has been removed.

Valleyfield Bridge (existing, Mile 45).—This is a combined railroad (New York Central) and highway structure across the Beauharnois Power Canal. Two old 100-ft fixed-girder spans have been replaced by a new 200-ft vertical lift span weighing 1,480 tons. One old pier has been removed.

It is of interest to note with reference to the foregoing two bridges that when the Beauharnois Power Development was constructed (initial stage completed during 1929-1932), the Canadian Government required that piers be constructed in the bridges across the canal at Valleyfield and at St. Louis suitable for future

lift spans. For use up to the time of completing the Seaway, a temporary pier in the middle of the lift span gap and two 100-ft spans were constructed. The recent modification has required the building of a new 200-ft span with towers and lifting machinery at each bridge, and the removal of the old spans and temporary piers. The new Valleyfield span was assembled on shore $\frac{1}{2}$ mile from the bridge. On a selected day in September 1958, the old short spans were removed by floating out on scows, and immediately following, the new span was floated into place on two other large steel scows. In early April 1959, the temporary pier weighing 750 tons was broken off at the ship channel grade, and the top part lifted up by two scows using four of the salvaged plate girders as a strong-back between the scows, and floated away from the ship channel. The St. Louis Bridge was handled in a similar way. At both of these bridges, the Seaway Authority has built the new lift spans, and Quebec Hydro has removed the old spans and temporary piers.

Cornwall Island Bridges - South and North Channels (new, Mile 81).—The piers for the South Channel Bridge were constructed by Canada. The superstructure was constructed by United States. The construction of the bridge across the North Channel is just starting (1960).

Iroquois (new, Mile 112).—A rolling lift bridge similar to the one at Côte Ste-Catherine has been constructed across the lower end of the Iroquois Lock. It is essentially a service bridge for use by the Authority and for access to the north end of the Iroquois Control dam.

LOCK OPERATIONS

The major factor limiting the capacity of the Seaway is the practical number of lockages which can be made in a day. The lockages per day are governed by the physical characteristics of the locks (hydraulic, mechanical and electrical), and by the speeds at which ships can be got into and out of the locks.

The lock physical characteristics consist of two basic elements:

1. The times required to open and close the gates and fenders; and
2. The times required to fill or empty the lock.

At the Canadian locks, the gates and fenders are electrically interlocked so that they operate in sequence.

The problem of getting ships into and out of the locks safely and quickly relates to the ships and their captains, to the lock-entrance arrangements and facilities, and also to the weather conditions.

The present operating time cycle under good weather conditions for the Canadian locks ranges about as follows:

Ship entering lock	15 to 25 min
Close fenders, then gates	3 min
Fill or empty lock	7 to 8 min
Open gates then fenders	3 min
Ship leaving lock	8 to 12 min
Total	36 to 51 min

The present average time cycle under good weather conditions is about 45 min, or about 32 lockages per day could be made if ships arrived steadily and uniformly at all locks.

Some improvements are possible in each of the foregoing time factors, but the greatest variable and the most rewarding place for gain is the time to get a ship into the lock. This feature involves good dispatching and clear instructions for the ships' captains, as well as providing adequate approach facilities.

Operations to this date (1960) have shown up a number of the critical spots which could influence traffic capacity. For example:

a. Ship movements at St. Lambert Lock are restricted by the many trains crossing Victoria Bridge (over 100 trains per day). These restrictions will be eliminated when the alternate railway bridge has been completed in 1961.

b. The Beauharnois locks require careful dispatching and good coordination between lockmasters and ships' captains. Because of the short distance between these locks, one slow ship will affect both locks, and the passage of one slow ship could cause twice the delay here compared to a delay at a single lock.

Traffic.—Traffic through the Seaway to the end of August, 1959 amounted to a little over 11,000,000 tons in about 2,000 ships upbound and 1,900 ships downbound. Of the total of about 3,900 ships passing through the locks, approximately 35% have been "Ocean" and 65% have been "Inland" type.

Maximum capacity of the Seaway is influenced greatly by three major factors entirely apart from the characteristics of the locks themselves. These three are:

(1) Uniformity of cargo traffic throughout the 8-month season;
(2) Reasonably equal upbound and downbound cargoes; and
(3) Reasonable proportion of large Lake vessels.

The Welland traffic up to 1958 never exceeded 24,000,000 tons of cargo per yr. This can be greatly increased. A total of 60,000,000 tons of cargo per yr through the St. Lawrence Seaway is possible if the foregoing three factors are reasonably attained.

Journal of the
WATERWAYS AND HARBORS DIVISION
Proceedings of the American Society of Civil Engineers

DESIGN AND CONSTRUCTION OF NAVY'S LARGEST DRYDOCK

By S. P. Zola[1] and P. M. Boothe,[2] F. ASCE

SYNOPSIS

This paper presents a technical description of the design and construction of the Navy's largest drydock at the Puget Sound Naval Shipyard, Bremerton, Washington. The ever increasing dimensions of naval ships since World War II, such as the "Super Carriers," require facilities capable of accommodating this class of vessel.

INTRODUCTION

In the old days of wooden ships and iron men the process of cleaning the ship bottom of barnacles and painting with pitch was called graving. While this name does not apply literally to the steel ships of today the title "Graving Dock" has been accepted down through the years as being synonymous with the name "Drydock." A graving drydock may be defined as a permanently fixed basin on shore into which a ship can be floated and the water removed.

Note.—Discussion open until August 1, 1960. To extend the closing date one month, a written request must be filed with the Executive Secretary, ASCE. This paper is part of the copyrighted Journal of the Waterways and Harbors Division, Proceedings of the American Society of Civil Engineers, Vol. 86, No. WW 1, March, 1960.

[1] Captain, Civ. Eng. Corps, U. S. Navy, Officer in Charge of Construction, Puget Sound Naval Shipyard, Bremerton, Wash.

[2] Captain, Civ. Eng. Corps, U. S. Navy, Resident Officer in Charge of Construction, Puget Sound Naval Shipyard, Bremerton, Wash.

The entrance, at or near the waters edge, is closed by a movable caisson or by gates.

Every ship requires at least an occasional drydocking. This may be for the purpose of normal periodic maintenance, for performance of alterations, including modernization and conversion, or for repairing battle damage. The common denominator, however, is the necessity to provide facilities that permit the underwater portions of the vessel to be exposed and available for the required work. Since the drydock, when dewatered, becomes, in effect, a repair shop it must be equipped with weight-handling equipment, compressed air for cleaning and sandblasting, power, water, oxygen, tank cleaning, and sewage-disposal facilities. In addition, a ship in drydock is completely dependent on outside sources for telephone, electricity, steam, fresh water, salt water, and sanitary sewer services to maintain living standards for the crew.

The size of naval drydocks has, by long custom, been associated with the largest class of warship that could be serviced, ranging from the small destroyer or submarine dock to the battleship dock. This latter could, until recently, accommodate the largest vessels of the Fleet. Naval strategy, tactics, and weapons development during and subsequent to World War II, however, relegated the battleship to the role of supporting fire power while emphasizing the supremacy of the carrier as the queen of the fleet. The development of carrier-based jet aircraft initiated such innovations in carrier design as the angled flight deck with its resulting overhang. To keep pace with the continued rapid and radical changes in aircraft the "Super Carrier" evolved from necessity into reality.

World War II carriers were not substantially larger than battleships, and presented no particular problems in connection with drydocking. With the advent of the Forrestal, Saratoga, Kitty Hawk, and Enterprise (nuclear) classes of carriers, however, a shortage of adequately sized drydocks for carrier repair became apparent. Although the hull of the new carriers will fit in the largest existing docks, the capability of effective underwater maintenance and repair is seriously impeded by the lack of adequate working clearances between the ship and drydock walls. Portal crane service is also hampered by the wide overhang of the angled flight deck which prevents passage of the cranes.

The completion of the Panama Canal in 1914 provided the U.S. Fleet with the capability to maneuver between the Atlantic and Pacific oceans with a minimum loss of time and thus established the two-ocean mobility concept. Subsequent ship design had been controlled by the limitation of the 100-ft wide canal locks until the development of the Forrestal. A major casualty to one of these vessels in the North Pacific could now entail a cruise more than halfway around the world due to lack of adequate drydocking facilities on the West Coast.

REQUIREMENTS

This creates an immediate requirement for repair facilities capable of accommodating the larger CVA class vessels which are already in service. This need is intensified by inclusion of future requirements for the CVA(N) (nuclear) class which are under construction.

The Bureau of Ships, which has responsibility for Naval Shipyard functions and operations as well as for design and development of new vessels, estab-

lished the basic criteria for the design of the new drydock. These relate to size of dock, proximity to adjacent facilities and requirements for various utilities. The Bureau of Yards and Docks is responsible for the design and construction of the Naval Shore Establishment public works and public utilities. Such responsibility includes translation of the operational criteria into design of the finished facility.

The Puget Sound Naval Shipyard in Bremerton, Wash. has had extensive experience in construction and repair of aircraft carriers. In the post-war era this yard has been a leader in carrier conversion and was a lead yard on the design of the Midway class and of certain Essex class carrier conversions. Sound economics and judgment dictated that such experience and potential be utilized for present day needs by selection of this shipyard as the location of the Navy's largest Carrier Repair Drydock.

SITE SELECTION-OPERATIONAL CONSIDERATIONS

After selecting the geographical area one of the more significant problems faced in the drydock planning stages was that of the site selection. A number of functional, operational, and economic factors affected the final determination and were weighed and balanced. Some fifteen possible sites were investigated, not only from the operational aspect but for the purpose of evaluating comparative soil structure. Serious consideration was given to an inshore location similar to the existing docks shown on Fig. 1 but the crowded condition of available working areas restricted such possibility. An offshore location, such as sites 1A and 2 in Fig. 1, would provide laydown and working areas adjacent to the dock without infringing on existing spaces but would involve appreciably higher costs. Site 1B represents a compromise between the inshore and offshore location concepts. Since the offshore location will provide some $13\frac{1}{4}$ acres of additional valuable area for future shipyard use and will provide the contractor with a working area creating the least interference during the 3 yr of construction, the additional cost involved was considered to be warranted.

ENGINEERING ECONOMICS

During the several glacial epochs in the geological history of Sinclair Inlet, the site of the Puget Sound Naval Shipyard, deposits left by the ice movements were sorted and shifted by tidal movements resulting in variable but rather distinctive subaqueous strata. Uppermost is a layer of highly compressable soft green organic clay varying from 2 ft to 40 ft in depth, which is unsuitable for foundation material. Underlying this, in a portion of the area, is as much as 12 ft of tan to gray sandy silt, most of which must be removed. Next is a layer of compact gray silty sand and gravel grading into medium sand and gravel, and cemented fine to coarse sand and gravel having excellent bearing value.

A total of seventeen final borings supplemented the data obtained from numerous preliminary studies, which included a steel sheep pile test cell driven to a depth of 40 ft below mud line and twelve test piles driven to refusal. These studies yielded information concerning the determination of the basic

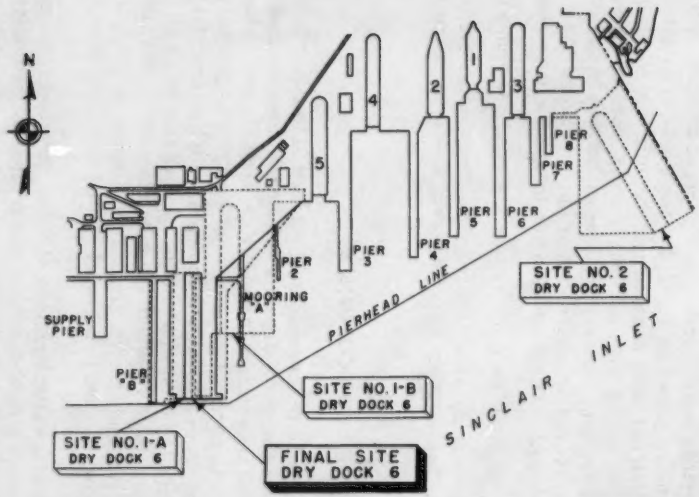

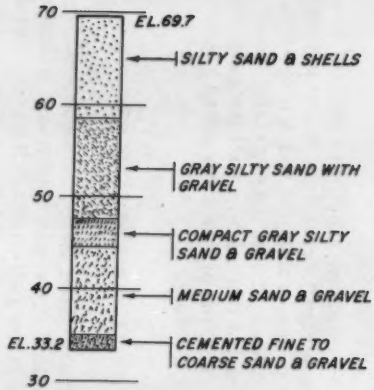

TYPICAL BORING LOG

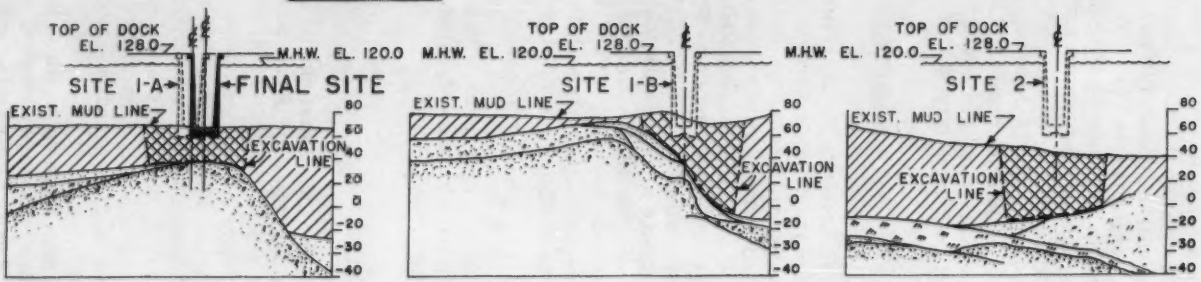

FIG. 1.—DRY DOCK SITES

drydock type, gave specific values on strength, permeability and consolidation properties of the underlying soils, and served in conjunction with the operational requirements to limit the final detailed investigations to the three sites shown in Fig. 1. Each of the final sites presented similar foundation problems, varying only in the depth to firm material and in the amount of soft overlay material to be dredged out. The final site is shown located over the high ridge of very compact gray coarse sand and gravel to minimize dredging.

The maximum tidal range is 20 ft although the average range between MLLW and MHHW is about 12 ft. The top of the mud line is approximately 54 ft below MHHW or 42 ft below MLLW. A sweep area outboard from the drydock entrance must be cleared so that no material will project above the elevation of the drydock floor or about 42 ft below MLLW.

Altogether 550,000 cu yd of unsuitable material must be removed by means of a suction dredge supplemented by clamshell and dump bottom scow. A deep water waste area one mile east of the site was used for disposal of material.

STABILITY OF DREDGED SLOPES UNDER WATER

The removal of unsuitable materials from the dredged area left side slopes as high as 40 ft in the clay stratum, requiring a slope of 1 vertical on 1.5 horizontal to provide a factor of safety greater than 2.0 to prevent material sliding into the dredged area. This comparatively steep slope is stable because of the low submerged weight of the clay and the fact that the soil strength increases in a linear ratio with the depth.

While the granular fill at the inboard end of the area has consolidated and strengthened a 15 ft underlying stratum of clay, the weight of this fill necessitates a flatter slope than the unburdened clay along the sides. On the assumption that failure could occur by rotation on a circular arc in the clay with active and passive failure wedges developing in the overlying granular material, a slope of 1 on 1.75 was determined to provide a safety factor of 1.2 submerged. To assure stability of this slope, control of ground water levels in the bank will be required when the area is dewatered.

TYPE OF DOCK

The underlying sand and gravel material was considered suitable for point bearing piles or other heavy foundation loads but pile penetration would be limited. Due to the variable thickness of the softer overlay material and the limited pile penetration where the clay stratum was thin or non-existent, foundation piling could not grip a sufficient mass of subsoil to hold down a dock floor of moderate thickness in an unrelieved dock.

To obtain the required mass of concrete to resist hydrostatic uplift in a gravity type dock, a 43 ft thick door floor slab would be required with the bottom of the slab 85 ft below MLLW. In view of the terrific construction problems and exorbitant cost involved, this type design was also discarded.

Studies were next made for a relieved type dock provided with underdrains and side drains which would dispose of sufficient ground water to reduce the hydrostatic head on the bottom and the sides to a predetermined acceptable height. Since foundation conditions were favorable, this type structure was determined to be the most economical. The design proceeded on the basis that

all of the soft material overlaying the natural gravel and glacial till would be removed as having very low permeability and bearing value.

Granular material which is plentiful in the Puget Sound area will be brought in to replace the soft material and to bring the moles up to grade. This material will then become the basic foundation for the outboard end of the drydock, the mole structures, and the temporary cellular cofferdam at the entrance end of the drydock site. The inboard end of the drydock and the moles will be founded on existing sand and gravel. The granular fill must be relatively clean, graded to specifications, and capable of compaction to a degree adequate to support loads of moderate intensity imposed by the flooded drydock weight or for the more localized ship loadings when the drydock is dewatered and a ship is supported on blocking.

COFFERDAMS AND STABILITY PROBLEMS

The design adopted for the Drydock dictates that the structure be built entirely in the dry, necessitating cofferdams surrounding the drydock area. The requirement for a working area necessitates fill, (moles), to be placed along both sides of the drydock to be utilized as a basis for dams on either side of the construction area. Lines of steel sheet piles will be driven in the central portion of each dam and across the inboard end to serve as the impervious core of the dam. The earthwork and cut-off walls will remain as a functional part of the final facility. A wall of interconnected sheet pile cells is connected to the sheet piles of the dams at the outboard end to complete the cofferdam surrounding the construction site. Along the moles and the outboard portion of cellular cofferdams, the sheet piling will be driven through the stratified glacial outwash into heterogeneous glacial till in order to minimize infiltration of ground water.

The width of the construction dams necessitates underwater fill material sloped to avoid encroaching on the drydock area or the area to be dredged for future ship berths. Granular material having the permeability and stability characteristics previously established will stand on underwater slopes of 1 on 2.75 if properly placed. Barges and flat scows, hydraulically flushed, are used to place the initial fill before pile driving is started for the sheet pile cut-off wall, thus providing support for the lower ends of the sheeting. Since the sheet piles should be driven before a substantial part of the upper portion of the dam fills are placed, precautions in placing the remaining fill are pertinent to the safety of the cut-off wall. Care must be exercised to avoid impact against the wall as well as excessive differential in heights of fill on either side.

The temporary cofferdam cells at the entrance to the dock must be filled with granular material of the same quality as used for the construction dams and other underwater fill. The material must be free draining so that excess hydrostatic pressure does not develop on the inner sheet piles and also that the weight of drained rather than submerged soil will contribute to the stability of the cells. Weep holes on the inner face of the sheet pile cells will be provided to drain the granular fill.

Limited space at the inboard end of the drydock and at the pumpwell creates stability problems requiring braced cofferdams in these areas. A steel sheet pile cofferdam at the inboard end will be necessary to permit excavation for the drydock with minimum demolition of existing buildings and to restrict

ground water flow. The cofferdam will be constructed in six stages with bracing placed in sequence with the excavation against sections of the concrete floor slab. For design of the sheeting, the active and passive diagrams were determined by Coulomb's equation considering the slope of the ground surface and neglecting frictional resistance between the soil and sheet piling. A trapezoidal pressure distribution was used in designing the braces in order to allow for possible redistribution of pressures upward during excavation. The sheeting is assumed to be simply supported at each wale. Ground-water levels were assumed to decrease progressively during excavation in order to obtain reasonable active pressures and an economical design.

In excavating for the pumpwell, a braced steel sheet pile cofferdam is required to retain the fill on the interior slope of the construction dam. The cofferdam will be constructed in eight stages with bracing placed against sections of the concrete floor slab. Design assumptions were essentially the same as those for the head end cofferdam. At the lowest stages of excavation, the sheeting is assumed to cantilever about the bottom wale.

The construction area will be dewatered by means chosen by the contractor. The rate of dewatering, however, will be limited in order that ground water draw-down does not lag to an extent that will cause ravelling of the berm faces or boiling up in the bottom. Temporary construction piezometers will be provided near the inner toe of the slope of the dam so that the differential head between the ground water levels and pool level can be controlled. The contractor will also provide facilities for emergency flooding and for flooding when the drydock has been completed. These facilities must be capable of equalizing the inside and outside water levels within a period of 12 hr without damage to either temporary or permanent structures. Dewatering the construction area will require pumping 135,000,000 gallons of free water from the enclosed pool in addition to 6,000,000 gallons of drainable pore water from the construction dams. After the initial dewatering a continuing underseepage is anticipated through the sheet pile wall estimated at 20,000 to 30,000 gpm.

DRYDOCK

The drydock structure will be 1,180 ft long from the head end to outboard face, 180 ft wide at the coping, and 61 ft deep.

A typical half section of the dock is shown in Fig. 2. The dock is roughly rectangular in shape with the vertical walls at each side supported on the floor slab. In turn the walls and sloping columns support a partitioned box structure which extends the full length of the dock and serves as tunnels for the electrical and mechanical services. The relatively thin dock floor slab is 7 ft thick with edges thickened to 12 ft under the side and head end walls. The side walls vary in thickness from 12 ft 6 in. at the floor line to 2 ft 9 in. just below the utility tunnel structure. The outboard 80 ft of these walls form an entrance structure 50 ft thick for the full height to contain the caisson seats and flooding culverts. The utility tunnels are supported, as shown, on the top of the dock wall and on precast concrete columns, 22 in. square, spaced at 16-ft centers. The utility tunnel walls serve as supporting structure for the crane tracks.

The sidewalls were designed as cantilevers supported by the floor slab. The lateral design loads on the wall were assumed to be due to pressure from cohesionless granular materials, surcharge, earthquake, and a controlled

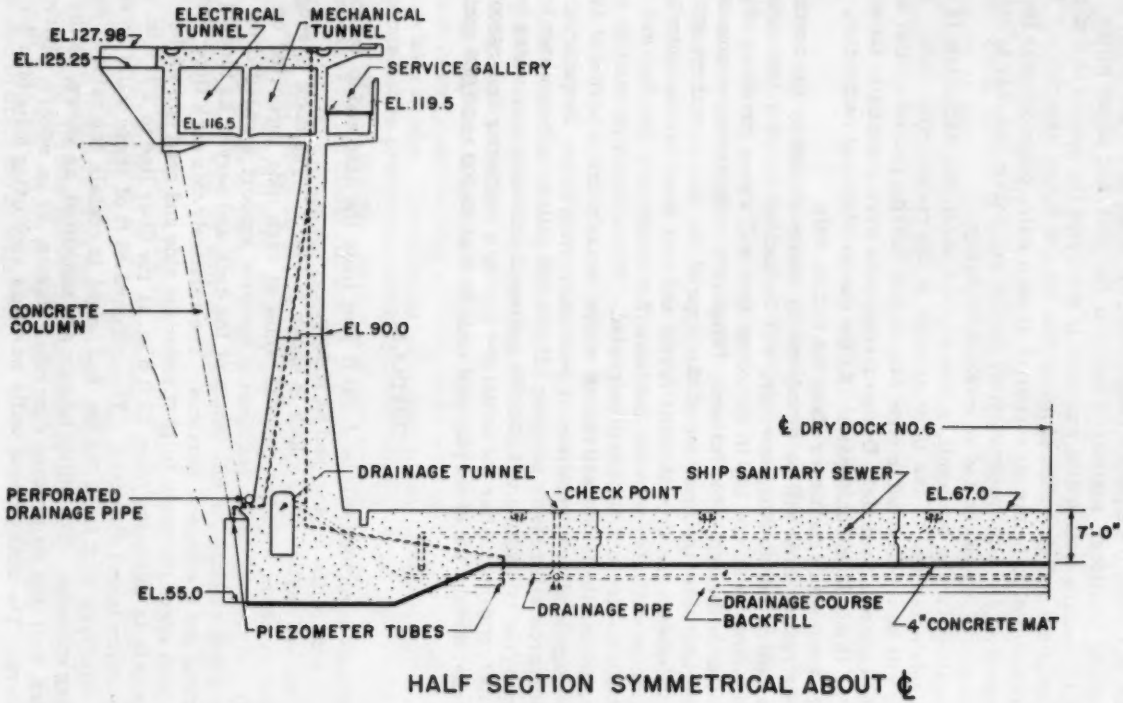

FIG. 2.—TYPICAL SECTION

hydrostatic pressure consistent with a water level on the outside of the wall at an elevation 10 ft above the top of the floor slab. Where walls are able to deflect to the extent required to produce an active state of stress, Rankine active pressures are assumed in the fill material behind the wall. Where walls were relatively rigid and unyielding, horizontal pressures were computed, using co-efficients between those for active and "at rest" pressures. The horizontal pressures produced by surcharge were assumed to be double the Boussinesq values. A close approximation of the lateral pressures on the sidewalls are those due to a fluid weighing 32 pcf from El. 128 to El. 76, a fluid weighing 82 pcf from El. 76 to El. 70 and a fluid weighing 100 pcf below El. 70, plus horizontal pressures caused by surcharge of 75 psf down to El. 115 and 150 psf below El. 115. Concrete was specified to have a 28-day strength of 3,500 psi for the walls and floor and 6,000 psi for the precast columns supporting the service galleries. The sidewalls of the drydock will be much thinner than the massive gravity walls which have been used for most existing graving docks. Considerable reinforcing was provided in these thin walls whereas practically no reinforcing is used in the customary massive gravity walls.

The effect of these walls on the floor was considered in determining the maximum transverse moment near the wall with blocking loads of a nuclear aircraft carrier on a battleship on the drydock floor. The 12 ft thick portion of the slab under the wall was considered to be an infinitely stiff section, 25 ft long. The center portion of the floor slab, 7 ft thick, was considered to be a semi-infinite (flexible) section. The elastic foundation method of analysis was used, assuming that the distribution of pressure on the soil foundation was proportional to the deflection of the floor slab. The co-efficient of subgrade reaction was assumed to be 260 kips per sq ft per ft and maximum soil pressure computed at 5.68 kips per sq ft.

PRESSURE RELIEF SYSTEM

The basis of the design of a relieved type structure not only means that there will be insufficient dead weight incorporated in it to prevent uplift but the strength in the slab and walls will be insufficient to resist the full hydrostatic pressures. The correct design of a drainage system for obtaining the required relief and its proper construction are of the utmost importance. The system must provide a satisfactory factor of safety against uplift for normal working conditions as well as against a critical differential between the draw-down inside and outside the dock during dewatering.

The first element to consider is permeability of the backfill which is of critical importance in a relieved type of structure. The material must be so graded that the ground water draw-down approximates that of the water within the dock. This is accomplished by: (1) Granular drainage course beneath the dock floor and outside the dock walls; (2) Granular backfill, having the required permeability and stability characteristics placed between the dock wall drainage course and the moles; (3) Sheet pile cut-off walls to minimize inflow.

The drainage course will be placed against several different soils and must conform to the gradation requirements for filter stability and permeability in each situation. A gradation was established to satisfy the requirements of a filter material against all backfill and natural materials encountered except

strata containing seams or lenses of very fine sand and silt. To prevent piping from any of these strata, a 1-ft layer of granular backfill will be placed beneath the drainage course in all areas where the dock is in cut.

The drainage course section outside the wall is shown in Fig. 3 and consists of a trapezoidal section approximately the shape of the active pressure wedge with a width of 5 ft at the base and 30 ft at the top. The gradation of the backfill placed between this drainage course and the moles required detailed study and balancing of the many factors involved. The material must be stable, of low compressibility and have sufficient permeability to allow the required rate of draw-down without resulting in high pumping rates while the drydock is dewatered. Conversely, the gradation should not be so restrictive as to require excessive processing and waste of the granular material locally available. Flow net studies indicated that the material should have a coefficient of permeability of approximately 0.05 ft per min.

The next basic element required is an adequate network of collector pipes under and around the drydock. After the drainage course of select material is placed under the drydock floor to permit ready percolation of seepage water, the underfloor drainage system is embedded as indicated on Fig. 3. This system is composed of a network of 8 in. perforated vitrified clay pipes with headers terminating in the sidewall drainage tunnels. The transverse headers are spaced on 48 ft centers except for the outboard end of the dock. In order to dispose of the heavier infiltration adjacent to the sheet pile cut-off wall along the dry dock entrance, the first four headers in this area are spaced at 24 ft centers. The longitudinal runs are spaced at 15 ft and $65\frac{1}{2}$ ft each side of the centerline of the drydock. At alternate intersections of the longitudinal and transverse lines, vertical risers are provided to the drydock floor in order to check the hydrostatic pressures and to permit flushing of the drainage system.

To protect the gravel drainage course from dirt and mortar and to prevent breakage of the collector pipes during construction a protective cover is required. This will consist of a membrane of impregnated paper or polyethylene covered with a 4 in. thick concrete subfloor. Exact adherence to the plans and specifications is imperative during this phase in order to assure satisfactory continued service of the drainage system. It is important both during and after laying of the collector pipe network to be alert for possible breakage and to insist upon replacement if any damage is discovered.

It will be noted that a continuous concrete cradle is provided along the outside of the dock wall to support the 12 in. vitrified clay collector pipe at the base of the wall drainage course. This pipe drains into the drainage tunnel by means of 8 in. cement asbestos branch pipes embedded in the wall at 24 ft centers. The supporting cradle will prevent dislodging the collector pipe and/or breakage of the branches into the tunnel but extreme care will be required during the backfill operation.

Flap type check valves will be provided at the tunnel ends of the drainage pipes as shown on Fig. 3. These will minimize the outflow of water into the drained ground while the drydock is being flooded and thus prevent undue disturbance of the select material drainage course and surrounding material. The flap valves will also speed up flooding of the dock by preventing flow from the tunnel into surrounding area.

The importance of the proper operation of the relief system cannot be overemphasized. If the system functions improperly a hydraulic differential

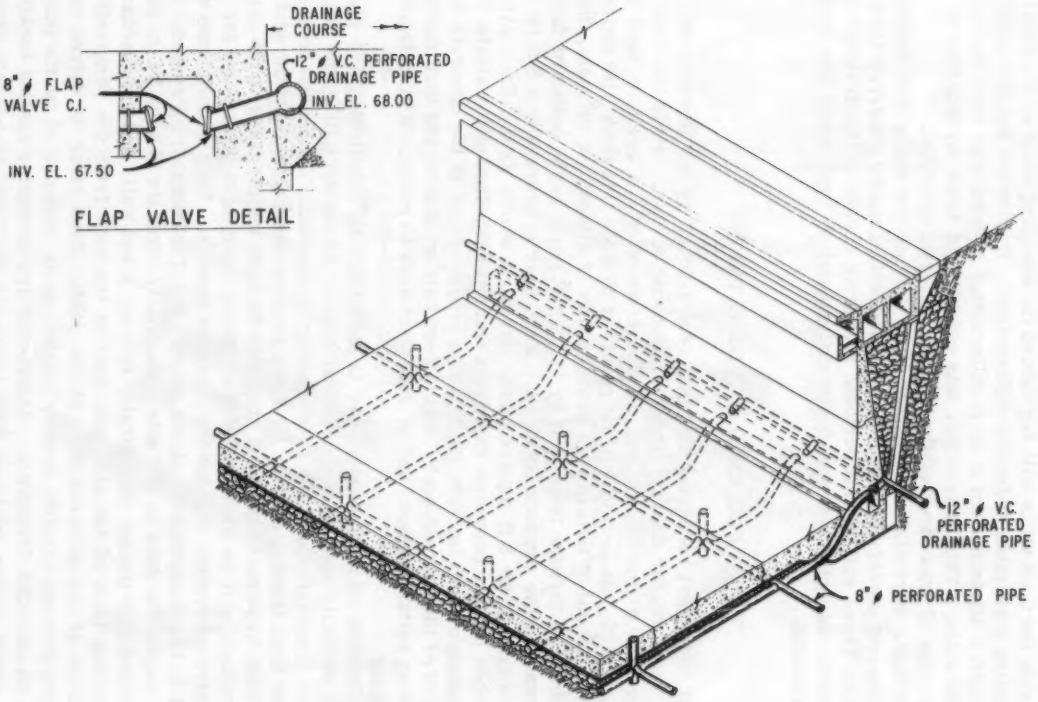
DRAINAGE COURSE
12" ø V.C. PERFORATED DRAINAGE PIPE
INV. EL. 68.00
8" ø FLAP VALVE C.I.
INV. EL. 67.50
FLAP VALVE DETAIL
12" ø V.C. PERFORATED DRAINAGE PIPE
8" ø PERFORATED PIPE

FIG. 3.—PRESSURE RELIEF SYSTEM

could arise to the extent at which rupture of the bottom slab or the walls or both could occur. The drainage system, then, must work properly and continuously for the life of the drydock. The design of the dock structure and the drainage and relief system have been predicated on the critical condition which could occur while the dock is being pumped out. The draw-down of the water-level outside the dock walls will lag behind the lowering level of the water inside, creating a variable hydraulic differential. To provide for this condition a conservative allowance for a 10 ft differential in head was used in the design of the walls. This differential was established from an analysis of the probable rates of draw-down of the backfill material specified.

To facilitate surveillance of water head outside the walls and under the slab, permanent piezometers will be installed which can be observed from the yard grade. These will permit periodic recurring checks of the drainage system operation as well as to watch the differential in head while the dock is being dewatered.

FLOODING AND DEWATERING

A most important recurring function of a drydock is the flooding and dewatering required for docking and/or undocking a ship. Since the time required for such a function is lost to productive effort, it must be held to a minimum. A 90-min period will be required to flood this dock with approximately 88 x 10^6 gal of water or an average flow of almost 1 x 10^6 gpm. Water will be admitted through twin 14 ft by 11 ft inlet ports in the outboard face of each sidewall at the drydock entrance. Each port converges to a 8 ft by 8 ft culvert containing an 8 ft square motor operated sluice gate. Each pair of culverts then further converge through a transition section into a single 11 ft by 10 ft passage which leads to the flooding cross culvert in the concrete floor just inboard of the caisson seat. This cross culvert discharges thru multiple floor opening suitably spaced and of sufficient area to minimize turbulence on the dock floor.

When flooding starts the operation is modulated by positioning the sluice gates only partially open to reduce initial surge. As the dock fills, the differential head diminishes and the gate opening is gradually increased to a full opening for final flooding stages. Grooves are provided outboard of the sluices gates in order to permit placing of stop logs to allow maintenance of the gates.

The drydock will be provided with separate pumping installations for the main dewatering system and for the drainage system. Both installations will be housed in the pumpwell as shown in Fig. 4. The dewatering system, designed to empty the dock in 226 min, essentially consists of four 54 in. centrifugal mixed flow pumps electrically driven, a wet well, and the discharge culvert running back of the east side wall of the dock from the pumpwell to the discharge at the entrance face of the dock. Each pump is driven by a 1500 hp synchronous electric motor, located on an upper level of the pumpwell, thru an extended driveshaft. The pumps are protected against backflow by 54 in. check valves equipped with hydraulic snubbers to prevent violent slam and 54 in. motor-operated gate valves, permitting complete closure of the discharge line for maintenance and safety to the pumpwell.

The pumps are located to have positive suction on the intake at all times during the dewatering period. Three of the main dewatering pumps take suction from a grating covered trench in the drydock floor thru 54 in. transition

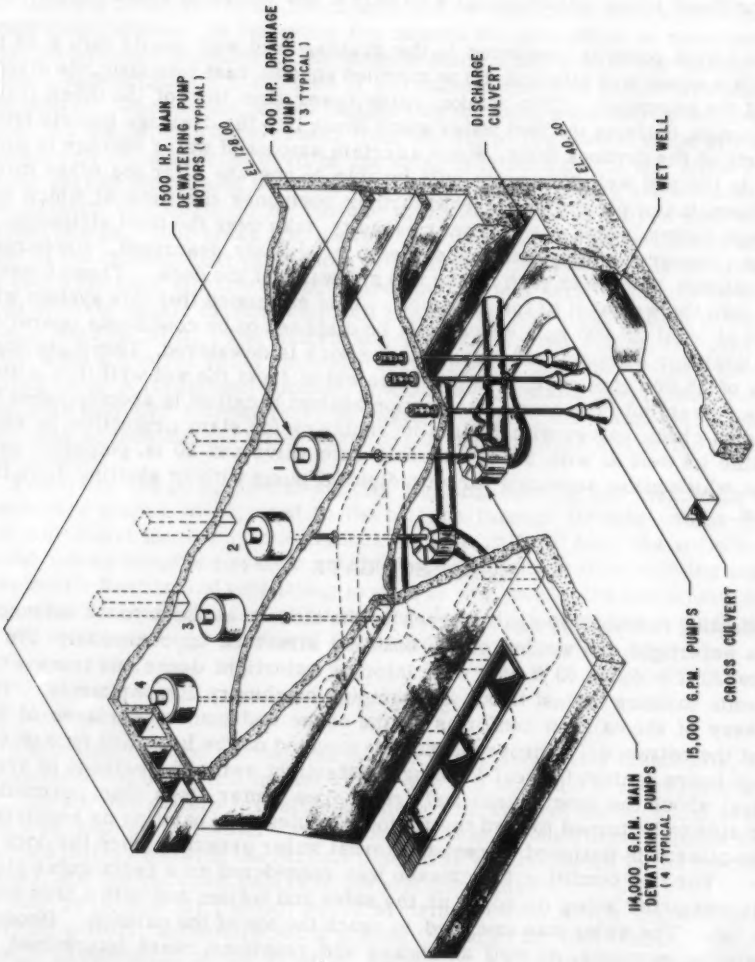

FIG. 4.—PUMP WELL

elbows and 7 ft square bell mouthed conduits cast in the concrete structure. A 7 ft square, motor operated sluice gate will be installed in each intake conduit. The trench, which is 12 ft by 62 ft in plan at floor level and 4 ft deep, facilitates conveying water to any one of the three pumps during the last stage of dewatering. The spillway length provided by the perimeter of this trench will feed sufficient water at the end of the drawdown to permit one main pump to be utilized to the fullest extent with only a few inches of water on the dock floor.

The fourth pump is connected to the drainage wet well cavity thru a 54 in. transition elbow and eliptical flare mouthed conduit cast into concrete structure of the pumpwell. This intake, being lower than that of the other three main pumps, collects the last water which flows into the drainage tunnels from all parts of the drydock floor. Since a certain amount of water storage is provided in the wet well this pump will be able to operate after the other three have been taken off the line. This further postpones the time at which the drainage pumps, which are of lesser capacity, take over the final stripping.

The pressure relief drainage system, previously described, discharges into drainage tunnels in each of the two sidewalls of the dock. These tunnels drain into the wet well of the pumpwell. It is estimated that this system will collect at least 20,000 gpm which must be disposed of by continuous operation of the drainage pumps at all times that the dock is dewatered. Three drainage pumps of 15,000 gpm each, will pump the water from the wet well thru a discharge culvert into the sound. Protection against backflow is accomplished by individual check valves with hydraulic snubbers for slam protection in each pumpline as well as with 36 in. manifold gate valve and 20 in. pumpline gate valves, which allow servicing for an individual pump without shutting down the system.

CAISSON GATE

A floating caisson-type gate serves as the closure at the drydock entrance. It is a watertight, all welded steel, box-like structure approximately 176 ft long by 20 ft wide by 63 ft high with interior watertight decks and transverse bulkheads forming ballast tanks and pumping machinery compartments. The periphery of the caisson conforms to the shape and contact surfaces of the seat at the entrance. A neoprene gasket mounted on the landward face of the caisson bears against the seat forming a watertight seal. The caisson is symmetrical about the longitudinal and transverse center lines thus permitting either side to be turned toward the drydock for cleaning, painting or repairing.

The caisson is designed to resist external water pressure when the dock is empty. For this condition the caisson was considered as a rectangular plate simply supported along its edges at the sides and bottom and with a free edge at the top. The water was assumed to reach the top of the caisson. Bending and twisting moments, as well as shears and reactions, were determined by using the elastic theory for rectangular plates subject to a triangular load.

Of the horizontal girders, only the main and top decks are watertight. The main deck of the caisson is at an elevation approximately 25 ft below the top deck. The main deck serves as the operating platform for the mechanical and electrical equipment contained in the caisson.

The main framing consists of a series of vertical frames and a series of horizontal girders. A frame near each end is watertight in order to provide

trim tanks. The top or weather deck is at the same elevation as the drydock coping and can be used as a roadway for pedestrian and light vehicular traffic.

The ballast tanks consist of a large center tank extending approximately three quarters of the length of the caission, and two end or trimming tanks. When closing the entrance to the flooded drydock the caisson is floated into position and then lowered into the seat by flooding these tanks. By regulating the flooding in the end tanks the caisson can be kept on an even keel during the seating operations. In removing the caisson the procedure is reversed. To provide adequate stability to the caisson when floating with the ballast tanks empty, approximately 1,860 tons of permanent concrete ballast are placed in the bottom. The amount of this ballast was partially governed by the requirement for the caisson to be raised from the sill at the lowest stage of the tide. Conversely the maximum draft of the caisson is such that it will come to rest in the seat at the highest tide that may occur. The flooding and unwatering of the caisson is controlled by the use of motor operated valves and electric driven pumps. The tanks are flooded through inlets or ports located on each side of the caisson near the bottom of the tanks. The center tank is unwatered by two 7500 gpm electric motor driven pumps and each trim tank by a 2000 gpm electric motor driven pump, all capable of operating against a total dynamic head of 30 ft. The pumps and motor operated valves are controlled from a main control panel centrally located in the machinery space above the center tank. A continuous bubbler, pneumatic-type water level indicating system with mercury manometer-type gages located at the main control panel is provided to indicate the water level in the ballast tanks and at the outside of the caisson.

Power for the pumping and also for lighting, heating and ventilation of the machinery spaces is supplied to the caisson through flexible cables from a 450 volt outlet located in the drydock service gallery near the entrance. A sound power telephone system provides intercommunication with the caisson. An electric heating and ventilating system is provided in the machinery spaces to reduce the humidity and eliminate the possibility of moisture condensation in the mechanical and electrical equipment.

UTILITIES

The electrical and mechanical tunnels are sized nearly identically, having a common height of 8 ft 9 in. and widths of 8 ft 5 in. and 8 ft 10 in., respectively. The service gallery is continuous along both sides of the dock and averages 6 ft 8 in. high by 6 ft wide. Fig. 5 is a section through these tunnels and the service gallery showing the various pipes that will be placed in the mechanical tunnel, and the rack and cables in the electrical tunnel.

The 14 in. line for the salt water system is shown with a connection to the service gallery, at which point a grating is placed for foot traffic. This system is independent of the existing PSNS salt water system which does not cover the waterfront area at the Carrier Repair Site. A study of the existing salt water system revealed that the cost of increasing the size of the distribution main, providing additional pump capacity, and extending the main into the area affected would be prohibitive. Therefore new pumping facilities and distribution mains were established within the new drydock area, specifically designed for this purpose.

Two 3500 gpm, 200 psi pumps in the pumpwell will supply the system with an emergency flow of 7,000 gpm at 150 psi residual pressure at the remotest outlet. In addition, provisions are made on the outboard end of the moles to augment the supply by the use of fire boats. An extension to the new compressor building will be used to provide cooling water for the 5,000 cfm compressor. Pipe sizes vary from $2\frac{1}{2}$ in. to 36 in., with approximately 6,400 ft of pipe being required. Approximately 280 tons of pipe and fittings will be installed.

The Existing PSNS fresh water distribution system was found to be adequate to handle the drydock requirements from an existing 12 in. main in the area. This main will be tapped opposite the west side mechanical tunnel with a 6 in. supply main, and opposite the east side tunnel with an 8 in. main. As noted in Fig. 5, one 6 in. line for the fresh water system is carried in the tunnel. Approximately 4,700 lineal ft of pipe, varying in size from $2\frac{1}{2}$ in. to 12

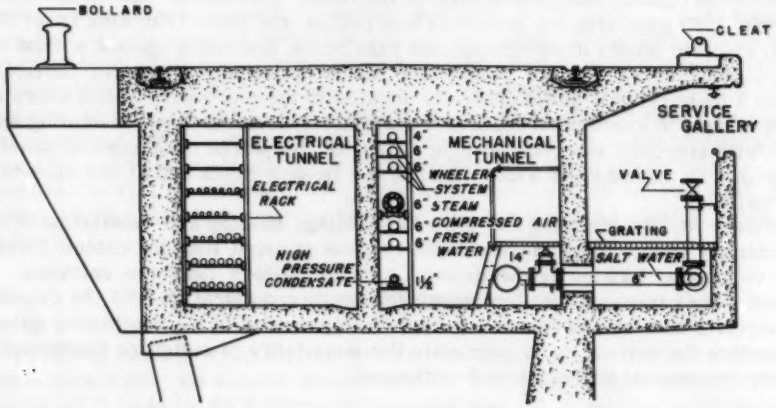

FIG. 5.—TUNNELS AND SERVICE GALLERY

in., will be required. The mains will be cement-lined cast iron pipe, while the service laterals will be zinc-coated iron pipe. Approximately 150 tons of pipe and fittings will be installed.

The requirement for compressed air at the Carrier Repair Site is difficult to determine. Changing ship design, variations in requirements in ships of the same class, and differences in repair operations make an accurate estimate of compressed air loads virtually impossible. Consideration was given to provide compressed air to care for the maximum demand load that could occur under the worst conditions but, as might be expected, this resulted in a highly over-designed system with excessively large mains and excessive costs. The final requirements were established after a study of the existing drydock loads and comparison with estimated requirements in the new dock for a large carrier. Since the existing air generation equipment was found to be loaded at approximately 95% of capacity and the existing distribution mains in the project area were of insufficient size to handle the expected load, it was found necessary to install a new 5,000 cfm at 100 psi compressor in a new building

near the repair site. A 10 in. steel main will be run under ground to the northwest corner of the dock from which the 6 in. line noted in Fig. 5 will loop through the mechanical tunnel. Altogether some 4,800 lineal ft of pipe varying in size from 3 in. to 10 in. and weighing approximately 54 tons will be required for the compressed air system.

As was the case with compressed air, the requirements for oxygen in the new Carrier Repair Site are extremely difficult to determine. The quantities required and sizing of the lines was determined in the same manner from studies of past requirements at Shipyard drydocks. The existing PSNS oxygen generation plant has sufficient capacity to handle the increase in load for the new facility and an existing distribution main in the vicinity will be tapped with a 4 in. extra strong wrought iron pipe with welded joints. This pipe will extend underground to the northeast corner of the drydock at which point the line will be teed and a 3 in. main carried down each side of the drydock, buried in the fill. It will be noted that the oxygen line is not shown in the tunnel since the hazards involved in handling oxygen required independent burial of the line. Service for the drydock will be provided by outlets crossing the tunnel and terminating in a box on the surface and adjacent to the curb. This system will carry oxygen at approximately 100 psig for use abroad ship and at dockside. The installation complies with National Board of Fire Underwriters requirements.

Steam will be provided to the drydock and other related facilities from an existing source in the vicinity. This will require a new concrete duct and piping to connect with the 6 in. steam and $1\frac{1}{2}$ in. condensate return system shown in the mechanical tunnel. Existing service along the quay wall to Mooring "A" will be rerouted to the north and temporary lines installed. The system consists of an insulated steam main of 80,000 lb per hr capacity and a high pressure condensate return line. Service connections will be provided at each mechanical service gallery station, in the service building, and at the three Wheeler manholes on the East mole. Approximately 10,300 ft of $\frac{1}{2}$ in. to 12 in. diameter pipe will be required, with an estimated total weight of 125 tons.

A process known as the Wheeler System is used to loosen oil sludge and remove it from shipboard storage tanks while the vessel is in drydock. To accomplish this operation, fresh water is taken into the Wheeler units, which are located on skids, and heated to near boiling with steam. The heated water is pumped through the high-pressure Wheeler line into the ship's oil tanks where it loosens the oil sludge and converts it to a froth. The dirty water and froth are removed through the suction line and are pumped into a floating tank at the seaward end of the dock. The Wheeler system valve bank will thus connect to the fresh water, steam, and compressed air as well as the 6 in. suction and discharge, and 4 in. high-pressure Wheeler system lines shown on Fig. 5. A total of 3,500 ft of 4 in. to 6 in. pipe is required with an estimated total weight of about 45 tons.

The ships sanitary sewer system consists of ten transverse 6 in. cast iron lateral sewer lines located at 96 ft centers in the floor of the dock. Provisions will be made for six connections to each lateral, except for the two inboard laterals which will provide for five connections each. The sewage will drain to a sewage wet well in the pumpwell, where pumps will transport it to a lift station in the Shipyard Interceptor Sewer System. Two 300 gpm at 90 ft

head suction pumps will be provided, each pump capable of passing 3 in. solids. The pumps will be driven by a 20 hp electric, open. drip-proof motor. The system is designed to serve a population of 3,100 men and contains 3,500 lineal ft of pipe, varying from 6 to 10 in. in diameter weighing approximately 80 tons.

Included in the electrical tunnel are telephone, fire alarm, and secondary services. Primary services are carried in ducts and manholes to the substations and pumpwell. Cables will be carried on racks as shown in Fig. 5 and terminated in boxes at the service stations which will be provided at approximately 150 ft intervals in the service gallery.

ELECTRICAL SYSTEM

Electrical energy is available in the Shipyard from three sources. The Bonneville Power Administration can deliver 27,000 kva through two transformer banks from a 115 kv supply to the PSNS 11.5 kv feeder system. The Puget Sound Power and Light Company can deliver 15,000 kva through a transformer bank from their 69 kv system. The Central Power Plant of the Shipyard can produce 18,000 kva of emergency power. Electrical energy is distributed underground by an 11.5 kv, three-phase system to substations scattered throughout the shipyard so that any one or all three sources of power can supply any load.

The primary feeder system to the Carrier Repair Site, shown in Fig. 6 is arranged to be flexible and to provide a maximum of service. As such it follows the pattern of the existing loop system which reaches any distribution substation from at least two main stations. Primary 11,500 volt power is received at substations 83, 84 and 85, and the compressor building to form a new loop following the established shipyard pattern. Each cable run terminates with a circuit breaker having 250,000 kva interrupting capacity and is protected by a pilot wire relay system. Connections to the Shipyard Primary 11,500 volt network will be made at existing Substation F, northwest of Drydock No. 4; and in Manhole No. 191 south of the new Compressor Building.

Transformer capacity of approximately 21,250 kva will be installed as follows:

Substation No. 83 - 9750 kva
Substation No. 84 - 3000 kva
Pumpwell Substation - 7500 kva
Compressor House - 1000 kva

The primary network cables shown by dash-dot line in Fig. 6 will be run through underground ducts and manholes between terminal points. The secondary cables at the drydock will be run between the substations and service galleries on cable racks installed in the electrical tunnel as previously shown. There will be seven shore to ship connections on each side of the dry dock, each providing a variety of voltages.

An approximation of the size of the installation can be gained by the following quantities required:

12 miles of 500,000 cm., 15 kv primary cable
8 miles of three-conductor cable

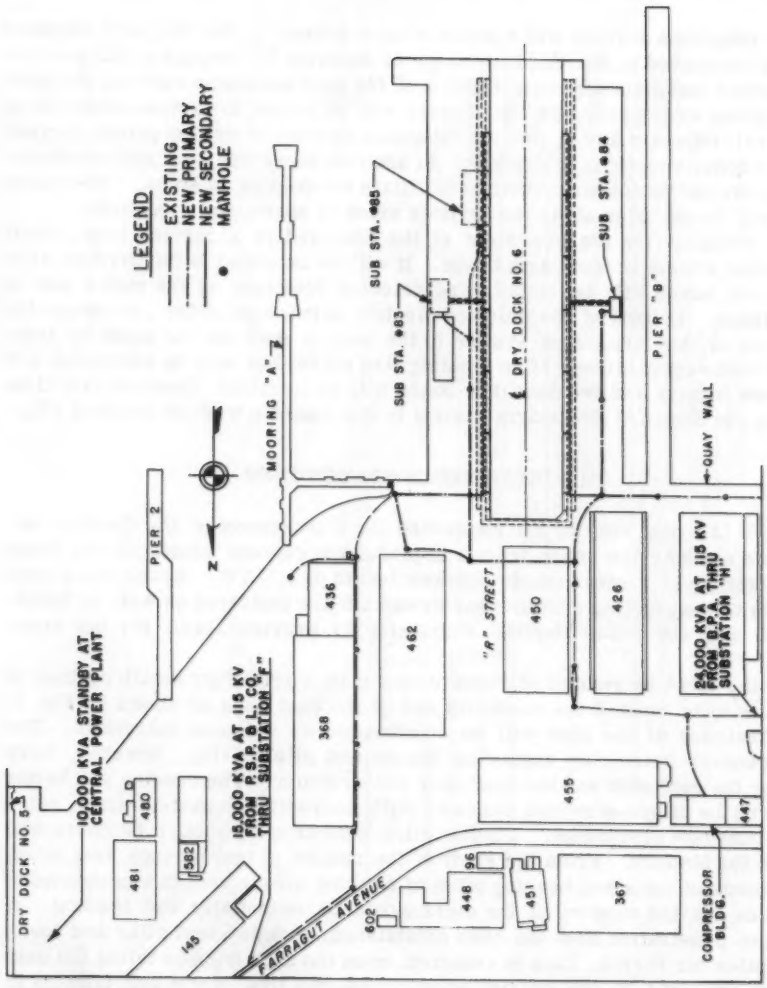

FIG. 6.—ELECTRICAL POWER

12 miles of miscellaneous cables
10 miles of underground duct
2 miles of underground steel conduit
1/2 mile of cable tunnel
Nine electrical manholes
Six steel floodlight towers, approximately 100 ft high

The telephone service will consist of an extension of the Shipyard standard system connected to the Yard exchange in Building 78 through a 202 position main frame and approximately 4,600 ft of 152 pair telephone cable in the main run. Cables with lesser number of pairs will be routed to various locations at the Carrier Repair Site to provide telephone service at needed points, including connections to ships in drydock. In addition there will be a self-contained sound powered telephone circuit to facilitate the docking of ships. The phone jacks will be installed along the drydock sides at appropriate locations.

The existing fire alarm system at the Shipyard is a service loop circuit with coded wheels in the alarm boxes. It will be extended to the drydock area and alarm boxes will be installed at selected locations on the moles and in substations. In each of the fourteen electric service galleries provisions for extension of this fire alarm system to the ship in dock can be made by temporary cable connections. One existing fire alarm box will be relocated, and eight new master and two auxiliary boxes will be installed. Connection will be made to the Shipyard fire alarm system in the manhole west of Building 450.

MISCELLANEOUS STRUCTURES

Fig. 7 is a plan view of the completed first increment of the Carrier Repair Site showing the crane tracks in place, the cassion seated in the inner seat which gives a clear inside drydock length of 1,122 ft. Crane track connections to the existing system near drydock 5 are indicated as well as Building 450 and 480 which require shortening to provide space for the crane tracks.

For the first increment of construction only a relatively small portion of Pier 9 is to be built at the southerly end of the east mole as shown in Fig. 7. The remainder of the pier will be constructed as a future increment. The same general principles regarding design and pile driving, however, were used for the pier stub and the final pier construction. The bearing and batter piles will be of pre-stressed concrete with conventional cast-in-place reinforced concrete pier decks. Timber piles backed up by rubber bumpers will be used for fenders. From the study of the results of test borings, test piles, and records of tests and bearing piles of existing structures, it was concluded that piles for the support of the piers would be essentially end bearing. A minimum penetration line has been established, both for test piles and foundation piles for Pier 9. This is required, even tho side friction in the fill may give the required 80 ton bearing value above this line, since skin friction in the fill may ultimately be decreased by settlement. The Contractor is allowed to jet to within 3 ft of minimum required penetration since this will tend to eliminate much of the unreliable skin friction. A design loading of 600 lb per sq ft is used for pier decks while bulkheads are designed with a surcharge of 300 lb per sq ft, assumed to act over an infinite length of wall.

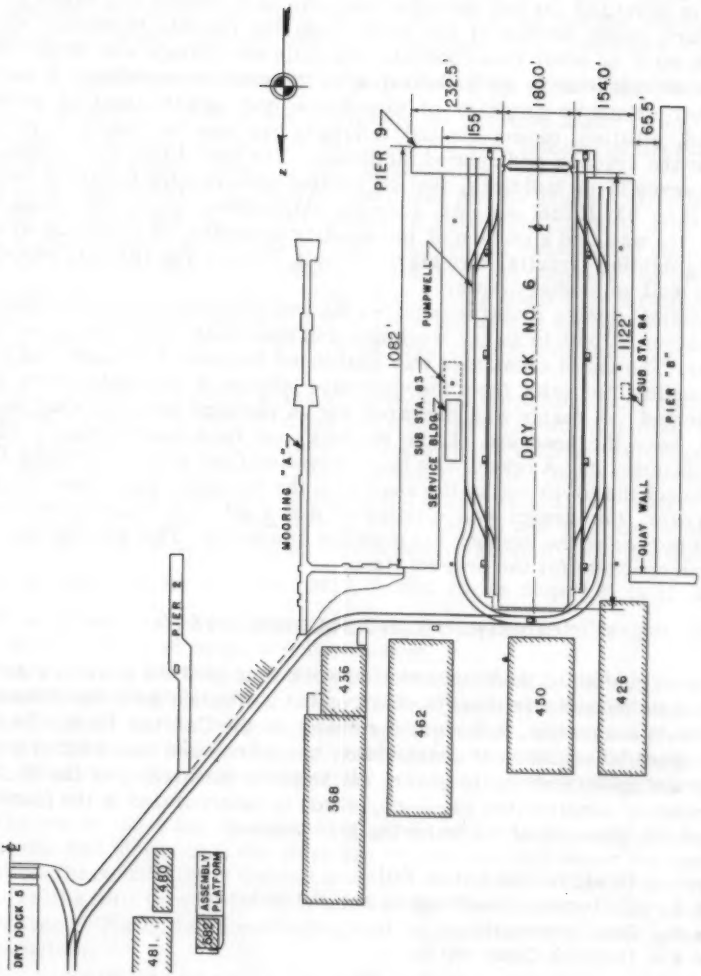

FIG. 7.—DRY DOCK NO. 6

The crane track installation on the concrete structure as shown in Fig. 5, is original for this project in such respects as: (1) The anchor bolts do not extend into the main structural concrete; (2) The slots in the main concrete to contain the rail and casing concrete slope inward at the sides to increase shear resistance and to provide for positive, inverted arch action for resisting uplift due to flexible foundation action; and (3) Non-shrink producing admixture is specified for the encasing concrete to minimize any slight movements which might develop at the sides from the flexible foundation action. For track work on other than concrete, the rails and fittings will be placed on treated wood ties to allow for reballasting in the event of settlement of the fill.

A rather extensive program of demolition and modification of existing structures, utilities, pavements and railroads has been necessary to provide space for the drydock and related facilities. The demolition will include removal of seven large buildings, fuel oil loading and transfer facilities including a 20 ft by 532 ft fuel oil pier, four old shipbuilding ways, 570 lineal ft of concrete sea wall and a portion of the existing underground electrical system containing lighting circuits, fire alarm circuit, 26 pair and 101 pair telephone cables as well as primary power.

The original design criteria required the use of elevators or escalators or a combination of both to carry workmen and materials to and from the drydock floor. The use of escalators was abandoned because of the cost and difficulty of sealing the units from the corrosive effects of salt water during the flooded period. A design was prepared for an elevator unit in a shaft on the east side near the head end of the drydock, set back approximately 100 ft from the coping line. A tunnel with floor elevation flush with the drydock floor would connect the lower end of the shaft with the drydock. For economic reasons however, this design was eliminated and a pit will be provided in the northeast corner of the drydock for possible future use. This pit will be filled with a lean concrete for the present time.

CONSTRUCTION REQUIREMENTS

The usual custom in Navy construction work is to give the general contractor the widest possible latitude in construction methods. In a significant departure from convention, however, the design of the Carrier Repair Site requires a specific sequence of construction operations and exact adherence to the plans and specifications to assure satisfactory functioning of the facility. This mandatory construction sequence, which is incorporated in the plans and specifications, consists of the following four phases:

Phase 1 - Dredging and Initial Fill
Phase 2 - Cofferdam Construction and Embankment
Phase 3 - Site Preparation
Phase 4 - Drydock Construction

The initial requirements of Phase 1 include the dredging and a portion of the demolition previously described. The fuel pier previously listed for removal was located in the area to be dredged, thus requiring early disposal. A prerequisite to demolition of the Fuel Pier, however was construction of a replacement fuel oil facility to preclude interference with Shipyard operations.

Removal of unsatisfactory foundation material by dredging has been previously covered. The dredged material was pumped through a 6,000 ft dis-

charge line to a disposal area in a deep portion of Sinclair Inlet. A thought-provoking problem arose when it was discovered that conventional sweeping methods, conducted after dredging to grade was accomplished, were unsuccessful in removing a boundary layer of loose silt. This layer, up to 3 ft in thickness, was in a flocculated semi-liquid state and was obviously unsatisfactory as a base for permanent fill. Although there was reasonable speculation that this layer could be displaced laterally as a mud wave by filling operations, this occurrence was by no means assured and the possibility of a plane of low shear strength and high compressibility remained a problem. The final solution was placement of a $\frac{3}{4}$ in. to 3 in. gravel blanket to assure foundation-to-fill interlock and to provide the required shear strength. Care was taken to restrict the gravel blanket to the area inboard of the cut-off wall to prevent a seepage channel of high permeability.

Fig. 8 shows the initial construction phase for the drydock after the dredging has been completed. It will consist of filling the dredged area to El. 70 with a select material barged in from a borrow pit constructed especially for this job about 3 miles across Sinclair Inlet from the Shipyard. At the option of the contractor, the fill may be humped where the sheet pile cut-off walls will be driven. Approximately 451,000 cu yd of fill will be deposited in this phase with a minimum placed in the dry dock area since it will later have to be removed.

Fig. 9 shows the second phase of drydock construction. The first operation during this phase has been to drive the sheet pile cut-off wall along each side of the dock and construct an eleven cell sheet pile cellular cofferdam around the outboard end of the dock. The contractor started phase 2 operations in a portion of the area where the dredging and initial backfill had been completed.

The area above the broken line in Sections A-A and B-B shows where additional backfill is to be placed. As shown in Section A-A, the fill will be brought to El. 116, or 7 ft above MLLW, and will be sloped $2\frac{3}{4}$ to 1. Fill work is being accomplished by hydraulic washing methods from barges. Approximately 605,000 cu yd of fill will be required.

A rock facing for tidal protection will be placed on the fill slope at the outboard side of the sheet piling. The width of the berm inboard of the cut-off wall will be 30 ft. As will be noted in Section B-B, the outboard side of the cellular cofferdam is driven into the subgrade, whereas the inboard piling are only driven into the first stage of the selected fill to predetermined cut-off grades.

The top of the piles in the cut-off walls and cellular cofferdams will be about one foot higher than the elevation of extreme high water for this area to preclude the possibility of topping and attendant possible loss of the structure. Pile lengths will vary from 95 ft to 99 ft for the outer face and 63 ft for the inner face. The cellular cofferdam will be removed in a later phase of the construction.

Site preparation, or construction phase 3, is shown in Fig. 10 and consists of dewatering the site, trimming the side slopes, necessary site excavation in the dry and the construction of the head-end and pumpwell cofferdams. As previously noted the dewatering procedures are the responsibility of the contractor but are subject to the approval of the Officer in Charge of Construction. The contractor will also make provision for a temporary flooding system of such size and capacity as to flood the drydock to a balanced water level

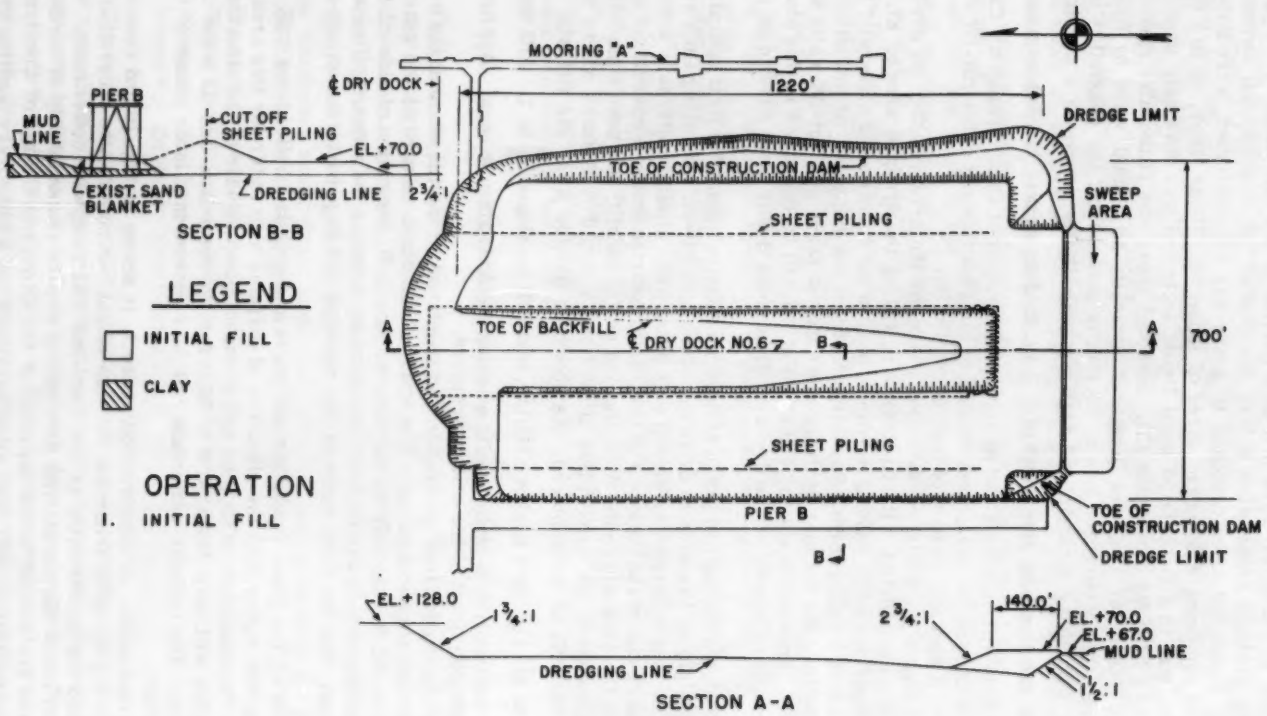

FIG. 8.—INITIAL FILL (PHASE 1B)

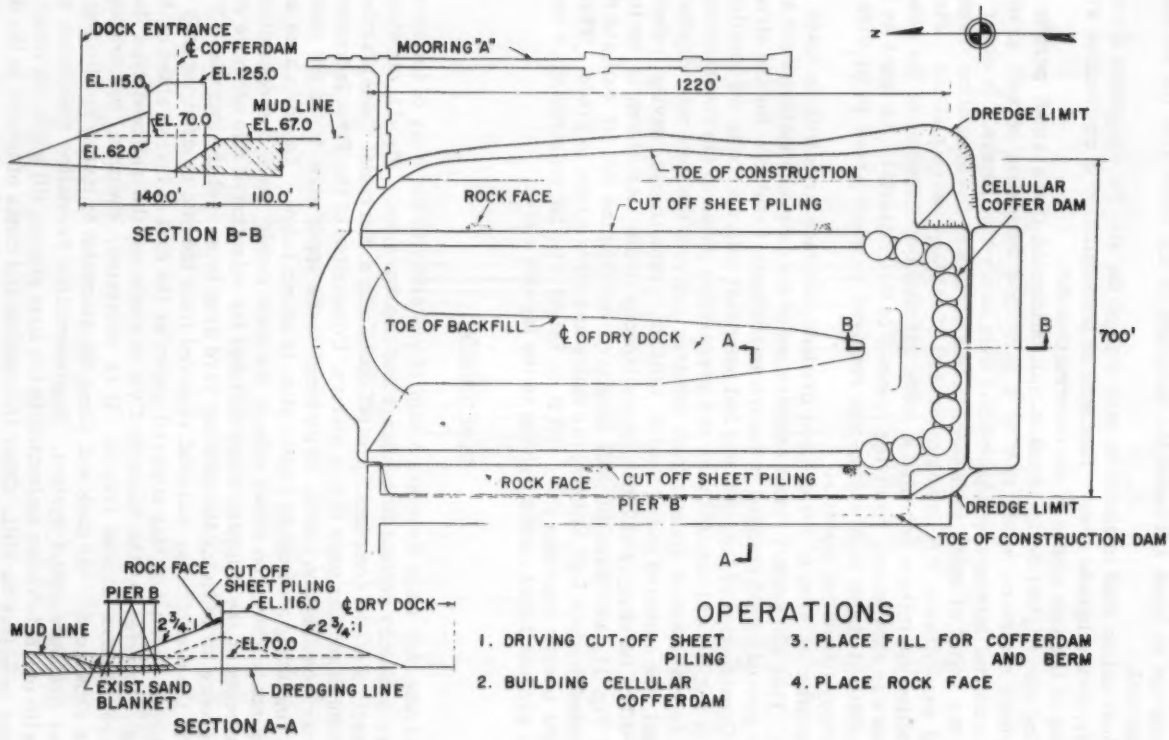

FIG. 9.—COFFERDAM AND BERM FILL (PHASE 2)

within a 12 hr period. This provision is made for the event of an emergency wherein damage to the cofferdam and existing structures might result if the area were not flooded. The ground water level after dewatering the site is to be maintained at least 2 ft below the subgrade of the excavation for the dock and pumpwell.

A construction road is shown on each side of the site for equipment access to the drydock subgrade area. This will be accomplished in conjunction with trimming of the side slopes of the construction dam.

During the original design work it was anticipated that a small portion of the drydock structure would rest on a stratified foundation of well graded gravel material interspersed with some hard sandy clay lenses. In order to insure the relief of uplift pressures in this portion of the foundation, twenty vertical sand drains, 2 ft in diameter and 15 ft deep, were planned. Field construction operations revealed a more extensive distribution of the sandy clay than was anticipated, requiring removal of this material. As much as 20 ft of additional depth of dredging was required in some areas to provide a satisfactory foundation material.

Excavation of most of the critical drydock subgrade area will be made in the dry. This will permit visual examination of the subgrade material and allow for possible field changes to insure an adequate foundation for the structure. Construction of the head end and pumpwell cofferdams in the locations shown in Fig. 10 will complete the site preparation phase of the construction.

The fourth phase of construction involves building the concrete drydock, pumpwell, the outboard end of Pier 9, utilities, crane tracks, paving, substations, utility building, and other miscellaneous items. As shown in Section B-B of Fig. 11, additional fill will be placed between the cut-off wall and the constructed drydock wall to bring the moles and other areas to grade. Three floodlight towers approximately 100 ft in height will be constructed on each mole to provide 3-foot candle lighting in the lay-down area.

CONCLUSION

The transition from the wooden ship of yesterday to the Navy of tomorrow provides a history replete with change and improvement. Fig. 12, showing a cross section of the completed project containing a Forrestal Class Carrier, could furnish another page in this history. Completion of the First Increment, now under construction (1960), is pictured in the upper view while the entire project, including a complete repair pier, is shown below. Laydown area and working space shown on either side of the dock result from the operational requirements of the shipyard which dictated the selection of this offshore site in preference to reducing the existing yard area by an inshore location. The extent of the organic clay material removed from the site by dredging may be noted by the overlay of this material shown at the east and west sides of the drawing. Dwarfed by the massive CVA it contains, the relieved type dock structure appears almost fragile. It is protected, however, by drainage courses shown under the deck and along the sidewalls to insure functioning of the vital pressure relief system. Representative foundation conditions are noted with one side shown embedded in the firm glacial till while the other is supported on select backfill. Other innovations and items of import in the design and construction of the Navy's largest drydock are the unique features of the flooding and dewatering systems, the prototype caisson and the prearranged compulsory phasing of the construction operations.

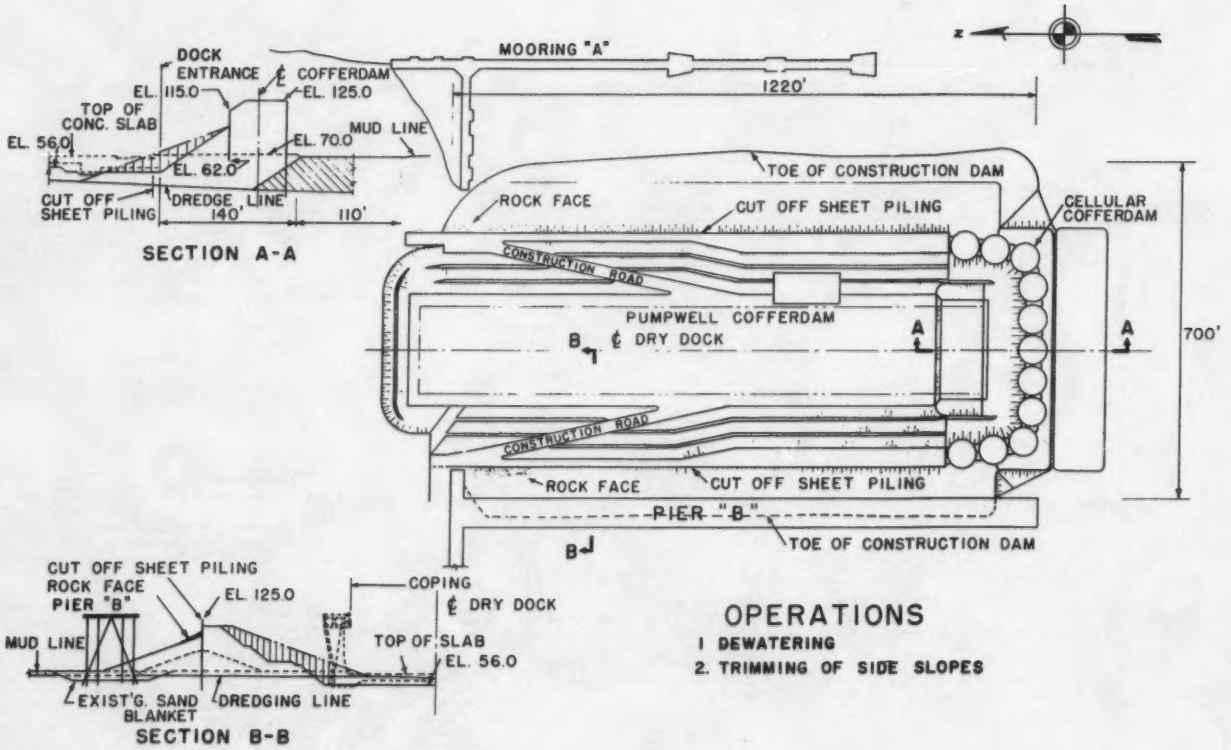

FIG. 10.—SITE PREPARATION (PHASE 3)

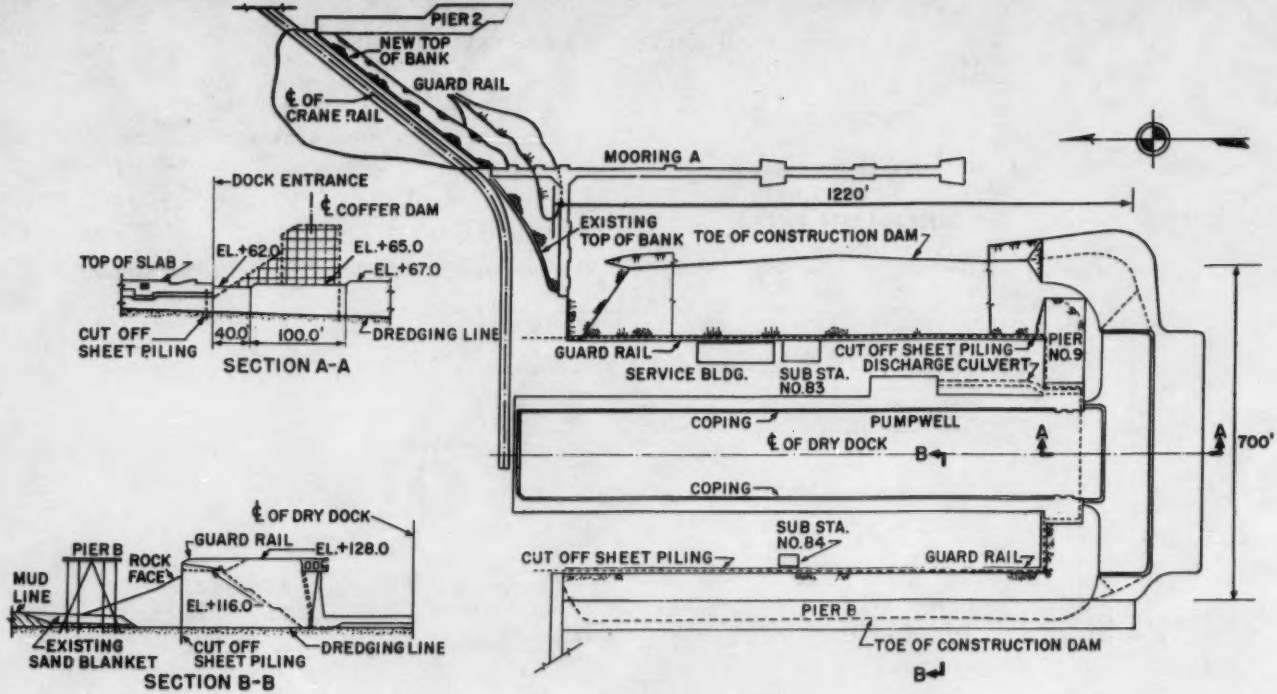

OPERATIONS

1. CONSTRUCT DRY DOCK
2. COMPLETE BACKFILL
3. REMOVAL OF ENTRANCE COFFERDAM CELLS
4. CONSTRUCTION OF PIER 9

FIG. 11.—DRY DOCK IN PLACE - INCREMENT I (PHASE 4)

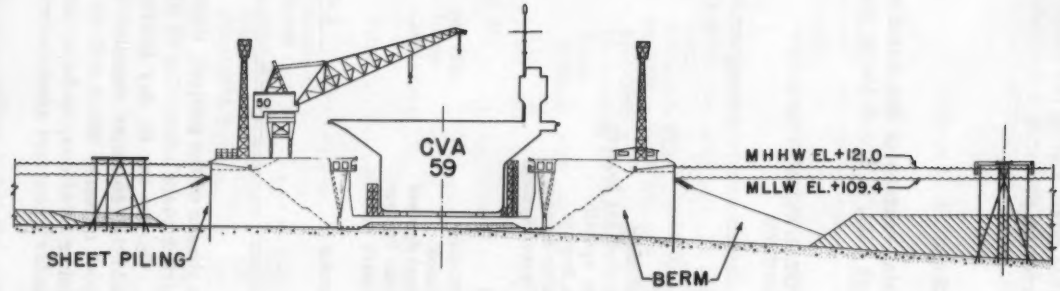

FIRST INCREMENT

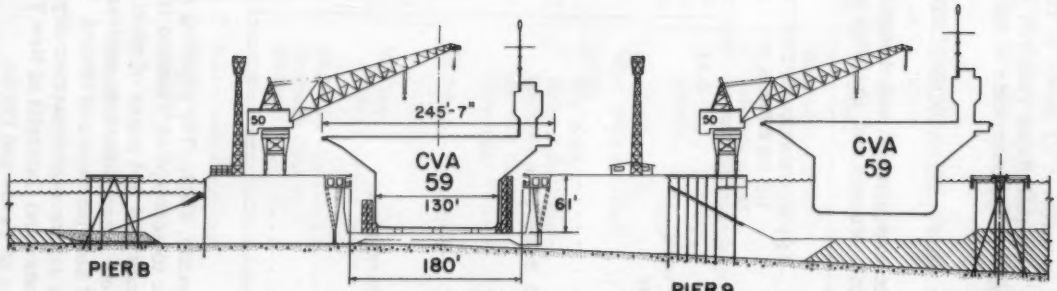

COMPLETED CONSTRUCTION

FIG. 12.—CARRIER REPAIR SITE

The relative workload for this project by construction categories is listed in Table 1. This shows a preponderance constituting over 75% of the job to be in the dock structure and associated marine work. A further concept of the scope of the project may be gained by review of a summary of the basic material quantities involved as shown in Table 2. This table, listing the quantities of major material items required for construction provides a comprehensive estimate of the magnitude of the project.

ACKNOWLEDGEMENTS

The project was planned and designed by a joint venture of the firms of Moran, Proctor, Mueser and Rutledge of New York City, N.Y. and Carey and Kramer of Seattle, Wash. The planning and design phases of the project, which required 3 yr to accomplish resulted in final contract plans consisting of 303 sheets drawings and 364 pages of specifications. During the 60 day bidding period 197 sets were issued to contractors in addition to those supplied to various AGC headquarters and others. The drydock caisson, which will be a prototype for future super-carrier drydocks at other locations, is being designed by Foster and Cafarelli of New York City under a contract administered by the Bureau of Yards and Docks.

Captain S.P. Zola, CEC USN, District Public Works Officer, Thirteen Naval District on behalf of the Chief, Bureau of Yards and Docks, awarded a contract in the amount of $21,645,000 for construction of the first increment of the project on 24 December 1959. Award was made to a joint venture of the following firms: Manson Construction and Engineering Company, Seattle,

TABLE 1.—APPROXIMATE PERCENTAGES OF TOTAL ESTIMATED COST OF DRY DOCK NO. 6, BY CATEGORIES

Demolition	0.6%	Mechanical	5.4%
Shipbuilding Ways		Piping in Docks	
Fuel Oil Pier		Pumps	
Buildings		Steam System	
Marine Work	25.0%	Compressed Air System	
Dredging		Wheeler System	
Cofferdam & Berm		Oxygen System	
Backfill		Salt Water System	
Drainage		Fresh Water System	
Structural	50.2%	Electrical	8.9%
Concrete		Pump Motors	
Reinforcing		Substations	
Misc. Structural Steel		Electrical System	
		Telephone System	
		Fire Alarm System	
Crane Tracks	4.1%	Miscellaneous	4.4%
Pavements	1.4%	Total	100.0%

Captain S.P. Zola, CEC USN, District Public Works Officer, Thirteen Naval District on behalf of the Chief, Bureau of Yards and Docks, awarded a contract in the amount of $21,645,000 for construction of the first increment of the project on 24 December 1959. Award was made to a joint venture of the following firms: Manson Construction and Engineering Company, Seattle,

Washington; J.A. Jones Construction Company, Charlotte, N.C.; Perini Corporation, Framingham, Mass.; Osberg Construction Co., Seattle, Washington. Captain P.M. Boothe, CEC USN, Public Works Officer of Puget Sound Naval Shipyard is the Resident Officer in Charge of Construction. The contract provides for completion within 1,065 calendar days after award, with a liquidated damage penalty of $5500 per calendar day for delay of completion. The

TABLE 2.—SUMMARY OF MATERIAL QUANTITIES (ESTIMATED) FOR DRY DOCK NO. 6

Material	Unit	Quantity
Dredging		
Total	CY	550,000
Fill & Backfill		
Initial Fill	CY	451,000
Berm Fill	CY	515,000
Cofferdam Fill	CY	90,500
Backfill : CY 352,000		
Spillover : CY 153,000		
Excavation: CY 100,000		
From		
C'Dam : CY 45,250	CY	53,750
Total	CY	1,110,250
Sheet Pile		
Berm	Tons	3,050
Cofferdam	Tons	2,390
Total	Tons	5,440
Concrete		
Dry Dock	CY	151,000
Pier 9	CY	900
Substation #83	CY	1,100
Floodlight Towers	CY	255
Total	CY	153,255
Prestressed Concrete Pile		
Total	LF	12,700
Reinforcing Steel		
Dry Dock	Tons	8,300
Pier 9	Tons	115
Substation #83	Tons	80
Floodlight Towers	Tons	15
Total	Tons	8,510
Misc. Iron & Struct. Steel		
Dry Dock	Tons	360
Rails & Rail Plates	Tons	320
Switches & Frogs	Tons	70
Service Building	Tons	35
Floodlight Towers	Tons	81
Total	Tons	866
Rip Rap		
Total	CY	8,400
Drainage Course		
Total	CY	92,000
Bituminous Concrete Pavement		
Total	SY	32,500
Concrete Masonry		
Total	SF	4,400

caisson, which is not yet under construction (1960), is estimated to cost an additional $1,000,000.

Throughout the 3 yr of planning and design, close coordination was necessary to resolve a multitude of technical and administrative problems and to meet scheduled dates. This project exemplifies the fine Navy teamwork of the sponsor bureau, the Bureau of Ships; the Bureau of Yards and Docks, which

has the responsibility for design and construction; the Puget Sound Naval Shipyard, the using activity; the District Public Works Officer; and the Architect and Engineer.

Without the full cooperation of all the members of the team, a project of this magnitude could not be accomplished.

The Carrier Repair Site, when completed in 1961, will provide West Coast facilities to service the largest fleet units that are in service, under construction, on the drawing boards or contemplated.

Journal of the
WATERWAYS AND HARBORS DIVISION
Proceedings of the American Society of Civil Engineers

WAVES IN NAVIGATION CANALS DUE TO LOCK FILLING

By Hans-Werner Partenscky[1]

SYNOPSIS

To allow for the increase in traffic on European canals it became necessary to replace existing locks or to improve efficiency. Such work resulted in the rapid flow of canal water. This paper is concerned with the effect of this flow on structures and ships.

INTRODUCTION

The increase of traffic intensity in European navigation canals made it necessary to replace some of the existing lock facilities by more modern ones or to improve the efficiency of the canals by the construction of additional lock chambers.

Filling and emptying times of the modern lock facilities are in general much shorter than was possible with lock chambers of the previous design. This was achieved by new filling and emptying systems (manifolds, culverts, etc.) without endangering the ships lying in the lock chamber. The filling times of the new locks are shortened by a high rate of increase of inflow from the upper pool due to a rapid rate of increase of the filling section.

Therefore the question arose as to what influence this rapid removal of the filling water and the greater peak discharges would have with respect to the water level and the navigation in the upper pool as well as in the upstream

Note.—Discussion open until August 1, 1960. To extend the closing date one month, a written request must be filed with the Executive Secretary, ASCE. This paper is part of the copyrighted Journal of the Waterways and Harbors Division, Proceedings of the American Society of Civil Engineers, Vol. 86, No. WW 1, March, 1960.

[1] Theodor Rehbock Hydrodynamics Lab., Karlsruhe, West Germany.

canal. In this regard it was important to determine limits which could be considered permissible with respect to navigation and its safety.

In the following, results are presented of extensive investigations by means of model tests carried out at the Theodor-Rehbock Hydro-dynamics Laboratory, Karlsruhe Institute of Technology, West Germany, as well as by measurements in the prototype. The complete description of these tests is available.[2]

Due to the extent of the whole investigations only the results dealing with the wave phenomena caused by lock filling are presented herein. Another publication[3] deals with the influence of the negative translation waves caused by lock filling on ships waiting in the upper pool as well as on ships or tugs moving in the upstream navigation canal. A short summary of these results is added at the end of this paper.

CALCULATIONS OF WAVE PHENOMENA

The following investigations deal with wave phenomena in the upper pool and in the upstream navigation canal caused by the filling of one or two lock chambers. However, the results of the tests can, by accounting for the positive character of these waves, also easily be applied to the wave phenomena which are caused by the emptying of a lock in the lower pool and in the downstream canal.

Wave Height and Wave Celerity.—In the following the formulas governing the wave characteristics such as wave height and celerity, etc., are presented without derivations. Definitions of the symbols used in the equations are as follows:

A = undisturbed submerged cross-sectional area, in square meters;
A_c = submerged cross-sectional area of the canal, in square meters;
A_f = submerged cross-sectional area of the upper pool, in square meters;
v = flow velocity of the canal water, in meters per second;
W = width of the water surface corresponding to a wave height z, in meters;
$W_m = 1/2\ (W_o + W)$ = mean width of the water surface, in meters;
W_o = width of the undisturbed water surface at any location, in meters;
z = wave height, in meters; and
ω = wave celerity referred to a fixed point at the shore, in meters per second

The equality in discharge removed from the upper pool and the inflow ΔQ into the lock chamber requires the following equations:

$$\Delta Q = z\, W_m \cdot \omega$$

or

$$dz = \frac{dQ}{\omega\, W_m} \qquad \text{(1)}$$

---

[2] "Der Einfluss der Schleusenfüllungen auf den Wasserstand und die Schiffahrt in einer Kanalhaltung," by H. W. Partenscky, 144. Arbeit aus dem Theodor-Rehbock-Laboratorium, Techn. Hochschule Karlsruhe, Germany.

[3] "Lock Fillings and Their Effect on Navigation," by H. W. Partenscky, Publication for the VIIIth Congress of the International Association for Hydraulic Research, Montreal, August, 1959.

The mean celerity ω of the negative translation wave can be calculated for cross sections which do not have vertical walls such as trapezoidal or quasi-circular profiles, as used in navigation canals, as follows:[4]

$$\omega = \sqrt{g\left(\frac{A}{W_m} - \frac{3}{2}z + \frac{W_m z^2}{2A}\right)} \pm V \quad \ldots\ldots\ldots \quad (2)$$

With small wave depths z the third term under the square root of Eq. 2 can be neglected, giving:

$$\omega = \sqrt{g\left[\left(\frac{A}{W_m}\right) - \frac{3}{2}z\right]} \pm V \quad \ldots\ldots\ldots\ldots\ldots \quad (3a)$$

or the St. Venant equation:

$$\omega = \sqrt{g\left(\frac{A}{W_m}\right)}\left(1 - \frac{3}{4}\frac{W_m}{A}z\right) \pm V \quad \ldots\ldots\ldots \quad (3b)$$

With small wave depths the Lagrange formula also gives sufficiently accurate results for approximate calculations:

$$\omega \approx \sqrt{g\left(\frac{A}{W_m}\right)} \pm V \quad \ldots\ldots\ldots\ldots\ldots\ldots \quad (4)$$

Wave Deformations Caused by Changes in Cross-Section.—

Sudden Changes in Cross Section.—Each change of the canal or upper pool cross section causes a deformation of the wave. The height of the transmitted wave is equal to the algebraic sum of the heights of the incident and the reflected wave. Using the indices 1, 2 and 3 for the incident, reflected, and transmitted wave, it follows:

$$z_3 = z_1 + z_2 \quad \ldots\ldots\ldots\ldots\ldots\ldots \quad (5)$$

In general, such narrowing of the cross section causes an increase in wave height of the incident wave, regardless of whether it is a positive or negative translation wave. Therefore, if the incident wave is positive, the transmitted wave will also be positive but of a greater height and the reflected wave will also be positive. On the other hand, if the incident wave is negative, a negative wave will be reflected and the depth of the transmitted wave will be increased (Fig. 1).

An enlargement of the cross section causes a transmitted wave which is of the same sense but smaller than the incident wave; the reflected wave is of the opposite sense and smaller than the incident wave (Fig. 2).

These phenomena are based on laws which can be derived from the equation of continuity and the conservation of energy. The former conditions require the following equation:

---

4 "Surges in Canals," by Dept. of the Army Corps of Engineers, Hydraulic Design Engineering Manual, Part CXVI, Chapter 6, March, 1949.

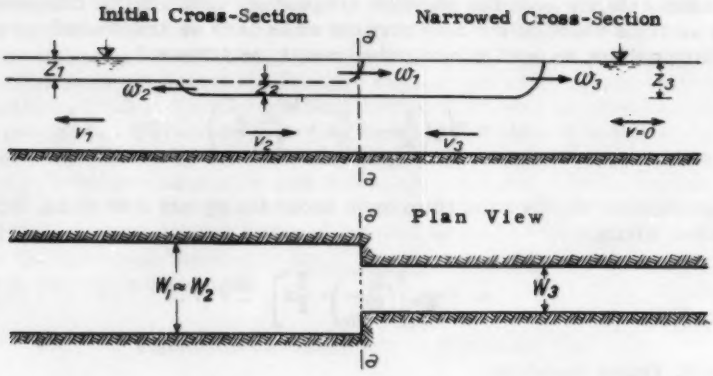

FIG. 1.—EFFECT OF ABRUPT CONTRACTION

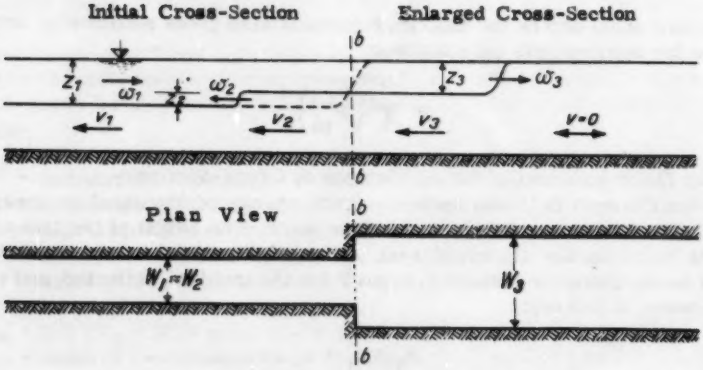

FIG. 2.—EFFECT OF ABRUPT ENLARGEMENT

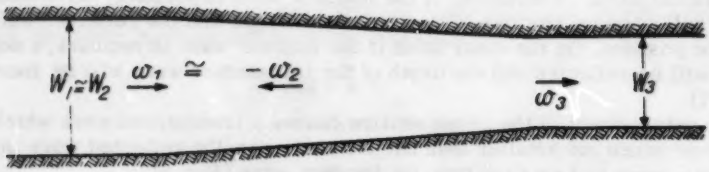

FIG. 3.—EFFECT OF GRADUAL CONTRACTION

$$W_3 z_3 \omega_3 \, dt = W_1 z_1 \omega_1 \, dt + W_2 z_2 \omega_2 \, dt \quad \ldots\ldots\ldots \quad (6)$$

With Eq. 5 for the heights of the transmitted and reflected waves the following formulas apply:

$$z_3 = z_1 \frac{\omega_1 W_1 - \omega_2 W_2}{\omega_3 W_3 - \omega_2 W_2} \quad \ldots\ldots\ldots\ldots\ldots \quad (7)$$

and

$$z_2 = z_1 \frac{\omega_1 W_1 - \omega_3 W_3}{\omega_3 W_3 - \omega_2 W_2} \quad \ldots\ldots\ldots\ldots\ldots \quad (8)$$

With the simplifying assumptions $\omega_1 \sim \omega_2$ and $W_1 \sim W_2$ it follows from Eqs. 7 and 8:

$$z_3 = z_1 \frac{2\omega_1 W_1}{\omega_3 W_3 + \omega_1 W_1} \quad \ldots\ldots\ldots\ldots\ldots \quad (9)$$

and

$$z_2 = z_1 \frac{\omega_1 W_1 - \omega_3 W_3}{\omega_1 W_1 + \omega_3 W_3} \quad \ldots\ldots\ldots\ldots\ldots \quad (10)$$

Gradual Changes in Cross Section.—For a gradual change in the cross section (Fig. 3) a calculation of the deformation in wave shape can be obtained by using Eqs. 5, 9, and 10. From Eq. 10 it follows:

$$\frac{z_3 - z_1}{z_1} = \frac{\omega_1 W_1 - \omega_3 W_3}{\omega_1 W_1 + \omega_3 W_3} \quad \ldots\ldots\ldots\ldots\ldots \quad (11)$$

For small changes in the cross section, it can be written:

$$z_3 = z_1 + d(z_1)$$

and

$$\omega_3 W_3 = \omega_1 W_1 + d(\omega_1 W_1)$$

From Eq. 11, it follows:

$$\frac{d(z_1)}{z_1} = -\frac{d(\omega_1 W_1)}{2\omega_3 W_1} \quad \ldots\ldots\ldots\ldots\ldots \quad (12)$$

Integrating and applying the appropriate limits:

$$z_3 = z_1 \sqrt{\frac{\omega_1 W_1}{\omega_3 W_3}} \quad \ldots\ldots\ldots\ldots\ldots\ldots (13)$$

With small wave heights the wave celerity can be calculated from Eq. 4. With $v = 0$ for the flow velocity in the upstream navigation canal, Eq. 13 gives:

$$z_3 = z_1 \sqrt[4]{\frac{A_1 W_1}{A_3 W_3}} \quad \ldots\ldots\ldots\ldots\ldots\ldots (14)$$

Special Cases for the Changes in the Cross Section.—If the incident wave reaches an end-wall of the canal, it follows with $W_3 = 0$ from Eq. 10 $z_2 = z_1$. That means that the height or depth of the resultant wave at the end wall is doubled.

Assuming that the wave front has reached the wall at the time $t = 0$, the shape of the resultant wave at any time $t > 0$ can be easily obtained when first it is assumed that the wave is progressing in a canal of uniform cross section. Thus, having obtained the extended location of the wave front at the time t, the wave, which is dashed in Fig. 4 has to be superimposed to that part of the incident wave which has not yet reached the wall (Fig. 4).

On the other hand, if an incident wave reaches a basin with a very large width, with $W_3 \to \infty$ it follows from Eq. 9 $z_3 \to 0$ and from Eq. 10 $z_2 \to - z_1$. That means that the incident and the reflected wave cancel out.

Crossing of Waves.—With the symbols of Fig. 5 for the crossing of two waves the following equations apply:

$$z_1 - z_4 = z_3 - z_2 \quad \ldots\ldots\ldots\ldots\ldots\ldots (15)$$

and

$$z_1 W_1 \omega_1 - z_4 W_4 \omega_4 = z_3 W_3 \omega_3 - z_2 W_2 \omega_2 \quad \ldots\ldots\ldots (16)$$

In these equations the ω - values have to be used corresponding to the direction of the wave motion and the z - values have to be provided with the corresponding sign depending on the sense of wave.

With the simplifying assumption that the mean widths and celerities of the waves travelling in the same direction remain unchanged during the crossing and furthermore neglecting the effect of energy loss it can be stated that the waves cross each other without changing their initial heights. During the superposition, the heights of the waves are added algebraically.

THEORETICAL INVESTIGATIONS OF THE FILLING PHENOMENA

The changes in water level in the upper pool and in the upstream navigation canal, caused by the removal of the filling water during the lock filling, depend primarily on the volume rate of inflow. For each kind of lock this depends on the lock size and filling system and is characterized by the filling curve $Q = f(t)$ (Fig. 6).

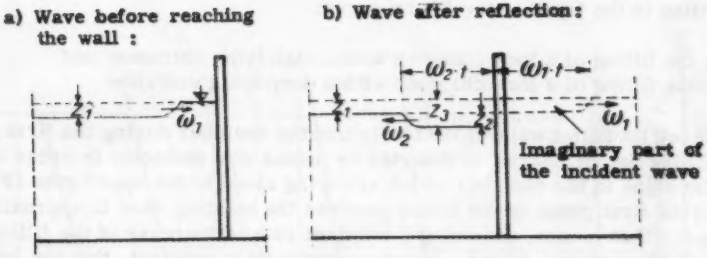

FIG. 4.—REFLECTION OF NEGATIVE WAVE AT VERTICAL WALL

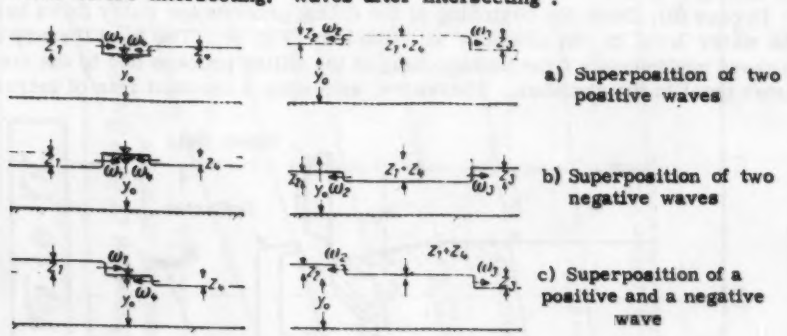
Waves before Intersecting:
Waves after Intersecting :
a) Superposition of two positive waves
b) Superposition of two negative waves
c) Superposition of a positive and a negative wave

FIG. 5.—SUPERPOSITION OF TWO WAVES

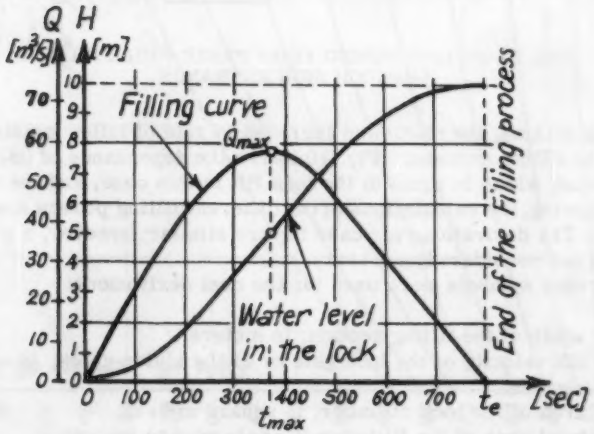

FIG. 6.—LOCK-FILLING CHARACTERISTICS

There are two different kinds of lock fillings which must be distinguished according to the trend of the filling curve:

(a) the filling of a lock chamber with a high lying entrance; and
(b) the filling of a lock chamber with a deep lying entrance

In case (a), the filling water flows freely into the chamber during the first phase. The filling jet of course is diverted by means of a deflector in order to protect the ships in the chamber which are lying close to the upper gate (Fig. 7). During the first phase of the filling process the existing head is approximately constant. That means, assuming a constant rate of increase of the filling section and a correction factor μ being approximately constant, that the increase in rate of inflow dQ/dt is also nearly constant. For case (a) in Fig. 8, the values dQ/dt are plotted versus the initial head H_O with the rate of increase of the filling section as the parameter.

In case (b), from the beginning of the filling process the water flows below the water level of the chamber into the lock (Fig. 9). The head thereby decreases continuously from the beginning of the filling process due to the rising water level in the chamber. Therefore, assuming a constant rate of increase

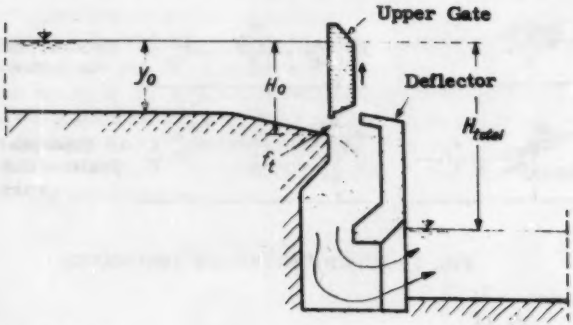

FIG. 7.—INFLOW DURING FIRST PHASE WHILE FILLING THROUGH HIGH ENTRANCE

of the filling section, the maximum increase in rate of inflow exists at the beginning of the filling process. Fig. 10 shows the dependance of $(dQ/dt)_{max}$ on the initial head, which is equal to the lock lift in this case, and the value n.

In the following, the calculations of the different filling phases are presented for case (b). The derivations for case (a) are similar; however, a presentation of them was not considered necessary.

The following symbols were used for the next derivations:

- b = width of the filling section, in meters;
- c = lift velocity of the lock gate or of the sluice gates, in meters per second;
- F = area of the lock chamber, in square meters;
- f_1 = total area of the filling section, in square meters;
- f_t = existing filling section at the time t, in square meters;
- H_o = initial head, in meters;

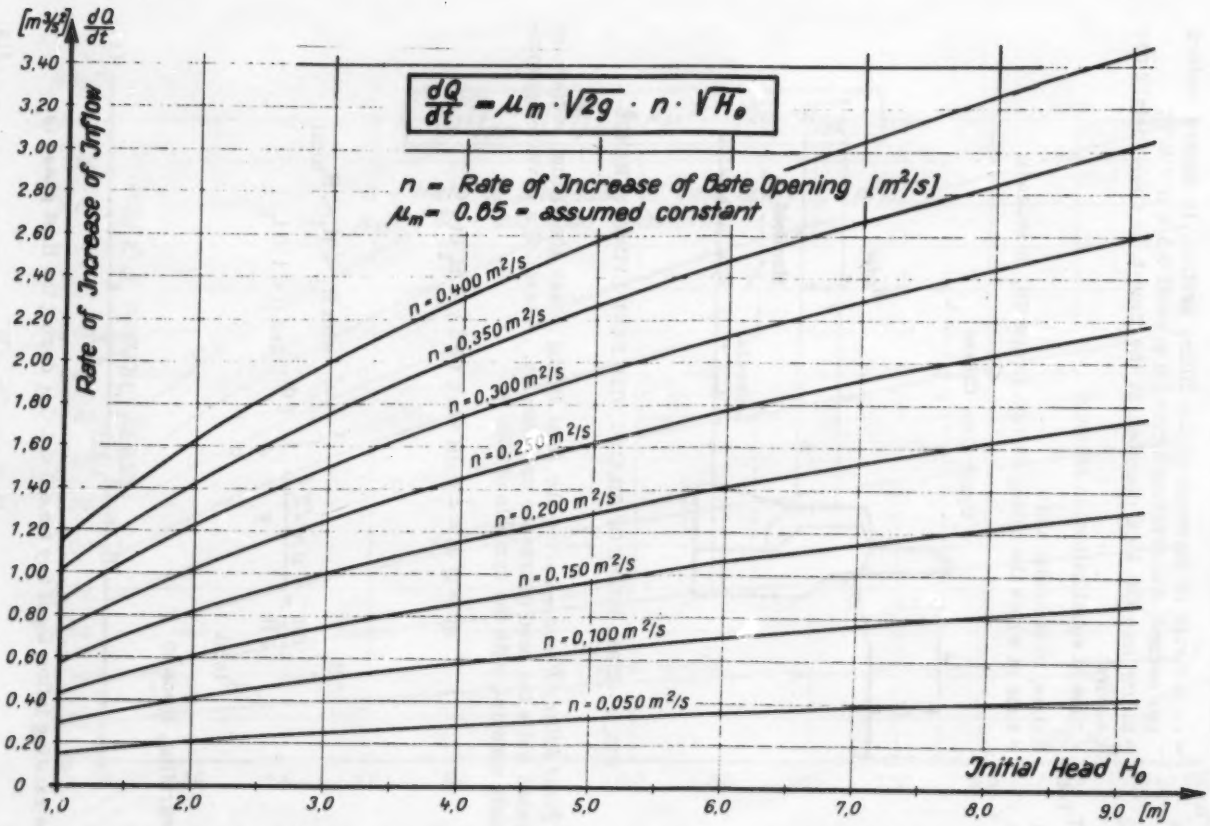

FIG. 8.—RATE OF INCREASE OF INFLOW DURING FIRST PHASE OF FILLING THROUGH HIGH INFLOW

H_t = existing head during the filling process at the time t, in meters;

H_{total} = lift of the lock, in meters;

n = c · b = rate of increase of the filling section, in square meters per second; = correction factor (in general $0.5 < \mu < 0.7$);

Q_t = inflow into the lock chamber at the time t, in cubic meters per second;

T_{Total} = time of equalization, in seconds;

t = time, in seconds; and

t_1 = time at which the filling section is opened, in seconds.

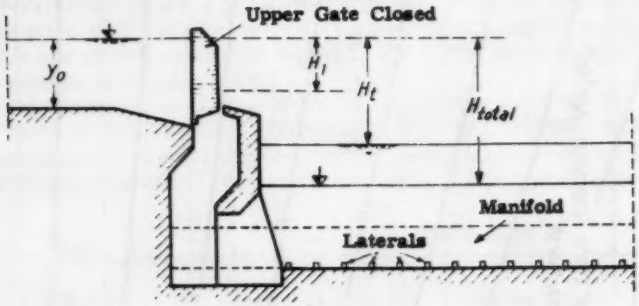

FIG. 9.—FIRST PHASE OF FILLING WITH DEEP LYING ENTRANCE

First Filling Phase.—During the first filling phase the filling section increases while the head decreases continuously. Assuming a μ-value approximately constant, with the symbols of Fig. 9

$$dV = Q\,dt = -F\,dH = \mu n t \sqrt{2g}\sqrt{H_t}\,dt$$

or

$$\int_{H_{total}}^{H_t} \frac{dH}{\sqrt{H}} = -\frac{\mu n \sqrt{2g}}{F} \int_0^t t\,dt \qquad \text{with } H_1 < H_t < H_{total} \text{ and } 0 < t < t_1$$

Integrating, leads to

$$\sqrt{H_t} = \sqrt{H_{total}} - \frac{\mu n \sqrt{2g}}{4F} t^2 \quad \ldots\ldots\ldots\ldots (17)$$

The existing inflow Q_t at any time $0 < t < t_1$ during the first phase is:

$$Q_t = \mu f_t \sqrt{2g}\sqrt{H_t} \quad \ldots\ldots\ldots\ldots\ldots (18)$$

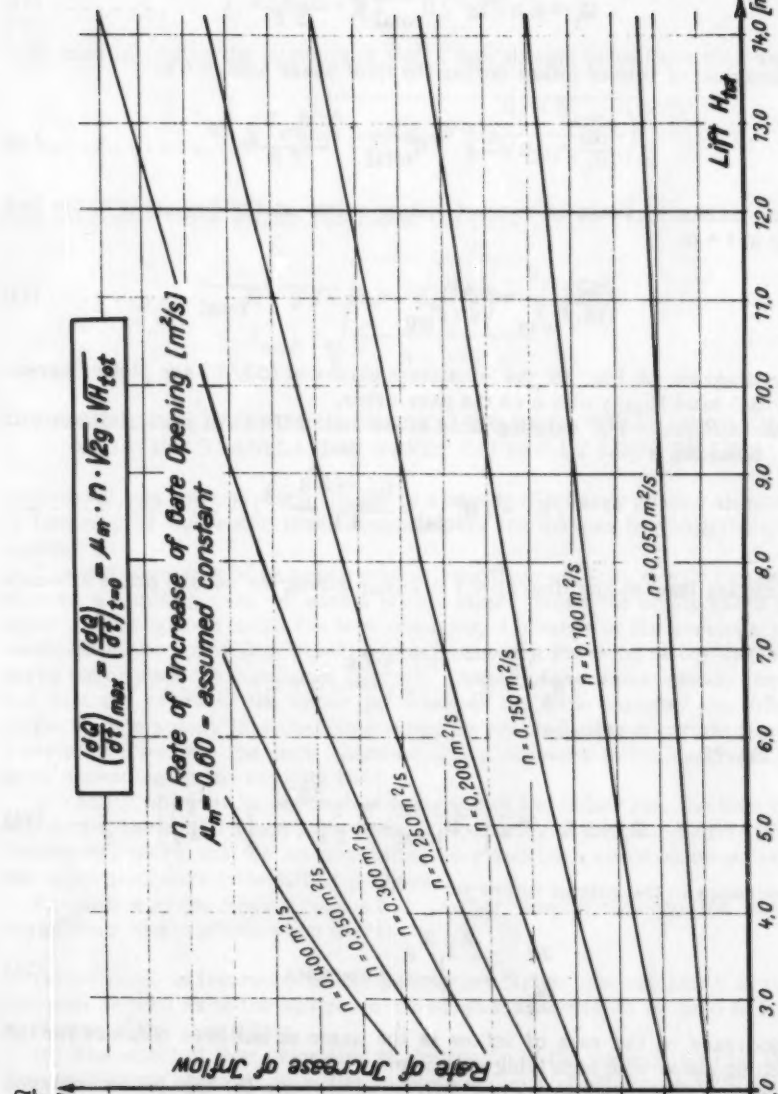

FIG. 10.—MAXIMUM RATE OF INCREASE OF INFLOW DURING FIRST PHASE OF FILLING THROUGH A DEEP LYING ENTRANCE

Using Eq. 17 it follows from Eq. 18 that:

$$Q_t = \mu n \sqrt{2g}\ \sqrt{H_{total}}\ t - \frac{\mu^2 n^2 g}{2 F}\ t^3 \quad \ldots\ldots\ldots (19)$$

The increase of rate of inflow during the first phase amounts to

$$\frac{dQ}{dt} = \mu n \sqrt{2 g}\ \sqrt{H_{total}} - \frac{3 \mu^2 n^2 g}{2 F}\ t^2 \quad \ldots\ldots\ldots (20)$$

The maximum increase of rate of inflow exists at the beginning of the lock filling at t = 0:

$$\left(\frac{dQ}{dt}\right)_{max} = \left(\frac{dQ}{dt}\right)_{t=0} = \mu n \sqrt{2 g}\ \sqrt{H_{total}} \quad \ldots\ldots\ldots (21)$$

In the diagram of Fig. 10 the maximum values of (dQ/dt) are plotted versus the initial head H_{total} with n as the parameter.

Second Phase.—The existing head at the end of the first phase follows with $t = t_1$, from Eq. 17:

$$\sqrt{H_1} = \sqrt{H_{total}} - \frac{\mu f_1 \sqrt{2 g}}{4 F}\ t_1 \quad \ldots\ldots\ldots\ldots (22)$$

The existing head at any time $t_1 < t < T_{total}$ during the second phase amounts to:

$$\sqrt{H_t} = \sqrt{H_1} - \frac{\mu f_1 \sqrt{2 g}}{2 F}\ (t - t_1) \quad \ldots\ldots\ldots\ldots (23)$$

Using Eq. 22:

$$Q_t = \mu f_1 \sqrt{2 g} \left[\sqrt{H_{total}} - \frac{\mu f_1 \sqrt{2 g}}{2 F}\ \left(t - \frac{t_1}{2}\right)\right] \ldots\ldots\ldots (24)$$

The increase in the rate of inflow is:

$$\frac{dQ}{dt} = \frac{-\mu^2 f_1^2 g}{F} = \text{constant} \quad \ldots\ldots\ldots\ldots\ldots (25)$$

The decrease of the rate of inflow is the same as has been obtained for the last filling phase with high lying entrance.[2]

Maximum Inflow During a Lock Filling.—For case (b) the inflow reaches its maximum value at the time $t_{max} < t_1$ From Eq. 20 with $\frac{dQ}{dt} = 0$ it follows:

$$t_{max} = \sqrt{\frac{4 F \sqrt{H_{total}}}{3 \mu n \sqrt{2g}}} \quad \ldots\ldots\ldots\ldots\ldots (26)$$

Using this value in Eq. 19 one obtains:

$$Q_{max} = \sqrt{\frac{16}{27} \mu \sqrt{2g}\ n\ F\ H_{total}^{3/2}} \quad \ldots\ldots\ldots\ldots (27)$$

In case (a), using the symbols of Fig. 7 one obtains in an analogous way:[2]

$$Q_{max} = \sqrt{\frac{16}{27} \mu \sqrt{2\,g}\ \ F\ n\ \left(\frac{H_0 + H_{total}}{2\sqrt{H_0}}\right)^3} \quad \ldots\ldots\ldots (23)$$

This maximum value will be reached at the time

$$t_{max} = \sqrt{\frac{4\ F\ \sqrt{H_0}\left(0.5 + \frac{H_{total}}{2\,H_0}\right)}{3\ \mu \sqrt{2g}\ n}} \quad \ldots\ldots\ldots\ldots (29)$$

THEORETICAL INVESTIGATIONS DEALING WITH THE SHAPE OF THE NEGATIVE TRANSLATION WAVES CAUSED BY LOCK FILLING

General.—In general, each change of a steady discharge causes an increase or lowering of the water level depending on the manner in which the change occurs.

The water volume of an upper pool at rest (flow velocity v = 0) can be considered a limiting case of such a steady state. When the sluice gates or the upper gate is opened to fill the lock chamber, a change of the previous steady condition in the upper pool results, which causes a lowering of the water level in the upper pool. Assuming a discrete change of the initial steady condition and that the areas of the upper pool and of the lock chamber are infinitely large, a new steady flow condition would be reached after a certain time with a certain inflow into the lock chamber and a decrease in the upstream water level depending on the velocity head.

In reality, however, a continuous variation of the inflow into the lock chamber during the equalization period exists according to the filling curve (Fig. 6). Therefore, there will be no possibility to establish a constant water level in the upper pool during the filling process.

Formation of the Wave Front.—For further considerations, the following simplifying assumptions were made:

(a) As usual in treatment of navigation canals, the flow velocity v in the upper pool as well as in the upstream canal was assumed to be zero before the beginning of the lock filling.

(b) The effect of flow velocities in the region of the wave caused by the inflow to the lock chamber upon the absolute velocity of all elements of the wave profile was considered to be negligible.

(c) Theoretically, each point of the wave profile has a different celerity ω corresponding to its distance from the bottom. However, because of the total water depth in the upstream navigation canal which is in general relatively great compared to the maximum depth of the negative surges the small differences in wave celerity can be neglected.

(d) The still water depth in the upper pool and the upstream navigation canal was assumed to be constant, the slope of the bottom was thereby assumed to be zero.

First of all, in the following considerations an unlimited upper pool length with a constant width W_f was assumed.

When the lock gates open, a water volume of ΔQ flows into the chamber in the first second. As a result of this removal the water level sinks in the upper pool by an amount z_1. The magnitude of the lowering depends on the discharge ΔQ, the width of the upper pool W_f and the wave celerity of the first negative wave element.

Assuming that the increase in rate of inflow is approximately constant (filling with high lying entrance), a water volume of $\Delta Q + \Delta Q = 2\,\Delta Q$ flows into the chamber in the second second. The water level in the upper pool sinks an additional amount, z_2, during this time due to the increase of inflow. Thus, a second wave element is created.

In a similar manner as the first and second wave elements, the third and all of the succeeding wave elements are formed, until the time $t = t_{max}$ (see Eqs. 26 and 29) the maximum inflow Q_{max} is reached (see Eqs. 27 and 28). The sum of all wave elements occurring up to this time form the front of the negative translation wave. The maximum lowering of the water level upstream can be approximated by the sum of the depths of all wave elements occurring till t_{max}:

$$z_{max} = \sum_{i=1}^{i=n} z_i \quad \ldots\ldots\ldots\ldots\ldots\ldots \quad (30)$$

Using Eq. 1

$$z_{max} \approx \frac{Q_{max}}{\omega_m W_m} \quad \ldots\ldots\ldots\ldots\ldots\ldots \quad (31)$$

The slope of the wave front can be calculated using the symbols of Fig. 11:

$$\tan \alpha = \frac{(z_1 + z_2)}{2} \frac{1}{dt} = S_w$$

With $\omega_1 \sim \omega_2 \sim \sqrt{g \frac{A_f}{W_f}} = \omega$

and $z_1 \sim z_2 = \frac{dQ}{\omega W_f}$

$$S_w = \frac{1}{g A_f} \frac{dQ}{dt} \quad \ldots\ldots\ldots\ldots\ldots\ldots \quad (32)$$

For a lock filling with deep lying entrance the increase in rate of inflow is in general not constant, but decreases continuously. By using Eq. 32 the slope of the wave front can be determined at any time $t \leq t_{max}$. The maximum slope of the wave front, however, which is decisive with regard to navigation, exists at the leading wave element. Using Eq. 20 and Fig. 10, respectively, the maximum slope can be calculated with Eq. 21.

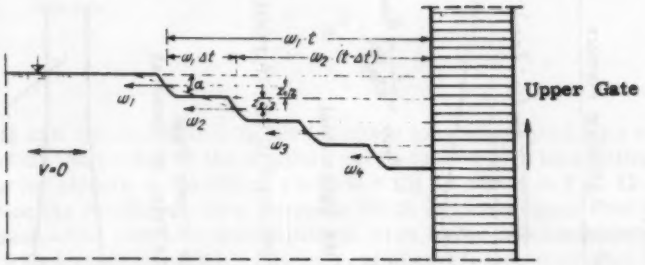

FIG. 11.—SLOPE OF WAVE FRONT

Formation of the Trailing Portion of the Wave.—When the rate of inflow decreases during an equalization period, the kinetic energy of that part of the inflow which can be no longer discharged into the lock chamber is transformed into potential energy in front of the points of removal. Therefore, the upstream water level rises in general in front of the upper gate in accordance with the inflow decrease.

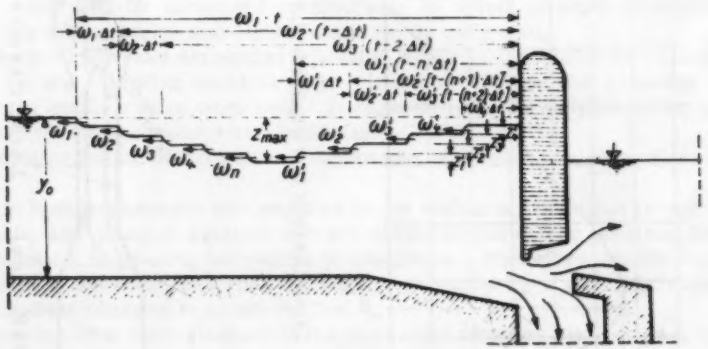

FIG. 12.—PROFILE OF WAVE DUE TO LOCK FILLING

Analogous to the considerations of the increase in rate of inflow during the first filling phase, for the last phase each change of the discharge during the time $t_{max} < t < T_{total}$ must cause a positive wave element, moving upstream against the previous flow direction. The sum of all positive wave elements form the trailing portion of the wave profile. At the time $t_{max} < t < T_{total}$ the wave can be shown as in Fig. 12.

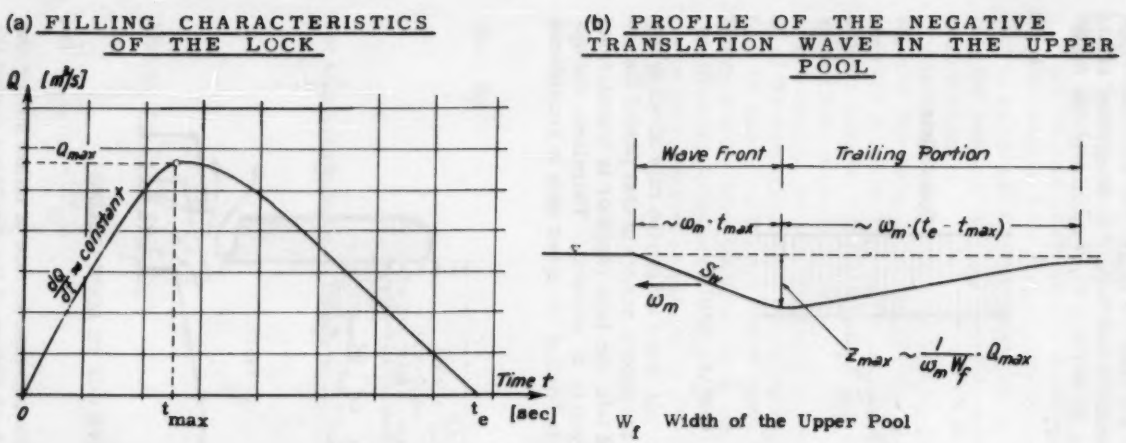

FIG. 13.—RELATION BETWEEN LOCK-FILLING CURVE AND WAVE PROFILE IN UPPER POOL

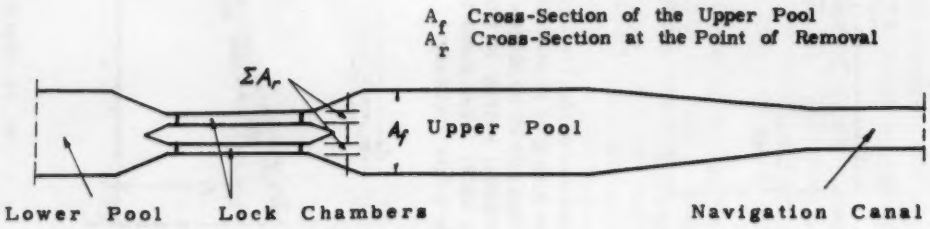

FIG. 14.—PLAN OF NAVIGATION FACILITIES

The slope of the trailing portion amounts to:

$$S'_w = \frac{1}{g\,A_f}\,\frac{dQ}{dt}$$

and with Eq. 25 to:

$$S'_w = -\frac{\mu^2 f_1^2}{A_f F} \quad \ldots\ldots\ldots\ldots\ldots\ldots (33)$$

Finally, it can be stated that in an infinitely long upper pool with a constant cross section the profile of the negative surge caused by a lock filling results in a distorted picture of the filling curve Q = f(t) as shown in Fig. 13.

Effect on the Profile due to a Variable Width Between Upper Pool and Navigation Canal.—The previous investigations were based on an infinitely long upper pool with a constant width. However, in general, the upper pool is gradually narrowed after a certain length (of about 700 to 1000 ft) to the regular width of the canal cross section depending on the size of the lock facilities and the traffic intensity in the canal. In order to guarantee safe entrance of the ships which are entering the upper pool, the transition between both of the cross sections takes place gradually, resulting in a relatively long transition region (Fig. 14).

Deformation of the Wave Front.—In passing the region of narrowing width between the upper pool and the navigation canal the negative translation wave will be deformed due to the continuous changes in cross section along this distance. This means that each wave element which forms the shape of the composite wave will be increased continuously in height or depth throughout the whole transition region and furthermore partly reflected.

The reflected wave elements (reflection waves of the first order) are superposed on the following incident wave elements. During the crossing of the waves the small loss in wave height is neglected and the heights of the crossing waves have to be added algebraically.

The deformation of the wave elements can be obtained by using Eqs. 13 or 14.

If the distance between two sections in the region of transition is sufficiently small, any desired number of wave deformations can be obtained for each wave element in passing the region of transition. Therefore, in the following the gradual decrease in cross section is replaced by a discrete number of small sudden changes in cross section.

When the first wave element of the wave front reaches the first step of narrowing, its depth z_1 increases according to Eqs. 13 or 14 and a negative reflection wave of the first order is sent back simultaneously. The latter superposes itself on the following part of the wave profile. The depth of the reflected wave is equal to the increase Δz of the incident wave element.

At the second narrowing, the new depth of the first wave element $(z_1 + \Delta Z)$ is increased again and a new negative reflection wave of the first order is sent back. This process is repeated at each new change of the cross section until the navigation canal is reached.

The depths of the second as well as of all following wave elements are increased at the profile steps in a way similar to those of the first wave element and negative reflection waves of the first order are reflected.

In travelling back, the reflection waves of the first order are again deformed at each change in cross section. But, because of their reverse direction, for them each change in cross section is an enlargement. That means that their depth decreases at each profile step and positive reflection waves of the second order are sent in the direction of the initial wave motion. The deformation of the latter at the profile steps results in reflection waves of the third and higher orders.

In general, however, the reflection waves of the second and higher orders can be neglected because of their small heights which have only an insignificant influence on the total wave profile.

With the simplifying assumption, that every wave element z_1 continues approximately with its previous celerity ω_i in the transition region, the slope of the wave front after reaching the navigation canal can be calculated by using Eq. 14:

$$S_{w_c} \approx \sqrt[4]{\frac{A_f W_f}{A_c W_c}} \; S_{w_f} = \alpha \, S_{w_f} \quad \ldots\ldots\ldots\ldots\ldots (34)$$

Deformation of the Trailing Portion of the Wave.—The deformation of the trailing portion in the transition region between upper pool and canal takes place in a way similar to that of the wave front. The height of each wave element will be increased according to Eqs. 13 or 14, and positive reflection waves of the first order will be sent back.

However, the following should be noted:

The negative reflection waves of the first order, which were sent back during the deformation of the wave front, are reflected again at the upper gates of the locks after having passed the upper pool and then pass the upper pool again in the opposite direction.

If the reflection waves reach the lock gates before the end of the equalization period, they superpose themselves to the incident wave elements caused by the last filling phase. That means that both waves travel in the same direction with about the same celerity, adding their heights.

With short lengths L_f of the upper pool and long equalization periods it is possible that the first negative reflection waves of the wave front arrive at the point of removal before the maximum discharge has been reached. In this case, the maximum lowering of the water level will be greater at this point than it would have been according to Eq. 31. This is the case, if $2\,L_f/\omega_m < t_{max}$, with ω_m = mean wave celerity.

If $2\,L_f/\omega_m > t_{max}$, greater total wave depths z_{max} at certain points in the upper pool can occur than would have been expected theoretically according to Eq. 31 depending on the superposition of negative reflection waves with incident negative wave elements of the wave front. At the point of removal however, the water level is already partly increased due to the increase in inflow when the negative reflection waves arrive. The latter, after reflecting again at the upper gates, superpose themselves on the primary positive wave elements of the trailing portion. In this case, the algebraic addition of all wave heights results in a decrease in slope of the trailing portion of the total wave profile.

Graphic Methods to Determine the Deformation of the Wave Profile.—It is not possible to represent the wave motion which depends on location and time in one diagram. On the contrary it is only possible either to plot the variation

of the water level at a certain place versus the time (hydrographs) or to determine the momentary wave profile for a specific time.

The second method was used in the following:

Method I based on a Distance-Time Diagram.—The continuous transition between upper pool and canal cross-section is approximated by several discrete changes in width (Fig. 15). Likewise the profile of the negative surge,

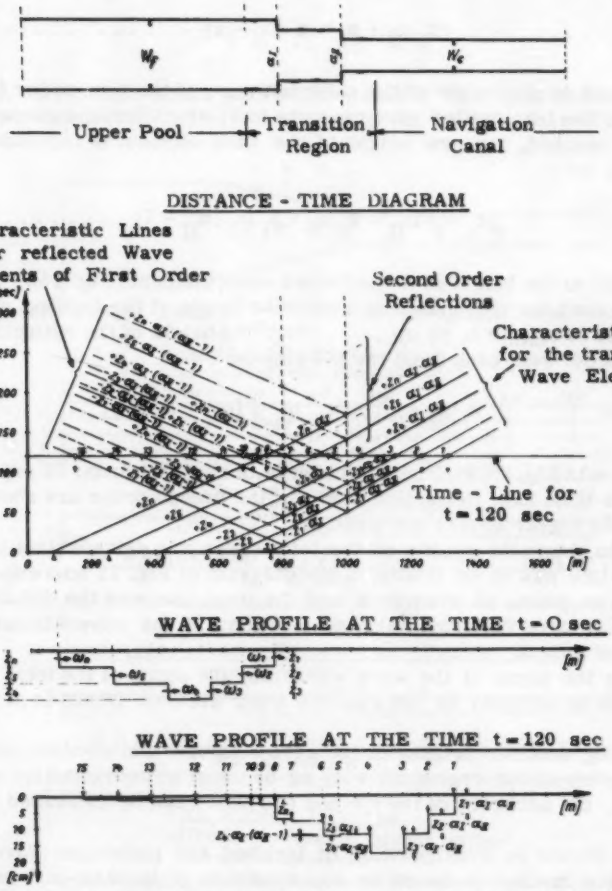
Upper Pool
Transition Region
Navigation Canal
DISTANCE - TIME DIAGRAM
Characteristic Lines for reflected Wave Elements of First Order
Second Order Reflections
Characteristic Lines for the transmitted Wave Elements
Time - Line for t = 120 sec
WAVE PROFILE AT THE TIME t = 0 sec
WAVE PROFILE AT THE TIME t = 120 sec

FIG. 15.—METHOD I TO DETERMINE WAVE DEFORMATION DUE TO TRANSITION REGION

as it would occur in an infinitely long upper pool with a constant width, corresponding to the filling curve is approximated by a number of small wave elements. Each of these wave elements has its own celerity ω_i depending on its depth.

In a distance-time diagram, for each of the wave elements a distance-time line is drawn with a slope corresponding to the appropriate wave celerity.

When a wave element reaches one of the assumed changes in width of the transition region, the height of the initial wave will be increased and a reflection wave of the first order will be sent back. The increase in wave height can be calculated with Eq. 14. The α-values are valid for the changes in width between two of the assumed neighboring cross-sections in this case.

The increase in wave height of an arbitrarily chosen wave element z_i after having passed the first change in width amounts to:

$$z_i \alpha_I - z_i = z_i (\alpha_I - 1) \quad \ldots\ldots\ldots\ldots\ldots\ldots (35)$$

which is equal to the height of the reflected wave of the first order (Fig. 15). The height of the transmitted wave amounts to $z_i \alpha_I$. When the second change in width is reached, the new height of the wave element is increased again. The increase is:

$$(z_i \alpha_I) \alpha_{II} - z_i \alpha_I = z_i \alpha_I (\alpha_{II} - 1) \quad \ldots\ldots\ldots\ldots\ldots (36)$$

which is equal to the height of the reflected wave element (Fig. 15).

Having passed the n^{th} change in width, the height of the incident wave element amounts to $z_{total} = z_i \alpha_I \alpha_{II} \ldots\ldots \alpha_n$. The height of the reflection wave of the first order sent back from the n^{th} step is:

$$z_i \alpha_I \alpha_{II} \ldots\ldots \alpha_{n-1} (\alpha_n - 1) \quad \ldots\ldots\ldots\ldots\ldots (37)$$

In the diagram in Fig. 15, each reflection wave of the first order is represented by a distance-time line. Reflection waves of the second order are shown; however, waves of higher orders are omitted.

In order to obtain the profile of the total surge at a certain time t, a horizontal time-line has to be drawn in the diagram of Fig. 15 corresponding to this time. The points of intersection of the time-line with the distance-time lines for each wave element yield the locations of the wave element fronts reached at the time t.

Observing the signs of the wave elements, the shape of the total surge at the time t can be obtained by drawing the wave element fronts in scale (Fig. 15).

By choosing smaller heights of the wave elements and smaller changes in width on the transition region as well as by considering reflection waves of higher order, the accuracy of the method described can be increased as much as desired.

Method II Based on Superposition of Incident and Reflection Waves.—The second graphic method is based on superposition of incident and reflection waves. Compared with method I it is less exact, but leads more quickly to approximately the same result.

In order to obtain the momentary shape of the surge at the time t, the profile of the negative translation wave that would result in an unlimited long upper pool with constant width, is drawn (see Fig. 16, incident wave) corresponding to the filling curve. Deformations of the incident wave caused by different celerities of the elements of the profile are not considered.

The region of transition between upper pool and canal is again divided into n steps as was shown with method I, (Fig. 16). The incident wave is deformed at each change in width and reflection waves of the first order are sent back.

The magnitude of each increase of the primary wave is the same as the height of the reflection wave of the first order, depending on the change in width between two neighboring cross-sections.

As the time t, the depths of the primary wave at the steps 0 to n are z_I, z_{II}, z_{III}, and z_n (Fig. 16).

Because of the narrowing I the depth z_I of the incident wave will be increased by an amount of:

$$z_I \alpha_I - z_I = z_I (\alpha_I - 1) \quad \ldots\ldots\ldots\ldots\ldots (38)$$

However, up to time t, the part of the incident wave lying between z_I and the first wave element of the wave has already passed the cross section I. That

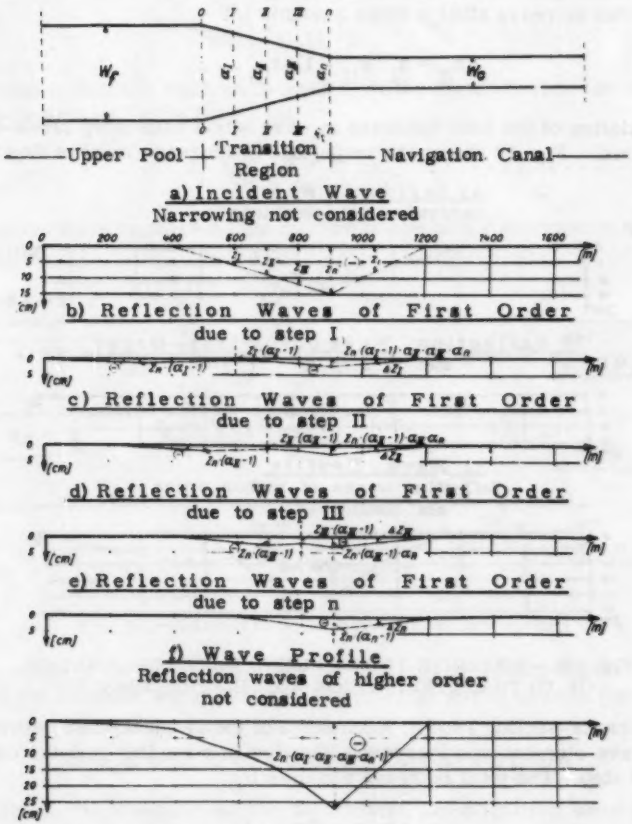

FIG. 16a.—METHOD II TO DETERMINE WAVE DEFORMATION DUE TO TRANSITION REGION-APPROXIMATION BY SEVERAL STEPS

means that each depth z_i of this part of the incident wave is already increased in passing step I by $z_i (\alpha_I - 1)$.

This increase will increase again when the wave depth reaches the step II. The additional increase is:

$$z_i (\alpha_I - 1) \alpha_{II} - z_i (\alpha_I - 1) = z_i (\alpha_I - 1) (\alpha_{II} - 1) \ldots\ldots\ldots (39)$$

The total increase in wave depth at step II is $z_i (\alpha_I - 1) \alpha_{II}$. The calculation of the total increase of the incident wave depth z_i after having passed the III, IV and n step, results in:

$$\Delta z_I = z_i (\alpha_I - 1) \alpha_{II} \alpha_{III} \ldots\ldots \alpha_n \ldots\ldots\ldots\ldots (40)$$

With cross section II (Fig. 16) the wave depth z_{II} is increased by an amount of $z_{II} (\alpha_{II} - 1)$. However, until time t the part of the incident wave lying between z_{II} and the first element of the wave has already passed step II. Each wave depth z_i of this part was increased by $z_i(\alpha_{II} - 1)$ in passing the cross section II. The total increase after n steps amounts to:

$$\Delta z_{II} = z_i (\alpha_{II} - 1) \alpha_{III} \ldots\ldots \alpha_n \ldots\ldots\ldots\ldots (41)$$

The calculation of the total increase in wave height caused by cross-section III is analogous. Fig. 17 shows the magnitude of increase in wave depth corres-

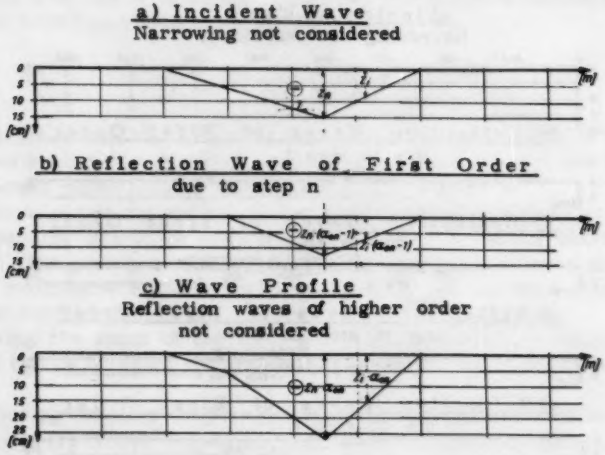

FIG. 16b.—METHOD II TO DETERMINE WAVE DEFORMATION DUE TO TRANSITION REGION-ROUGH APPROXIMATION

ponding to cross-section I to III. Each depth of the incident wave between n and the first wave element was increased likewise in a similar manner until passing the n^{th} step. The total increase amounts to:

$$\Delta z_n = z_i (\alpha_n - 1) \ldots\ldots\ldots\ldots\ldots\ldots (42)$$

In general it is true that each depth, z_i, of the incident wave which, up to the time t, has passed the arbitrarily chosen cross-section causes a reflection wave with a depth of $\Delta z_m = z_i (\alpha_m - 1)$. Considering only reflection waves of the first order, the decrease of Δz_m, when the reflection wave reaches the section of enlargement in width (m - 1), (m - 2), etc. can be neglected.

Furthermore, it is assumed that the celerities of the reflection waves are approximately the same as those of the incident waves.

Using these assumptions, it follows that the reflection wave, pertaining to the cross section m, has the same shape as that part of the incident wave which has already passed the cross-section m at the time t but is distorted in height by the factor (α_m - 1) and reflected from the cross-section m (Fig. 16).

Finally, the profile of the composite wave at the time t can be obtained by adding algebraically the heights of the incident, reflection and incremental wave at each point.

Simplified Method II.—For rough calculation of the wave profile, the choice of only one reflection cross section can be considered sufficient. The corresponding α-value for this cross section, in general placed in the middle or at the end of the transition region, results from the total change in width between upper pool and canal. Using the symbols of Fig. 16:

$$\alpha_{0n} = \alpha_I \, \alpha_{II} \, \alpha_{III} \cdots \alpha_n \quad \ldots\ldots\ldots\ldots\ldots (44)$$

The increase in depth of each wave depth z_i of the incident wave having passed the cross-section up to the time t is:

$$z_i \, \alpha_{0n} - z_i = z_i \, (\alpha_{0n} - 1) \quad \ldots\ldots\ldots\ldots\ldots (45)$$

The reflection wave appears as the mirror image of the increase in wave depth (Fig. 16(b)).

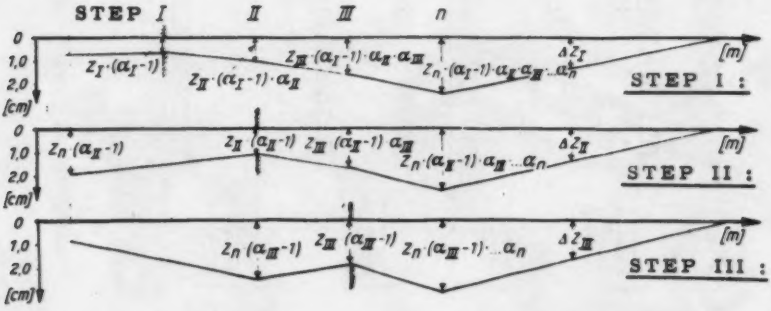

FIG. 17.—MAGNITUDE OF WAVE AMPLIFICATION

The profile of the total wave can be obtained by adding algebraically the heights of the incident, reflection and incremental waves at each point.

MODEL TESTS TO VERIFY THE WAVE THEORY

The Model.—The results of the theoretical investigations were confirmed by model tests. These tests were designed to give information about the wave profile caused by water removal in the upper pool as well as on the deformation of the negative surge when passing the region of transition between upper pool and upstream navigation canal.

The investigations were carried out on an undistorted model (scale 1:35) built from concrete with a total length of approximately 130 ft. (The model in-

M_1 , M_2 , M_3 , M_4 = Locations of the Wave Gages

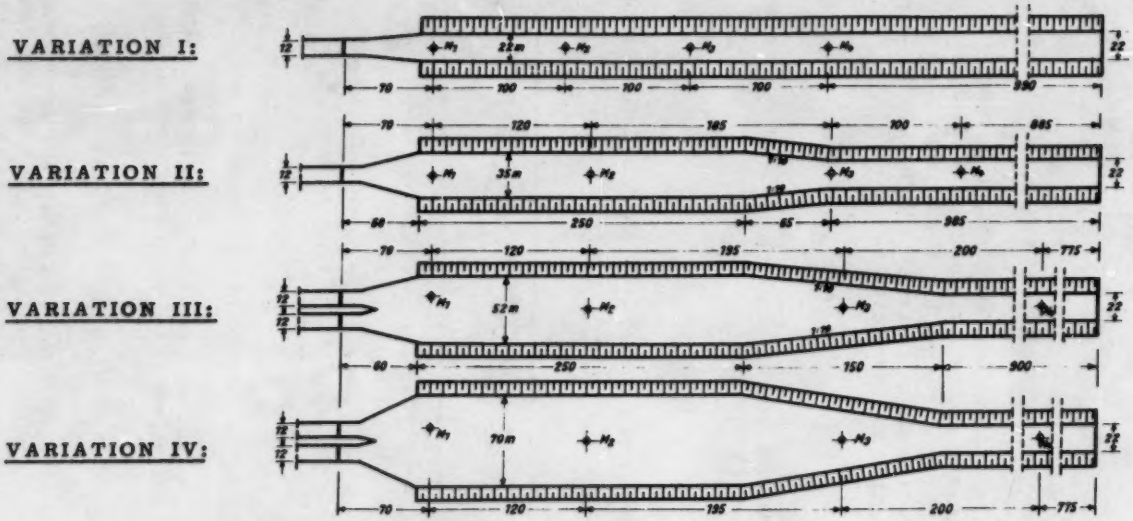

FIG. 18.—FOUR UPPER-POOL VARIATIONS

cluded a lock chamber, the upper pool and the region of transition connected to a section of the navigation canal of sufficient length.

The side slopes of both the cross sections of the upper pool as well as of the navigation canal were the same 1:3, the slope of the bottom was zero. During the tests the initial water depth upstream from the lock was uniform $y_0 = 3.50$ m (~10.5 ft.).

All together, investigations were made with four different widths of the upper pool such as $W_f = 43.0$ m, 56.0 m, 73.0 m and 91.0 m as shown in Fig. 18. The width of the water surface in the upstream navigation canal was $W_c = 43.0$ m and was the same for all tests.

The waves in the upper pool and the navigation canal were measured by an electrical method developed at the Theodor-Rehbock Hydrodynamics Laboratory, Karlsruhe Institute of Technology, Germany. Adjustable gages provided with two needle electrodes which extend vertically through the water were used as the sensing elements. The electrical current flowing between the two electrodes varied in proportion to their submergence, which changed with each change of the water level.

The variations of the water level height were recorded by means of a light-point-line-tracer equipped with four moving coil galvanometers. During the same run, the four units of the recorder permitted measurement of the wave profile at four different points simultaneously. Thus, it was possible to obtain the deformation of the wave as it passed the region of transition. Fig. 18 shows the distribution of the measuring gauges for the four variations tested in the model.

Results of the Model Tests.—

Determination of the Slope of the Wave Front.—It was assumed for the theoretical investigations and the derivation of Eq. 32 that the filling water would be removed from an infinitely long upper pool with a constant width. However, this assumption is not generally valid. In reality, the upper part is narrowed to the normal width of the navigation canal after a certain length. But, also, at the point of removal, (for instance, in front of the upper gate of the lock chamber) the width of the upper pool assumed for Eq. 32 is not applicable but gradually increases to the width of the upper pool (Fig. 18, Variation I and II). Furthermore, with double locks, a sudden increase in width to the final width of the upper pool usually occurs at the end of the lock entrance (Fig. 18, Variations III and IV).

According to the laws for wave deformation caused by such a sudden or continuous enlargement of the cross section, each negative wave element of the total wave profile must be decreased in height resulting in positive reflection waves of the first order which are sent back. Because of the short length of the transition region, the latter rapidly reach the upper gate of the lock chamber and are reflected and superposed on the following incident wave elements at the point of removal.

It is difficult to determine theoretically the effect of these superpositions on the slope of the surge front in the upper pool. Therefore, the effect was investigated empirically by means of model tests. Considering the increase in width between the lock and the upper pool, a correction factor β for the wave slope was necessary. In the model investigations it was found that this factor β depended on the relation between the width of the point of removal (in general equal to the lock width) and the width of the upper pool as shown in Fig. 19.

Using Eq. 32 the final slope of the surge front in the upper pool can be determined as:

$$S_{w_f} = \beta \frac{1}{g\,A_f} \frac{dQ}{dt} \quad \ldots\ldots\ldots\ldots\ldots\ldots\ldots (46)$$

If the cross section, A_f, of the upper pool as well as the increase of rate of inflow during the first phase of the lock filling are known, the slope of the wave front in the upper pool can be determined by means of Fig. 19.

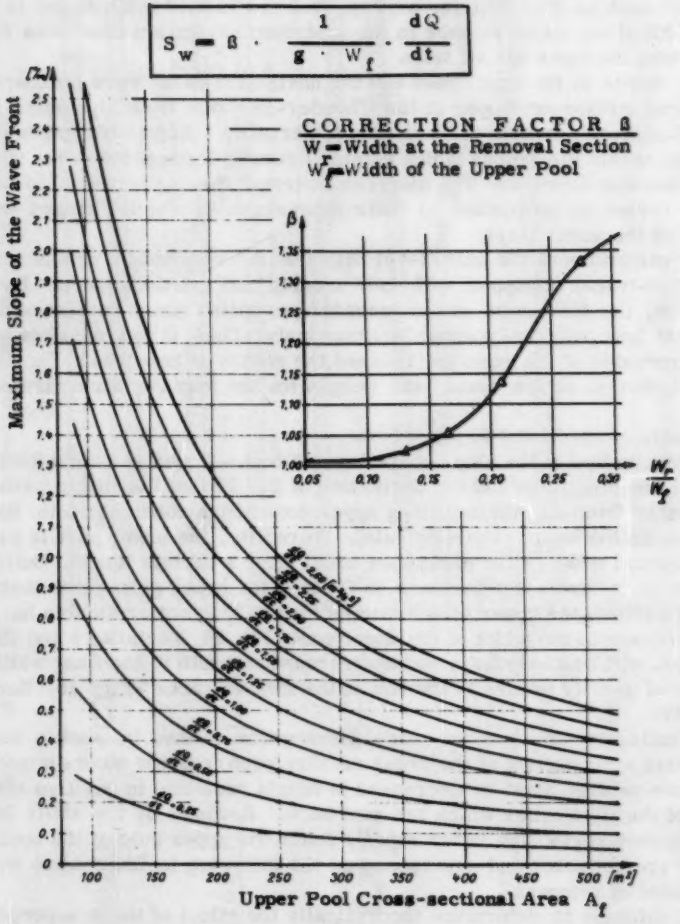
$S_w = \beta \cdot \frac{1}{g \cdot W_f} \cdot \frac{dQ}{dt}$
CORRECTION FACTOR β
W = Width at the Removal Section
W_f = Width of the Upper Pool
Maximum Slope of the Wave Front
β
$\frac{W_r}{W_f}$
Upper Pool Cross-sectional Area A_f

FIG. 19.—MAXIMUM SLOPE OF WAVE FRONT IN UPPER POOL

If double locks are filled simultaneously, Fig. 19 also permits one to determine the maximum slope of the negative surge which must be expected in the upper pool. In this case, however, the sum of the widths of the two points of removal has to be considered as W_r in order to determine the factor β (Fig. 19). That means that in general W_r is equal to the sum of the two lock widths.

Maximum Wave Depths in the Upper Pool.—The curves of water level in the lock chamber during the equalization period corresponding to different lengths of the lock, lifts, filling cross sections and rates of release were determined by model tests. From these the corresponding filling curves and the maximum inflow Q_{max} were determined.

The maximum depths of the surges measured in the model were in good agreement with those calculated by Eq. 31.

Increase of the Wave Depth Between the Upper Pool and Canal.—The dependance of the surge depth in the navigation canal on that in the upper pool, resulting from Eq. 14 for Variations II, III and IV are shown in Fig. 20.

The maximum wave depths as obtained from the model tests in the upper pool and navigation canal were plotted as measured points in the same diagram of Fig. 20. The small deviations of the measured values from the theory are caused by the superposition of the primary wave with negative reflection waves in the upper pool. Depending on the measuring point in the upper pool, the deviations can vary within a narrow range since the total wave depth at each point in the upper pool depends on the location of this point as well as on the length of the upper pool and the length of the wave front.

Increase of the Surge Slope Between the Upper Pool and Canal.—Fig. 21 shows the relationship between the wave slope in the upper pool and the navigation canal resulting from Eq. 34 for variations II, III, and IV. Due to the superposition with negative reflection waves, the measured wave slopes plotted in the same diagram deviate slightly from the theory. The slopes of the surges measured were greater in the upper pool than they would have been in a very long upper pool at a measuring point located at a great distance from the transition region.

Since the deviations between experimental results and theory were small, Eq. 34 is considered to be adequate for practical applications.

MEASUREMENTS IN THE PROTOTYPE AT THE DORTMUND-EMS-CANAL

General Introduction.—In December, 1956, extensive measurements in the West-German Dortmund-Ems-Navigation-Canal were carried out by the Theodor-Rehbock-Hydrodynamics Laboratory of the Karlsruhe Institute of Technology. The investigations included the recording of the negative surges in the part of the navigation canal between Meppen and Varloh caused by the fillings of the Meppen lock facilities as well as measurements at the mooring lines of ships lying in the upper pool of the Meppen locks during the lock filling.

Investigations were also carried out concerning the forces in the tow ropes of tugs in motion. In particular, the purpose of the investigations was to determine whether a simultaneous filling of the two Meppen locks would be permissible with regard to navigation upstream.

The Meppen lock facilities consist of two lock chambers, each of which is 39 ft wide and 575 ft and 346 ft long respectively. The lift of both lock is H_{total} = 24.6 ft.

In general, the filling of each lock takes place from two storage basins with the final amounts of the filling water entering through the upper gate being removed from the upper pool. However, during the tests both of the locks were entirely filled through the upper gate in order to obtain critical conditions in the upper pool and the navigation canal, that is, the filling water was removed only from the upper pool.

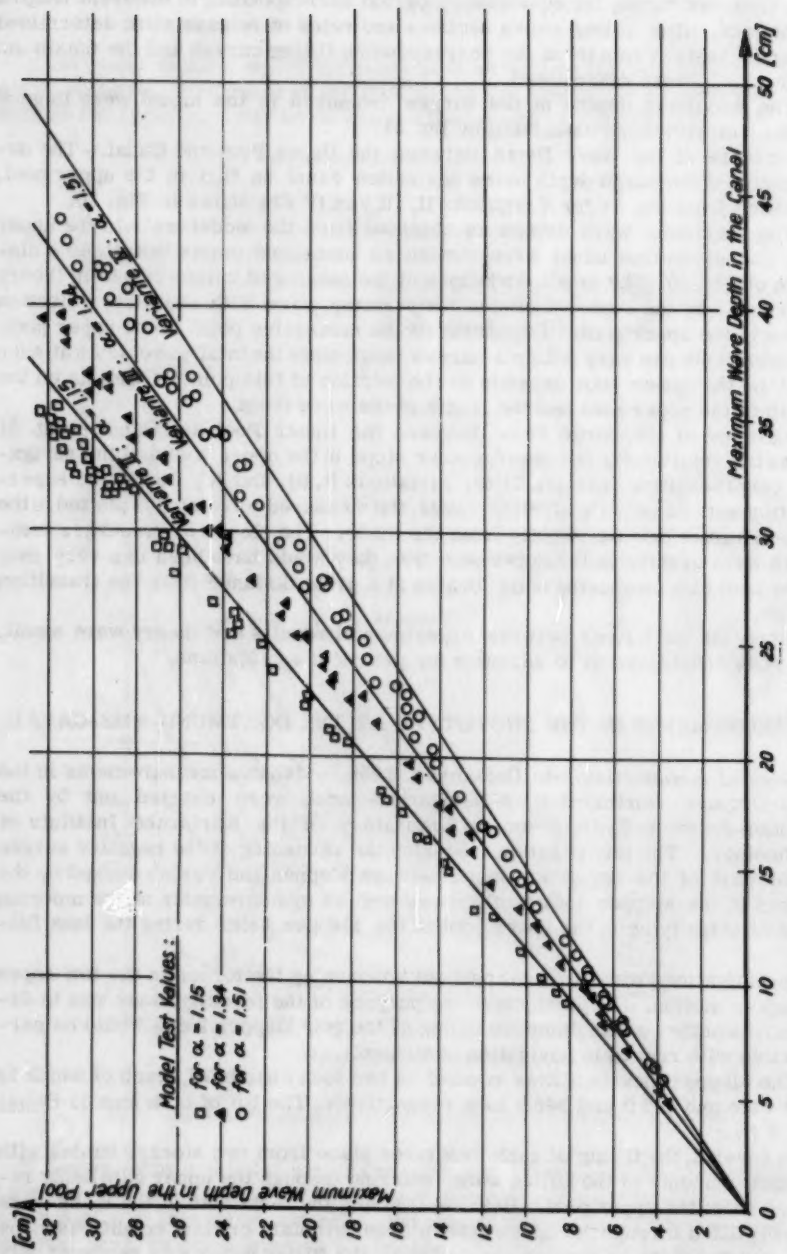
Maximum Wave Depth in the Upper Pool [cm]
Maximum Wave Depth in the Canal [cm]
Model Test Values :
□ for α = 1.15
▲ for α = 1.34
○ for α = 1.51
Variante I : α = 1.51
Variante II : α = 1.34
Variante III : α = 1.15

FIG. 20.—RELATION BETWEEN VAVE DEPTH IN UPPER POOL AND IN CANAL

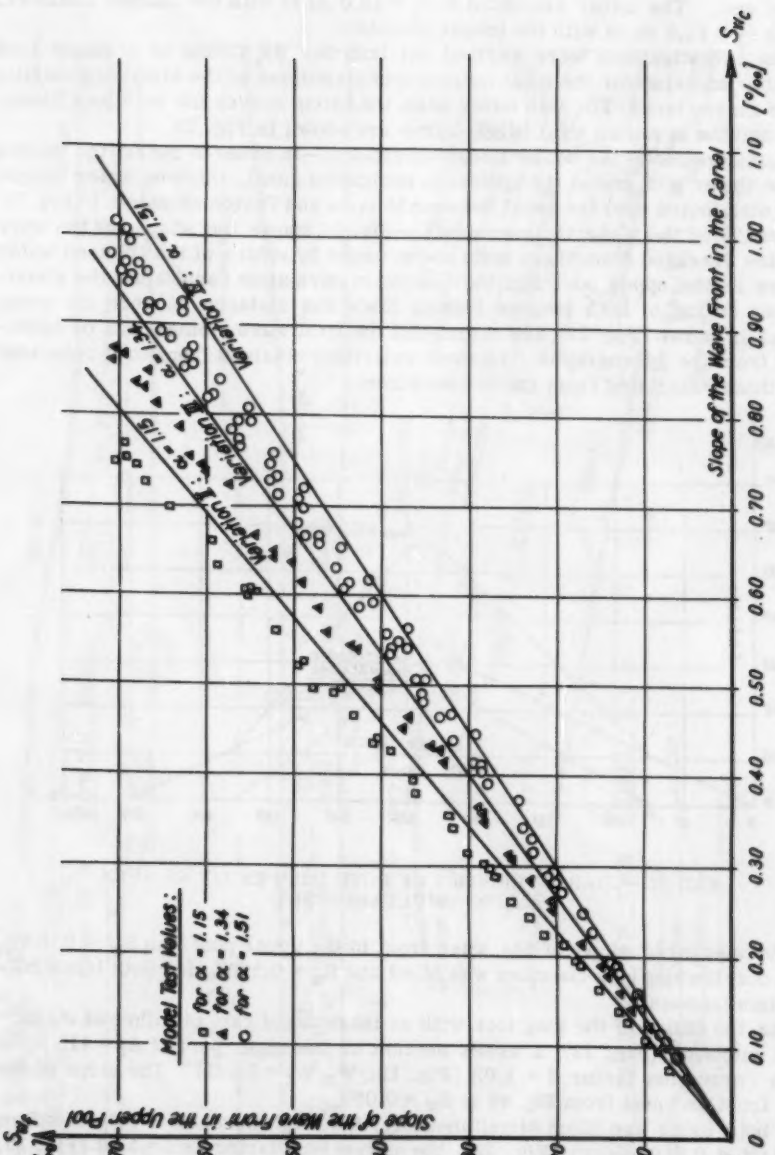
Slope of the Wave Front in the Upper Pool
Slope of the Wave Front in the Canal
Model Test Values:
for α = 1.15
for α = 1.34
for α = 1.51
Variation I: α = 1.15
Variation II: α = 1.34
Variation III: α = 1.51

FIG. 21.—RELATION BETWEEN WAVE SLOPE IN UPPER POOL AND IN CANAL

During the tests the lift velocity of the upper gates of both locks was c = 3.0 mm per sec, the rate of increase of the filling cross section was n = 0.036 sq m per sec. The latter amounted to f_1 = 12.0 sq m with the shorter chamber, and to f_1 = 11.5 sq m with the longer chamber.

The investigations were carried out both for the filling of a single lock chamber and also for the most unfavorable conditions of the simultaneous filling of the two locks. For this latter case, the filling curves for both lock chambers and the resulting total filling curve are shown in Fig. 22.

Measurement of the Water Level Variations.—In order to record the surges in the upper pool and in the upstream navigation canal, thirteen water gauges were distributed over the canal between Meppen and Varloh as shown in Fig. 23.

Results of the Wave Measurements.—Fig. 24 shows the shapes of the wave profiles averaged from three tests as recorded by means of the thirteen water gauges in the upper pool and the upstream navigation canal after the simultaneous filling of both Meppen locks. Since the distance between the water gauges is known (Fig. 23), the celerity of the first wave element can be calculated from the hydrographs. The wave celerities obtained from Eq. 4 coincided with those calculated from the measurements.

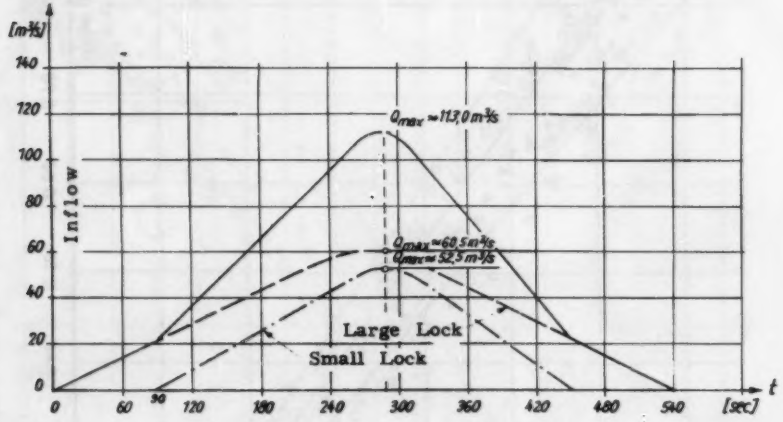

FIG. 22.—CHARACTERISTICS OF BOTH MEPPEN LOCKS WHEN FILLING SIMULTANEOUSLY

The measured slope of the wave front in the upper pool was $S_W \sim 0.055‰$ when only the long lock chamber was filled and $S_W \sim 0.135‰$ for both locks filling simultaneously.

For the filling of the long lock with an increase of rate of inflow of $dQ/dt = 0.245\ m^3/sec^2$ (Fig. 22), a cross section of the upper pool of A_f = 415 sq m and a correction factor β = 1.02 (Fig. 19, $W_r/W_f = 0.093$). The slope of the wave front as found from Eq. 46 is $S_W = 0.06‰$.

If both locks are filled simultaneously, the total increase of rate of inflow is $dQ/dt = 0.510\ m^3/s^2$ (Fig. 22), the correction factor is $\beta = 1.07$ (Fig. 19, $W_r/W_f = 0.186$). With these values the slope of the wave front as computed from Eq. 46 is $S_W = 0.134‰$.

The measurements confirm the accuracy of Eq. 45. Passing the transition region between the upper pool and the navigation canal, the slope of the wave front is increased because of the decrease in cross section. Therefore at

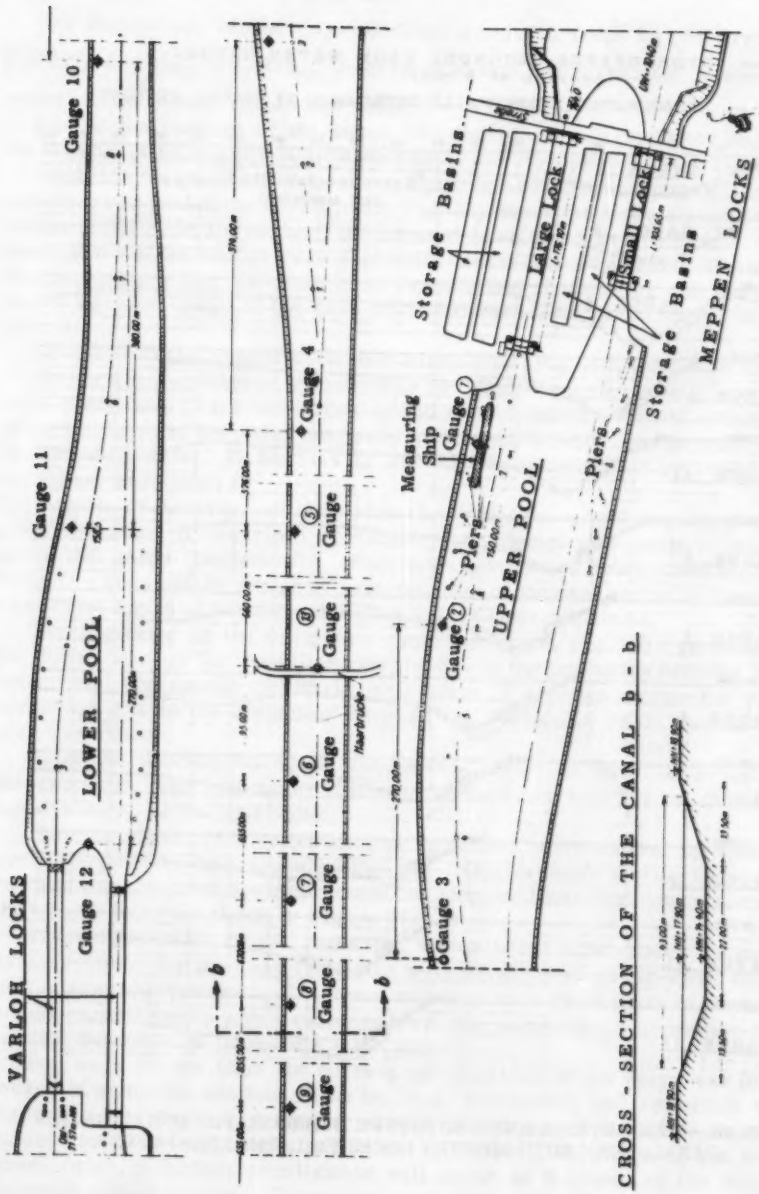

FIG. 23.—LOCATION OF WATER GAUGES IN NAVIGATION CANAL BETWEEN MEPPEN AND VARLOH

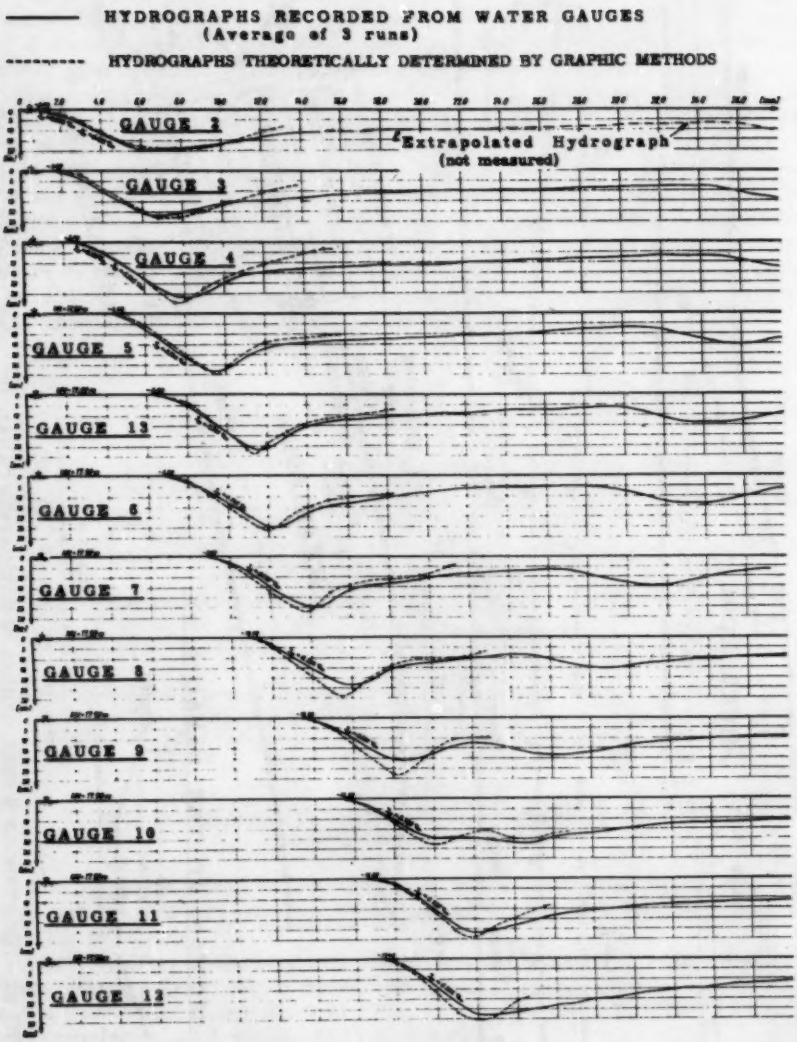

FIG. 24.—THEORETICAL AND PROTOTYPE HYDROGRAPHS IN NAVIGATION CANAL WHEN BOTH MEPPEN LOCKS FILL SIMULTANEOUSLY

gauge 4 (Fig. 23) the slope of the measured wave front was $S_{w_1} \sim 0.100‰$ and $S_{w_2} \sim 0.246‰$ respectively (Fig. 24).

The theoretical values obtained from $\alpha = 1.815$ from Eq. 34 are: $S_{w_1} = 0.0995‰$ and $S_{w_2} = 0.245‰$. According to that, the agreement between theoretical and observed values was good.

During the passage of the canal, the wave front will be flatter because of the difference in celerity of all elements of the wave profile (Fig. 24).

When the surge reaches the transition region between the navigation canal and the lower pool of the Varloh locks (Fig. 23), the wave slope should decrease further. However, the parts of the incident wave which are reflected from the lower gates of the Varloh locks superpose on the following parts of the incident wave such that the final wave recorded at Stations 11 and 12 (Fig. 23) shows a greater slope of the wave front than measured in the navigation canal (Fig. 24).

As shown in the results of the measurements (Fig. 24), the surge reflected at Varloh was recorded at Stations 2 to 10. However, as a result of the loss of wave energy due to friction, crossing and reflections of the wave elements, the slope and depth of the reflected surge were considerably smaller than those of the primary wave. At Stations 11 and 12 the primary and reflected surge superpose each other.

Analysis of the Surge, Measured in the Prototype.—Applying the simplified graphic method II described previously, an attempt was made to obtain the measured surge theoretically. The wave profile was determined for certain times (t = constant) by means of superposition of incident and reflection waves. Reflection waves of second and higher orders were neglected.

The beginning of the navigation canal (section 4, Fig. 23) was assumed as the cross section for wave deformation due to the transition between Meppen upper pool and canal. Similarly, at Station 11 a cross section for wave deformation due to the transition between the navigation canal and the Varloh pool was chosen.

First the incident wave was constructed as would have occurred in the Meppen upper pool (due to the filling curve shown in Fig. 22) by assuming an infinite length of the upper pool.

The magnitude of the reflection and increment wave caused by changes in cross section was determined by Eq. 14. Uniform cross section for wave reflection was assumed upstream from the Meppen locks and downstream from the Varloh locks as shown in Figure 25.

The shaded parts of the reflection waves which extend over the assumed cross sections for the wave reflection were superposed on the wave elements in the Meppen upper pool. The same was done with those parts of the incident and increment waves which extended past the assumed cross section for reflection downstream from the Varloh locks.

For each chosen time the corresponding profile of the surge was found by means of algebraic addition of the incident, increment, and reflection waves. However, the resulting irregular shapes of the waves cannot be expected in nature since the irregularity is a result of the assumed shape of the incident wave. Also, a further equalization will occur as a result of the reflection waves of higher orders. These circumstances were taken into account by the dot-dash correction lines for the wave profile (Fig. 25).

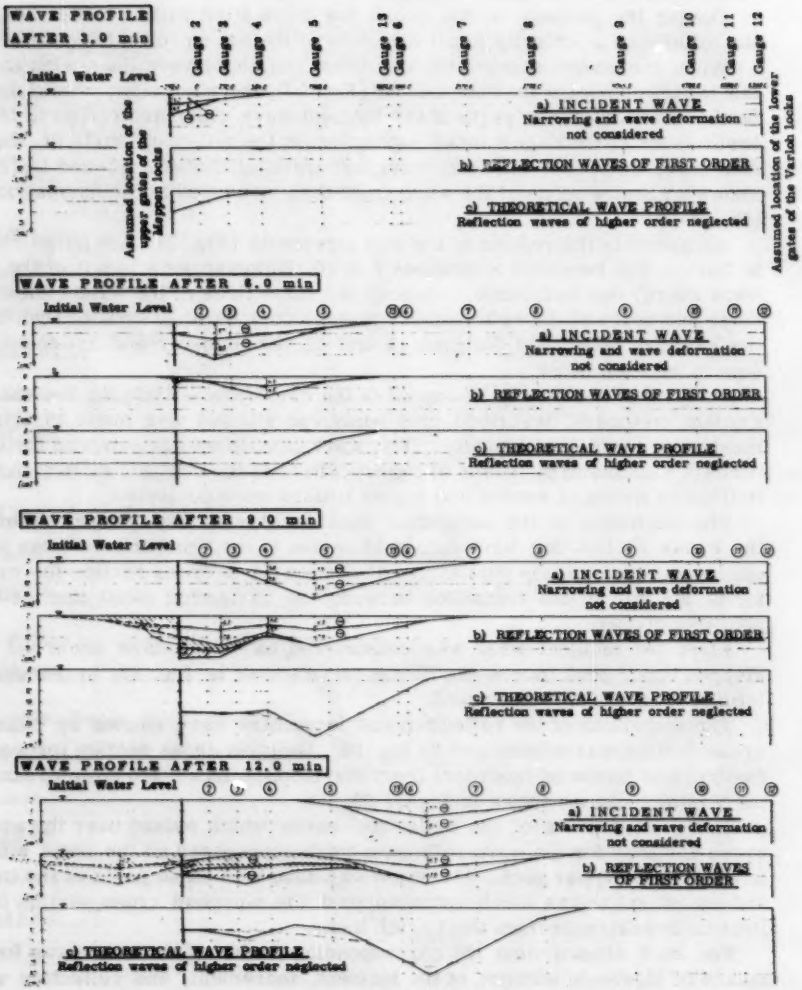
WAVE PROFILE AFTER 3.0 min
Gauge 2
Gauge 3
Gauge 4
Gauge 5
Gauge 13
Gauge 6
Gauge 7
Gauge 8
Gauge 9
Gauge 10
Gauge 11
Gauge 12
Initial Water Level
a) INCIDENT WAVE
Narrowing and wave deformation not considered
b) REFLECTION WAVES OF FIRST ORDER
c) THEORETICAL WAVE PROFILE
Reflection waves of higher order neglected
Assumed location of the upper gates of the Mayyan locks
Assumed location of the lower gates of the Varioh locks
WAVE PROFILE AFTER 6.0 min
Initial Water Level
a) INCIDENT WAVE
Narrowing and wave deformation not considered
b) REFLECTION WAVES OF FIRST ORDER
c) THEORETICAL WAVE PROFILE
Reflection waves of higher order neglected
WAVE PROFILE AFTER 9.0 min
Initial Water Level
a) INCIDENT WAVE
Narrowing and wave deformation not considered
b) REFLECTION WAVES OF FIRST ORDER
c) THEORETICAL WAVE PROFILE
Reflection waves of higher order neglected
WAVE PROFILE AFTER 12.0 min
Initial Water Level
a) INCIDENT WAVE
Narrowing and wave deformation not considered
b) REFLECTION WAVES OF FIRST ORDER
c) THEORETICAL WAVE PROFILE
Reflection waves of higher order neglected

FIG. 25.—THEORETICAL ANALYSIS OF NEGATIVE SURGE IN NAVIGATION CANAL SIMULTANEOUSLY THROUGH

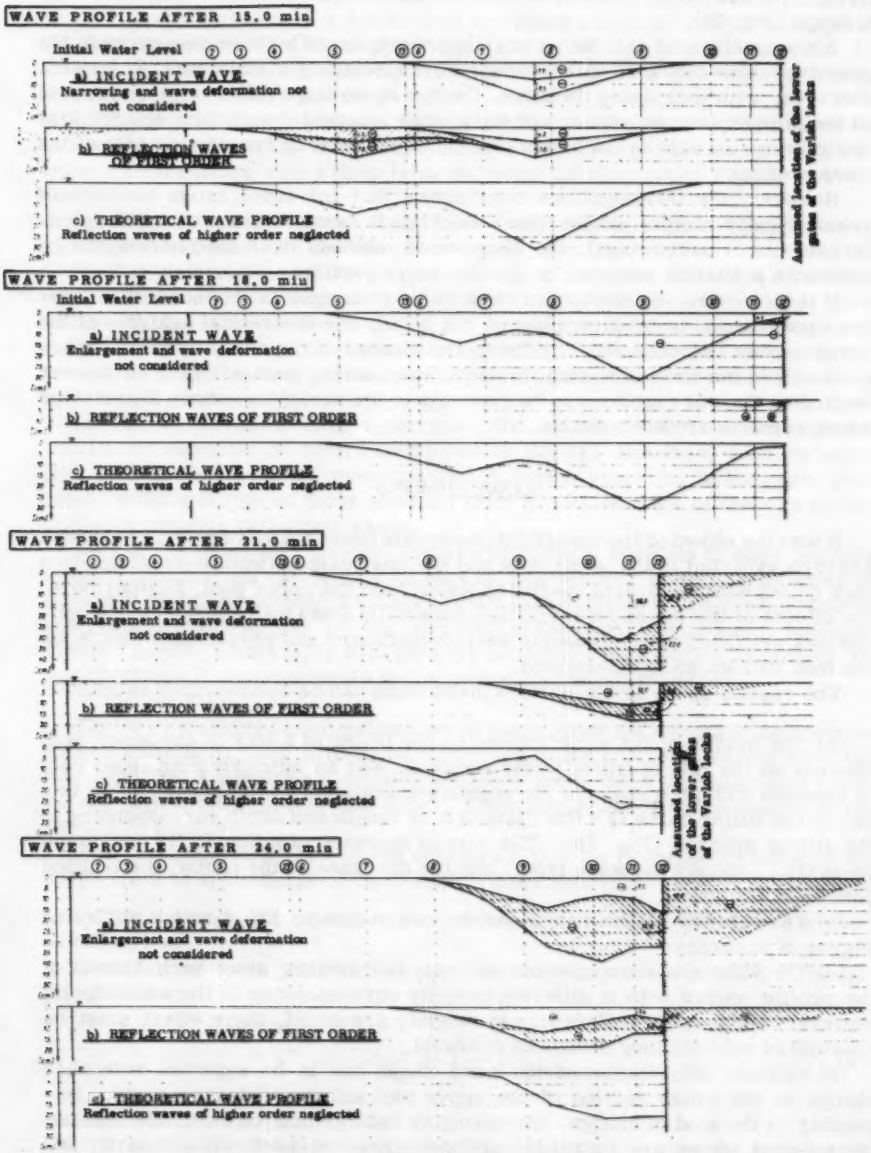
WAVE PROFILE AFTER 15.0 min
Initial Water Level
a) INCIDENT WAVE
Narrowing and wave deformation not considered
b) REFLECTION WAVES OF FIRST ORDER
c) THEORETICAL WAVE PROFILE
Reflection waves of higher order neglected
Assumed location of the lower gates of the Varloh locks
WAVE PROFILE AFTER 18.0 min
Initial Water Level
a) INCIDENT WAVE
Enlargement and wave deformation not considered
b) REFLECTION WAVES OF FIRST ORDER
c) THEORETICAL WAVE PROFILE
Reflection waves of higher order neglected
WAVE PROFILE AFTER 21.0 min
a) INCIDENT WAVE
Enlargement and wave deformation not considered
b) REFLECTION WAVES OF FIRST ORDER
c) THEORETICAL WAVE PROFILE
Reflection waves of higher order neglected
Assumed location of the lower gates of the Varloh locks
WAVE PROFILE AFTER 24.0 min
a) INCIDENT WAVE
Enlargement and wave deformation not considered
b) REFLECTION WAVES OF FIRST ORDER
c) THEORETICAL WAVE PROFILE
Reflection waves of higher order neglected

BETWEEN MEPPEN AND VARLOH WHILE FILLING BOTH MEPPEN LOCKS THEIR UPPER GATES

The lineated hydrograph is constructed by transferring the depths of the surge obtained by the graphic method for each station and time (Fig. 25) onto a graph (Fig. 24).

A comparison of the theoretical hydrographs with those measured in the prototype shows a good correspondence especially for Stations 2, 3, 4 and 5. However, with increasing distance, the two recordings differ slightly because of the simplifying assumptions of the graphic method (neglecting energy loss of the surge as well as the assumption of equal celerity for all elements of the wave profile).

However, the investigations have shown that for canal cross sections of geometrically simple shapes (such as straight canal sections with steady enlargements or narrowings), the theoretical methods described herein can be used with sufficient accuracy to predict surge profiles.

If the plan view of a navigation canal is more complicated because of irregular cross-sections or branching of the canal, the theoretical analysis of the surge profile becomes difficult due to the number of the reflections and superpositions of the wave elements. In such cases, model tests will give an answer regarding the wave motions to be expected in the navigation canal, if prototype measurements are not possible.

CONCLUSIONS

It was the object of the investigations to determine the wave phenomena which are to be expected in the upper pool and the upstream navigation canal due to a lock filling with removal of the filling water from the upper pool. Furthermore, the effects of the waves on navigation, especially when both chambers of a double lock are filled simultaneously were investigated and permissible limits for the lock fillings were determined.

The results of the investigations prescribed can be summarized as follows:

(a) The profile of the surge caused by the filling of a lock in the upper pool depends on the rate of filling water removal. For an infinitely long upper pool of constant width the shape of the negative translation wave appears as an image of the filling curve $Q = f(t)$ distorted in length and depth corresponding to the filling process (Fig. 13). The rate of increase of inflow to the maximum value Q_{max} causes the wave front; and the decrease of the inflow, the trailing portion of the wave.

(b) The celerity of the surge can be calculated by Eq. 4 with a sufficient degree of accuracy.

(c) The wave shape changes continuously in travelling since each element of the profile moves with a different celerity corresponding to the water depth. However, because the differences in celerity are small, their effect must be considered only for long distances of travel.

(d) Another deformation of the wave shape has to be expected with each change in the cross section of the upper pool and the navigation canal. Depending on the kind of change, narrowing or enlargement of the cross section, the incident waves are increased and decreased respectively and partly reflected. The superposition of the reflection waves with the following wave elements of the incident wave leads to a change in shape of the resulting wave.

(e) The slope of the surge front in the upper pool can be obtained from Eq. 46 as well as from the diagram of Fig. 19. The influence of the enlargement be-

tween the point of water removal and the upper pool is accounted for by the correction factor β which was obtained empirically from model tests (Fig. 19).

(f) If both chambers of a double lock are filled simultaneously, the slope of the resulting wave front in the upper pool can be determined either by Eq. 46 or Fig. 19. However, the sum of both cross-sections of water removal has to be considered to determine the β-factor.

(g) During the first phase of a lock filling, the maximum rate of increase in inflow can be obtained by means of Fig. 8 for the filling with a high lying entrance; for the filling with a deep lying entrance the diagram of Fig. 10 must be used.

(h) The deformation of the surge front due to the transition region between upper pool and canal can be determined by Eq. 34.

(i) The deformation of the trailing portion of the wave due to the transition region depends not only on the variation in cross-section between upper pool and canal, but also on the fact that the superpositions of reflection waves of the surge front cause on additional deformation. In each case, the total deformation of the trailing portion of the surge can best be determined by using the graphic methods.

(j) For an infinitely long upper pool, the maximum depth of the negative translation wave can be determined by using Eq. 31. However, with an upper pool of limited length, the maximum wave depths occurring in the upper pool can be a little larger as those obtained from Eq. 31 because of the superposition with negative reflection waves.

(k) The investigations showed that the theoretical analysis of wave motions in navigation canals due to lock fillings is possible with a sufficient degree of accuracy using the graphic methods if the cross sections of the canal and pools are geometrically simple and the alignment of the canal is reasonably straight. In other cases, model tests will give the necessary information regarding the wave motions if measurements in the prototype are not feasible.

Further extensive investigations were made about the effects of the negative surges caused by lock fillings on navigation in the upstream region from the lock facilities.[2] However, a detailed presentation of these investigations would extend beyond the limits of this paper. Therefore, only a short summary of the results is possible.

The investigations[2] led to the conclusion that the permissible slope of the surge front is approximately $S_{w_f} \leq 1.3‰$. When this value is used, with an appropriate mooring, the ropes are stressed to a maximum of 25% to 30% of their breaking load.

If the filling curve of a lock is given, the necessary cross section of the upper pool is

$$A_f \geq \frac{\beta}{\eta} \left(\frac{dQ}{dt}\right) \text{ given} \quad \ldots\ldots\ldots\ldots\ldots\ldots (47)$$

where $0.01 \leq \eta \leq 0.013$.

On the other hand, for a given cross section of the upper pool the permissible increase of inflow during the first phase of a lock filling should not exceed the following value:

$$\left(\frac{dQ}{dt}\right) \leq \eta \frac{A_f}{\beta} \quad \ldots\ldots\ldots\ldots\ldots\ldots (48)$$

Investigations made on existing navigation facilities showed, even with the most modern locks, that the maximum increase in inflow was only 30% of the permissible value given by Eq. 48.

ACKNOWLEDGMENT

The writer wishes to express his appreciation and thanks to E. h. Heinrich Wittmann, Professor of Hydraulics and Head of the Theodor-Rehbock Hydrodynamics Laboratory, Karlsruhe Institute of Technology, for his help and stimulating advice and for having made available to him during the investigations, facilities and personnel of the Karlsruhe Institute.

Appreciation is also due to the staff of the German Wasser-und Schiffahrtsdirektion, both in Muenster and Meppen, Ems.

The helpful suggestions given to the writer during the preparation of this paper by Robert G. Dean, Research Assistant at the M.I.T. Hydrodynamics Laboratory is gratefully acknowledged.

Journal of the
WATERWAYS AND HARBORS DIVISION
Proceedings of the American Society of Civil Engineers

MEAN DIRECTION OF WAVES AND OF WAVE ENERGY

By Omar J. Lillevang,[1] M. ASCE

SYNOPSIS

Reliable predictions of erosion/accretion effects of new coastal works are necessary. A vector technique related to wave direction and duration statistics is devised, tested on Santa Barbara historical shoaling records and demonstrated as a design aid for a small craft harbor plan on a sandy reach of California coast.

INTRODUCTION

Instances are rare, indeed none comes to mind, where works constructed on a sandy coast have not changed the configuration of adjoining beaches, or initiated shoaling phenomena where formerly none existed, or caused new erosive action. The ability to make predictions on technically reliable bases of how coastal works will change shore and shoal characteristics is an obvious need.

Basing predictions of shoal and shore changes on a background of long observational experience, firm knowledge of wave phenomena and intuitive art

Note.—Discussion open until August 1, 1960. To extend the closing date one month, a written request must be filed with the Executive Secretary, ASCE. This paper is part of the copyrighted Journal of the Waterways and Harbors Division, Proceedings of the American Society of Civil Engineers, Vol. 86, No. WW 1, March, 1960.

[1] Sr. Engr., Leeds, Hill and Jewett, Cons. Engrs., Los Angeles, California.

should not be deprecated, for many problems have been successfully handled in this way when competent practitioners have been involved.

Model studies have been used for prediction with varying degrees of reliability. Even small, relatively inexpensive distorted-scale models have given useful qualitative information, but the writer is acutely aware from personal experience that it may be easier for one to build, operate and evaluate the results of such a model than to find acceptance of the model's performance.

World War II needs of our fighting forces caused great strides to be made in the development of techniques for analyzing and describing wave development, motion, force, and other phenomena which have engineering significance. These techniques have continued to evolve and have been subjected to wholesome criticism. When found worthy, each has improved the reliability of coastal engineering practice to the benefit of both the engineer and of those who utilize engineering services.

In connection with studies for a proposed harbor development on a sandy reach of California's coast, the writer has devised an application of wave energy and direction data which is described in this paper so its usefulness may be considered and so modifications or further applications may be suggested, if warranted. The methods have not been derived from rigorously theoretical procedures. Their application involves a series of defined assumptions which permit a reviewer to duplicate the steps that have been taken to predict movement and deposition of sand in wave-affected waters.

HYPOTHESIS

The configurations of sand deposits which occur as the result of wave action, or because of the interception of wave action, must be related to the direction of wave motion at the locality. Waves expend work which is applied in the direction of the motion of water particles within the waves. It is hypothesized that in mature shoals and beaches their outline will bear a distinguishable relationship to the mean direction of all wave energy which has been applied at that location. If this hypothesis is acceptable, the first need becomes a consistently reproducible definition of the mean direction of wave energy at a specific location from basic data.

BASIC WAVE INFORMATION

Comprehensive data on wave occurrence are sparse and generally only a few engineers are aware of their existence, extent or nature. Many compilations are considered proprietary because they have been made by hindcast methods from meteorological information, and the computations have been performed at considerable expense to the commissioning entity. Actual records of wave height and period have been made mechanically and electrically at shore stations, but thus far no adequate wave direction recorder is known to have been developed.

On July 1, 1947, Scripps Institution of Oceanography of the University of California submitted a report under contract with the Los Angeles District Engineer, Corps of Engineers, U.S. Army, entitled "A Statistical Study of Wave Conditions at Five Open Sea Localities Along the California Coast." The report is often referred to as SIO-68. The Scripps report compiled statistics for each of the selected localities by hindcasting waves from all storms of

consequence in the North Pacific and Hawaiian area which were shown on daily weather charts of that ocean expanse in the years 1936, 1937 and 1938. Unfortunately, insufficient data on Southern Hemisphere storms existed for the Weather Bureau to map their occurrence, location, and extent during the years covered by SIO-68. Therefore the Scripps report does not present statistical data on all the wave trains which approach the coast of southern California.

As an extension of the hindcast records of wave action, SIO-68 presented computations of the annual energy of the waves at the offshore stations, broken down by azimuth directions and wave periods. Data from the Scripps report are utilized to describe the procedures which are the subject of this paper.

DIRECTION AND MAGNITUDE OF WAVE ENERGY

Statistics for all SIO-68 stations are for waves in deep water where they are not modified by shore or island effects. Almost without exception, deep water wave directions are changed as the waves advance past islands and through shallow waters to break on the coast. Their energy per unit length of crest is usually modified with the "bending" of the waves due to variations in the submerged terrain. When the waves are so refracted that the loci of perpendiculars to their crests (orthogonals) converge, the waves tend to increase in height, thus expressing their greater energy content per unit of crest length. Consistently, when the wave orthogonals diverge, the waves decrease in height. For all practical purposes there is no transmission of wave energy across orthogonals.

Wave refraction diagrams are maps or charts of the orthogonals of waves of defined period and deep water azimuth. They define the direction and energy content of the waves at any point of interest. The energy per unit of wave crest length between two selected orthogonals varies from place to place along the path of advance of the wave inversely as the ratio of the spaces between the orthogonals at the points selected for comparison.

With each characteristic wave direction and relative energy content at a point of interest determined from refraction diagram studies, vector representations can be used to weight the effect of several directions of wave action and establish the mean direction of the energy of all the waves considered.

ENERGY VECTOR CONCEPT APPLIED AT SANTA BARBARA

A usefulness in predicting the position of mature shoals deposited in the wave lee of a breakwater tip is implied when one examines an application of the resultant energy vector procedure at Santa Barbara Harbor, Calif. The history of the breakwater tip shoal there beings over 25 yr ago and is well documented. Geographically the location is such that southern swell does not deliver any effective wave energy, and thus the Scripps wave work data are not incomplete for Santa Barbara studies.

Fig. 1 shows the geographical relationship of Santa Barbara to ocean wave approach. Fig. 2 presents graphically under the sloping lines the annual work of waves at Scripps Station D, the nearest of the statistical stations in the study to Santa Barbara. The work is for all waves of the plotted periods occurring within a 22.5° sector centered at the azimuth shown.

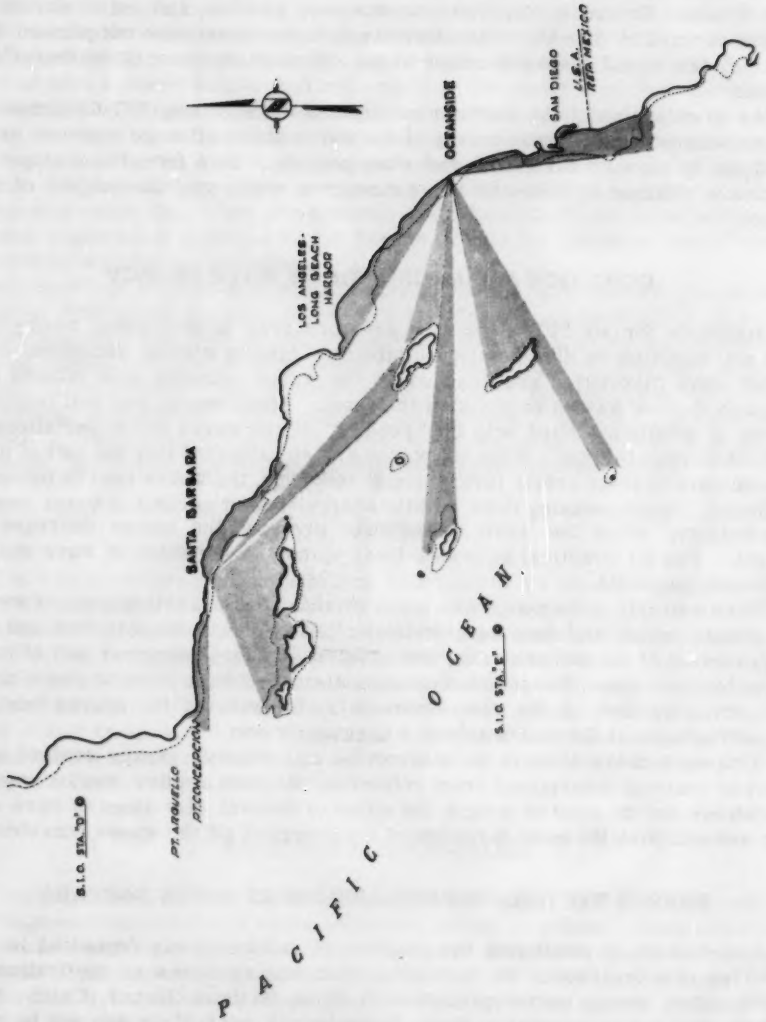

FIG. 1.—WAVE EXPOSURE

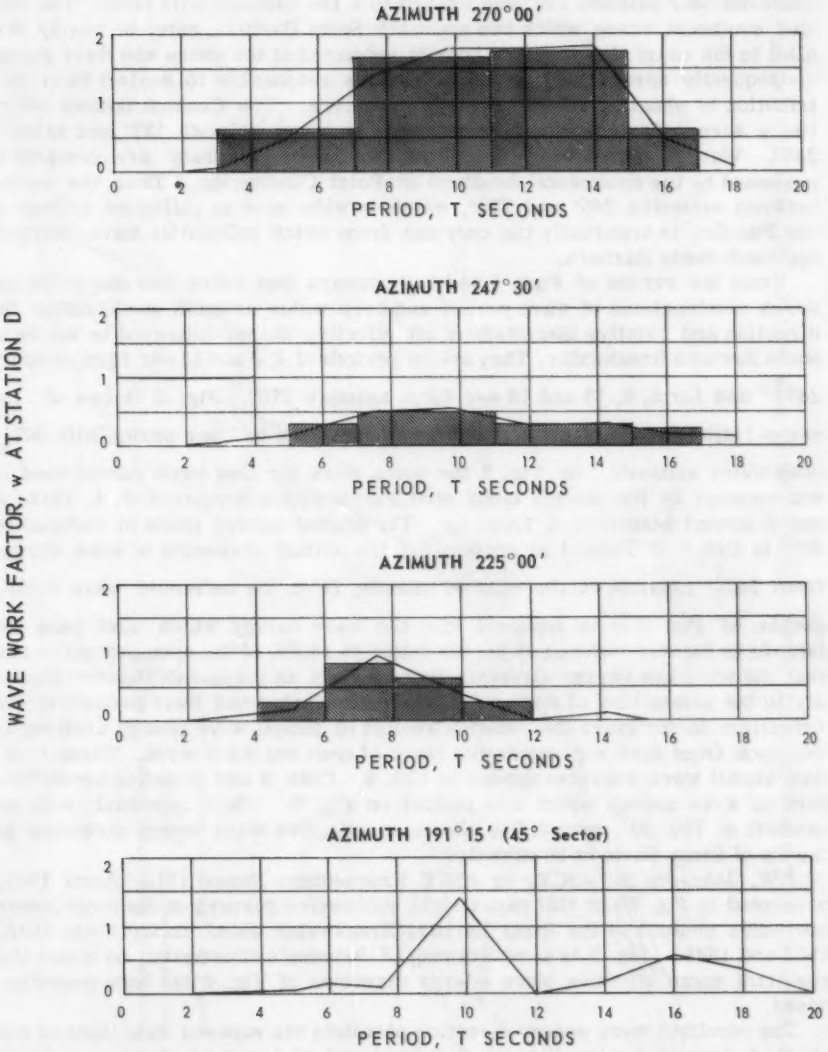

FIG. 2.—ANNUAL WORK BY WAVES AT SANTA BARBARA HARBOR

Examination of Fig. 1 leads to the conclusion that, other than local chop, waves from the southeast have an open sector of approach of only about 12°, centered near azimuth 130° and limited to a 150 nautical mile fetch. The limited southeast waves which can approach Santa Barbara move so nearly parallel to the coast that they are heavily refracted at the shore and their energy consequently spread so thin that it appears reasonable to neglect their contribution to shoaling effects at the breakwaters. The Channel Islands effectively screen Santa Barbara from waves between azimuth 137° and azimuth 245°. Waves approaching from the northwest quadrant are completely screened by the continental headland at Point Concepcion. Thus the sector between azimuths 245° and 270°, which is wide open to unlimited fetches of the Pacific, is apparently the only one from which influential wave energies approach Santa Barbara.

From the review of Figs. 1 and 2 it appears that refraction diagrams for seven combinations of wave period and deep water azimuth would define the direction and relative magnitude of all effective energy delivered by waves at Santa Barbara Breakwater. They are for periods of 6, 9 and 13 sec from azimuth $247\frac{1}{2}°$ and for 5, 9, 13 and 16 sec from azimuth 270°. Fig. 3 is one of the seven refraction diagrams and is for waves from 5 to 7 sec period with $247\frac{1}{2}°$ deep water azimuth. On Fig. 2 the wave work for that wave period band is represented by the shaded block of 0.3 units ordinate value (Col. 4, Table 1) and 2 second width (Col. 5, Table 1). The shaded energy block is reduced by 40% in Col. 7 of Table 1 to account for the partial screening of wave energy from $247\frac{1}{2}°$ azimuth by the channel islands; from the refracted wave orthogonals of Fig. 3 it is apparent that the wave energy which does pass the islands is further reduced at the shoreline to 16.3% of the open sea value and that the wave and energy direction there has an azimuth of 204° 00'. Multiplying the summation of work by the exposure factor and their product by the refraction factor gives the relative amount of annual wave energy arriving at the coast from each representative block of open sea wave work. These relative annual wave energies appear in Col. 9. Cols. 9 and 10 define seven vectors of wave energy which are plotted on Fig. 4. Their resultant, with an azimuth of 190° 20', may define the mean effective wave energy direction at the tip of Santa Barbara Breakwater.

J.W. Johnson, M. ASCE, in ASCE Proceedings Paper 1211, April 1957, presented in Fig. 20 of that paper eight successive surveys of the mean lower low water contour of the Santa Barbara Breakwater shoal during 1948, 1949, 1950 and 1951. Fig. 5 is a re-drawing of Johnson's illustration on which the resultant mean effective wave energy direction of Fig. 4 has been superimposed.

The resultant wave energy direction parallels the exposed-side limit of the shoal at mean lower low water. This apparent fit is not so clear on earlier, less detailed surveys. There are indications that the degree of alignment of the shoal limit with the resultant energy vector improves with the maturity of the shoaling conditions. The sparse number of earlier condition surveys available which show the slope of the submerged accretions against the seaward face of the breakwater allow some inference that their seaward slope has flattened with time. Trends of clockwise rotation of the shoal limit with time, and therefore perhaps with maturing of the submerged accretion against the breakwater face, may be appraised by reference to Fig. 6.

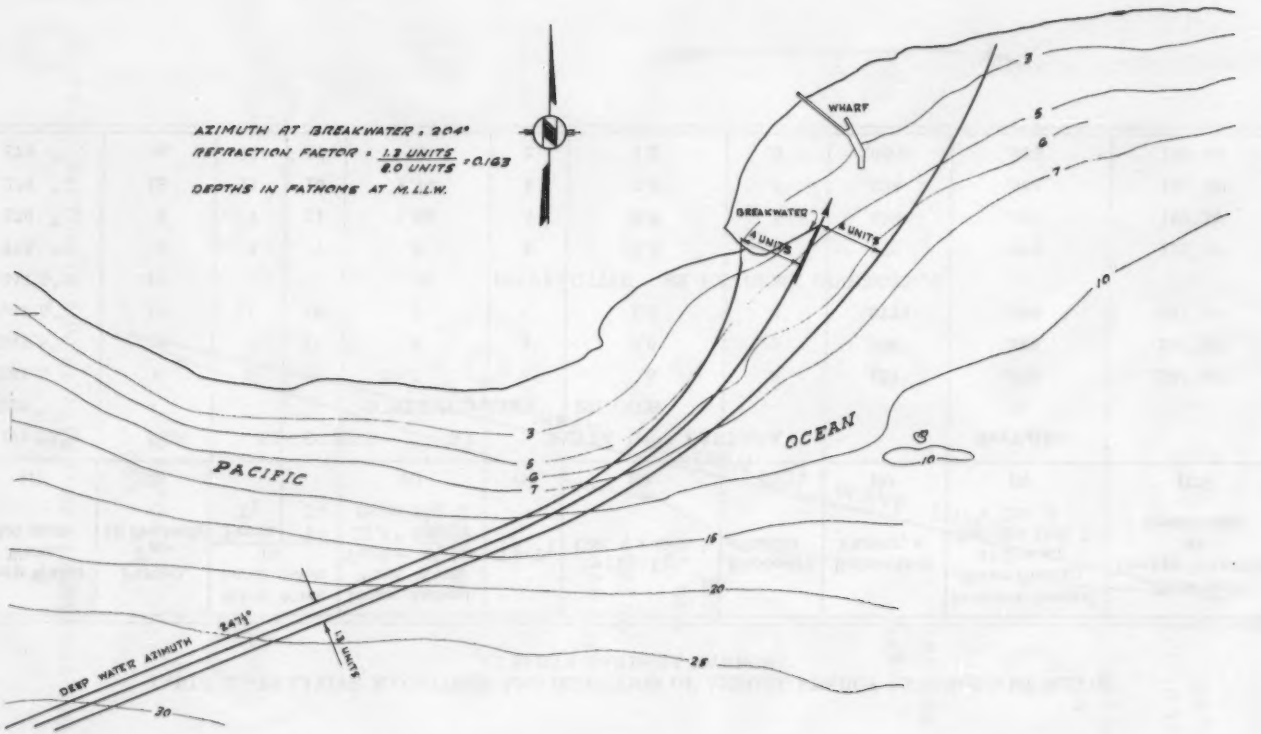

FIG. 3.—WAVE REFRACTION AT SANTA BARBARA FOR 6-SEC PERIOD WAVES WITH 247 1/2° DEEP WATER AZIMUTH

TABLE 1.—RELATIVE MAGNITUDE AND DIRECTION OF ANNUAL ENERGY EXPENDED BY WAVES AT SANTA BARBARA HARBOR

Deep Water Wave Azimuth	Period, T_m, in Seconds	Wave Work Subdivision (3)		Mean Annual Wave Work Factor, w, for 22.5° Sector from Fig. 2	T_2-T_1	$w(T_2-T_1)$, Col. 4 x Col. 5	Exposure Factor	Refraction Factor, e	Relative Annual Wave Energy at Coast, Col. 6 x Col. 7 x Col. 8	Wave and Energy Direction at Breakwater
		From T_1	To T_2							
(1)	(2)			(4)	(5)	(6)	(7)	(8)	(9)	(10)
191.25°	NON	EFFECTIVE AT			SANTA		BARBARA		Negligible	-
225°	-	-	-	SCREENED	BY	ISLANDS	-	-	-	-
247.5°	6	5	7	.3	2	.6	.6	.163	.059	204°00'
247.5°	9	7	11	.5	4	2.0	.6	.300	.360	196°30'
247.5°	13	11	15	.3	4	1.2	.6	.0775	.056	187°00'
247.5°	16	-	-	.25	INEFFECTIVE BY EXTREME DIVERGENCE				-	-
270. °	5	3	7	.6	4	2.4	.5	.070	.084	210°00'
270 °	9	7	11	1.65	4	6.6	.5	.088	.291	185°30'
270 °	13	11	15	1.75	4	7.0	.5	.024	.084	182°30'
270 °	16	15	17	.6	2	1.2	.5	.0655	.039	189°00'

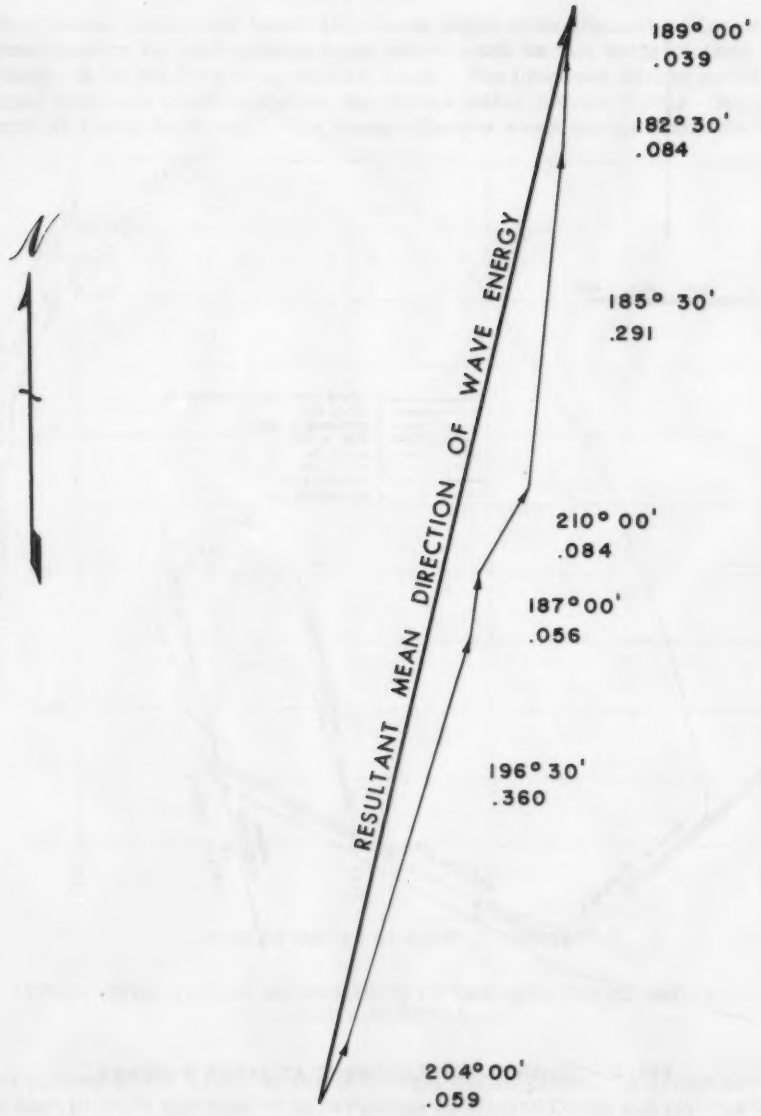

FIG. 4.—VECTORS OF ANNUAL WAVE WORK AT SANTA BARBARA

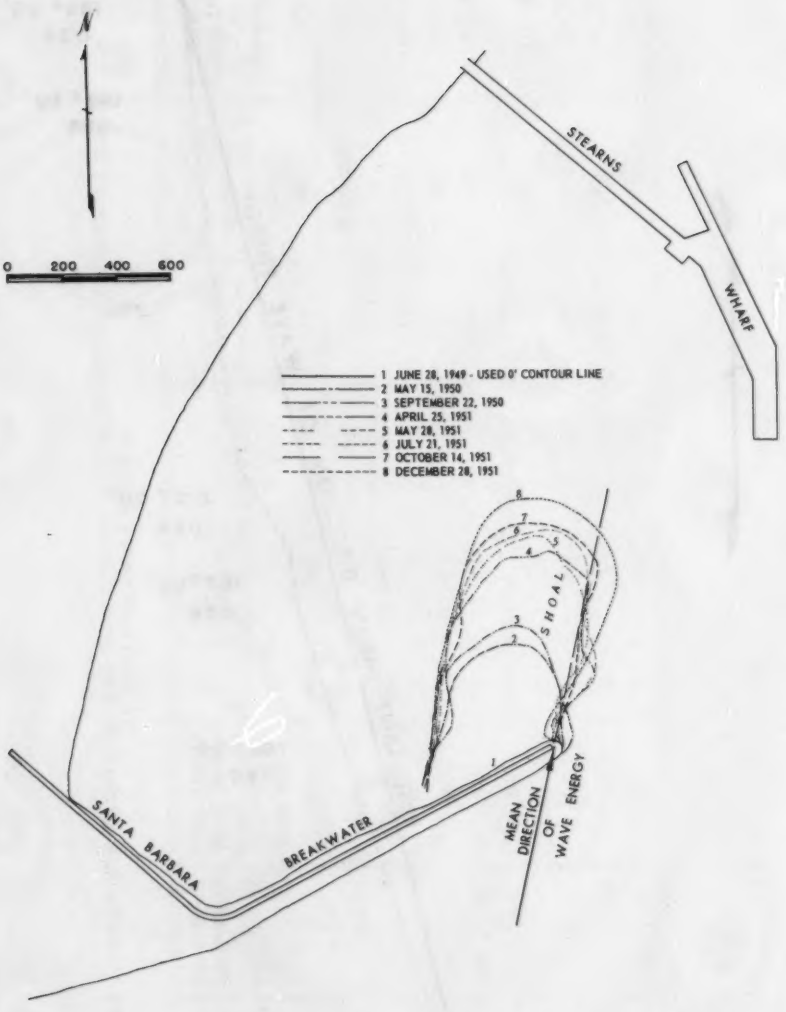

FIG. 5.—TIP SHOAL DEVELOPMENT AT SANTA BARBARA

ENERGY DIRECTION AND SAND DEPOSITS AT DEL MAR HARBOR

How future shoals and beach accretions might aline themselves is a significant concern in the design of a new small craft harbor being planned for development by the City of Oceanside, Calif. The proposed harbor would be dredged from low lands alongside the United States Marine Corps' Del Mar Harbor at Camp Pendleton. The mean effective wave energy approach has

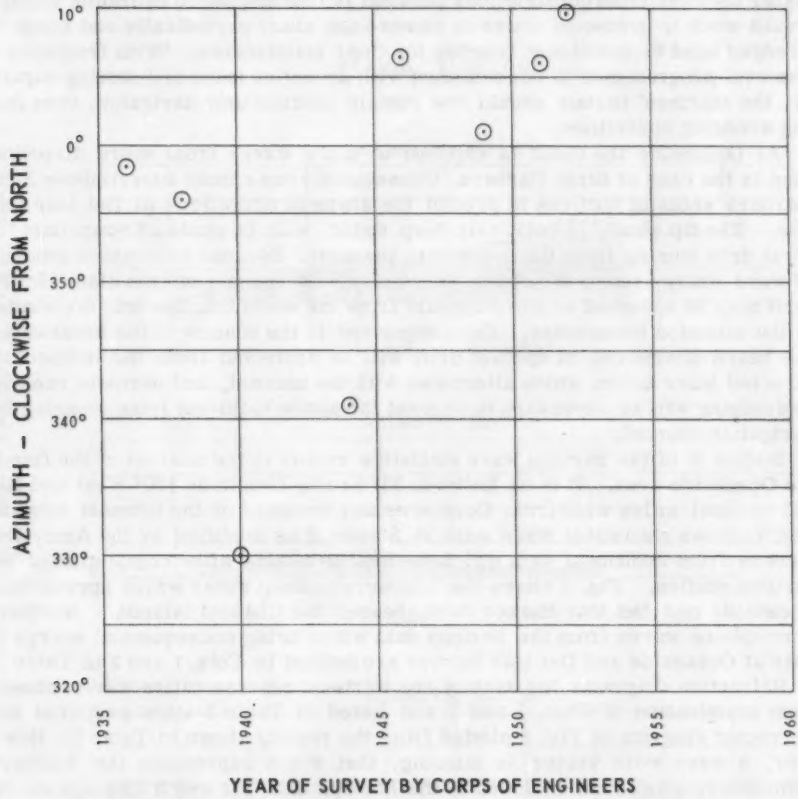

FIG. 6.—DIRECTION OF EXPOSED SIDE OF BREAKWATER TIP SHOAL AT SANTA BARBARA

been applied by the writer as one of several design guides. A prime concern has been to avoid any conflict in navigation by Marine Corps and civilian craft while gaining the advantage of two harbors being served by one capital expenditure for works which make littoral drift bypassing possible.

In early 1958 the breakwater at the small Marine Corps amphibious training harbor was extended 2,300 ft, generally parallel to the shoreline. As a result of the extension a physical arrangement very similar to that at Santa Barbara now exists. Prior to the breakwater extension it was difficult and

hazardous, and therefore expensive, to remove accretions of littoral drift which occurred in the harbor entrance, and the dredging plant completely occupied the entrance during excavation. On one occasion accretions were removed before the breakwater was extended, and the harbor entrance became clogged again within 9 months.

The design for the modification (by James W. Dunham, M. ASCE) was conceived to fix the location of downcoast drift deposits in the lee of the breakwater tip away from constrictions between jetties and where hydraulic dredges would work in protected water to remove the shoal periodically and pump the dredged sand to downcoast beaches for their maintenance. With frequency of removal programmed to be consistent with accretion rates and storing capacity, the Marines' harbor should now remain continuously navigable, even during dredging operations.

At Oceanside the coast is exposed to more waves from more directions than is the case at Santa Barbara. Consequently one cannot superimpose Santa Barbara shoaling outlines to predict the shape of accretions at Del Mar Harbor. The tip shoal, in relatively deep water, will be made of downcoast littoral drift coming from the beaches to the north. Because substantial amounts of wave energy reach the shore seasonally with upcoast effects also, littoral drift may be expected to move upcoast from the south beaches into the shadow of the extended breakwater. Once deposited in the shadow of the breakwater, the beach accretions of upcoast drift will be protected from the downcoast-directed wave action which alternates with the upcoast, and periodic removal by dredging will be necessary to prevent the shore build-out from clogging the navigation channel.

Station E of the Scripps wave statistics report is the nearest of the five to the Oceanside area. It is at Latitude 33° North, Longitude 120° West and lies 130 nautical miles west from Oceanside and seaward of the Channel islands. Fig. 7 shows statistical wave work at Station E as modified by the Army Engineers from additional data which became available after completion of the Scripps studies. Fig. 1 shows the exposure to deep water waves approaching Oceanside and Del Mar Harbor from beyond the Channel islands. Northern Hemisphere waves from the Scripps data which bring consequential energy to bear at Oceanside and Del Mar Harbor are defined by Cols. 1 and 2 of Table 2.

Refraction diagrams for each of the thirteen representative waves chosen from examination of Figs. 1 and 7 and listed in Table 2 were prepared and the vector diagram of Fig. 8 plotted from the results shown in Table 2. However, a wave work vector is missing, that which represents the Southern Hemisphere swells not included in the Scripps data but which impinge on the Oceanside coast each summer when winter storms south of the equator generate them and send them to California waters.

The southern swells arriving in the Oceanside reach of the California coast are known to have periods of about 20 sec. To determine the direction of a southern swell vector, refraction diagrams for 20 sec waves of 180° and 190° deep water azimuths were prepared, and it was found that their refracted directions at the tip of Del Mar Harbor breakwater were azimuth 214° 50' and azimuth 216° 15' respectively. Azimuth 215° 35' was selected as a representative southern swell direction.

To complete the vector diagram for Del Mar Harbor by giving the directed southern swell a relative energy magnitude, a littoral drift factor approach was utilized. On August 16, 1958, the Army's Los Angeles District Engineer's

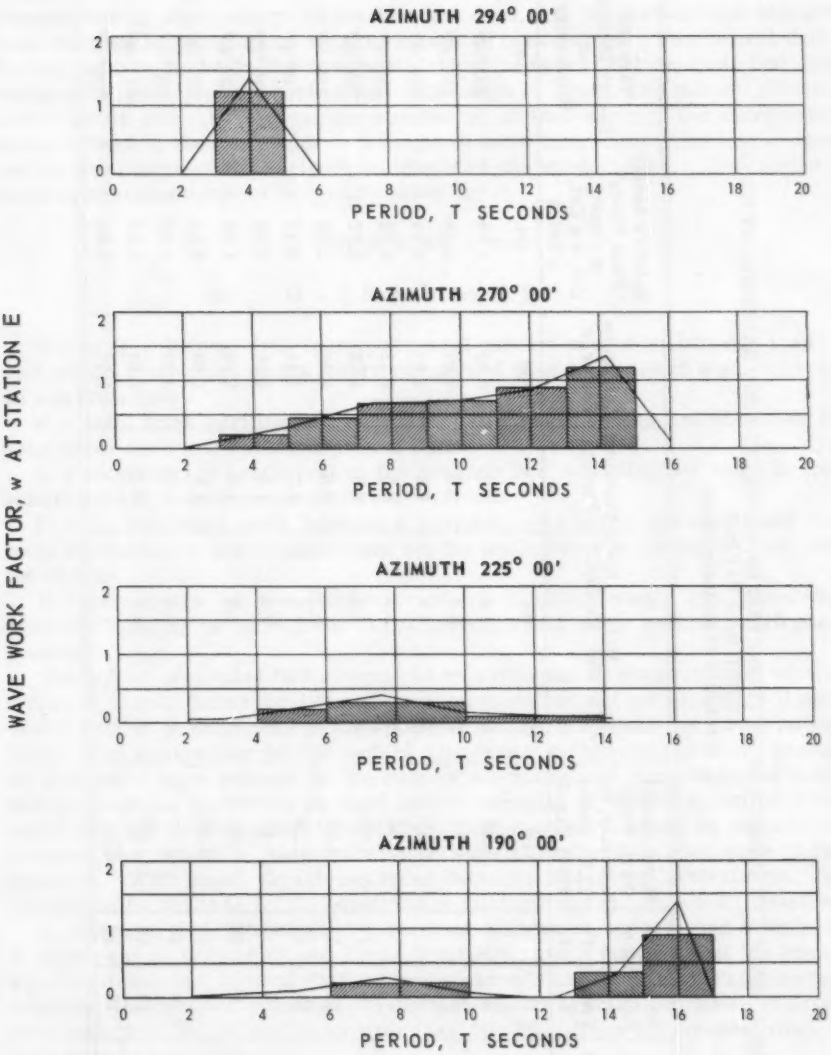

FIG. 7.—ANNUAL WORK BY WAVES AT DEL MAR HARBOR

TABLE 2.—RELATIVE MAGNITUDE AND DIRECTION OF ANNUAL ENERGY EXPENDED BY WAVES AT DEL MAR HARBOR
(Exclusive of Southern Swell)

Deep Water Wave Azimuth	Period, T_m, in Seconds	Wave Work Subdivision (3) From T_1	To T_2	Mean Annual Wave Work Factor, w, for 22.5° Sector from Fig. 7	T_2-T_1	$w(T_2-T_1)$, Col. 4 x Col. 5	Exposure Factor	Refraction Factor, e	Relative Annual Wave Energy at Coast, Col. 6 x Col. 7 x Col. 8	Wave and Energy Direction at Breakwater
(1)	(2)			(4)	(5)	(6)	(7)	(8)	(9)	(10)
294°	4	3	5	1.20	2	2.4	0.7	0.89	1.50	291°00'
270°	4	3	5	0.20	2	0.4	0.5	0.96	0.19	267°45'
270°	6	5	7	0.45	2	0.9	0.5	1.00	0.45	265°40'
270°	8	7	9	0.65	2	1.3	0.5	1.11	0.72	259°30'
270°	10	9	11	0.70	2	1.4	0.5	1.02	0.72	253°50'
270°	12	11	13	0.90	2	1.8	0.5	1.00	0.90	250°15'
270°	14	13	15	1.20	2	2.4	0.5	1.18	1.42	246°55'
225°	5	4	6	0.20	2	0.4	1.5	1.00	0.60	226°20'
225°	8	6	10	0.30	4	1.2	1.5	1.04	1.88	227°20'
225°	12	10	14	0.10	4	0.4	1.5	1.09	0.65	227°55'
190°	8	6	10	0.20	4	0.8	0.75	0.87	0.52	203°00'
190°	14	13	15	0.35	2	0.7	0.75	1.03	0.54	214°00'
190°	16	15	17	0.90	2	1.8	0.75	1.00	1.35	216°40'

office presented a derivation of a littoral drift factor. The District Engineer emphasized that the derived relationships, which describe the quantity of sand transported by wave energy in the breaker zone, are theoretical and had not been verified by experiment or other means of observation. The littoral drift factor, Q, was based on the assumption from mathematical analysis that for waves of a given energy content per unit length of crest, the rate of littoral drift varies with the alongshore component of that energy, the component being related to the energy per unit length of wave crest multiplied by the sine and by the cosine of the angle of incidence of the wave energy. The mathematical representation of the relationship is:

$$Q = K\ w\ E \sin I \cos I$$

$$\text{or} \qquad Q = \frac{1}{2} K\ w\ E \sin (2\ I)$$

Where Q = littoral drift factor, the total amount moved in littoral transport past a given point on the shore per unit of time by waves of a given period and direction.

w = total work performed by all waves of a given period and direction in deep water during the selected unit of time.

E = wave energy coefficient at the breaker line, adjusting for width of exposure sector, convergence or divergence, etc.

I = the incidence angle between a perpendicular to the shore line and the wave orthogonal at the breaker line; or, the angle between the wave crest and the shore.

K = a constant for the particular shore condition under consideration, probably relating to sand grain characteristics and other related beach phenomena.

The writer concluded that absence of experimental or observational verification of the Q factor for littoral draft computation did not eliminate it as a useful tool if its empirical parts wholly or nearly disappear by cancellation. Thus, if an expression for the sum of all upcoast components of wave energy at Oceanside were equated to the sum of all downcoast components of wave energy, and the quantities of sand moved annually in either direction were equal (50 : 50), any uncertainties of the Q-factor equation would be immaterial because they would be included in identical multipliers on each side of the equation. With small departures from balanced reversing littoral drift, the uncertainties in the Q-factor equation are minimal and possibly not important.

It is known that littoral sand movement alternates upcoast and downcoast in each year at Oceanside and Camp Pendleton, and it appears that the annual average downcoast littoral drift quantity exceeds the annual average upcoast quantity; the ratio of downcoast to upcoast annual average quantities is probably less than 70 : 30 and is greater than 50 : 50. Thus for consideration, it may be said for Oceanside:

$$Q_d = R_q\ Q_u \quad \ldots\ldots\ldots\ldots\ldots\ldots \quad (1)$$

where Q_d = Annual downcoast littoral drift

$$= \frac{1}{2} K\ (w\ E)_D \sin \left(2\ I_D\right) \quad \ldots\ldots\ldots\ldots\ldots\ldots\ldots\ldots \quad (2)$$

the subscript D referring to the resultant relative wave energy vector D shown on Fig. 8

and Q_u = Annual upcoast littoral drift

$$= \frac{1}{2} K (w\ E)_U \sin \left(2\ I_U\right) \quad \ldots\ldots\ldots\ldots\ldots\ldots \quad (3)$$

the subscript U relating to the resultant vector for all upcoast waves, including the unknown southern swell energy

and R_q = the ratio of downcoast to upcoast annual littoral drift quantities.

The value Q_u may be divided in two parts, the known upcoast relative energy magnitude and direction represented by the resultant vector B on Fig. 8, and the unknown magnitude but known direction of southern swell energy, S. The division of Q_u is:

$$Q_u = Q_B + Q_S \quad \ldots\ldots\ldots\ldots\ldots\ldots \quad (4)$$

$$= \frac{1}{2} K (w\ E)_B \sin \left(2\ I_B\right) + \frac{1}{2} K(w\ E)_S \sin \left(2\ I_S\right) \quad \ldots\ldots \quad (5)$$

Substituting Eqs. 2 and 5 into Eq. 1 there results:

$$(w\ E)_S = \frac{(w\ E)_D \sin \left(2\ I_D\right) - R_q\ (w\ E)_B \sin \left(2\ I_B\right)}{R_q \sin \left(2\ I_S\right)} \quad \ldots\ldots\ldots \quad (6)$$

The factors (w E) in the development may be represented by the scale values of the relative energy vectors. The angles I may be represented by the incidence angles of the respective vectors with the normal to a Corps of Engineers Beach Erosion Board baseline, which parallels the general coastline on an azimuth of 325° 25'. The following values may be taken from Fig. 8.

$(w\ E)_D$	= 5.65	Relative energy with downcoast effect
I_D	= 27° 30'	Incidence angle of $(w\ E)_D$
$(w\ E)_B$	= 5.50	Relative energy of upcoast waves, excepting southern swell
I_B	= 14° 30'	Incidence angle of $(w\ E)_B$
I_S	= 19° 50'	Incidence angle of southern swell

Substituting these values in Eq. 6 and using a 60 : 40 ratio for R_q, the computed relative energy at the coast of swell from the Southern Hemisphere becomes:

$$(w\ E)_S = 0.66$$

With 63.5 : 36.5 substituted for R_q, the computed magnitude of $(w\ E)_S$ is zero. It is not reasonable to say there is no southern swell energy effective in beach transport at this locality, so this ratio value trial was rejected. With R_q of 55 : 45 used with the vector data, $(w\ E)_S$ became 1.78, roughly equivalent to one-fourth of all energy delivered to the coast by waves of upcoast effect. Statistics specifically compiled for amphibious maneuver planning have been accumulated for 8 yr at a Camp Pendleton surf and weather station. The Marine Corps has not rendered an opinion thereon, but examination of these

classified data did not indicate that so high a percentage of upcoast energy is delivered at the Oceanside-Del Mar Harbor shoreline by southern swell. Work by a field group from the Beach Erosion Board in charge of D.R. Forrest, M. ASCE, compiled wave observations at Mission Beach (San Diego) in 1950 which indicate that southern swell delivered less than 5% of the wave energy at that location in the year. Adoption of the 60 : 40 littoral quantity direction ratio appeared to be justified. The result of adding the southern swell relative wave energy vector from the 60 : 40 computation to the diagram of Fig. 8 is shown by the complete vector diagram on Fig. 9. On that vector diagram resultant energy directions for any combinations of statistical waves and the computed southern swell are definable and were used as guides in delineating the outline of the expected shoal behind the breakwater tip and the anticipated shoreline accretion in its shadow. Vector R is the resultant of all waves, including the estimated southern swell; vector D is for all downcoast

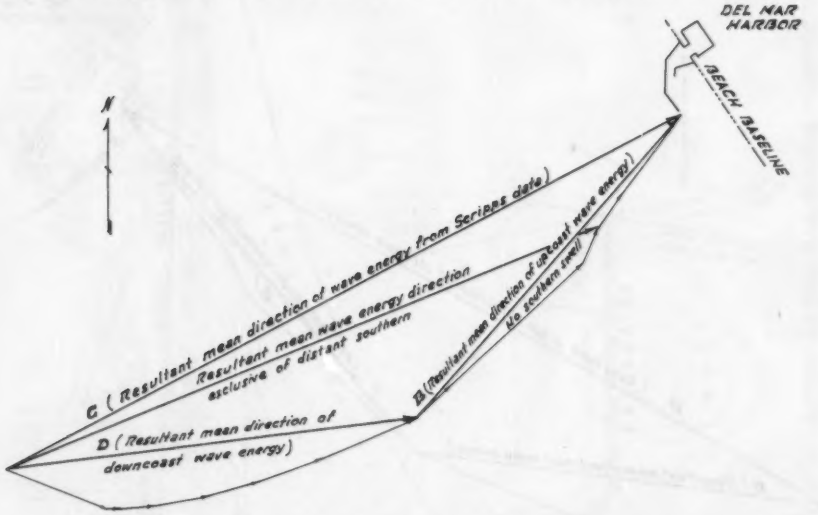
DEL MAR HARBOR
BEACH BASELINE
N
C (Resultant mean direction of wave energy from Scripps data)
Resultant mean wave energy direction exclusive of distant southern
B (Resultant mean direction of upcoast wave energy) Ue southern swell
D (Resultant mean direction of downcoast wave energy)

FIG. 8.—VECTORS OF ANNUAL WORK AT OCEANSIDE, EXCLUSIVE OF SOUTHERN SWELL

waves; vector U is for all upcoast waves, including southern swell. Fig. 9 was also used as a design guide for location and alignment of the entrance to the proposed Oceanside Harbor.

Relying upon the energy vector resultant for all waves at Oceanside (R, Fig. 9 as one guide, it was predicted that the littoral drift moving downcoast to the tip of the Del Mar Harbor north breakwater will form a shoal in the breakwater's shadow which will be shaped about as shown on Fig. 10. The shoal indicated contains 300,000 cu yd. Its underwater slopes are consistent with those noted on accretions in the throat of the entrance to Del Mar Harbor before its modification and rehabilitation. The width of shoal shown was arbitrarily set at 500 ft, which is roughly one and one-half wave lengths at the breakwater depth for a 12-sec wave. The shoal is not likely to be narrower when it has actually formed. If wider, its extension toward shore will be slower, and navigability of the Del Mar entrance will be feasible for longer periods of time between maintenance removals of the sand.

During periods of upcoast wave action, which occur each year, sand in littoral transport along the beach and in the breaker zone will move against the south jetty of Del Mar Harbor, deposit and form a fillet accretion with a shoreline which is expected to be aligned with the diffracted front of the mean upcoast-directed wave. Resultant vector U of Figs. 9 and 10 describes the mean wave direction at the breakwater tip for upcoast-directed waves. The fillet accretion cannot be removed by natural wave erosion and may have an outline as shown on Fig. 10 when 220,000 cu yd have been deposited.

OCEANSIDE HARBOR ENTRANCE DESIGN

The extreme downcoast limit of the tip shoal at the end of Del Mar Harbor breakwater was a determining factor in locating a public harbor entrance.

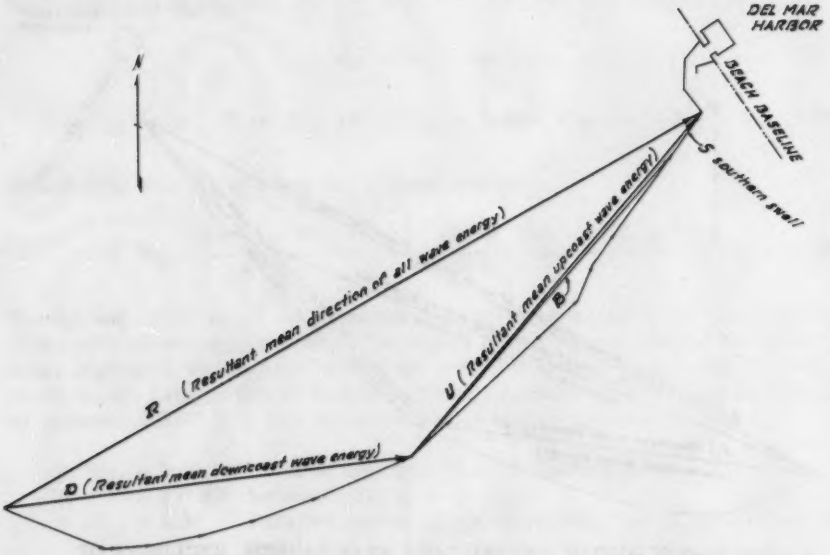
DEL MAR HARBOR
BEACH BASELINE
S southern swell
R (Resultant mean direction of all wave energy)
U (Resultant mean upcoast wave energy)
D (Resultant mean downcoast wave energy)

FIG. 9.—VECTORS OF ANNUAL WORK AT OCEANSIDE, SOUTHERN SWELL ADDED

Fig. 11 shows the position and features of the proposed Oceanside Harbor entrance. The dotted lines on the diffraction diagram on Figs. 10 and 11 show lines of equal change in height of the diffracted waves. The line marked K = 1.17, for example, is the locus of points in the wave after it passes the breakwater tip where the wave height is 117% of its height just seaward of the breakwater. The downcoast entrance jetty for the proposed harbor was located and aligned so that the fairway for Del Mar Harbor entrance would not become less than 400 ft wide unless the tip shoal were allowed to grow to a size which would clot Del Mar Harbor entrance whether a public harbor existed or not. The downcoast jetty for the proposed harbor was also located so as to restrain upcoast littoral drift from entering the sheltered beach between the proposed harbor entrance and Del Mar Harbor south jetty, where it

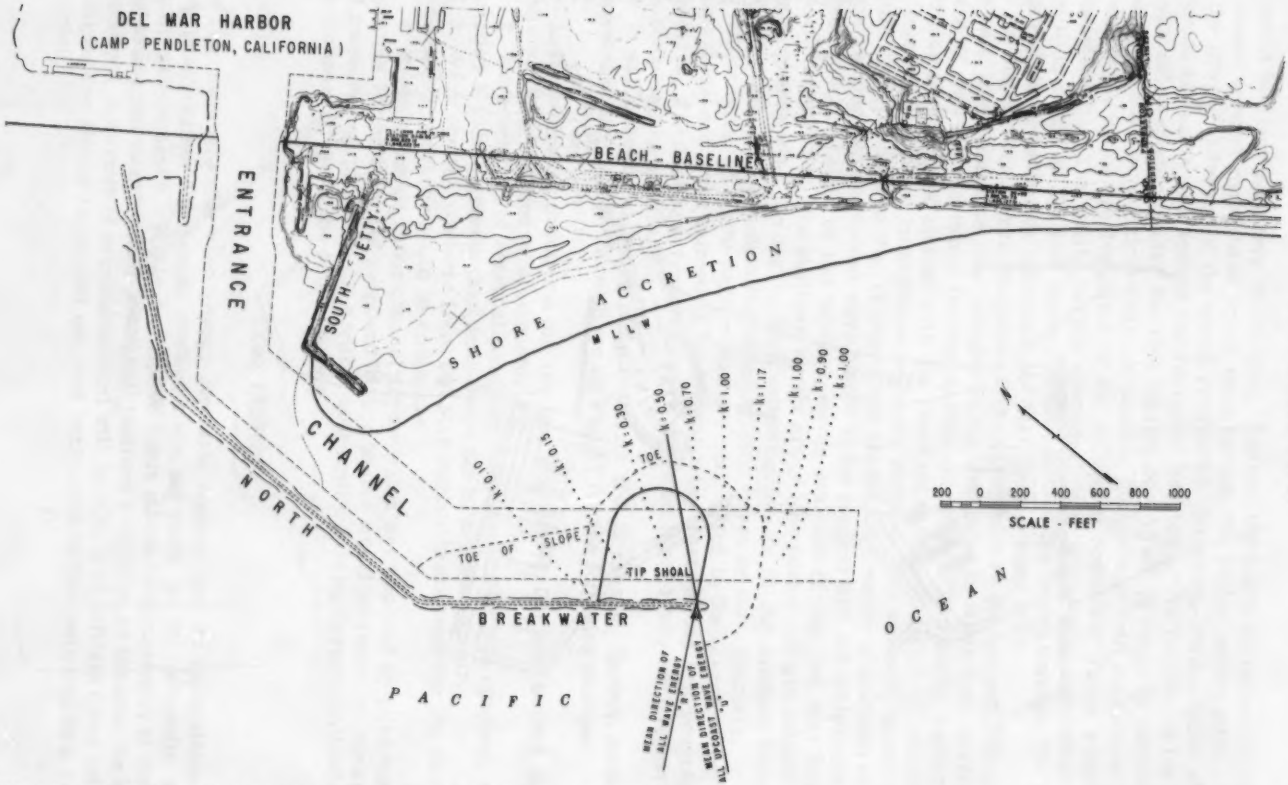

FIG. 10.—PREDICTEN SHOALING AND SHORE ACCRETION AT DEL MAR HARBOR WITHOUT OCEANSIDE HARBOR DEVELOPMENT

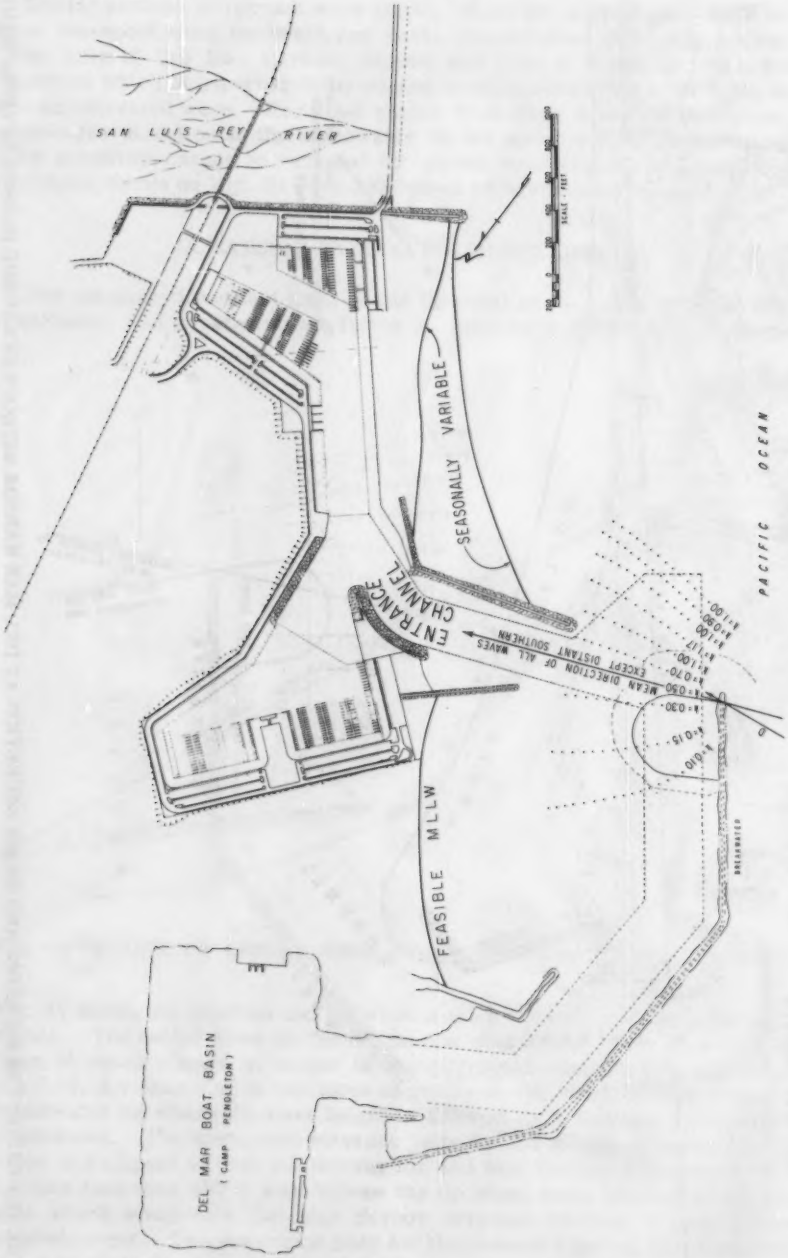

FIG. 11.—PLAN FOR OCEANSIDE HARBOR

would be removable only by dredging. Instead, the beach accretion during the annual upocast drift phase would form against the public harbor jetty. With the littoral influence of the waves reversed in direction, the accretion should erode and move back toward the downcoast beaches. The location of the jetty was selected to minimize the risk that its root to shore might be severed by concentrated wave action while yet causing the upcoast drift accretions to be where the major erosive effect of the diffracted downcoast waves would act beneficially. The public harbor downcoast jetty would also supplement the stilling effect of Del Mar Harbor breakwater on the beach between the proposed public harbor entrance and Del Mar Harbor south jetty.

A sloping-crest groin perpendicular to the shore on the upcoast side of the public habor entrance was included in the design to stabilize the downcoast end of the beach between the two harbor entrances. The public harbor entrance channel was aligned with the resultant energy direction of all waves except those moving from distant southern storms. The wave diffraction pattern superimposed on Fig. 11 shows that except when waves of southern origin are running, the diffracted wave height in the channel will not materially exceed 50% the height of the incident waves seaward of the Del Mar Harbor north breakwater. The southern swells are of long period and are usually low in amplitude when moving in 20-ft water depths, as in the dredged channel. Small craft are not badly affected taking such waves on their quarters.

Other features of the harbor plan are not related to the energy vector design guide and were related to land availability restrictions and geographic features. The harbor arrangements are shown on Fig. 11 only for interest and to complete the picture.

It was considered undesirable to locate the Oceanside Harbor entrance downcoast from the position shown on Fig. 11 for the following reasons:

1. Its beneficial protection for the beach adjoining Del Mar Harbor south jetty would be reduced or eliminated.
2. Wave removal of seasonal beach accretions would be less efficient; diffraction k values greater than unity would not be brought to bear.
3. Wave shelter available from Del Mar Harbor breakwater for the Oceanside Harbor entrance would be minimized.
4. Restrictions on inner channel layout which are imposed by topographic features inland from the proposed harbor basins would increase the severity of maneuvering problems for civilian boat traffic turning toward destinations in the inner areas of the public harbor.

CONCLUSIONS

The mean effective wave energy direction concept and its applications to practical engineering design problems are not pure, in the scientific and mathematical sense. If this description leads others to a consensus of worth and to suggest modifications which will improve reliability or broaden the applications, a warmth of accomplishment will be felt. If significant flaws exist, their nature should be pointed out, and such constructive acts will be a real service.

Journal of the

WATERWAYS AND HARBORS DIVISION

Proceedings of the American Society of Civil Engineers

CONTENTS

DISCUSSION

Generalities on Coastal Processes and Protection by J. B. Schijf (March, 1959. Discussion: September, 1959. Discussion closed).
by J. B. Schijf (Closure) 147

The Effect of Seiches at Conneaut Harbor, by I. A. Hunt. (June, 1959. Prior discussion: December, 1959. Discussion closed.)
by Basil W. Wilson (corrections). 149

Laboratory Investigation of Rubble-Mound Breakwaters by Robert Y. Hudson. (September, 1959. Prior discussion: none. Discussion closed).
by Jose Reis de Carvalho and Daniel Vera-Cruz 151
by William H. Booth, Jr. 154
by Francis B. Slichter. 156
by Leland B. Jones 157

An Electric Analog Model of a Tidal Estuary by H. A. Einstein and James A. Harder. (September, 1959. Prior discussion: none. Discussion closed).
by G. B. Fenwick 161

A Breasting Dolphin for Berthing Supertankers by John M. Weis and Virgil Blancato. (September, 1959. Prior discussion: none. Discussion closed).
by W. F. Manning 163
by Nicholas Bilonok 164
by Jerome M. Richolson 168

A Case of Critical Surging of a Moored Ship, by Basil W. Wilson. (December, 1959. Prior discussion: none. Discussion closes: May 1, 1960).
Corrections 169

Note.—This paper is a part of the copyrighted Journal of the Waterways and Harbors Division, Proceedings of the American Society of Civil Engineers, Vol. 86, No. WW 1, March, 1960.

GENERALITIES ON COASTAL PROCESSES AND PROTECTION[a]

Closure by J. B. Schijf

J. B. SCHIJF.[1]—The author wishes to thank Mr. Silvester for his interest.

The author's purpose has been to emphasize the need for a clear understanding of the physical processes active on the coast as a basis for the design of coastal protection works, and in particular the necessity of distinguishing between the effects of transverse and lengthwise displacements of coastal material by waves and the effects of currents.

Mr. Silvester's comments, in the author's opinion, indicate an agreement with the general term of his paper, in the light of which a slightly different emphasis on some matters of detail does not seem to warrant a lengthy discussion on his part. On a few points, however, he wishes to classify his meaning.

If the author has created the impression that he considers groins as ineffective, he wants to correct this. Perhaps it is to be attributed to the numerous instances of indiscriminate use of groins he has seen, probably on the assumption that what is useful in one place should be so in another. The author knows cases where groins are ineffective, where they are effective enough and where they are too effective. The point is not so much if groins are effective or not, but if they are the most effective (and least harmful) means in the given conditions. May we agree in considering them a more permanent commitment than artificial supply?

In spite of the fact that sand can be transported by waves and wave-induced currents in depths of 10 or 20 m, the author maintains that groins are not the proper type of structure to control the flow in a tidal channel, at least as long as we understand by a groin a rather shallow structure on a gently sloping shore. There is a very marked difference in the scouring action on the tip of a construction of waves and of the eddying flow in a steep-sided tidal channel encroaching on a stretch of coast. This is one of the points the author has sought to underline in his paper.

---

[a] March, 1959, by J. B. Schijf.

[1] Chf., Central Research Div., the Rijkswaterstaat, 's-Gravenhage.

THE EFFECT OF SEICHES AT CONNEAUT HARBOR[a]

Corrections to the Discussion by Basil W. Wilson

CORRECTIONS TO THE DISCUSSION BY BASIL W. WILSON[b].–

p. 181 1st line after Eq. (16) amend "ζ" to "ξ"
p. 181 3rd line after Eq. (16) amend (16) to (6)
p. 181 4th line after Eq. (16) amend "ζ" to "ξ"
p. 181 2nd line after Eq. (19) amend "ζ" to "ξ"
p. 181 3rd line after Eq. (19) amend "ζ" to "ξ"
p. 181 last paragraph, 1st line amend "ζ" to "ξ"
p. 182 4th line above Eq. (22) amend "ζ" to "ξ"
p. 182 3rd line above Eq. (22) amend "ζ" to "ξ"

---

[a] June, 1959, by I. A. Hunt
[b] December, 1959.

LABORATORY INVESTIGATION OF RUBBLE-MOUND BREAKWATERS[a]

Discussion by Jose Reis de Carvalho and Daniel Vera-Cruz, William H. Booth, Jr., Francis B. Slichter and Leland B. Jones

JOSÉ REIS DE CARVALHO[1] and DANIEL VERA-CRUZ.[2]—The writers have followed the extensive and valuable work done in the Waterways Experiment Station on breakwater stability, of which Mr. Hudson's paper is a part. The paper shows the new trend in the study program of that station due to the difficulty in obtaining the exact value of the friction coefficient in Irribarren's formula, the accurate determination of which was the purpose of the former program. In spite of the considerable work already carried out, much remains to be done before the design engineer will be able to achieve an optimum design. For that purpose, the design engineer must not only know how to design the armor cover layer, but also, especially when dealing with great depths, to design the underwater slopes below the lower level of the cover layer. He must also know how to solve the problems involved in the singular points of breakwaters, such as curves and heads. When dealing with shallow depths, the situation is very different from that prevailing at great depths, especially on sandy bottoms when the waves break just before or on the breakwater toe. In this case, even when measures are taken against the setting down of the toe, the increased specific gravity of the water resulting from the great amounts of sand stirred up, must be taken into account. Believing that this is an extremely important point, the writers suggest that, although the experimental conditions during the tests are presented in the text, it would be preferable to stress in the figures of the paper summing up the experimental results that these, due to the test conditions, have a restricted field of application.

The Formula Proposed by the Author.—The author considers that the armor units acted upon by the wave are subjected to two principal forces: a drag force and an inertia force. It is the opinion of the writers that the inertia force is very important and that, if the influence of the term $\frac{\partial V}{\partial t}$ could be investigated, a better understanding of the phenomena occurring in a breakwater would result. However, it being difficult to determine this influence, the author includes this term in the same coefficient which involves the drag coefficient, the virtual-mass coefficient and the shape of the units.

To establish the incipient instability condition, the author makes the resultant of the two forces developed by the waves equal to the buoyant weight of the armor unit. The author, however, takes only the magnitude of those forces into consideration, neglecting their directions. It is the opinion of the writers

[a] September, 1959, by Robert Y. Hudson.
[1] Ass't. Research, Laboratório Nacional de Engeharia Civil, Lisbon.
[2] Ass't. Research, Laboratório Nacional de Engeharia Civil, Lisbon.

that an effort must be made to express the vectorial character of the forces, which is supposed to be all the more important the steeper the slopes. With these simplifications, the proposed formula is:

$$\frac{\gamma_r^{1/3}}{(S_r-1)W_r^{1/3}} = f\left(\alpha, \frac{H}{\lambda}, \frac{d}{\lambda}, C_d, C_n, K_a, K_v, \ldots\right) \ldots\ldots (1)$$

Where the first member is a dimensionless parameter and the symbols are those defined in the paper.

For the test conditions, the author found,

$$\frac{\gamma_r^{1/3} H}{W_r^{1/3}(S_r-1)} = a\,(\cot\alpha)^{1/3} = \left(K_\Delta \cot\alpha\right)^{1/3} \ldots\ldots\ldots (2)$$

in which K_Δ is the shape coefficient, numerical values of which are presented for quarry-stone and tetrapod-shaped units.

Criteria of Stability.—One of the chief advantages of the author's paper lies, no doubt, in the adoption of numerical, consequently well defined, stability criteria. In all the experimental studies so far carried out, both at European laboratories and in those previously described by the Waterways Experiment Station, the criterion left an important part of the experimenter's personal judgment in regard its definition and above all its appreciation. It has thus been impossible to make an accurate comparison of the very numerous results already obtained by the different laboratories where the subject was studied.

The writers believe, nevertheless, that a real effort should be attempted to improve the stability criterion established by the author, for the no-damage condition at least, so that the results can be generalized for use in the design of similar structures.

In fact, the geometrical characteristics of the breakwater sections used in the tests on the quarry-stone armor units and the tetrapod armor units being considerably dissimilar, the results obtained are not comparable, since, as the author states himself, the percentage of damage is proportionally higher for the cover layer of smaller volume. It seems that the most adequate criterion for the no-damage condition should be one in which only the active portion of the breakwater and one or two layers of the protective cover were taken into account.

As regards the tests for determination of the damage or safety factor, it seems that the results obtained apply only to the types of breakwater sections tested. It suffices to point out that, according to the author himself, failure of the tetrapod cover layer occurs for values of $H/H_{D=0}$ slightly exceeding 1.3, while for identical values of $H/H_{D=0}$ in the quarry-stone armor unit tests, only 5% to 15% damages were observed. Consequently, we believe that safety factors should be determined for each particular case, as it is very difficult, if not impossible, to find a criterion of stability in which the multiple causes conducive to damage in breakwater subjected to waves with a $H > H_{D=0}$ could be considered.

Iribarren's Formula.—In the deduction of his formula, Iribarren considers as the principal resistant force the one resulting from friction between blocks. His formula, as presented in Hudson's paper, is:

$$W_r = \frac{K' \gamma_r^3 H^3 \mu^3}{(\mu \cos \alpha - \sin \alpha)^3 \left(S_r - 1\right)^3} \quad \ldots\ldots\ldots\ldots \quad (3)$$

With regard to μ, Iribarren says that it will be very close to the tangent of the natural slope of the layer-units. According to Iribarren, μ is greater than 1, but he recommends that one use $\mu = 1$, which would introduce a certain safety factor. This point must be explained and the writers need to present here the conditions near the quarry-stone breakwater, the observation of which permitted Iribarren to determine the coefficient to be used with quarry-stone breakwaters. Iribarren used the non-homogeneous expression of Eq. 3,

$$W_r = \frac{N H^3 S_r \mu^3}{(\mu \cos \alpha - \sin \alpha)^3 \left(S_r - 1\right)^3} \quad \ldots\ldots\ldots\ldots \quad (4)$$

where

$$N = K' \gamma_w \quad \ldots\ldots\ldots\ldots\ldots\ldots \quad (5)$$

The breakwater observed by Iribarren was of quarry stone with a sandy bottom, its water depth in high water was 4.5 m and the slope toe lay at the low-water level. The stones had a weight of 3 metric tons, $S_r = 2.65$ and the equilibrium slope was cot $\alpha = 3.1$. Iribarren assumed that the height of the maximum wave was H = 4.5 m (water depth in high water) and $\mu = 1$. A value of N results equal to 0.015. If, according to Iribarren, one takes $\mu > 1$, a new value would result for N. Let us call this new value N'. It is easy to see that $N' > N$ and that, with such a value N' and the corresponding μ, no safety factor would have been introduced by taking $\mu = 1$ and the corresponding value of N. If now, according to Iribarren, we assume that N and N' are not variable with the slope, it can be seen by a simple computation, that $\mu = 1$ as an unsafe assumption when cot $\alpha < 3.1$, and a safe one when cot $\alpha > 3.1$. However, the safety factor introduced in these slopes varies with the slope, and this variation can be very important (for example, if the actual value is $\mu = 1.09$, the safety factor with $\mu = 1$ is about 1.1 if cot $\alpha = 2$ and 2.2 if cot $\alpha = 1.25$). The difficulty in defining with exactitude what is the natural slope, makes the use of Iribarren's formula too uncertain.

Besides, it is the opinion of the writers that, owing to the particular conditions near the quarry-stone breakwater observed by Iribarren (very small depths and sandy bottom), the generalization of the coefficient determined is very problematical.

Comparison Between Hudson's and Iribarren's Formulas.—Let us consider Eq. 2. We can give a similar expression to Iribarren's Eq. 3:

$$\frac{\gamma_r^{1/3} H}{W_r^{1/3}\left(S_r - 1\right)} = \frac{(\mu \cos \alpha - \sin \alpha)}{K'^{1/3} \mu} \quad \ldots\ldots\ldots\ldots (6)$$

Let $\left(\frac{1}{K'}\right)^{1/3} = K$, and let us equate the two second members of Eqs. 2 and 6:

$$K \cos \alpha - \frac{K}{\mu} \sin \alpha = K_\Delta^{1/3} (\cot \alpha)^{1/3}$$

$$K \left(\cos \alpha - \frac{1}{\mu} \sin \alpha\right) = a (\cot \alpha)^{1/3}$$

$$K = \frac{a (\cot \alpha)^{1/3}}{\cos \alpha - \frac{1}{\mu} \sin \alpha} = a \frac{(\cot \alpha)^{1/3}}{\cos \alpha - \frac{1}{\mu} \sin \alpha}$$

$$K'^{1/3} = \frac{\cos \alpha - \frac{\sin \alpha}{\mu}}{a (\cot \alpha)^{1/3}}$$

$$K' = \frac{\left(\cos \alpha - \frac{\sin \alpha}{\mu}\right) 3}{K_\Delta \cot \alpha} \quad \ldots\ldots\ldots\ldots\ldots (7)$$

This expression relates Iribarren's coefficient K' with Hudson's coefficient K_Δ. And, K_Δ being a constant for the test conditions, the expression above shows that Iribarren's coefficient is a function of the slope α.

Using Eq. 7 we can always suppose $\mu = 1$ when cot α is greater than one. By this means, the writers think that Iribarren's formula is susceptible of experimental verification, provided that its coefficient is not considered a constant.

Summing up, the writers think that the great merit of Hudson's coefficient lies in the important advantage of being constant, whatever the slope. It should not, however, be called a shape coefficient, as it necessarily involves the friction as well and is also dependent on the physical nature of the surface of the blocks.

WILLIAM H. BOOTH, F. ASCE.[3]—Due to the peculiar character of rubble structures and the phenomena of wave action thereon, it has been difficult, in the past, to arrive at designs which are both safe, from a structural standpoint, as well as being economical to construct. The many variables present in the phenomena of waves attacking a rubble structure greatly complicate the problem of analysis. The science of rubble breakwater structures is still in an early stage of development. The writer of the paper has done a great service to the engineering profession in presenting the model data developed to date. However, much work remains to be done.

---

[a] September, 1959, by Robert Y. Hudson.

[3] Chf., Maritime Sect., Structural Branch, Engrg. Div., Civ. Works, Office, Chf. of Engrs., Washington, D. C.

Until recent years, the design of rubble-mound breakwaters was usually based on observed performance of like structures without any regard to the wave characteristics at the proposed location. As a result, several rubble-mound structures have been damaged and maintenance costs have been high.

The original purpose of the laboratory investigation was to provide data from which an efficient design of rubble-mound breakwaters could be selected for different conditions of use and wave attack. It was believed that the results of the investigation would allow the formulation of equations for more scientific designs. The original investigation has been expanded and the results to date are contained in the paper.

The new stability formula presented has been used to determine the weight of armour units for rubble-mound structures on several projects constructed by the Corps of Engineers. However, the values of the experimentally determined coefficient (K_{Δ}) should not be considered as final at this stage of the testing program. Additional model studies of rubble-mound breakwaters are being conducted in a wave tank capable of producing 6-ft waves. Information from these studies will provide data on scale effects. The wave tank is located at the Beach Erosion Board, Washington, D. C.

The weight of the tetrapods described by John E. Deignan,[4] F. ASCE was determined from results of the small scale model study. His paper presents some of the problems encountered in the design and construction of projects of this nature. From a structural and hydraulic standpoint, the tetrapod is considered to have a desirable shape for good stability when subjected to wave forces. However, an indicated royalty cost in the United States of $3.00 per cu yd of tetrapod volume may limit its use to a small number of projects due to economy.

The tribar has been patented in the United States by R. Q. Palmer. The patent provides for the manufacture and use by or for the Government for governmental purposes without royalty payment. Patent applications are pending in several countries. This shape of armour unit has been manufactured and used for the repair of the breakwater at Nawiliwili Harbor, Island of Kauai. The project is under the jurisdiction of the U. S. Army Engineer District, Honolulu. The weight of the units was determined under the same testing program. This breakwater is a rubble-mound structure about 2,150 ft in length which had been damaged by storm waves. Quarry rock of sufficient weight to insure stability of the breakwater, without excessively flat slopes, was not available. Since preliminary model studies indicated that the tribar was slightly better than the tetrapod, it was decided to prepare three alternate plans for reconstruction of the breakwater. One plan was designed to use only stone. Two other plans were designed using precast concrete shapes on the seaward slope. One of these called for the use of 20-ton tetrapods and the other called for the use of 17.8-ton tribars. The tribar armour facing as well as the tetrapod armour facing, requires a solid backing to present ravelling when subjected to design wave overtop the structure. Therefore, both plans provided for concrete caps. Bids for the reconstruction were opened by the Honolulu District Engineer on April 30, 1958. The low bid was on the tribar plan. Since completion of the project, the breakwater has been subjected to heavy wave action. Preliminary information available at this time, (December 1959), indicates

---

[4] "Breakwater at Crescent City, California," Proceedings, ASCE, Journal of the Waterways and Harbors Division, September, 1959.

minor shifting of the tribars down the slope. The maximum measured distance was about 9 in. This movement was expected due to the consolidation of the rubble-mound and the tribar cover layer.

It is desired to emphasize the point that weight of armour units, determined in accordance with experimental data presented, will not necessarily apply to the seaward end, or head, of breakwaters. The ends are subjected to severe wave action and must be strengthened accordingly. In 1958, storm waves moved tetrapods weighing approximately 33 tons each off the heads of the breakwaters at Kahului Harbor, Territory of Hawaii. The tetrapods on the head were of the same weight as those designed and placed on the seaward slope of the breakwater. The expanded laboratory investigation program includes tests for the treatment of the head of breakwaters. It is hoped the investigation can be continued in order to provide sufficient data to insure safe and economical designs of rubble structures.

FRANCIS B. SLICHTER, F. ASCE.[5]—The author's development of hydraulic model testing procedures and formulas for evaluating test results are significant contributions toward rationalizing the variables involved in breakwater design.

To be effective, a breakwater must accomplish its purpose of reducing the waves generated by severe storms to tolerable levels in the designated harbor area. Often, several alternative breakwater layouts can be developed which although not equal in performance may give acceptable results. Consequently, decision on the layout to be selected will depend upon an economic analysis considering first cost, maintenance costs, and relative performance in protecting the harbor area. In fact, economic limitations can force the acceptance of a breakwater design which allows severe harbor disturbance or breakwater damage during critical storm periods.

Breakwater design is far removed from status as a science where application of formulas will lead to an exact solution. In addition to gaps in knowledge of wave phenomena wherefrom we derive the "design wave," we lack finite information on the reaction of the breakwater armour units and of its core material and foundation under the complex hydraulic impact of the waves. When we adopt a design using armour units of pre-cast concrete, we must accept unknown limitations imposed by structural strength of fabricated units and durability of concrete (and reinforcing steel, if used) in seawater. Therefore, although the guide lines contributed by the author's work are valuable aids, the design of breakwaters must remain largely in an area dominated by sound judgment based on observations of past experience.

In an effort to augment its experience record on fabricated armour units, the Corps of Engineers has constructed a tetrapod armoured breakwater at Crescent City, Calif., and has used the tribar shape in reconstruction of the breakwater at Nawaliwili Harbor, Island of Kauai, Hawaii. The weights of individual armour units are 25 tons, and 17.8 tons, respectively. Observations over several years are anticipated before conclusive data can be assembled as design criteria.

The value of experience is demonstrated by that of the Corps of Engineers at Kahului Harbor, Island of Maui, Hawaii. At this harbor two breakwaters converge to form the harbor entrance. The design wave height which is in the

---

[a] September, 1959, by Robert Y. Hudson.

[5] Chf., Engrg. Div., Civ. Works, Office, Chf. of Engrs., Washington, D. C.

general magnitude of 28 ft actually will overtop the breakwater. The breakwaters were repaired in 1952, with armour stone of 12-ton weight. In the storm of March 1954, the ends of both breakwaters were damaged to the extent that restoration was essential to continued harbor use. Past experience with breakwater heads subjected to wave attack from divergent sources has demonstrated a requirement for monolithic cast-in-place concrete blocks with weight of several hundred tons. However, funds in the amount needed for such head construction were not available, and it was decided to rebuild the heads with the same weight armour unit selected for the breakwater proper. Consequently, the 33-ton units of the tetrapod shape used on the breakwater were also placed around each head. In December 1958, the breakwater was subjected to a storm delivering waves of design magnitude. Examination, subsequent to the storm, revealed that the tetrapods had been stripped from the face of each breakwater head. Some of the 33-ton tetrapods had been moved over 100 ft into the interior of the harbor. In fairness to Neyrpic (Grenoble, France), inventors of the tetrapod, their representative had advised that tetrapods used in armouring the head should be of greater weight than those used on the breakwater proper.

In view of the magnitude of the weight scale ratio between the author's model armour unit and the prototype (over 300,000 for the Kahului tetrapod), it is doubted that there is any practical design significance in abandoning the Iribarren formula with its troublesome friction coefficient in favor of the author's new formula. On the other hand, the derivation of the author's formula results in a valuable tool for his use in evaluation of his model test data.

In developing his formula for stability, the author has considered that friction between armour units can be neglected. This assumption is questioned, in particular for fabricated shapes such as the tetrapod and tribar. It would appear that part of the large differences between stone and fabricated shapes in test values for K could be attributed to reactions caused by shear forces between units. Further research to explore the relative effects of unit-shape, porosity and reaction between units should contribute information useful in breakwater design.

Further work also is needed in developing criteria for armour shapes and in placement procedures for aid in design of the seaward end (head) of a breakwater.

LELAND B. JONES,[6] F. ASCE.—The advantages of the formula developed by Mr. Hudson are evident when one considers the uncertainties inherent in breakwater design. Use of the formula with the shape factor K_Δ, if selected with reasonable care, should lead to consistently better design than use of Iribarren's formula where the accurate selection of the friction factor is both critical to accurate design and difficult to do, especially when manufactured shapes are used.

Since close control can be maintained in sizes and shapes of materials used for breakwater construction, testing of uniform materials leads to practicable design and reduces the number of variables that would otherwise require testing. Also, breakwaters are usually constructed in relatively shallow water, and it has not been necessary to investigate reduction in stability requirements very far below the water surface. For these reasons, rubble-mound breakwater investigations have been confined primarily to testing the stability of uni-

---

[a] September, 1959, by Robert Y. Hudson.

[6] Civ. Engr., Chf. of Soils Sect., Corps of Engrs., Walla Walla, Wash.

form size quarry stone and manufactured units at elevations within the range of wave action.

When railroads, highways, and other structures are constructed along lakes and reservoirs it is often necessary to protect them against wave action, but it has not been considered economical to require uniform size materials or manufactured units for this purpose. Instead, riprap consisting of quarry-run rock having a graduation range is used. The selection of rock sizes and other riprap features has not always been very rational, and often they have been based upon the engineer's judgement, supplemented by experience and the limited amount of available data. In the past some effort has been made to utilize breakwater design criteria for determining required rock sizes needed for graded riprap, but there has always been an uncertainty as to the effects of gradation and how to determine the significant rock sizes.

Development of flood control, navigation, and water power along the lower Columbia and Snake Rivers, in Oregon and Washington, makes a more precise knowledge of riprap requirements necessary. The Corps of Engineers has completed three dams on the lower Columbia River: Bonneville, The Dalles and McNary. Construction is just commencing (1960) on John Day Dam on the Columbia River, and Ice Harbor Dam on the lower Snake River is nearing completion. Three more dams are authorized for construction on the lower Snake River downstream of Lewiston, Idaho. All of these completed, under construction, and authorized projects have these things in common: all are in deep, narrow, steep-walled canyons; all have railroad and highway relocations that are or will be located along the edges of the reservoirs with high fills extending well below the water surface; and all are subject to relatively severe wave action. Riprap design for each of the completed projects was based primarily on Corps of Engineer's experience criteria, but required rock sizes were compared with W_r in Iribarren's formula, in which the assumed friction factor was 1.05. There was some question as to the validity of this assumption because W_r might represent a stone-size smaller than maximum size, water pressures inside the riprap might assume greater importance than in open, one-size stone, and the friction factor might be in error. It was found by measurement that dumped rock fill generally assumed outside slopes of 1 vertical on 1.3 or 1.4 horizontal, which could mean that a friction factor of 0.75 or 0.8 might be more reasonable. If the friction value were 0.75 the stone weight would be increased four times for a 1 on 2 slope.

Completion of Bonneville, The Dalles, and McNary Dams has given the Corps of Engineers, highway departments, and railroad companies with relocations along the reservoirs opportunity to observe the effects of wave action. It is obvious now that additional study is required for adequate and economical riprap design. More than 100 miles of riprap have been provided along the completed projects, and several hundred miles of riprap will be required along projects under construction and authorized. Inadequacies and overdesign can result in substantial extra cost here, where they would not be particularly important on smaller jobs.

As a result, the Waterways Experiment Station is investigating the following features of riprap design and other protection against wave action. These tests are being made for the Walla Walla district, Corps of Engineers, under the direct supervision of the writer.

1. Effects of wave heights and wave periods on graded riprap at the water surface and at variable depths below water surface;

2. necessary depth of riprap toe below water surface when embankment is rock fill;
3. necessary depth of riprap or rock fill toe below water surface when embankment is gravel;
4. height of wave ride-up and depth of wave rundown for graded riprap;
5. limited tests for variable riprap slopes; and
6. comparative effects of wave action on riprap for angles of attack of 30°, 60°, and 90°.

While the testing program has not progressed to the point where results can be published, it has produced some interesting trends, as suspected, and these trends may become important factors in riprap design. For example:

a. The value of W_r for quarry stone, as determined from the author's formula, was compared with results of model tests for graded riprap. Preliminary data indicate the riprap stone size comparable to W_r may be in the order of 20% by weight or 50% by size of the maximum size stone. This was based on tests for well graded riprap where the minimum size stone was about 6% by weight of the maximum size. On this basis, it might be necessary to require more uniform stone sizes where wave action is severe and available stone sizes tend to be small, or where the volume of material required for graded riprap would make the cost excessive.

b. Tests on river gravel having 2-in. maximum size and underwater slope of 1 vertical on 2 horizontal indicate that gravel fill may require riprap protection for 10 ft below water surface for wave heights in the order of 4 ft or 5 ft, and for about 30 ft below for wave heights in the order of 8 ft. The wave period appears to have considerable effect on stability of the gravel. It is interesting to note that the gravel, when tested for damage by wave action at water surface, resisted wave heights of about 0.5 ft.

Since tests are incomplete, it is not possible to present firm conclusions. However, it is believed that the work being performed on riprap is of general interest. These studies are, of necessity, geared to problems and materials typical of the Columbia and Snake River areas, but it is expected that significant data will be obtained to be of value on other related work. It will also be a starting point for future expansion of riprap testing.

AN ELECTRIC ANALOG MODEL OF A TIDAL ESTUARY[a]

Discussion by G. B. Fenwick

G. B. FENWICK,[1] F. ASCE.—It is hoped that the authors will, in the future, extend the scope of their very interesting paper to include at least the major results obtained from the electric analog model of the Delta Region, as well as the engineering significance of these results.

The paper explains the use of the analog model in predicting tidal elevations, as well as flow discharges and average velocities at any desired points throughout the maze of Delta channels, both for existing conditions and with the channel system modified by various possible combinations of channel barriers, cutoffs, and enlargements. The further statement in the paper that it is hoped to derive from the predicted flow velocities (cross-sectional averages) the extents of expected salinity intrusions in the Delta channel complex creates some question as to possible methods of accomplishing such derivations.

In many tidal channels the presence of varying degrees of salinity produces density effects which cause the surface and subsurface currents in a given cross-section to be out of phase, and opposite in direction during a considerable portion of each tidal cycle. In such a case, it appears that the average velocity indicated by an electric analog model would be difficult to interpret in terms of total salinity intrusion into the upstream channel complex, particularly when flows in the different interconnected channels involved are also out of phase with each other.

On the other hand, could it be that density effects in the upper portions of the Delta channel are so small that the average velocities obtained from the analog model may, in this particular case, provide a sufficient basis for determining expected salinity intrusion? It would be interesting to obtain comparisons of the results of the electric analog model with those of the hydraulic model of the San Francisco Bay area for the reaches where these two models overlap.

---

[a] September, 1959, by H. A. Einstein and James A. Harder.

[1] Chf., Rivers and Harbors Branch, U. S. Army Engr. Waterways Experiment Sta., Vicksburg, Miss.

A BREASTING DOLPHIN FOR BERTHING SUPERTANKERS[a]

Discussion by W. F. Manning, Nicholas Bilonok and Jerome M. Richolson

W. F. MANNING,[1] M. ASCE.—Commendations are in order for the author's bringing to rest a rather weighty problem. The writer's views on the few aspects listed below are hereby "tossed into the ring" in hopes that further discussion will result in some clarification.

The free-body diagram (Fig. 1) should have another vertical force, that developed on the face of the fender due to friction with the ship's hull as the fender rides up the under action of P. Such additional vertical force will, in effect, increase the weight W of fender. Also the energy absorbing capacity of the fender system, and the force P will be increased. Assuming the coefficient of friction between the ship's hull and the fender to be 0.25, the value of P required to move the fender becomes 3.52 W as compared to 1.85 W from Eq. 105 for A = 45°. Similarly a coefficient of friction of 0.10 results in P = 2.28 W. Complete retraction of fender due to such loads, P, results in energy absorption of 7,800 and 5,060 in-tons respectively, bracketing the required capacity of 6,350 in-tons obtained from Eq. 1.01. Meanwhile, within limitations of the same assumption and keeping the fender weight at 37 kips, P for the individual fender movement ranges between 130 and 84.5 kips. The increased energy absorbing capacity of the fender is a desirable result of this phenomenon, but the effect of increased P value on the ship's hull and the fender attachment brackets should be analyzed.

The reaction of the supporting pin (Fig. 1) on its inclined support brackets should include a friction force in addition to the normal force that has been taken into account. Insertion of such friction force into Eq. 1.07 and 1.08 yields a resultant moment on the dolphin cylinders at the point of fixity of 80 P, which is simply the cantilever moment of the applied load, P. One should expect to get the same answer by analyzing a free body obtained by considering the whole dolphin above a plane at the "point of fixity" level.

Based on the capacity of the four dolphin cylinders, per Eq. 102, the average load per lin ft of fender = (4) (129) ÷ (6) (20) = 4.30 kips per lin ft. Allowable uniformly distributed load on the two 24 WF 120 wales, assuming 30 ft simple spans and yield-point stress of 33 kips per sq in. in bending about weak axis, is found to be about 2.06 kips per lin ft. This leaves some 11.0 kips per lin ft to be supplied by the remaining portions of fender, which is almost double the 6.0-kip-per-lin-ft fender pressure on the ship's hull listed under "Design Criteria." Also, torsion due to fender bracket supports would further add to the wale stresses.

---

[a] September, 1959, by John M. Weis and Virgil Blancato.
[1] Design Engr., Socony Mobil Oil Co.-Dallas, Tex.
[a] September, 1959, by John A. Weis and Virgil Blancato.

The capacity of the dolphin cylinders to absorb energy is very sensitive to the cantilevered length. For example, using an effective cantilever length of 70 ft, instead of the 80 ft illustrated, increases the allowable value of P by 14% while decreasing the corresponding deflection by 33%. The resulting energy absorbing capacity is some 25% below that for the illustrated case. However, strength is the main requirement of the cylinders, as it has been pointed out that the capacity of the retractable fenders can be sufficient to care for the applied energy. Thus the dolphin system becomes merely a structure affixing the fender system to the firm bottom below 50 ft of water. Probably no other structural element would be more efficient in this regard.

NICHOLAS BILONOK.[2]—The paper presented by the authors shows how the heaviest load of a berthing ship may be absorbed by the elastic deformation of the dolphin breasting structure.

The design of dolphins and other maritime structures for lateral loads is a subject which is dealt with in some textbooks. The author's results fully confirm the usefulness of the general methods of analysis applied and are a welcome addition to the literature of a dolphin breasting type structure design.

The writer adds the following discussion in the hope that it may throw further light on another type of dolphin structure for berthing ships.

The critical factor in estimating berthing impact loads is the assumed speed of approach of the ship; some factors which will influence the berthing speed are:

1. The location of the dolphin. Enclosed harbors minimize the risk of winds blowing a ship against a dolphin. To open channels or exposed situations, the dolphins are more liable to impact at higher speed of approach.
2. The presence of river or tidal currents will obviously increase the risk of serious impact due to an error of judgment of the pilot, whereas a ship coming alongside in still water has a better chance of making a smooth approach.
3. The larger the ship, the greater the care with which it is handled when berthing.

The estimate of approach-speed at berthing is thus a matter of judgment for the designing engineer in consultation with pilots and other persons who have experience in berthing of the ships.

The lateral forces assumed to act on the dolphins always include impact of the ship tying up alongside of them. In order for a ship to attain a position parallel to the center-line of dolphins, it is customary to pull the ship itself toward the dolphins by means of its hoisting winches, ropes, and the mooring posts.

This horizontal pull in the direction of the ship, cannot, of course, exceed the capacity of the winch. In approaching the dolphins with a speed of 1 ft per sec is commonly used in practice,[3] the ship will be brought to a standstill by making contacts with the fender system of the structure. A considerable amount of kinetic energy is delivered to the structure, which must be absorbed by the elasticity of the dolphins themselves.[4]

---

[2] Civ. Engr., Engrg. Div. Corps of Engrs., U. S. Army, Philadelphia, Pa.

[3] "The Design of Piers, Jetties, and Dolphins," by D. A. Hopkins, Proceedings Paper 727, June, 1955.

[4] "Substructure Analysis and Design," by P. Andeson, M. S. Ph. Dr.

The Army Engineers use a unique system of dredging to maintain the ship channel in the Delaware River between Philadelphia and the Atlantic Ocean (about 97 miles). This new system developed by the Army Engineers, several years ago, is called the Sump Rehandling System.

On the left in Fig. D1, is the Sump Rehandler New Orleans, a hopper dredge, which has been converted to a rehandling unit by equipping it with high-powered pumping machinery.

On the right is the sea-going hopper dredge Comber, which has been outfitted with snorkel, which can be seen extending from the side toward the New Orleans.

When the Comber has dredged sufficient material from the channel to load its bins, it ties up alongside the New Orleans, and discharges the material

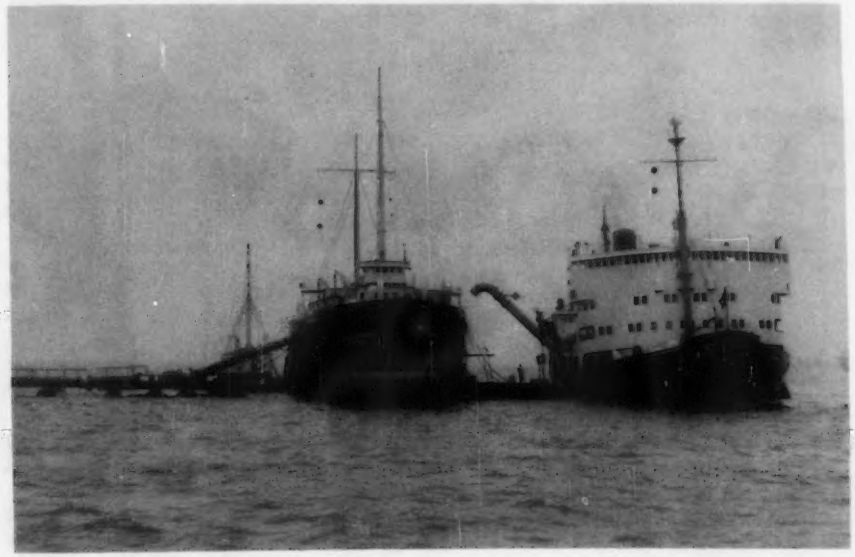

FIG. 1

through the snorkel into the bins of the Sump Rehandler New Orleans. The New Orleans then pumps the material ashore through a floating pipeline into a disposal area, where the solid materials settle to the bottom of the disposal area and the water returns to the river.

To maintain this operation, five rehandling stations were established and the dolphin-type berthing facilities constructed. At each rehandling station, two dolphins were constructed 209 ft apart (Fig. D2).

Each dolphin consists of a sheet pile cell 25.5 ft in diameter, with timber piling and rubber fender system. The spacing between dolphins and fender system were specified by the Marine Division.

Design criteria have been assumed such, that the dolphin will be capable of absorbing normal berthing forces of the hopper dredge Comber, as well as energies due to excessive weather conditions occuring while berthing in an exposed situation:

Water depth: 37 ft at mean high water; berthing speed of ship: 1 ft per sec; displacement of ship: 13,760 long tons; angle of approach with line parallel to the two dolphins; 10°; tidal range: 6 ft; ice pressure: 12 tons per sq ft, at high water level; wind pressure: 30 lb per sq ft of exposed area; longitudinal area of Comber: 16,800 sq ft.

Dolphin Cell Design.—The dolphin cell 25.5 ft in diameter, was formed with MP 112 interlocking steel sheet piling, filled with sand and gravel. The design assumptions and stability computations were considered similar to cofferdam design. The steel sheet piling forming the enclosure of the cellular dolphin has sufficient penetration into the underlying soil. Steel sheet piling (80 ft long)

FIG. 2

was driven in water depth of 37 ft, with a penetration of 39 ft below river bottom, which is more than 2/3 depth of water.[4,5]

The forces considered in dolphin design:

1. The effective kinetic energy, of the hopper dredge Comber,

$$E_A = \frac{M V^2 C}{2 g} = \frac{13{,}670 \times 1^2 \times 0.5 \times 12 \times 1.12}{2 \times 32.2} = 1426 \text{ in.-tons}$$

has been computed by the same equation as Eq. 1.01, except coefficient energy absorbed by dolphin C = 0.5 and speed of approach 1 ft per sec was introduced.[3]

2. Blows from floating ice of 10-in. thick with pressure of 12 tons per sq ft on exposed area. Pressure reduction factor[6] for rounded surface is equal 0.5.

$$P_i = 0.5 \times 12 \times 0.83 \times 25.5 = 127 \text{ tons}$$

---

5 "Stability and Stiffness of Cellular Cofferdam," by K. Terzaghi, Transactions of the ASCE, 1945, Vol. 110, pp. 1083-1210.

6 "Shore Protection and Design," Technical Report No. 4, Corps of Engrs., U. S. Army, June, 1954.

3. The pressure exerted by current water is assumed to occur at the water surface and the circular area exposed to the current is reduced by a coefficient of 2/3. Current pressure is:

$$P_c = 20 \text{ tons.}$$

Total ice and current pressure is:

$$P = P_i + P_c = 127 + 20 = 147 \text{ tons.}$$

4. Wind pressure on longitudinal area of hopper dredge Comber exposed to the wind applied to one dolphin is:

$$W_1 = \frac{16{,}800 \times 30}{2 \times 2{,}000} = 126 \text{ tons.}$$

The greatest impact will be produced by ice and water current P = 147 tons, on which all computations were based. Coefficient stability has been found at the river bottom equal to 1.6 and, at the bottom of sheet piling, 1.9. Maximum tension stress in the sheet pile and interlocks occur at a point above river bottom,[4] which are 4,000 lb per in.[2] and 1,510 lb. per lin in. of lock, respectively, which are less than allowable[6] of 12,000 lb per in.[2]

The shearing resistance in the vertical neutral plane has been increased by the welding of locks at the top of piles and by two band plates, also welded to the piles.

The fender system consists of rubber cylinders and timber piles which provide protection for berthing ships, and also provide the additional energy absorption.

This type of dolphin, constructed in an exposed area is considered to be a practical and economical solution of berthing for hopper dredge Comber, for unloading purposes.

Acknowledgements.—The writer wishes to acknowledge the use of material from the U. S. Army Engineer District, Philadelphia, Pa., Corps of Engineers, in preparation of this discussion. Particular acknowledgment is given to C. E. McGurk and J. B. Cavallero, who were supervisors for the dolphin design; the writer was the structural designer.

References.—

1. "Design of Miscellaneous Structures, Breakwaters, Jetties, and Piling," Preliminary Engineering Manual, Part CXXIX, Corps of Engineers, U. S. Army., Chapters 4 and 6.
2. "Some Dolphins Design," by D. H. Little, Journal Inst. C. E., No. 1, 1946-47.
3. "Some Designs for Flexible Fenders," by D. H. Little, Broc. Inst. C. E., February, 1953.
4. "Data Book for Civil Engineers," by E. E. Seelye.

---

[7] "Steel Sheet Piling," Catalogue of U. S. Steel Co.

[a] September, 1959, by John M. Weis and Virgil Blancato.

JEROME M. RICHOLSON.[8]—In this paper the authors have described a breasting dolphin capable of berthing supertankers of 100,000 tons and certain modifications to an earlier design of a retractable fender system for the dock-side berthing of vessels of similar tonnage. These changes consist, essentially, of replacing a number of the wooden structural members, that is, walers and rear vertical holding posts with steel I-beams, as well as a redesign of the hinging brackets to permit a greater retraction and energy absorption.

For the past several years the Naval Material Laboratory, at the New York Naval Shipyard, has been investigating a number of tropical hardwoods, some of which show considerable merit as marine construction timbers. in fact, two of these foreign species are currently (1960) undergoing evaluation at the New York Naval Shipyard in an experimental installation of the initial design of retractable fender system.

It would appear that both the breasting dolphin and the redesigned retractable fender system have almost practical universal application. However, under certain circumstances—for example, tropical ports adjacent to hardwood timber tracts as are common to many port cities of South America and Africa—economic considerations and local labor conditions may make it more desirable to utilize, as much as possible, the heavy marine timber species indigenous to that vicinity than to attempt to fabricate and install the large-sectioned steel members, or have them purchased and shipped from a distant foreign country. Assuming the probability of such a situation arising, it is suggested that the authors indicate the maximum tonnage that could be safely berthed by the breasting dolphin, or the redesigned retractable fender system, if all of the structural members were constructed of wooden timbers rather than steel beams.

---

8 Supervisory Wood Technologist, Naval Material Lab., N. Y. Naval Shipyard, Brooklyn, N. Y.

A CASE OF CRITICAL SURGING OF A MOORED SHIP[a]

Corrections

CORRECTIONS.–

p. 160 line 2 from bottom after "have had" insert "at"

p. 161 2nd paragraph, 1st line delete "A'B" at end of line

p. 163 2nd paragraph, 3rd line amend "losding" to "loading"

p. 165 top line after "ship" insert "the"

p. 166 2nd paragraph, last line elevate ϵ to line level

p. 167 1st paragraph, 1st line after Eq. (19) amend "of" to "or"

p. 175 (new addition)
Below S_0 insert:
dS stretch of mooring line under tension (=S - S_0)

p. 176 line ϕ
elevate ϵ to line level.

[a] December, 1959, by Basil W. Wilson.

PROCEEDINGS PAPERS

The technical papers published in the past year are identified by number below. Technical division sponsorship is indicated by an abbreviation at the end of each Paper Number, the symbols referring to: Air Transport (AT), City Planning (CP), Construction (CO), Engineering Mechanics (EM), Highway (HW), Hydraulics (HY), Irrigation and Drainage (ID), Pipeline (PL), Power (PO), Sanitary Engineering (SA), Soil Mechanics and Foundations (SM), Structural (ST), Surveying and Mapping (SU), and Waterways and Harbors (WW) divisions. Papers processed in the Department of Conditions of Practice are identified by the symbol (PP). For titles and cover sheets, refer to the appropriate issue of "Civil Engineering." Beginning with Volume 32 (January 1962) papers were published in Journals of the various Technical Divisions. To locate papers in the Journals, the symbols after the paper number are followed by a numeral designating the issue of a particular Journal in which the paper appeared. For example, Paper 2270 is identified as 2270(ST9) which indicates that the paper is contained in the ninth issue of the Journal of the Structural Division during 1962.

VOLUME 85 (1959)

MARCH: 1900(ST3), 1901(HY3), 1902(ST3), 1903(ID3), 1904(EM2), 1905(HW1), 1906(SA2), 1907(AT1), 1908(CP1), 1909(ST3), 1910(ST3), 1911(ST3), 1912(ST3), 1913(ST3), 1914(ST3), 1915(ST3), 1916(WW1), 1917(WW1), 1918(WW1), 1919(WW1), 1920(WW1), 1921(WW1), 1922(WW1), 1923(WW1), 1924(SA2), 1925(SA2)[c], 1926(HW1), 1927(WW1), 1928(ST3)[c], 1929(ST3)[c].

APRIL: 1930(EM2), 1931(EM2), 1932(EM2), 1933(HW2), 1934(HY3), 1935(HY4), 1936(HY4), 1937(HY4), 1938(EM2), 1939(SM2), 1940(SM2), 2001(SM2), 2002(ST4), 2003(ST4), 2004(ST4), 2005(ST4), 2006(PO3), 2007(HW2)[c], 2008(EM2)[c], 2009(ST4)[c], 2010(SM2)[c], 2011(SM4)[c], 2012(HY4)[c], 2013(PO2)[c].

MAY: 2014(AT2), 2015(AT2), 2016(AT2), 2017(HY3), 2018(HY3), 2019(HY3), 2020(HY3), 2021(HY3), 2022(HY3), 2023(PL3), 2024(PL3), 2025(PP1), 2026(PP1), 2027(PP1), 2028(PP1), 2029(PP1), 2030(SA3), 2031(SA3), 2032(SA3), 2033(SA3), 2034(ST5), 2035(ST5), 2036(ST5), 2037(ST5), 2038(PL2), 2039(PL2), 2040(PL2), 2041(PL2)[c], 2042(PP1)[c], 2043(ST5)[c], 2044(SA3)[c], 2045(HY3)[c], 2046(PP1), 2047(PP1).

JUNE: 2048(CP1), 2049(CP1), 2050(CP1), 2051(CP1), 2052(CP1), 2053(CP1), 2054(CP1), 2055(CP1), 2056(ST6), 2057(HY6), 2058(HY6), 2059(HW2), 2060(PO2), 2061(SM3), 2062(SM3), 2063(SM3), 2064(SM3), 2065(WW2), 2066(WW2), 2067(WW2), 2068(WW2), 2069(WW2), 2070(WW2), 2071(WW2), 2072(CP1)[c], 2073(SU2)[c], 2074(ST6)[c], 2075(ST6)[c], 2076(EM3)[c], 2077(EM3)[c], 2078(WW2)[c].

JULY: 2079(HY7), 2080(HY7), 2081(HY7), 2082(HY7), 2083(HY7), 2084(HY7), 2085(HY7), 2086(HY7), 2087(SA4), 2088(SA4), 2089(SA4), 2090(SA4), 2091(EM3), 2092(EM3), 2093(EM3), 2094(EM3), 2095(SM3), 2096(SM3), 2097(HY7)[c], 2098(SA4)[c], 2099(EM3)[c], 2100(AT3), 2101(AT3), 2102(AT3), 2103(AT3), 2104(AT3), 2105(AT3), 2106(AT3), 2107(AT3), 2108(AT3), 2109(AT3), 2110(AT3), 2111(AT3), 2112(AT3), 2113(AT3), 2114(AT3), 2115(AT3), 2116(AT3), 2117(AT3), 2118(AT3), 2119(AT3), 2120(AT3), 2121(AT3), 2122(AT3), 2123(AT3), 2124(AT3), 2125(AT3).

AUGUST: 2126(HY8), 2127(HY8), 2128(HY8), 2129(HY8), 2130(PO3), 2131(PO4), 2132(PO4), 2133(PO4), 2134(SM4), 2135(SM4), 2136(SM4), 2137(SM4), 2138(ST8), 2139(PO3)[c], 2140(SM4)[c].

SEPTEMBER: 2141(CO2), 2142(CO2), 2143(CO2), 2144(WW3), 2145(WW3), 2146(WW3), 2147(HY9), 2148(HY9), 2149(HY9), 2150(HY9), 2151(ID3), 2152(ST7)[c], 2153(ID3), 2154(ID3), 2155(ID3), 2156(ID3), 2157(ID3), 2158(ID3), 2159(ID3), 2160(ID3), 2161(SA5), 2162(SA5), 2163(ST7), 2164(ST7), 2165(SU1), 2166(SU1), 2167(WW3), 2168(WW3), 2169(WW3), 2170(WW3), 2171(WW3), 2172(WW3), 2173(WW3), 2174(WW3), 2175(WW3), 2176(WW3), 2177(WW3), 2178(CO2)[c], 2179(ID3)[c], 2180(ID3)[c], 2181(SA5)[c], 2182(HY9)[c], 2183(SU1)[c], 2184(WW3)[c], 2185(PP2)[c], 2186(ST7)[c], 2187(PP2), 2188(PP2).

OCTOBER: 2189(AT4), 2190(AT4), 2191(AT4), 2192(AT4), 2193(AT4), 2194(EM4), 2195(EM4), 2196(EM4), 2197(EM4), 2198(EM4), 2199(EM4), 2200(HY10), 2201(HY10), 2202(HY10), 2203(PL3), 2204(PL3), 2205(PL3), 2206(PO5), 2207(PO5), 2208(PO5), 2209(PO5), 2210(SM5), 2211(SM5), 2212(SM5), 2213(SM5), 2214(SM5), 2215(SM5), 2216(SM5), 2217(SM5), 2218(ST8), 2219(ST8), 2220(SM5), 2221(ST8), 2222(ST8), 2223(ST8), 2224(WW4), 2225(HY10), 2226(PO5), 2227(PO5), 2228(PO5), 2229(ST8), 2230(EM5), 2231(EM5), 2232(AT4)[c], 2233(PL3)[c], 2234(EM4)[c], 2235(HY10)[c], 2236(WW4)[c], 2237(ST8)[c], 2238(PO5)[c], 2239(ST8), 2240(PL3).

NOVEMBER: 2241(HY11), 2242(HY11), 2243(HY11), 2244(HY11), 2245(HY11), 2246(HY11), 2246(SA6), 2247(SA6), 2248(SA6), 2249(SA6), 2250(SA6), 2251(SA6), 2252(SA6), 2253(SA6), 2254(SA6), 2255(SA6), 2256(SA6), 2257(ST9), 2258(ST9), 2259(ST9), 2260(ST9), 2261(ST9), 2262(ST9)[c], 2263(ST9), 2263(HY11), 2264(ST9), 2265(HY11), 2266(SA6), 2267(SA6), 2268(SA6), 2269(HY11)[c], 2270(ST9).

DECEMBER: 2271(HY12), 2272(CP2), 2273(HW4), 2274(HW4), 2275(HW4), 2276(HW4), 2277(HW4), 2278(HW4), 2279(HW4), 2280(HW4), 2281(ID4), 2282(SM6), 2283(SM6), 2284(SM6), 2285(PO6), 2286(PO6), 2287(PO6), 2288(PO6), 2289(PO6), 2290(PO6), 2291(PO6), 2292(SM6), 2293(SM6), 2294(SM6), 2295(SM6), 2296(SM6), 2297(SM6), 2298(WW4), 2299(WW4), 2300(WW4), 2301(WW4), 2302(WW4), 2303(WW4), 2304(WW4), 2305(ST10), 2306(CP2), 2307(CP2), 2308(ST10), 2309(CP2), 2310(HY12), 2311(HY12), 2312(PO6), 2313(PO6), 2314(ST10), 2315(HY12), 2316(HY12), 2317(HY12), 2318(WW4), 2319(SM6), 2320(SM6), 2321(ST10), 2322(ST10), 2323(HW4)[c], 2324(CP2)[c], 2325(SM6)[c], 2326(WW4)[c], 2327(EM5)[c], 2328(PO6)[c], 2329(ST10)[c], 2330(CP2).

VOLUME 86 (1960)

JANUARY: 2331(EM1), 2332(EM1), 2333(EM1), 2334(EM1), 2335(HY1), 2336(HY1), 2337(EM1), 2338(EM1), 2339(HY1), 2340(HY1), 2341(SA1), 2342(EM1), 2343(SA1), 2344(ST1), 2345(ST1), 2346(ST1), 2347(ST1), 2348(EM1)[c], 2349(HY1)[c], 2350(ST1), 2351(ST1), 2352(SA1)[c], 2353(ST1)[c], 2354(ST1).

FEBRUARY: 2355(CO1), 2356(CO1), 2357(CO1), 2358(CP1), 2359(CO1), 2360(CO1), 2361(PO1), 2362(HY2), 2363(ST2), 2364(HY2), 2365(SU1), 2366(HY2), 2367(HY2), 2368(SM1), 2369(SM1), 2370(SU1), 2371(HY2), 2372(PO1), 2373(SM1), 2374(HY2), 2375(PO1), 2376(HY2), 2377(CO1)[c], 2378(SU1), 2379(ST2), 2380(SU1), 2381(HY2)[c], 2382(ST2), 2383(SU1), 2384(ST2), 2385(SU1), 2386(SM1), 2387(SU1), 2388(SM1), 2389(ST2)[c], 2390(EM1)[c], 2391(PO1)[c].

MARCH: 2392(ID1), 2393(ID1), 2394(ID1), 2395(ID1), 2396(ID1), 2397(ID1), 2398(ID1), 2399(ID1), 2400(ID1), 2401(ID1), 2402(ID1), 2403(ID1), 2404(ID1), 2405(ID1), 2406(ID1), 2407(SA2), 2408(SA2), 2409(HY3), 2410(ST3), 2411(SA2), 2412(WW1), 2413(WW1), 2414(WW1), 2415(HY3), 2416(HY3), 2417(HW2), 2418(WW1)[c], 2419(WW1)[c], 2420(WW1), 2421(WW1), 2422(WW1), 2423(SA2), 2424(SA2)[c], 2425(HY3)[c], 2426(ST3)[c].

[c] Discussion of several papers, grouped by division.

AMERICAN SOCIETY OF CIVIL ENGINEERS

OFFICERS FOR 1960

PRESIDENT

FRANK A. MARSTON

VICE-PRESIDENTS

Term expires October, 1960:
PAUL L. HOLLAND
LEONARD D. KNAPP

Term expires October, 1961:
CHARLES B. MOLINEAUX
LAWRENCE A. ELSENER

DIRECTORS

Term expires October, 1960:
PHILIP C. RUTLEDGE
WESTON S. EVANS
TILTON E. SHELBURNE
CRAIG A. HAZELET
LEONARD D. MATTESON
JOHN E. RINNE

Term expires October, 1961:
THOMAS J. FRATAR
EARL F. O'BRIEN
SAMUEL B. VENTRES
CHARLES W. BRITZIUS
WAYNE G. O'HARRA
FRED H. RHODES, JR.
N. T. VEATCH

Term expires October, 1962:
ELMER E. TIMBY
SAMUEL S. BAXTER
THOMAS M. NILES
TRENT R. DAMES
WOODROW W. BAREN
BERNHARD DORNBLATT

PAST PRESIDENTS

Members of the Board

LOUIS R. HOWSON
FRANCIS S. FRIEL

EXECUTIVE SECRETARY
WILLIAM H. WISELY

TREASURER
E. LAWRENCE CHANDLER

ASSISTANT SECRETARY
E. LAWRENCE CHANDLER

ASSISTANT TREASURER
ENOCH R. NEEDLES

PROCEEDINGS OF THE SOCIETY

HAROLD T. LARSEN
Manager of Technical Publications

PAUL A. PARISH
Editor of Technical Publications

MARVIN L. SCHECHTER
Associate Editor of Technical Publications

IRVIN J. SCHWARTZ
Assistant Editor of Technical Publications

COMMITTEE ON PUBLICATIONS

PHILIP C. RUTLEDGE, *Chairman*

THOMAS M. NILES, *Vice-Chairman*

TILTON E. SHELBURNE
WESTON S. EVANS
WAYNE G. O'HARRA
BERNHARD DORNBLATT

PART 2

MARCH 1960 — 9 NO. WW 1
VOLUME 86 PART 2

Your attention is invited

NEWS OF THE WATERWAYS AND HARBORS DIVISION OF ASCE

JOURNAL OF THE WATERWAYS AND HARBORS DIVISION
PROCEEDINGS OF THE AMERICAN SOCIETY OF CIVIL ENGINEERS

Journal of the
WATERWAYS AND HARBORS DIVISION
Proceedings of the American Society of Civil Engineers

NEWS

March, 1960

Waterways Projects Nominated for Awards

Two waterways projects have been nominated by ASCE directors for the "Outstanding Civil Engineering Achievement of 1959" award.

The St. Lawrence Project, the power and seaway development on the St. Lawrence River, was nominated for the award by Earl F. O'Brien, of Syracuse, N. Y., ASCE Director for District 3 (upper New York State and areas in Canada). The St. Lawrence River project opened the Great Lakes to four-fifths of the world's shipping. By use of four locks, each approximately 900 feet long, 80 feet wide and 30 feet deep, the ocean-going vessels are lifted 224 feet between Montreal and the Thousand Islands on the St. Lawrence River. A major part of the overall project is the power dam which will develop 1,880,000 kilowatts of power. The river drains an area of 300,000 square miles and has an average annual flow of 236,000 cubic feet per second, all of which passes through the project.

The Wilson Lock project at Wilson Dam, Alabama, was nominated by Don H. Mattern, of Knoxville, Tenn., who is ASCE Director for District 10 (the states of Alabama, Florida, Georgia, North Carolina, South Carolina and portions of Tennessee). Constructed at Muscle Shoals by the Tennessee Valley Authority, Wilson Lock has a lift of 100 feet, probably the world's largest single-lift lock. On-site construction began in July of 1956, and in November of 1959 the new lock was placed in commercial operation. Related improvements include the lowering of the three-mile Florence Canal 10 feet by an unique procedure to keep traffic moving, and the construction of a new high-level highway bridge of curved girder design.

These projects are among 12 nominations made throughout the country for the outstanding civil engineering achievement. Judging will be by a jury of engineering magazine editors, and the winner will be announced by the Society's Board of Direction at ASCE's national convention in New Orleans in March.

ASCE Coordinating Committees

The ASCE Coordinating Committee on Transportation, composed of representatives of the Waterways and Harbors Division, the Air Transport Division,

Note.—No. 1960-9 is part of the copyrighted Journal of the Waterways and Harbors Division, Proceedings of the American Society of Civil Engineers, Vol. 86, WW 1, March, 1960.
Copyright 1960 by the American Society of Civil Engineers.

Highways Division, Pipeline Division, and City Planning Division, held its initial meetings during 1959. The chairman of the Committee is Thomas J. Fratar, ASCE Director from District 1 and a member of the Division's Committee on Ports and Harbors. The Waterways and Harbors representative on the Committee is Roger H. Gilman. The Committee plans to direct its efforts along the following lines:

a) Encourage contacts and exchanges between the five technical committees.

b) Act as a focal point for initiating studies and disseminating information.

c) Effectuate a detailed study of existing technical divisions to avoid overlaps.

d) Study work of technical committes with respect to other associations and organizations such as American Association of Port Authorities, Inst. of Traffic Engineers, etc.

The Waterways and Harbors Division is represented on the ASCE Water Resources Coordinating Committee by Col. L. B. Feagin of the Division Executive Committee. As a result of the Coordinating Committee's recommendations, the Division's purpose was changed during 1959 to the following:

Purpose: The advancement and dissemination of engineering knowledge concerning the utilization of waterways and harbors, and the protection and development of ocean and other water frontage. This includes studies in the following fields: floods and methods of protection, droughts and methods of alleviation, tidal action, wave action, and unusual phenomena which affect the stability of shore lines and the navigable capacity or usefulness of waterways and harbors; port development and operation; types of structures and equipment used in navigation, shore protection and flood control engineering, their design, construction, maintenance, and the suitability of materials for such use; and the economics of waterborne transportation.

The statements of purpose of several of the Division's Technical Committees were also changed.

The Division Executive Committee has recommended that these Coordinating Committees emphasize expansion of the scope of existing divisions and liaison among divisions rather than the creation of new divisions.

Princeton University Conference

The Princeton University Conference on Shipping and Navigation Problems of the Great Lakes and St. Lawrence Seaway was held on January 19 - 20, 1960 under the direction of Admiral W. Mack Angas, Chairman of the Department of Civil Engineering at Princeton University. The papers presented at the Conference are listed below.

1. Surface Elevations of the Great Lakes

Harley F. Lawhead
U. S. Corps of Engineers

In the design of harbors and improved channels, cognizance must be taken of anticipated variations in lake levels as well as a trend toward the use of

larger vessels in lake commerce.

2. Water Level Disturbances in the Great Lakes and Their Effect on Navigation

Leonas Bajorunas
United States Lake Survey

Disturbances of the water levels in the Great Lakes, due to winds and variation of barometric pressure, are transmitted into connecting rivers and harbors, reducing depths in navigation channels and creating currents in harbors.

3. Navigation Problems of the St. Lawrence Seaway and the Great Lakes

R. J. Burnside
St. Lawrence Seaway Authority

A review of the navigating and operating problems encountered during the first year's operation of the Seaway with special emphasis on the probability of bottlenecks developing in one or more sections of the system. Proposed adjustments with special reference to the Welland Canal will be considered.

4. The Ice Problem

Real Admiral E. H. Thiele
United States Coast Guard

The Great Lakes navigation season is limited by weather and ice conditions to about eight months. The author discusses the problems involved in winter navigation as presently conceived and the possibilities for the future.

5. The Ocean-Lake Ship

Hugh C. Downer
Marine Transportation Consultant

A review of the technical and economic problems involved in the development of ships that are efficient in dual ocean and Ocean-Seaway-Great Lakes service.

6. The Great Lakes Port Developments

Austin E. Brant, Jr.
Tippetts-Abbett-McCarthy-Stratton

A review of the present status of harbor and terminal facilities at Great Lakes ports and an analysis of the effect of the Seaway on these ports.

7. The Effect of the Seaway on the Great Lakes Traffic Pattern

Rear Admiral Lyndon Spencer
United States Coast Guard, Retired
Lake Carriers' Association

A description of the bulk trade on the Great Lakes, the types of vessels engaged in the trade, the commodities transported, the flow of traffic and changes to that flow resulting from construction of the St. Lawrence Seaway.

The proceedings of the Conference are planned for publication during the spring.

SPECIAL HYDRAULICS PROGRAM AT MIT

Massachusetts Institute of Technology is planning a special summer program on "Estuary and Coastline Hydrodynamics," to be given at MIT from June 20 through July 1, 1960. This two-week program is intended to meet the needs of engineers engaged in the design and development of all types of marine structures in which gravity wave action and tidal phenomena are important. A general and concise review of the theory will be given including the most recent results of experimental and analytical research. Topics include: generation and transformation of waves, damping by boundary layer action, wave refraction and diffraction, resonant conditions in harbors, interaction of waves and marine structures, coastal currents, sediment erosion and deposition, tidal dynamics of estuaries and inlets, saline and fresh water interaction, steady and unsteady diffusion processes in estuaries, coastal and tidal models. The lectures will be given by the staff of the Hydrodynamics Laboratory of the Department of Civil and Sanitary Engineering and will be coordinated with presentations by other distinguished experts in the field. Dr. Arthur T. Ippen, Professor of Hydraulics, will be in charge of the program.

AAPA Committee Report on Construction and Maintenance

At the annual convention of the American Association of Port Authorities in December 1959, the report submitted by the AAPA Committee on Construction and Maintenance included the following papers which may be of interest to members of the Waterways and Harbors Division.

1. Bulk Unloading Dock, Pier 4 Terminal No. 4
   Portland, Oregon

   Thane E. Brown, Chief Engineer
   The Commission of Public Docks
   Portland, Oregon

2. Reconversion of Piers 38 and 40 South
   Port of Philadelphia, Philadelphia, Penna.

   Thomas C. Brown
   Chief, Division of Port Operations
   Department of Commerce
   City of Philadelphia

3. Future Development Trends for Shipside Facilities

   B. N. Hoffmaster, Chief Harbor Engineer
   Port of Long Beach, California

4. Redesign and Conversion of Port Facilities
   for Modern Operations

   John S. Wilson
   Engineer of Design (Marine Terminals)
   The Port of New York Authority

5. A Discussion of the General Problem of Redesigning and the Conversion of an Old Established Port into a Modern Port

John D. M. Luttman-Johnson
Senior Engineer
Fay, Spofford & Thorndike, Inc.
Boston, Massachusetts

6. A Discussion of the Problem of Conversion for Seaway Navigation of Established Wharves in Great Lakes Ports

Clifford W. Morgan, General Manager
Port of Hamilton, Canada

7. Description of Atlantic Sugar Refineries Limited New Wharf Facilities for Unloading and Handling Bulk Sugar at the Port of Saint John, New Brunswick

D. M. Vye, Port Manager
National Harbours Board
Port of Saint John
New Brunswick, Canada

These papers have been published in "Committee Reports" of the Association.

For Your Calendar

March 7-11, 1960	ASCE, New Orleans Convention
June 19-23, 1960	ASCE, Reno Convention
October 9-13, 1960	ASCE, Boston Convention
April 10-15, 1961	ASCE, Phoenix Convention
October 16-20, 1961	ASCE, New York Convention
February, 1962	ASCE, Houston Convention
May, 1962	ASCE, Omaha Convention
October 15-19, 1962	ASCE, Detroit Convention

Newsletter Publication

The next issue of the Waterways and Harbors Division Journal will be in June 1960. The deadline for submission of material for that issue is April 29, 1960. If you have any material which might be useable in the newsletter, please send it to:

Austin E. Brant, Jr.
Editor, Waterways and Harbors
Division Newsletter
Tippetts-Abbett-McCarthy-Stratton
375 Park Avenue
New York 22, N. Y.